The *C. elegans* RAS/MAPK and WNT Signalling Pathways are Modified by Polymorphic Genes and Molecular Oxygen

---

Dissertation

zur

Erlangung der naturwissenschaftlichen Doktorwürde
(Dr. sc. nat.)

vorgelegt der

Mathematisch-naturwissenschaftlichen Fakultät

der

Universität Zürich

von

Sabrina Maxeiner

aus

Buchs ZH

Promotionskommission

Prof. Dr. Alex Hajnal (Vorsitz)
Prof. Dr. Konrad Basler
Prof. Dr. Jan Kammenga
Prof. Dr. Beatrice Beck-Schimmer

Zürich, 2018

ZUSAMMENFASSUNG

Die weltweit zweithäufigste menschliche Todesursache ist Krebs. Während fundamentale Signaltransduktionswege wie z.B. WNT, RAS/MAPK und NOTCH in direkten Zusammenhang mit der Krankheit gebracht wurden, ist die Beschreibung von mitwirkenden Modifikatoren erst in den Kinderschuhen. Modifikatoren (Risikofaktoren) haben alleine kleine Effekte, die allerdings quantitativ den Ausgang einer Krankheit beeinflussen und daher vielversprechende therapeutische Angriffspunkte darstellen. Obwohl genomweite Assoziationsstudien (GWAS) zur Identifikation von Risikofaktoren beigetragen haben, sind sie eingeschränkt durch limitierte Stichproben. Wir haben *C. elegans* als Model verwendet, um solche Modifikatoren zu identifizieren, da genetisch unterschiedliche Wildisolate existieren und fehlerhafte WNT, RAS/MAPK und NOTCH Signalaktivität auffällige phänotypische Veränderungen mit sich bringt, besonders während der Entwicklung der Vulva.

In unserer Studie haben wir CB4856 / N2 Inzuchtlinien benutzt, die wir mit einer Funktionsverlustmutation in *ß-catenin* oder einer Funktionsgewinnmutation in *RAS* genetisch sensibilisiert hatten. Mit diesen Linien verifizierten wir eine zuvor vermutete Region quantitativer Merkmale (engl. QTL) für RAS/MAPK Signalaktivität auf dem ersten Chromosom und schränkten diese positionell ein (QTL1a). Des Weiteren verifizierten wir eine Region quantitativer Merkmale, ebenfalls auf dem ersten Chromosom, für WNT Signalaktivität und unterteilten diese in zwei kleinere Regionen, nachdem die eingekreuzte DNA Sequenz rekombiniert hatte (QTL1A und QTL1B). In einem ersten Projekt haben wir durch RNA Interferenz innerhalb von QTL1B und QTL1a generelle Modifikatoren sowie Risikofaktoren spezifisch für den genetischen Hintergrund gefunden, die wir noch nicht weiter charakterisiert haben. In einem zweiten Projekt haben wir den Zusammenhang zwischen polymorphen Kandidatengenen und assoziierten zellulären Signalwegen der vorgängig beschriebenen QTL1b Region mit dem RAS/MAPK Signaltransduktionsweg charakterisiert. Zwei Gene interessierten uns besonders: *pfd-3* ist ein Ortholog von VHL binding protein 1 und *F44F1.1* ist ein Paralog eines vermuteten Calpains. Beide Gene supprimieren den Eiablagedefekt in *egl-9* Mutanten. Dies impliziert eine Verbindung zum stark konservierten Hypoxiereaktionsweg, der durch die *C. elegans* Gene *hif-1, egl-9* und *vhl-1* kodiert und durch Sauerstoff reguliert wird. Wir haben die aktivierende G13E Mutation in das *RAS* Wurmgen *let-60* von CB4856 und N2 eingefügt und entdeckten, dass starke Hypoxie (0.5% O_2) die RAS/MAPK Signalaktivität in der Vulva ungeachtet des genetischen Hintergrundes auf dasselbe Niveau supprimierte, wohingegen milde Hypoxie (> 0.5% O_2) keinen Effekt zeigte. Dieses Resultat war erstaunlich, da CB4856 einen höheren Level an RAS/MAPK Grundsignalaktivität besitzt und deutet auf eine genetische Komponente hin, die Sauerstoff in Verbindung setzt mit RAS/MAPK und darüber hinaus die natürliche Differenz in der RAS/MAPK Signalstärke eliminiert. Tatsächlich entdeckten wir, dass der Verlust von VHL-1 oder EGL-9 die RAS/MAPK Signalaktivität von *let-60(n1046)* Mutanten verringerte, während ein Funktionsverlust von HIF-1 die Signalaktivität

erhöhte. Zusätzlich zeigen wir, dass Hypoxie die RAS/MAPK Signalaktivität auch in der exkretorischen Kanalzelle und der Keimbahn inhibiert, wobei der hypoxische Effekt im letzteren Gewebe HIF-1 abhängig zu sein scheint. Dem gegenüber gestellt ist der hypoxische Effekt in der Vulva unabhängig von HIF-1 und benötigt stattdessen wahrscheinlich Serotonin. Unter normoxischen Bedingungen ist der inhibitorische Effekt durch HIF-1 auf RAS/MAPK Signalaktivität gewebsspezifisch und abhängig von dem HIF-1 Zielgen NHR-57, das in den ventralen Pn.p Zellen inklusive der vulva-spezifischen Vorläuferzellen exprimiert ist, allerdings am markantesten in jenen Pn.p Zellen, die keine Vulva formen können. Zuletzt zeigen wir, dass das HIF-1 Hydroxylase-Protein EGL-9 ein Zielgen des NOTCH Signalweges ist und schlagen ein Szenario vor, in dem EGL-9 mit NHR-57 konkurriert, um vulva-spezifische Kompetenz aufrecht zu erhalten. Unsere Resultate decken einen neuen Mechanismus auf, durch den die RAS/MAPK und NOTCH Signaltransduktionswege die Umweltkomponente Sauerstoff integrieren um die Festlegung von Zellschicksalen zu kontrollieren.

SUMMARY

The worldwide second leading cause of human death is cancer. Fundamental signalling pathways such as WNT, RAS/MAPK and NOTCH have been linked to the disease, however the description of contributing genetic modifiers is only at the beginning. Modifiers (risk factors or susceptibility genes) have small effects on their own but quantitatively change disease outcome and are thus promising therapeutic targets. Genome-wide association studies (GWAS) have helped in identifying risk factors but are limited by sample number. We have used *C. elegans* as a model to identify such modifiers, since genetically divergent wild isolates exist and erroneous WNT, RAS/MAPK and NOTCH signalling pathway activity causes easily discernible phenotypic outcomes, especially during vulval development.

By using CB4856 / N2 introgression lines genetically sensitised with a *ß-catenin(lf)* or *RAS(gf)* mutation, we verified and spatially refined a previously identified quantitative trait locus (QTL) for RAS/MAPK signalling on LG I (QTL1a) and another QTL on LG I for WNT signalling, which we subdivided into two smaller QTLs upon recombination in the introgression (QTL1A and QTL1B). In a first project, we identified general as well as isolate-specific candidate modifiers within QTL1B and QTL1a by RNAi that await further characterisation. Secondly, we characterised the connection of polymorphic candidates within the previously described QTL1b and associated cellular pathways with RAS/MAPK signalling. Two genes in the QTL1b region attracted our attention: *pfd-3* is an ortholog of VHL binding protein 1 and *F44F1.1* is a paralog of a probable calpain. Both were described to suppress the *egl-9* mutant phenotype. This suggests a link to the highly conserved hypoxia response pathway, which is encoded by the worm *hif-1, egl-9* and *vhl-1* genes. We introduced into the CB4856 and N2 wild strains the activating G13E mutation in the worm *RAS* gene *let-60* and found that severe hypoxia (0.5% O_2) suppressed RAS/MAPK activity in the vulva to equal levels irrespective of the genetic background, whereas mild hypoxia (> 0.5% O_2) had no effect. This was striking, since CB4856 inherently exhibits higher ground RAS/MAPK levels and suggests a genetic component that links oxygen sensing to RAS/MAPK signalling. Indeed, we found that a loss of VHL-1 or EGL-9 reduces whereas a loss in HIF-1 function increases RAS/MAPK signalling strength in *let-60(gf)* mutants. We further show that hypoxia inhibits RAS/MAPK activity in the duct cell and the germline. In the latter tissue, the hypoxic effect is completely HIF-1 dependent while it appears to be partially HIF-1 independent and regulated through serotonin in the vulva. In normoxic conditions, the inhibitory effect of HIF-1 on RAS/MAPK activity in the vulva is cell autonomous and depends on the HIF-1 target gene NHR-57. Interestingly, NHR-57 is expressed in the ventral Pn.p cells including the vulval precursor cells (VPCs), but expression is most prominent in those VPCs that are incompetent of forming the vulva. Finally, we show that the HIF-1 hydroxylase EGL-9 is a target of the NOTCH pathway. We propose a competition between NOTCH signalling and NHR-57 to maintain the VPCs competent to differentiate. Our findings reveal a novel mechanism, by which the RAS/MAPK and NOTCH pathways integrate oxygen in order to control cell fate specification.

Contents

Introduction

1

1.1 The model organism *C. elegans*

Caenorhabditis elegans is a small, free-living, non-parasitic nematode that primarily inhabits soil (Altun and Hall 2009). It feeds on bacteria and develops through four larval stages until it reaches adulthood and a length of approximately 1 mm (**Fig. 1.1A**). Each larval stage is terminated by a moulting event and is accompanied by an increase in size. If the worm encounters food shortage, overcrowding or inadequate temperature, it can enter an alternative L3 stage as a dauer larva (Golden and Riddle 1982). The dauer larvae arrest in development and can endure for several months until the situation improves.

The predominant sex of *C. elegans* is the hermaphrodite, although males exist at a frequency of 0.1% and can arise from spontaneous nondisjunction of the X chromosome or after a hermaphrodite has mated with a male (**Fig. 1.1B**). Hermaphrodites self-fertilise by producing sperm and eggs in a sequential manner, thus a population can arise from a single worm and is clonal (Herman 2005). One hermaphrodite can produce approximately 300 offspring during its life – a highly appreciated fact among geneticists.

The wild-type (wt) strain of *C. elegans*, N2, was isolated in Bristol, England, and established as a model organism in 1965 by Sydney Brenner (Brenner 1974). It has since gained in popularity in studies on behaviour, developmental and cell biology due to several key aspects. These include its short life cycle of only 3.5 days, a large number of progeny, small size, transparency, a small genome of which the sequence was known by 1998 (The *C. elegans* Sequencing Consortium 1998), its convenience of cultivation in the laboratory, where it feeds on *E. coli* OP50 seeded on agar plates, the simplicity of applying RNAi by feeding (Timmons and Fire 1998) as well as its invariant cell lineage, a feature known as eutely (Martini 1923). Sydney Brenner, H. Robert Horvitz and John E. Sulston received the Nobel Prize for Physiology and Medicine in 2002 for their work on describing the cell lineage: Hermaphrodites consist of 959 somatic cells (131 of originally 1090 cells die by apoptosis) and males comprise 1031 somatic cells (Sulston and Horvitz 1977; Sulston et al. 1983).

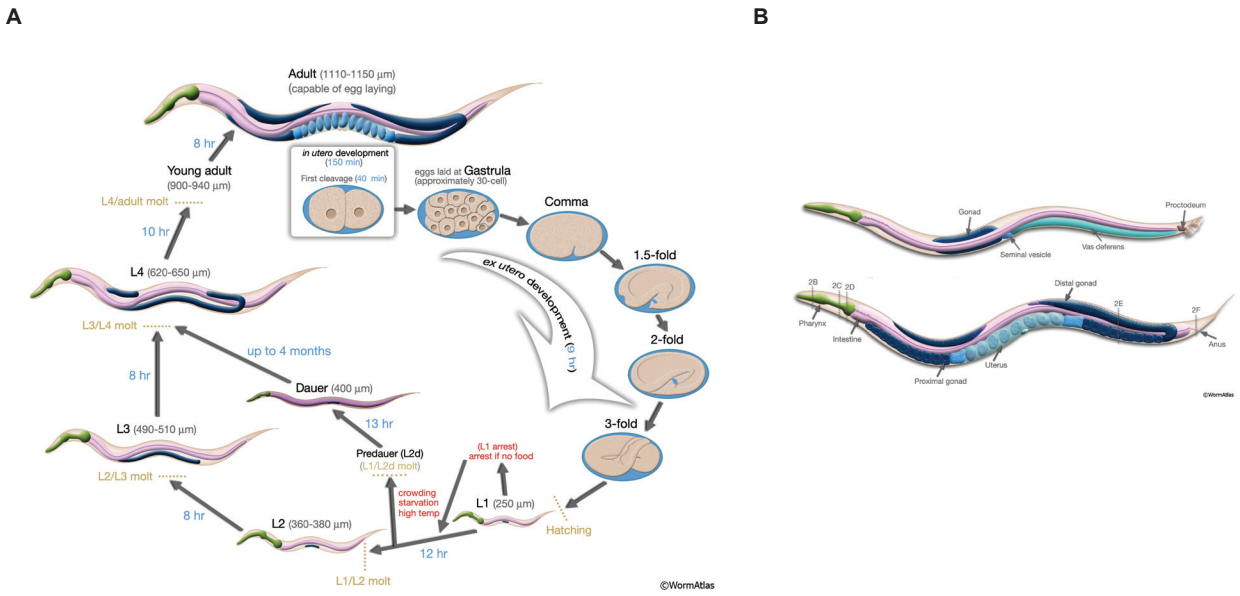

Figure 1.1. Schematic representation of the *C. elegans* life cycle and sexes. **(A)** The worm passes four larval stages before it reaches adulthood. An alternative L2 dauer stage allows endurance in unfavourable environmental conditions. Each larval stage is terminated by a moulting event and accompanied by an increase in size. At 20 °C, one life cycle is completed after approximately three days. **(B)** *C. elegans* males are slightly smaller (top) than hermaphrodites (bottom). Males have only one gonad arm to exclusively produce sperm whereas hermaphrodites produce oocytes and sperm sequentially and in two gonad arms. The vulva of the hermaphrodite serves as the egg-laying and mating organ. Figures adaptes from WormAtlas.

In addition to the wild-type N2 strain, genetically divergent isolates were collected for developmental, evolutionary or population studies (Wicks et al. 2001; Thompson et al. 2015): CB4857 from mushrooms in Claremont (California), RC301 from compost in the Botanical Garden of Freiburg (Germany), CB4856 from a pineapple field in Hawaii and AB2 from soil in Adelaide (Australia) (Hodgkin 1993) to name only a few. The CB4856 strain is one of the most divergent isolates from N2 with 3.3 Mb of N2 sequence absent in CB4856 and 1.4 Mb CB4856 sequence not present in N2 (Thompson et al. 2015) which demonstrates the power of employing *C. elegans* wild isolates to study natural variation and quantitative traits (de Bono and Bargmann 1998; Jansen and Nap 2001; Li et al. 2006; Palopoli et al. 2008; McGrath et al. 2009; Ghosh et al. 2012).

1.2 Vulval development

The formation of the *C. elegans* hermaphrodite vulva is an excellent tool to study organogenesis, signal transduction and a network of intercellular signalling pathways including epidermal growth factor (EGF) signalling, Notch mediated lateral signalling and WNT signalling (Sternberg and Horvitz 1986; Kornfeld 1997). The vulva is the worm's organ for egg-laying and copulation with males and connects the uterus to the environment (Kornfeld 1997). Aberrant signalling is easily visible, as the vulva is wrongly or not formed. It is built up of only 22 polarised ventral epidermal cells. The development of the organ starts in the early L1 larva, when twelve ventral neuroectoblasts P1 - P12 divide and give rise to anterior neurons or glia cells (Pn.a) and posterior Pn.p cells, of which six (P3.p - P8.p) will form the vulval precursor cell (VPC) equivalence group (Sulston and Horvitz 1977) (**Fig. 1.2**). The remaining posterior daughters P1.p, P2.p and P9.p - P12.p fuse with *hyp7*, the syncytial hypodermis. P3.p fuses with the hypodermis in 50% of the cases (Sulston and White 1980).

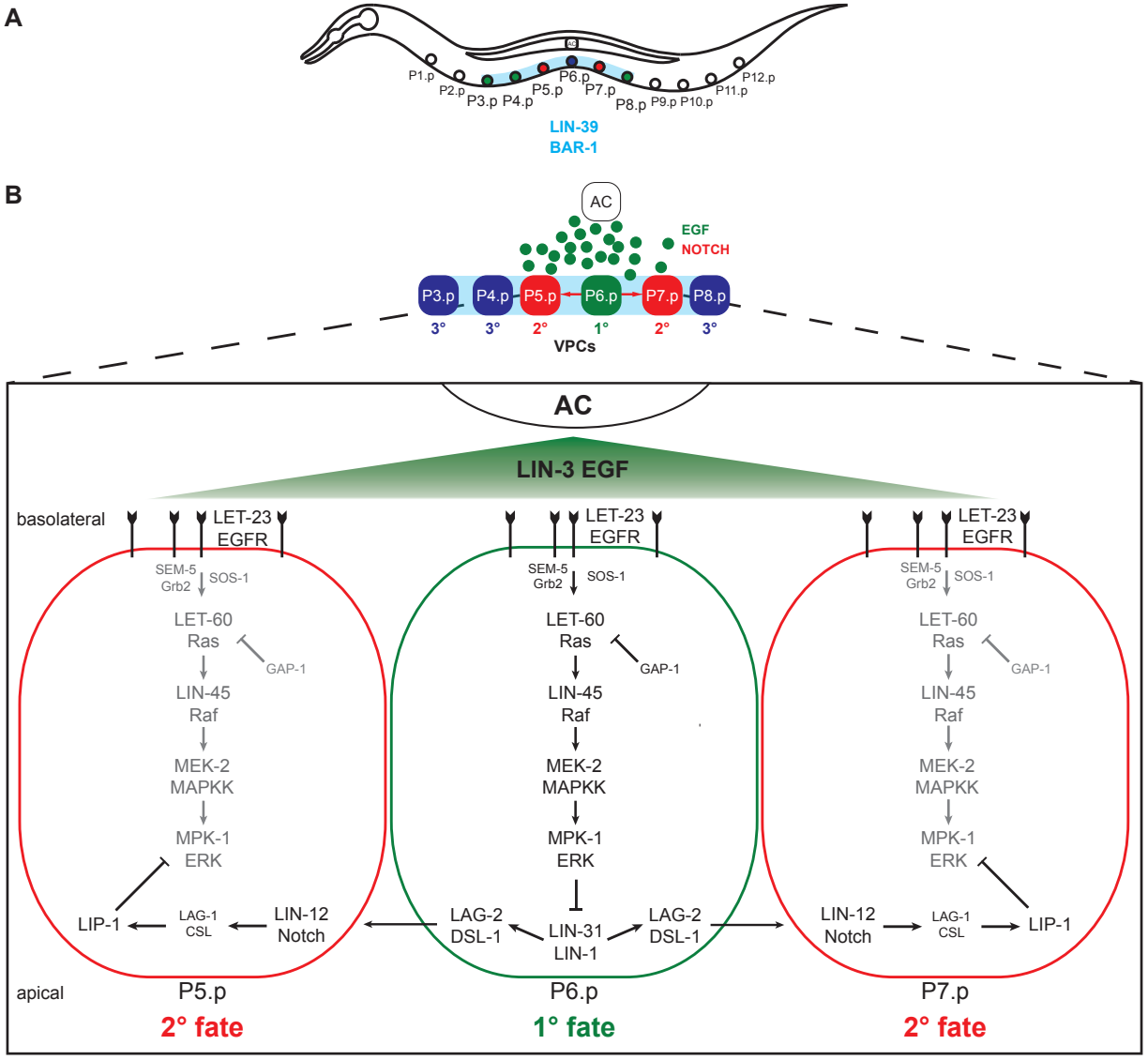

Figure 1.2. Development of the *C. elegans* hermaphrodite vulva. **(A)** Only six of the twelve ventral epidermal cells make up the vulval competence group that is defined by the presence of LIN-39 and BAR-1 (light blue). **(B)** Consecutive and interconnected inductive LIN-3/EGF and lateral LIN-12/NOTCH signalling during the L2 and early L3 stages determine the pattern cell fate acquisition and subsequent cell division. P6.p adopts the 1° cell fate and generates eight descendants, while P5.p and P7.p acquire the 2° cell fate and give rise to seven descendants each. P3.p, P4.p and P8.p fuse to the hypodermal syncytium *hyp7* as uninduced 3° VPCs after one round of cell division.

1.2.1 WNT signalling establishes the vulval fate and cell polarity

The VPCs, P3.p - P8.p, are specified via *lin-39*, a Hox gene preventing the fusion of the VPCs to *hyp7* and conferring vulval cell fate competence (Clark et al. 1993) (**Fig. 1.2A**). WNT signalling is necessary to maintain *lin-39* expression in P3.p - P8.p (Eisenmann et al. 1998). Compromising mutations in ß-catenin (*bar-1*) or Wntless (*mig-14*) cause too few cells to adopt a vulval cell fate and an underinduced phenotype (Eisenmann and Kim 2000; Bänziger et al. 2006). As opposed to vertebrates or *Drosophila*, the function of ß-catenin in cell adhesion, non-canonical signalling and canonical signalling is separated onto the three *C. elegans* ß-catenin genes, *hmp-2* (Natarajan et al. 2001), *wrm-1* (Korswagen et al. 2000) and *bar-1* (Eisenmann et al. 1998). A fourth ß-catenin, SYS-1, regulates asymmetric cell divisions in the early embryo in a variant of canonical signalling (Miskowski et al. 2001). Presumably, several rather than one single WNT ligand and receptor mediate WNT signalling in the vulva (Gleason et al. 2006). The *C. elegans* genome encodes five WNT ligands (*lin-44, egl-20, mom-2, cwn-1* and *cwn-2*) (Shackleford et al. 1993; Herman et al. 1995; Rocheleau et al. 1997; Thorpe et al. 1997; Maloof et al. 1999), four Frizzled related WNT receptors (*lin-17, mom-5, mig-1* and *cfz-2*) (Sawa et al. 1996; Rocheleau et al. 1997; Ruvkun and Hobert 1998) and one Ryk/Derailed related WNT receptor (*lin-18*) (Inoue et al. 2004) and defects in VPC specification can be observed only if several ligand and/or receptor genes are mutated (Gleason et al. 2006). The *C. elegans* WNT, Axin, APC, CK1, GSK-3ß and TCF homologues *mig-14* (Thorpe et al. 1997), *pry-1* (Korswagen 2002), *apr-1* (Rocheleau et al. 1997), *kin-19* (Peters et al. 1999), *gsk-3* (Schlesinger et al. 1999) and *pop-1* (Rocheleau et al. 1997) contribute to vulval development, indicating that a canonical WNT pathway is active in the VPCs (Gleason et al. 2002). In animals mutant for *pry-1, apr-1, kin-19* or *gsk-3* P3.p, P4.p and P8.p can adopt a vulval cell fate (Gleason et al. 2002). Conversely, loss of POP-1 can suppress this overinduced phenotype.
In addition to the role in vulval fate specification, WNT signalling is involved in patterning the fates of the P6.p descendants VulE and VulF into vulE-vulF-vulF-vulE (anterior to posterior) (Wang and Sternberg 2000) and establishing a mirrored polarity of P7.p in respect to P5.p (Kornfeld 1997; Inoue et al. 2004). Mutant animals exhibiting the default polarity of P7.p often display a reversal of the vulval lineage, which results in an additional invagination posterior to the main vulva (also known as “Bivulva”) (Green et al. 2008).

1.2.2 EGFR/RAS/MAPK and DELTA/NOTCH activity confer 1° and 2° cell fates

During the L2 stage, the gonadal anchor cell (AC) residing above the VPCs and closest to P6.p secretes the inductive LIN-3/EGF signal in a graded manner (Kornfeld 1997) (**Fig. 1.2B**). LET-23/EGFR is present on the basolateral membrane of the VPCs, receives LIN-3/EGF and activates a downstream RAS/MAPK cascade that involves LET-60/RAS (Han and Sternberg 1990), LIN-45/BRAF (Han et al. 1993), MEK-2/MEK (Church et al. 1995) and MPK-1/ERK (Lackner et al. 1994; Sundaram et al. 1996; Tan and Kim 1999; Moghal and Sternberg 2003). The cascade is strongest in P6.p and confers the 1° cell fate (Yoo et al. 2004). LIN-1, an ETS family transcription factor, is a target of the RAS/MAPK cascade and inhibitor of vulval induction (Beitel et al. 1995). LIN-1 forms a complex with LIN-31 which is disrupted by phosphorylation of MPK-1/ERK and the loss of LIN-1 results in a highly penetrant and strong Multivulva (Muv) phenotype (Tan et al. 1998). Another target of the cascade is *egl-17/FGF* which guides the migration of sex myoblast precursors during the formation of the vulval and uterine muscles via another RAS/MAPK cascade downstream of EGL-15/FGFR (Sundaram et al. 1996; Burdine et al. 1998). Positive factors of the cascade include SUR-2, EOR-1, LIN-25 and EOR-2 (Tuck and Greenwald 1995; Singh and Han 1995; Howard 2002).

RAS/MAPK signalling in P6.p leads to the expression of the NOTCH transmembrane ligands *apx-1* and *lag-2* and the secreted ligand *dsl-1* and the activation of LIN-12/NOTCH in P5.p and P7.p to confer the 2° and inhibit the 1° cell fate (Greenwald et al. 1983; Chen and Greenwald 2004). The low dose of both LIN-3/EGF and LIN-12/NOTCH signal that is received by P3.p, P4.p and P8.p results in these cells adopting the uninduced 3° cell fate and fusing to *hyp7* after one cell division (Sternberg and Horvitz 1986). Extensive coupling and crosstalk between LET-23/EGFR and LIN-12/NOTCH signalling ensures such an invariable 3°-3°-2°-1°-2°-3° cell fate patterning (Berset et al. 2001; Yoo et al. 2004). LET-23/EGFR activation leads not only to the adoption of the 1° cell fate but also to the endocytosis and downregulation of LIN-12/NOTCH in the same cell, P6.p (Shaye and Greenwald 2002), and to the upregulation of lateral inhibitory signals to prevent the neighbouring P5.p and P7.p from adopting the 1° cell fate (Sternberg 1988). Vice versa, the MAPK phosphatase *lip-1, dpy-23* and the *lst-1, -2, -3* and *-4* genes are targets of LIN-12/NOTCH and inhibit RAS/MAPK signalling in P5.p and P7.p (Berset et al. 2001; Yoo et al. 2004).

1.2.3 Morphogenetic events complete the vulva

During the L3 and L4 stages, 1° and 2° cells divide three times to give rise to the 22 vulval cells (Kornfeld 1997). The 1° cell lineage generates vulE and vulF cells in a mirror symmetrical fashion (E-F-F-E) around the AC (Sharma-Kishore et al. 1999), which is dependent on WNT and RAS/MAPK signalling (Inoue et al. 2004) (see 1.2.1, 1.2.2). The 2° fate cells produce a symmetrical patterning of vulA, vulB1, vulB2, vulC and vulD (ABCD and DCBA) due to a WNT

signal from the AC. The vulval muscles vm1 innervate between vulE and vulF cells, whereas the vm2 muscles insert between the vulC and vulD cells to provide the musculature for egg-laying (Burdine et al. 1998; Sharma-Kishore et al. 1999). The vulF cells express LIN-3/EGF to activate RAS/MAPK in the future uv1 cell and establish the vulval-uterine connection (Chang et al. 1999) (see also 1.4.4). The vulval cells move towards the AC, which breaks down the basement membrane between the gonad and the developing vulva to invade between the two vulF cells (Sherwood and Sternberg 2003). The seven types of vulval cells fuse pair-wise to build toroids (Sharma-Kishore et al. 1999). The formation of the hermaphrodite vulva is completed during the L4-to-adult moult by eversion.

1.2.4 Vulval induction index as a readout for signalling strength

During wt vulval development, P3.p to P8.p divide once during the L3 stage and prior to induction by LIN-3/EGF, with P3.p dividing only in 50% of the cases (Sulston and White 1980; Kornfeld 1997) (**Fig. 1.3A**). In response to LIN-3/EGF, P5.p, P6.p and P7.p divide three more times to give rise to eight (P6.p) or seven daughter cells (P5.p and P7.p) (Kornfeld 1997), hence three VPCs became induced which determines a vulval induction index (VI) of three (**Fig. 1.3**). In cases of enhanced signalling activity, e.g. as a result of *let-60/RAS* gain-of-function or *pry-1/Axin* loss-of-function mutations, P3.p, P4.p or P8.p can be induced and cause excessive invaginations (**Fig. 1.3B**, middle). This Muv phenotype is caused by ectopically dividing VPCs and can increase the VI to a maximum of six, if all VPCs are fully induced. If only one Pn.px of a VPC divides, it is counted as half induction (0.5). Conversely, the reduced signalling strength in *bar-1/ß-catenin* or *let-23/EGFR* mutant animals leads to too few induced cells and a Vulvaless (Vul) phenotype with a VI below three and minimally 0 (**Fig. 1.3B**, bottom). To determine the VI, the cells within the invaginations and the undivided Pn.p cells are counted while scanning the worm from the tail, since P3.p can sometimes fuse with the hypodermis prior to the Pn.px stage (Sulston and Horvitz 1977).

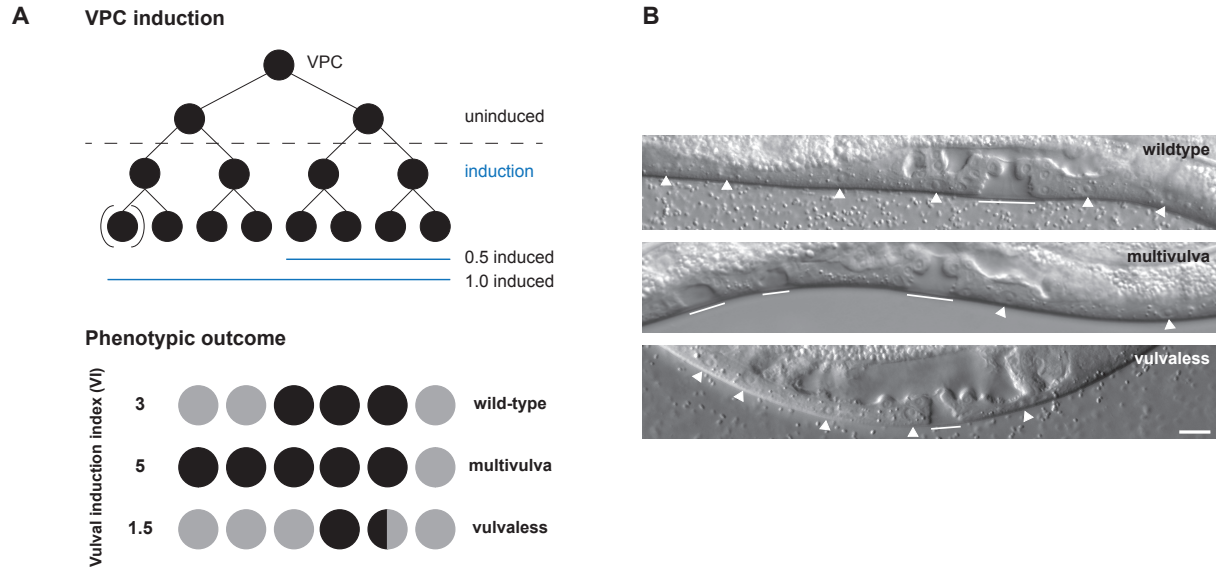

Figure 1.3. Vulval induction index. **(A**, top**)** Each VPC divides once prior to induction by LIN-3/EGF to produce two daughter cells. Upon induction, each daughter cell can be induced independently. Induction of one daughter cell results in only this cell dividing whereas its sister does not undergo division and a VI of 0.5 is determined for a given VPC. A full induction is counted if both daughter cells of a VPC have divided. **(A**, bottom**)** Example VIs of wild-type (= 3), Multivulva (> 3) and Vulvaless (< 3) phenotypes. The VI ranges between one to six induced VPCs. Nomarski images in **(B)** show the situation depicted schematically in **(A**, bottom**)**. The bars indicate invaginations formed by induced VPCs and the triangles indicate uninduced, undivided VPCs. The scale bar indicates 10 µm.

1.2.5 Robustness of the system

In wild-type animals, the 3°-3°-2°-1°-2°-3° vulval fate patterning is invariant (Félix and Barkoulas 2012). This robustness is achieved by redundancy and extensive crosstalk between the EGFR/RAS/MAPK, Notch and WNT pathways and ensures that naturally occurring stochastic fluctuations are buffered and do not result in visible phenotypes (Gleason et al. 2002; Yoo et al. 2004; Gleason et al. 2006). The intrinsic variability and contributing factors have been and are being described in detail to understand how such a simple cellular system can deal with and interpret natural fluctuation to generate a solid functional unit (van Zon et al. 2015; Huelsz-Prince and van Zon 2017).
Due to this robustness, the identification of regulators is only possible in combination with sensitising mutations in core pathway members that challenge the balanced system to an extent sufficient to reveal minor changes in signalling phenotypically. The terms „regulator“, „modifier“ and „fine-tuning“ underscore the nature of such candidates: A defect in a regulating gene does not necessarily cause a phenotype but can enhance or suppress a sensitising mutation. One example is one of the worms GTPase activating proteins, GAP-1, which turns LET-60/RAS into its inactive form during vulval development (Hajnal et al. 1997). A mutation in *gap-1* does not cause a Muv by itself but can enhance overactivated and rescue compromised RAS/MAPK signalling. Robustness is further exemplified by the lack of phenotypes in single mutants for *sli-1* (c-Cbl) (Yoon et al. 1995), *sra-13* (Battu et al. 2003), *unc-101* and *apm-1* (medium chains of adaptin) (Lee et al. 1994; Jaegal Shim 2000) or for genes of one of two classes containing so called synMuv genes (Ferguson and Horvitz 1989). These genes cause a Muv when combined with further defective regulators or enhance the outcome of a sensitising mutation. Apart from genetic influences, the environment contributes strongly to variation. A Vul can be partially suppressed when worms had been starved, gone through dauer or cultivated in liquid medium instead of NGM plates (Horvitz and Ferguson 1985; Moghal et al. 2003). Our lab has further observed that vulval induction of mutants carrying overactivated RAS is reduced on crowded NGM plates and variable in terms of the type of food source provided (I. Nakdimon, doctoral thesis). Finally, Zn ions inhibit RAS/MAPK signalling strength in a sensitised setting (Bruinsma et al. 2002; Yoder et al. 2003) as does the serotonin metabolite 5-HIAA (Schmid et al. 2015). Thus, although biological systems are highly robust against changes, fluctuations can become visible under certain conditions and can even cause profoundly different outcomes – a fact that is frequently underestimated but just as important.

1.2.6 Inequality in the vulval competence group

The vulval competence group that comprises P3.p to P8.p is often referred to as “vulval equivalence group” as all the Pn.p cells are able to adopt 1°, 2° or 3° cell fates as shown by ablation experiments (Sternberg and Horvitz 1986). However, this notion is not entirely correct as the following findings suggest. The homeodomain transcription factor, *mab-5*, which is related to the Antennapedia, Ultrabithorax and abdominal-A family of homeodomain genes, is expressed in P7.p and P8.p where it reduces the sensitivity to inductive LIN-3/EGF signalling (Salser et al. 1993; Clandinin et al. 1997). Expression of another homeodomain protein LIN-39 in all the VPCs is promoted by WNT and RAS/MAPK signalling and confers a vulval fate and sensitivity to inductive signalling (Eisenmann et al. 1998; Maloof et al. 1999). Moreover, the zinc-finger protein SEM-4 is present in the VPCs with strongest expression in P7.p and acts in concert with LIN-39 to specify vulval cell fates (Grant et al. 2000). Finally, Gleason et al. (2006) found defects especially in the adoption of anterior vulval fates if they combined mutations in three WNT ligands *lin-44, cwn-1* and *egl-20*. Using fluorescent reporter genes, they and others found enhanced expression of these ligands in the posterior of the worm and proposed a graded action of WNT ligands on vulval cell fate specification (Whangbo and Kenyon 1999; Coudreuse 2006; Gleason et al. 2006; Zinovyeva et al. 2008). Although all six VPCs are able to respond to inductive signalling by LIN-3/EGF and lateral signalling via LIN-12/NOTCH (Greenwald et al. 1983; Ferguson et al. 1987), they do so with unequal sensitivity, which should be taken into consideration during studies on vulval cell fate determination.

1.3 WNT signalling

WNT signalling is fundamental during the patterning of early embryos, in establishing cell polarity, in the regulation of cell migration and proliferation, as well as during the maintenance of adult tissue (Logan and Nusse 2004; Clevers and Nusse 2012). WNT pathways are divided into canonical and non-canonical signalling (Sugimura and Li 2010; Clevers and Nusse 2012). The WNT ligands can act as long-range morphogens to impose spatial information as exemplified in the *Drosophila* wing disc (van den Heuvel et al. 1989). Alternatively, short-range signalling takes place e.g. between *engrailed* and *wingless* expressing cells to establish cell fate boundaries and segments in the early fruit fly embryo (Swarup and Verheyen 2012) or in the maintenance of a stem cell niche that gives rise to a range of differentiated cells like hair follicle cells (DasGupta and Fuchs 1999) or the various types of intestinal crypt cells (Satoh et al. 2000; Crosnier et al. 2006). The importance of WNT signalling during these processes foreshadows its significance in a number of diseases.

1.3.1 The WNT/ß-catenin pathway

During canonical WNT signalling, the signal transduced by WNT ligands arrives in the nucleus through the inhibition of an inhibitory destruction complex in the cytoplasm (Logan and Nusse 2004). Lipid modification of WNTs via palmitoylation is essential for their secretion and function as becomes obvious in fruit flies mutant for a gene that regulates WNT secretion, *porcupine*. These flies show phenotypes similar to the loss of WNTs themselves (*wingless* in *Drosophila*) (Kadowaki et al. 1996; Clevers and Nusse 2012). Given the necessity of lipid modification, the identification of small molecules inhibiting this process are promising drugs in diseases caused by deregulated WNT signalling (Lu et al. 2009). In the absence of a WNT signal, ß-catenin resides in a cytoplasmic complex consisting of the scaffold protein Axin, Dishevelled (Dvl), glycogen synthase kinase-3ß (GSK-3ß), casein kinase 1 (CK1) and Adenomatous Polyposis Coli (APC) (Hart et al. 1998; Amit 2002; Weis and Stamos 2013). ß-catenin is phosphorylated by GSK-3ß and CK1 and the recruitment of the E3 ubiquitin ligase ß-TrCP causes its proteasomal degradation (Aberle et al. 1997; Xiao et al. 2014) (**Fig. 1.4**, left). Upon WNT ligand binding to a seven-transmembrane (7TM) Frizzled receptor and in presence of a single-pass TM Frizzled co-receptor LRP5/6 (low density lipoprotein (LDL) receptor-related protein), Axin leaves the destruction complex which loses activity and ß-catenin is stabilised (Cliffe et al. 2003) (**Fig. 1.4**, right). Liberated ß-catenin translocates to the nucleus to displace the transcriptional repressor Groucho from TCF/LEF DNA-binding proteins and itself interact with TCF/LEF as well as co-activators and histone modification proteins to promote target gene expression (van de Wetering et al. 1997; Miller and Moon 1997). WNT targets include not only components of the pathway itself to supply a negative feedback (Cadigan et al. 1998; Sato et al. 1999), but also genes whose products are involved in proliferation, such as *MYC* or *CCND1* (He 1998; Tetsu and McCormick 1999).

Non-canonical WNT signalling does not employ ß-catenin and TCF/LEF to exert its function (Veeman et al. 2003). Also, co-receptor function is not fulfilled by LRP5/6 but by members of the ROR and RYK family of tyrosine kinase receptors (Sugimura and Li 2010; van Amerongen 2012). Non-canonical signalling through WNT ligands organises cell polarity, cell migrations and more generally cytoskeletal rearrangements in the planar cell polarity pathway that recruits the small GTPases RHO and RAC (Axelrod 2009; Gómez-Orte et al. 2013) (**Fig. 1.5**, left). Other downstream effects include phospholipase C regulated calcium signalling and actin remodelling via CDC42 or negative regulation of the canonical WNT pathway involving ß-catenin (Sugimura and Li 2010) (**Fig. 1.5**, right).

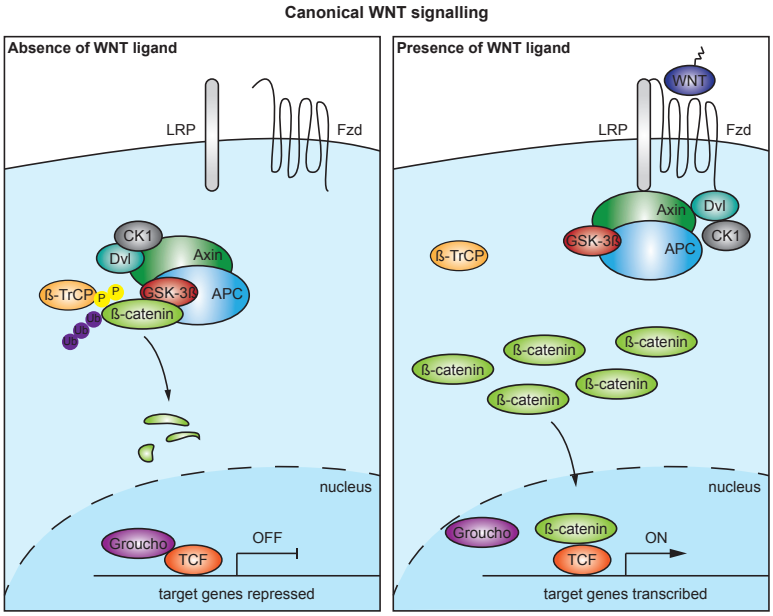

Figure 1.4. Canonical WNT signalling pathway. (Left) Without ligand binding, ß-catenin resides in a cytoplasmic complex with Axin, Dishevelled (Dvl), glycogen synthase kinase-3ß (GSK-3ß), casein kinase 1 (CK1) and Adenomatous Polyposis Coli (APC). ß-catenin is phosphorylated and the recruitment of the E3 ubiquitin ligase ß-TrCP causes proteasomal degradation. (Right) Upon WNT ligand binding to the 7TM receptor Frizzled (Fzd) and in presence of its co-receptor LRP5/6, the destruction complex is disassembled and ß-catenin can enter the nucleus. Transcriptional repressors like Groucho are displaced and ß-catenin enhances expression of target genes through the interaction with TCF/LEF and co-activators.

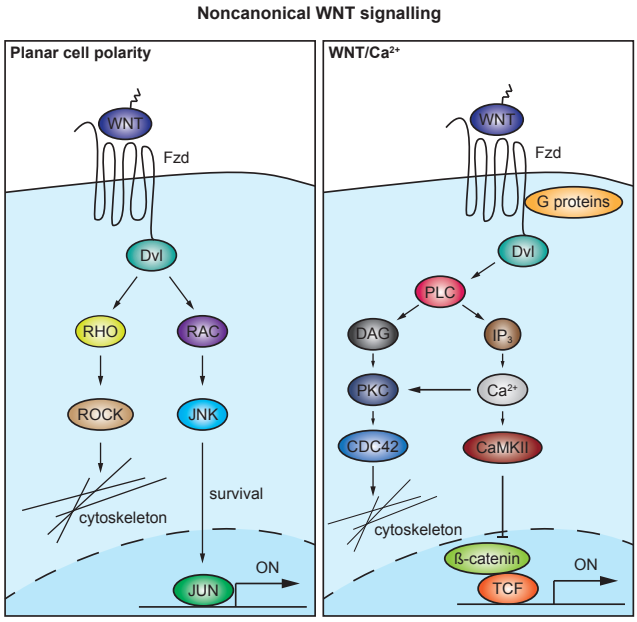

Figure 1.5. Noncanonical WNT signalling pathway. (Left) The planar cell polarity pathway recruits the small GTPases RHO and RAC to impinge on the cytoskeleton or cell survival. (Right) In the WNT/Calcium signalling pathway, WNT binding triggers the recruitment of PLC to produce the second messengers IP3 and DAG and induce calcium dependent cell signalling responses or cytoskeletal rearrangements.

1.3.2 WNT signalling during disease

Mutations affecting the stabilisation of ß-catenin, i.e. phosphorylation of ß-catenin itself or the function of the destruction complex, contribute to cancer development as a consequence of constitutive pathway activation (Yost et al. 1996; Giles et al. 2003). A famous example is familial adenomatous polyposis (FAP), in which a defective copy of APC was inherited and the second allele is lost thereafter in a subset of cells (Kinzler et al. 1991; Nishisho et al. 1991). In combination with the loss of further tumour suppressor genes or activating mutations in proto-oncogenes, initially benign polyps can become malignant (Kinzler and Vogelstein 1996; Ivanov et al. 2006). Strikingly, approx. 80% of colorectal cancers originate from the complete loss of APC, which highlights the importance of the pathway in cell proliferative events (Wood et al. 2007; Nishisho et al. 1991). Furthermore, a loss of Axin was found in hepatocellular carcinoma (Rubinfeld et al. 1997). Mutations preventing the phosphorylation and hence degradation of ß-catenin have been associated with colon cancer and melanoma (Rubinfeld et al. 1997; Reya and Clevers 2005) and TCF/LEF was found to be lost in sebaceous skin tumour (Takeda et al. 2006). It is worth mentioning that defective WNT signalling is further involved in bone density defects (Gong et al. 2001; Boyden et al. 2002), type II diabetes (Kanazawa et al. 2004; Christodoulides et al. 2006) and other diseases.

1.3.3 Other roles of ß-catenin

ß-catenin does not only act to mediate transcriptional responses but also plays a role in microtubule organisation at the centrosome (Huang et al. 2007). Furthermore, it is found in cell adhesion complexes together with E-cadherin and α-catenin (reviewed in detail in (Nelson and Nusse 2004; Valenta et al. 2012)). This is of special interest, since the stable pool of ß-catenin in cell junctions is unavailable for signalling and coordinated with the cytoplasmic unstable pool (Gumbiner 2000; Logan and Nusse 2004). The different functions of ß-catenin are highlighted in *C. elegans*. While *Drosophila* and vertebrates possess one ß-catenin to carry out all functions, *C. elegans* has split the roles of ß-catenin onto four proteins (Korswagen et al. 2000). ß-catenin-armadillo-related (BAR-1) is the main signalling member of the canonical WNT pathway (Maloof et al. 1999) and participates in vulval cell fate specification (see 1.2.1), Q neuroblast migration or the specification of the P12 fate through interaction with POP-1, the worm TCF. Another ß-catenin, *humpback* (*hmp-2*), interacts with HMR-1 (cadherin) and HMP-1 (α-catenin) at cell junctions (Korswagen et al. 2000). WRM-1 (Worm armadillo 1) and SYS-1 (symmetrical sister cell hermaphrodite gonad defect 1) act in a worm-specific variation of the canonical pathway to regulate asymmetric cell divisions (Takeshita 2005; Gómez-Orte et al. 2013). Here, the members of the destruction complex, APR-1 (APC), PRY-1 (Axin) and GSK-3 (GSK-3ß) act as activators rather than repressors (Park et al. 2004). A polarized WNT signal induces the complex and hence WRM-1, which displaces POP-1 from the nucleus into the cytoplasm upon which SYS-1 can turn

on transcription (Bowerman et al. 1999; Lo et al. 2004). Thus, the outcome of this type of pathway is the same as in all canonical WNT pathways, i.e. transcription is turned on upon WNT ligand binding. As in *Drosophila* and vertebrates, an association with of SYS-1 with the centrosome has been observed (Vora and Phillips 2015).

1.4 RAS signalling

Signalling through RAS (rat sarcoma) regulates multiple developmental events such as proliferation, cell differentiation, cytoskeletal rearrangements, apoptosis or survival and is highly conserved (Satoh et al. 1992; Downward 2003). The small GTP-binding protein RAS acts as a molecular switch to direct downstream pathways through effector proteins like RAF, PI3K, PLCE or RALGEF (Rodriguez-Viciana et al. 2004; Repasky et al. 2004) (**Fig. 1.6**).

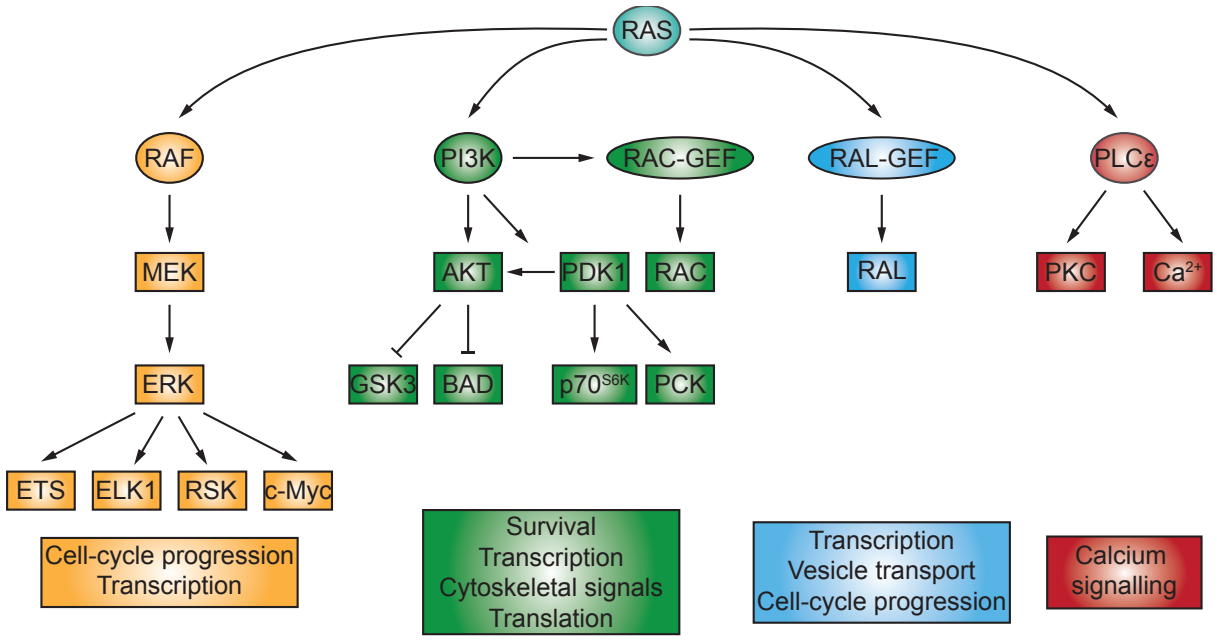

Figure 1.6. Effector pathways downstream of RAS. The small GTP-binding protein RAS activates several effectors to control various cellular events. Activation of the RAF protein kinase initiates the mitogen-activated protein (MAP) kinase cascade that phosphorylates ERK. ERK targets are present both in the cytosol and the nucleus and comprise transcription factors like ETS family members, ELK1 or c-Myc as well as the 90 kDa ribosomal protein S6 kinases (RSKs) to impact on transcription. Activation of phosphoinositide 3-kinases (PI3Ks) results in the second messenger PIP3 that promotes survival signalling through AKT or in active RAC GTPases that influence cytoskeletal architecture. RAL guanine exchange factors promote RAS-related RAL proteins and the stimulation of PLCE leads to an accumulation of diacyglycerol DAG and IP3 and signalling by PKC and calcium. Figure adapted from Downward (2003).

1.4.1 The GTPase-binding protein RAS

Initially, RAS was discovered in retroviruses that showed a strong carcinogenic potential (Harvey 1964; Kirsten and Mayer 1967; Peters et al. 1974; Rasheed et al. 1978; Cox and Der 2014 for review). Subsequently, mutations that prevent GTP hydrolysis (positions G12, G13 and Q61) were found in 20-30% of all human cancers (Forbes et al. 2010; Prior et al. 2012). Within the three isoforms encoded by the *RAS* locus, mutations in *KRAS* are predominant (86%) whereas *NRAS* and *HRAS* are less frequently mutated in cancers (11% and 3% respectively) (Fernandez-Medarde and Santos 2011; Beukers et al. 2014).
As a master regulatory switch, the RAS protein is subject to extensive regulation. Activation is achieved through the exchange of GDP for GTP, which is mediated by guanine nucleotide exchange factors (GEFs) containing a CDC25 homology catalytic domain, e.g. the *son of sevenless* gene product SOS (Vigil et al. 2010; Cherfils and Zeghouf 2013). Conversely, GTPase-activating proteins (GAPs) enhance the low intrinsic GTPase activity of RAS to mediate inactivation. Furthermore, signalling activity strongly depends on RAS subcellular localisation (Prior and Hancock 2012). Substantial post-translational modifications involving stable farnesylation, proteolysis, methylation as well as reversible palmitoylation allow the localisation at the plasma membrane, where most of the signalling originates from. Depalmitoylated RAS accumulates in the cytosol and arrives at the Golgi apparatus, where re-palmitoylation takes place to shuttle RAS back to the plasma membrane (Rocks et al. 2010). While NRAS and HRAS participate in this palmitoylation cycle, the KRAS isoform cannot undergo palmitoylation (Ahearn et al. 2011). Instead, basic residues within the hypervariable region of KRAS promote its solubilisation by binding of the prenyl-binding protein PDEδ and facilitated trafficking to the plasma membrane (Chandra et al. 2011). These basic residues in KRAS have further been shown to be essential for calmodulin binding and removal from the plasma membrane (Villalonga et al. 2001) as well as for phosphorylation by PKC and induction of apoptosis at mitochondria (Bivona et al. 2006). Thus, numerous studies aim at developing small molecules to interfere with one of the many steps of RAS modification (Downward 2003; Roberts and Der 2007; Spiegel et al. 2014).

1.4.2 The EGFR/RAS/MAPK signalling pathway

Extracellular signals such as growth factors, cytokines and hormones bind to and activate cell surface proteins such as receptor tyrosine kinases or G-protein coupled 7TM receptors (Satoh et al. 1992), the modules upstream of RAS. One of the signal transduction pathways that has been studied in great detail is initiated by epidermal growth factor (EGF) and its receptor (EGFR) and involves the downstream kinases RAF, MAP kinase-ERK kinase (MEK1/2) and extracellular-signal regulated kinase (ERK1/2, MAPK) (Scaltriti and Baselga 2006) (**Fig. 1.7**). Ligand binding causes EGFR dimerisation, auto-phosphorylation within the cytoplasmic domain and binding of the SHC adaptor protein (Ravichandran 2001), which interacts with GRB2 (Ravichandran

et al. 1995). The stable association of GRB2 with SOS and the localisation of RAS at the plasma membrane facilitate the exchange of GDP for GTP and thus the activation of RAS and a downstream mitogen-activated kinase (MAPK) cascade (Schlessinger 1993). In this cascade, RAS binds the RAF serine/threonine kinase at the membrane, which in turn relays the signal to MEK1 and MEK2 via phosphorylation (Crews et al. 1992). MEKs are dual specificity kinases of ERK1 and ERK2, i.e. they phosphorylate both threonine and tyrosine residues (Crews et al. 1992). Phosphorylated ERK translocates to the nucleus and phosphorylates transcription factors including ELK1, ETS, HIF1A (see also 1.6.3) or MYC upon which gene expression is enhanced, e.g. of proteins required for cell cycle progression (cyclin D1, c-Fos) (Marais et al. 1993; Price et al. 1996; Sears 2000; Berra et al. 2000; Murphy et al. 2002). Further transcription factor targets are the nuclear receptors estrogen receptor (ER) (Kato et al. 1995) or peroxisome proliferator-activated receptor gamma (PPARG) (Farmer 2005). Phosphorylation of ELK1, MYC, HIF1A and ER is activating whereas phosphorylation renders ETS and PPARG inactive.

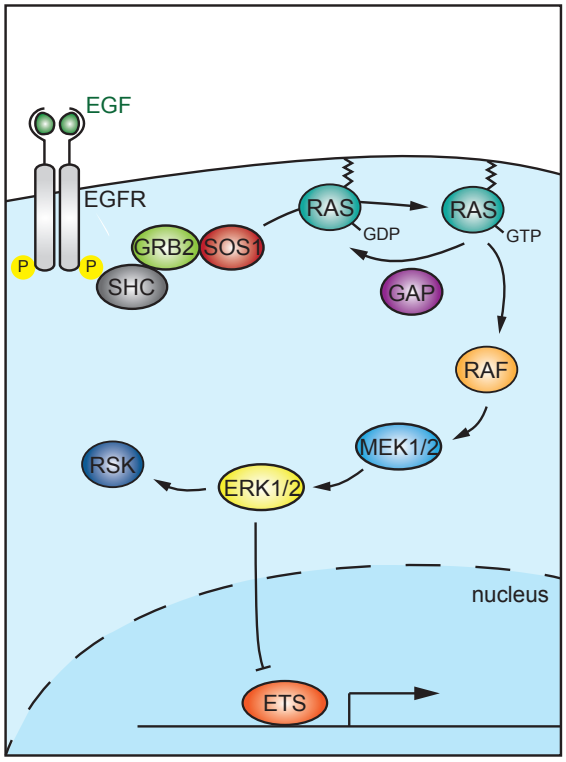

Figure 1.7. EGFR/RAS/MAPK signalling pathway. The binding of epidermal growth factor (EGF) leads to EGF receptor dimerisation and auto-phosphorylation, upon which the adaptor protein SHC binds. SHC recruits GRB2 which is associated with the RAS-GEF SOS1. The localisation of RAS at the membrane facilitates the exchange of GDP for GTP by SOS1 and RAS activation, which is counteracted by GAP. Active RAS promotes the RAF kinase, which phosphorylates the MEK1/2 dual specificity kinases. MEK1/2 in turn activate ERK1/2, which phosphorylates targets both in the nucleus and the cytoplasm to elicit various cellular responses.

1.4.3 Non-nuclear ERK functions

Activated ERK1/2 is sorted into and to a number of cellular compartments to exert several functions. Some examples are described below and the interested reader is referred to extensive reviews (e.g. Kolch 2005; Wortzel and Seger 2011).
Within the cytosol, ERK phosphorylates components of its upstream cascade to establish a negative feedback loop (Brummer et al. 2003), the MAPK-interacting Kinases (MNKs) which enhance the activity of EIF4E and hence general translation efficiency (Waskiewicz 1997) or the 90 kDa ribosomal protein S6 kinases (RSKs) that regulate transcription (Chen et al. 1992). ERK1/2 prevents apoptosis by phosphorylating BCL2 at mitochondria (Deng et al. 2000) and has been detected to accumulate in mitochondria (Galli et al. 2009). The co-localisation of ERK1/2 with endosomes is mainly thought to enhance signalling by bringing the components of the cascade into close proximity with the activated and internalising RTKs (Schaeffer 1998; Luttrell et al. 2001). Interactions with microtubules and actin filaments not only ensures the proper transport and localisation of ERK1/2 throughout the cell (Reszka et al. 1995) but also regulates cell motility through direct phosphorylation of myosin light chain kinase (MLCK) (Klemke et al. 1997). Finally, an ERK1 splice variant is involved in the fragmentation of the Golgi apparatus at the onset of mitosis, which occurs to distribute the Golgi building blocks to the emerging daughter cells (Shaul and Seger 2006; Persico et al. 2010).

1.4.4 RAS/MAPK signalling in *C. elegans* tissues other than the vulva

The single *C. elegans* orthologue of mammalian N-, H- and KRAS, LET-60 (Han and Sternberg 1990), controls a MAPK cascade downstream of LET-23/EGFR in the vulval tissue (Aroian and Sternberg 1991; Kornfeld 1997) (see 1.2.2), during induction of the excretory duct cell fate, during P12 development and in the specification of the uterine uv1 fate (Chang et al. 1999). A MAPK cascade acts downstream of the worm FGF receptor, EGL-15, to regulate sex myoblast migration (in response to EGL-17/FGF) (DeVore et al. 1995; Burdine et al. 1998) and axon guidance (in response to FGF-like LET-756) (Bülow et al. 2004). Downstream of the insulin-like receptor DAF-2, RAS/MAPK promotes the exit from pachytene during meiosis in the germline (Church and Lambie 2003; Lopez et al. 2013) and it is required for chemotaxis (Iino et al. 2000; Battu et al. 2003). In differentiated muscle, RAS/MAPK activates protein degradation (Szewcyk et al. 2002). The loss of LET-60/RAS can thus cause the lack of a duct cell (Abdus-Saboor et al. 2011), a P12 to P11 cell fate transformation (Jiang and Sternberg 1998), defects in the vulval-uterine connection (Chang et al. 1999), defects in sex myoblast migration and vulval muscle function (Burdine et al. 1998), axon guidance defects (Bülow et al. 2004), sterility due to arresting germ cells in the pachytene (Church and Lambie 2003) or altered chemotaxis (Iino et al. 2000). Null mutants of *let-60* die as zygotes, probably due to loss of the duct cell and associated osmoregulation (Nelson and Riddle 1984; Sundaram et al. 1997).

1.5 NOTCH signalling

1.5.1 Core components of NOTCH signalling

Both the ligands and receptor proteins of the NOTCH pathway exclusively encode TM proteins (Kimble and Simpson 1997). As a consequence, LIN-12/NOTCH acts in cell fate decision events via cell-cell interactions and close physical cell contacts (Greenwald 1994; Kimble and Simpson 1997). The core components of the NOTCH signalling pathway are the DSL ligands (originating from the first ligands identified, Delta, Serrate and LAG-2), LNG receptors (LIN-12, NOTCH and GLP-1) and the CSL proteins (CBF-1, Su(H) and LAG-1) (**Fig. 1.8A**). The DSL ligands are present on signalling cells and contain a TM domain, epidermal growth factor (EGF)-like repeats (Lieber et al. 1992; Gao et al. 1997; Bray 2006), as well as a DSL domain and a N-terminal motif that have signalling activity (Lieber et al. 1992; Gao et al. 1997). Both CSL proteins and LNG receptors are present in receiving cells (Bray 2006) and the latter consist of extracellular EGF-like repeats involved in ligand binding (Fehon et al. 1990; Rebay et al. 1991; Lieber et al. 1992), LNR repeats (for LIN-12/Notch Repeat repeats) with negative signalling activity (Lieber et al. 1993; Bray 2006), a TM region as well as intracellularly a RAM domain and cdc10/ankyrin repeats (ANK repeats) that interact with CSL proteins (Greenwald and Seydoux 1990; Roehl and Kimble 1993; Lieber et al. 1993), a transcriptional activation domain (TAD) (Hori et al. 2013) and a C-terminal PEST domain through which the receptor can be degraded (Öberg et al. 2001; Hori et al. 2013) (**Fig. 1.8A**).

The NOTCH signalling pathway is highly conserved in all animals (Artavanis-Tsakonas 1999; D'Souza et al. 2008). In *Drosophila melanogaster*, Delta and Serrate are the DSL ligands that activate the only Notch receptor (Bray 2006). Five mammalian ligands have been described, three Delta-like ligands DLL1, DLL3 and DLL4 and two Serrate homologues Jagged 1 and 2 that activate one of four Notch receptors (NOTCH1-4) (D'Souza et al. 2008). In *C. elegans, lin-12* and *glp-1* encode the two Notch receptors while *apx-1, lag-2, arg-1* and *dsl-1* are the DSL ligands (Lambie and Kimble 1991; Mello et al. 1994; Mickey et al. 1996; Artavanis-Tsakonas 1999; Chen and Greenwald 2004). The CSL proteins are Su(H) in *Drosophila*, CBF1 in mammals and LAG-1 in the worm (Bray 2006). Although the ligands and receptors act in different tissues, they are interchangeable to some extent: In *C. elegans*, APX-1 has been shown to rescue the loss of LAG-2 (Fitzgerald and Greenwald 1995) as does GLP-1 in *lin-12(lf)* mutants (Fitzgerald et al. 1993). Similarly, the overexpression of Serrate can substitute for Delta during early *Drosophila* development (Gu et al. 1995). Thus, organisms appear to have several NOTCH receptors and DSL ligands that are at least partially interchangeable. The presence of several different components of one NOTCH pathway has been proposed to help achieve a temporally and spatially distinctive pattern of expression to carry out the numerous differing tasks during development (Weinmaster et al. 1992; Swiatek et al. 1994).

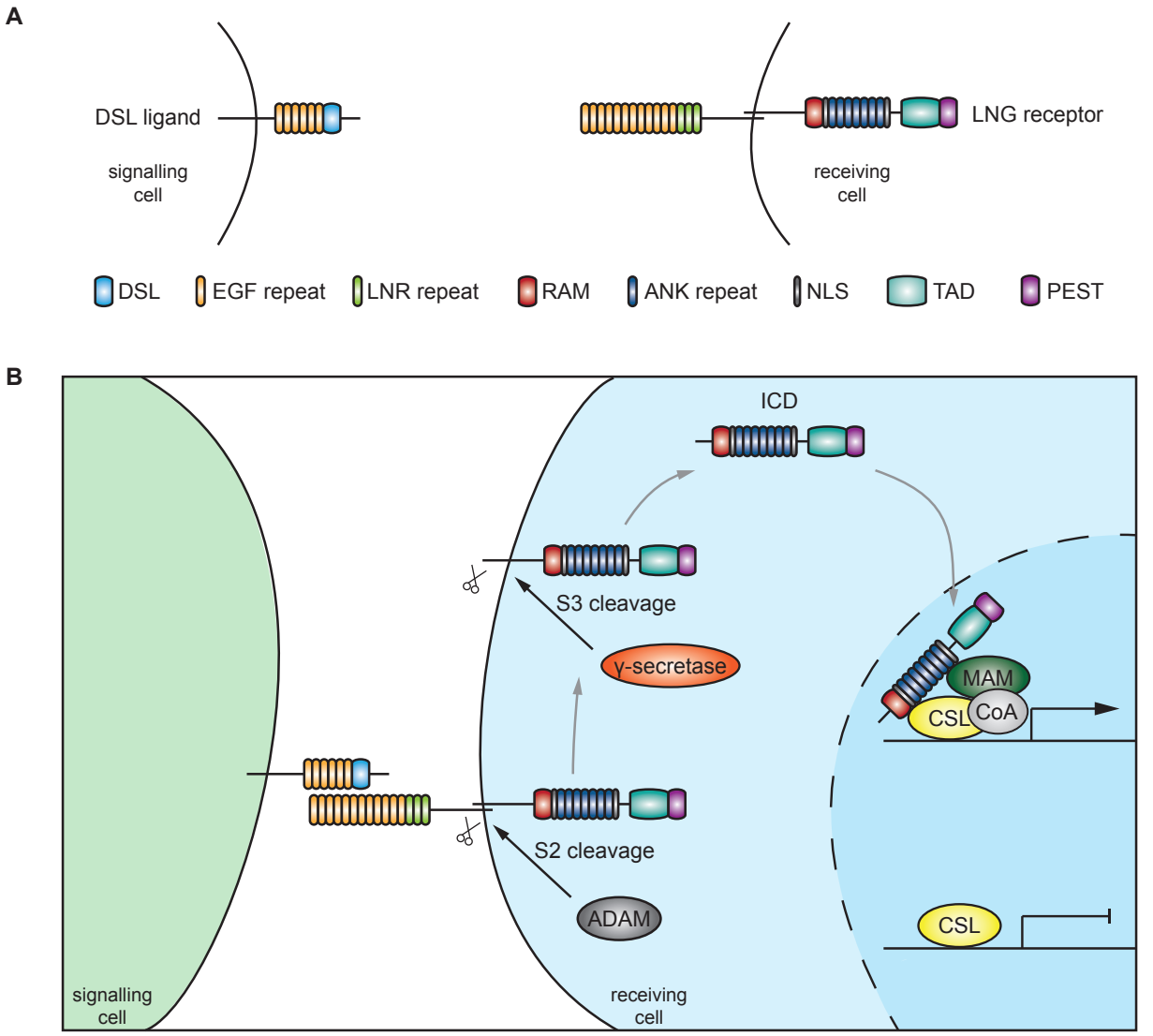

Figure 1.8. NOTCH signalling pathway. **(A)** DSL ligands are present on the signalling cell and consist of EGF repeats and a DSL domain. LNG receptors are present on receiving cells and comprise extracellular EGF and LNR repeats. The intracellular fraction contains a RAM domain, ANK repeats, a TAD and a PEST domain next to nuclear localisation signals. **(B)** Binding of a DSL ligand to a LNG receptor leads to the cleavage of the extracellular receptor domain by a metalloproteinase ADAM. The extracellular part is endocytosed with the DSL ligand by the signalling cell. A second cleavage event carried out by a γ-secretase complex releases the NOTCH intracellular domain (NICD), which enters the nucleus and activates gene expression in cooperation with Mastermind and co-activators.

1.5.2 The signalling pathway

In the absence of DSL ligands, the CSL proteins form transcriptional repressor complexes on NOTCH target gene sequences (Bray 2006) (**Fig. 1.8B**). Upon ligand binding, the extracellular domain of Notch receptors is cleaved (S2 cleavage) by a metalloproteinase ADAM (Hori et al. 2013) and endocytosed with the DSL ligand on the signal sending cell (Bray 2006). The LNR re-

peats prevent the S2 cleavage event in the absence of DSL ligand and thereby restrict signalling (Bray 2006; Kopan and Ilagan 2013). A second cleavage event (S3) involving Presenilin within a γ-secretase complex releases the NOTCH intracellular domain (ICD) (Struhl et al. 1993; Brou et al. 2000). The NICD enters the nucleus and forms a transcriptional complex via the RAM and ANK domains with CSL protein, Mastermind and co-activators to activate gene expression (Bray 2006; Choi et al. 2012). Thus, NOTCH signalling activity converts the function of CSL proteins from repression to activation. NICD is subject to both stabilisation through phosphorylation by kinases like GSK-3ß (Espinosa et al. 2003) (see also WNT signalling) as well as to degradation via SEL10 (Hubbard et al. 1997), an E3 ubiquitin ligase that interacts with the NOTCH intracellular PEST domain (Öberg et al. 2001) and has been implicated in regulating *C. elegans* LIN-45/BRAF in a negative feedback loop (de la Cova and Greenwald 2012). These regulatory interactions imply a tight link of the Notch pathway to other developmentally fundamental signalling pathways.

1.5.3 NOTCH signalling during development

Notch signalling is employed in various developmental cell fate decision events (Artavanis-Tsakonas et al. 1995; Bray 2006; Hori et al. 2013). During „lateral inhibition“, Notch specifies one of two cell fates within a group of developmentally equivalent cells (Hori et al. 2013). Initially, cells express the same amount of Notch receptor and ligand and the balance is tipped to either by an inductive signal or stochastic fluctuation. Signal amplification through positive feedback loops fortifies the imbalance in that the signal sending cell (expressing the ligand) activates NOTCH in the receiving cell that enhances receptor expression and vice versa (Bray 2006). This results in the ligand expressing cell adopting one cell fate and the receptor expressing cell adopting another. Prominent examples for lateral inhibition are the AC vs. ventral-uterine (VU) decision during *C. elegans* gonad development (Wilkinson et al. 1994) (see below), VPC fate acquisition (see 1.2.2) or the decision of a neuronal vs. ectodermal cell fate in *Drosophila*, where NOTCH represses neurogenesis (Campos-Ortega 1994). Another mechanism to confer different fates among cells is achieved through the asymmetric inheritance of NOTCH regulators. In *Drosophila*, the NOTCH inhibitor Numb is asymmetrically distributed to daughter cells of the sensory organ precursor (SOP) (Frise et al. 1996; Artavanis-Tsakonas 1999). In two consecutive cell divisions and asymmetric Numb segregation, the SOP will give rise to two cells with active NOTCH signalling, a socket and a sheath cell, as well as two cells with suppressed NOTCH activity due to presence of Numb, a hair cell and a neuron. Finally, NOTCH can act to induce non-equivalent cells. NOTCH mediated induction is presented by the DTC in the *C. elegans* germline that expresses the DSL ligand LAG-2 (Crittenden et al. 2003). LAG-2 binds GLP-1 and induces germline mitosis (see also 1.5.4). Induction by NOTCH signalling further establishes the dorso-ventral wing margin during *Drosophila* wing disc development (Doherty et al. 1996). Here, dorsal cells induce ventral cells to express *wingless* and vice versa and this pattern depends on Delta, Serrate and Notch.

Oncogenic receptor forms lack the regulatory extracellular or intracellular PEST domains, transduce signal independently of DSL ligands (Struhl et al. 1993; Lieber et al. 1993) and have been associated with T cell leukemia (TAN-1 (Ellisen et al. 1991)) or mouse breast cancer (INT-3 (Gallahan and Callahan 1987; Robbins et al. 1992)). It is poorly understood how NOTCH activation can contribute to transformation. However, its involvement in cellular differentiation and crosstalk to other fundamental signalling pathways is likely to play a role (Radtke and Raj 2003). Surprisingly, NOTCH has also been associated with a tumour suppressive function, as it induces differentiation in mammalian skin and a cell-cycle arrest (Nicolas et al. 2003; Radtke and Raj 2003). These contradicting findings highlight the importance of a given cellular context and appreciate the many outcomes of NOTCH signalling activity.

1.5.4 NOTCH signalling in *C. elegans* tissues other than the vulva

In *C. elegans*, NOTCH signalling is crucial in several instances during early embryo development where the ligand *apx-1* and the receptors *glp-1* and *lin-12* are used (Lambie and Kimble 1991 and reviewed in Priess 2005) as well as embryonic and larval cell fate decisions and mitosis in the germline (Kimble and Simpson 1997). Prior to vulval induction, the ligand *lag-2* acts through LIN-12/NOTCH in the VU vs. AC precursor fate decision process and promotes the VU fate in a feedback mechanism (Greenwald et al. 1983; Seydoux and Greenwald 1989; Wilkinson et al. 1994; Park et al. 2013). In animals mutant for *lin-12* or with impaired cell movement resulting in lack of precursor cell contact, two ACs develop and overactivation of LIN-12 results in the absence of any AC (Greenwald et al. 1983; Hedgecock et al. 1990). Later during development, the AC induces descendants of the VU cell via LIN-12 to adopt the pi cell fate (Newman et al. 1995). These pi cells will be induced by the vulF cells (see 1.4.4) and RAS/MAPK activity to become uv1 cells and contribute to the vulval-uterine connection for functional egg-laying (Chang et al. 1999). LIN-12 has also been found to regulate spontaneous reversal rate of the worm in cooperation with the glutamate receptor *glr-1* (Chao et al. 2005). Another Notch receptor in *C. elegans*, GLP-1 (Pepper et al. 2003), is crucial during the development of the germline and its maintenance in the adult worm (Kimble and White 1981). The two distal tip cells (DTCs) in the gonad express the ligand LAG-2 and activate NOTCH signalling via GLP-1 and the CSL protein LAG-1, which leads to mitotic divisions of germ cells (Kimble and White 1981; Henderson et al. 1994). In the absence of the DTCs or GLP-1, germ cells enter meiosis and the pool of mitotic stem cells is lost.

1.6 The relevance of oxygen during development and disease

Molecular oxygen is a double-edged sword. On the one hand, it serves as an external energy source that participates in a variety of metabolic processes and acts as the terminal electron acceptor molecule in the electron transport chain during mitochondrial aerobic respiration (Gleadle and Ratcliffe 2001). The obligatory dependence of organisms on oxygen is exemplified by elaborate mechanisms that ensure oxygen homeostasis as well as a number of pathologies associated with inappropriate oxygen supply. On the other hand, the metabolism of oxygen produces reactive oxygen species (ROS) that are toxic to cells. It is thus not surprising that oxygen availability dictates the expression of genes involved in energy metabolism, defence against oxygen toxicity or further metabolic pathways that require molecular oxygen. One such example is erythropoiesis, the production of red blood cells (Goldberg et al. 1988). Erythrocytes circulate in our body and deliver oxygen from the lungs to all tissues by means of the oxygen-transport metalloprotein haemoglobin. Situations including oxygen shortage (hypoxia), bleeding (haemorrhage) or a decrease in the number of red blood cells or haemoglobin (anaemia, e.g. as a result of blood donation) cause a rise in erythropoietin (EPO), the hormone that controls erythropoiesis, and a boost in erythrocyte production (Goldberg et al. 1988). In addition to adjusting the number of red blood cells, the vasculature is modified to match the given metabolic needs through a process known as angiogenesis. Analogously, individuals living in higher altitudes with lower oxygen pressure exhibit an increased amount of erythrocytes (polycythaemia), myoglobin, mitochondrial volume density and respiratory enzymes (Storz et al. 2010). Although some level of oxygen deficiency is crucial during embryonic development to stimulate vascularisation (Patterson and Zhang 2010), prolonged hypoxia can result in irreversible tissue damage by inducing cell death via necrosis or apoptosis (Banasiak et al. 2000). Hypoxia is characteristic of various pathological conditions such as ischaemia (the restriction of blood supply to tissues), stroke, inflammation, thrombosis, anaemia, artherosclerosis and solid tumours (Harris 2002; Vannucci 2004; Hare 2004; Hultén and Levin 2009; Eltzschig and Carmeliet 2011; Bovill and van der Vliet 2011; Ferdinand and Roffe 2016) and triggers a range of cellular responses as discussed below.

1.6.1 Acute cellular responses to hypoxia

In the case of restricted oxygen availability, both immediate and more gradual changes occur within cells, the latter comprising altered gene expression, which is introduced below. Ventilation is tuned such that the gas exchange between the lungs and the environment is optimised and this process is governed by oxygen sensing cells within the carotid bodies in the artery (Ureña et al. 1994). The opening of potassium channels on the membrane of these cells is inhibited by hypoxia, which leads to the opening of calcium channels with consequent calcium influx and the release of the neurotransmitter dopamine to stimulate ventilation. Although not fully understood, it is assumed that oxygen is sensed through redox state dependent structural changes that dictate the activity of

ion channels (Kemp and Peers 2007; Muralidharan et al. 2016). Acute responses to hypoxia further act to conserve energy via the downregulation of translation through multiple pathways (Koritzinsky et al. 2005; Wouters et al. 2005; Koritzinsky et al. 2006). One of these includes the unfolded protein response (UPR), which is induced by an accumulation of un- or misfolded proteins during hypoxic insult (Koumenis et al. 2007). The endoplasmatic reticulum (ER) kinase PERK is part of the UPR and phosphorylates EIF2A to inhibit translation initiation (Koumenis et al. 2002). Other pathways are the hypoxic inhibition of the mammalian target of rapamycin mTOR that integrates metabolic signals with protein synthesis or the disruption of the mRNA cap-binding complex by targeting eukaryotic translation initiation factor 4E (EIF4E) (Wouters and Koritzinsky 2008).

1.6.2 Transcriptional cellular responses to hypoxia: HIF1A

In early studies on erythropoietin induction by hypoxia, it became clear that cells also respond to changes in oxygen pressure more gradually, i.e. through transcriptional programmes. A *cis*-acting 5'-G/ACGTG-3' hypoxia-response element (HRE) was found to be required for EPO transcription (Beck et al. 1991; Semenza et al. 1991; Pugh et al. 1991; Madan and Curtin 1993) and soon thereafter, the nuclear hypoxia inducible factor HIF was purified using the EPO sequence (Semenza and Wang 1992; Wang and Semenza 1993). These studies revealed the existence of a heterodimeric transcription factor complex consisting of an oxygen-degradable HIF1A subunit and a constitutive HIF1B subunit (also known as ARNT) (Maxwell et al. 1999). Both subunits are basic helix-loop-helix (bHLH) transcription factors of PAS domain family proteins (named after their first characterisation in *Drosophila* Per and Sim and mammalian ARNT proteins) (Wang et al. 1995). The description of HREs that are bound by HIF1 triggered the discovery of many further HIF1 target genes, among which vascular endothelial growth factor (VEGF) (Shweiki et al. 1992), Glucose transporter-1,3 (Chen et al. 2001) or endothelin (Kourembanas et al. 1991) (a more detailed list is reviewed in (Harris 2002)). The von Hippel-Lindau protein VHL is a substrate recognition subunit of the ubiquitin protein ligase complex that promotes proteasomal degradation of the HIF1A subunit at normoxia (Salceda and Caro 1997; Huang et al. 1998; Maxwell et al. 1999). Binding of pVHL was found to require prolyl hydroxylation of HIF1A at residues P^{564} and P^{402} within a conserved LXXLAP motif in an oxygen-dependent degradation (ODD) domain (Huang et al. 1998; Yu et al. 2001; Masson et al. 2001) (**Fig. 1.9**). The hydroxylation step is carried out by 2-oxoglutarate and iron dependent prolyl hydroxylase domain (PHD) proteins (dioxygenases, also called EGLN) that were described in 2001 in mammalian cell culture and *C. elegans* (Ivan et al. 2001; Jaakkola et al. 2001; Yu et al. 2001; Epstein et al. 2001). Three such dioxygenases exist and PHD2 (EGLN1) appears to be the prime HIFA hydroxylase (Berra et al. 2003). The conserved interaction of HIFA, PHD2 and VHL is known as the hypoxia response pathway. In addition to destabilising prolyl hydroxylation, the inhibitory hydroxylation of an asparagine residue in the HIF1A transactivation domain by factor inhibiting HIF1 (FIH1) provides further regulation (Mahon 2001).

Mammalian genomes encode three *HIFA* isoforms regulated by oxygen and one constitutive *HIF1B* gene. HIF1A is expressed ubiquitously, whereas expression of HIF2A appears more tissue-specific, e.g. in vascular endothelium or kidney epithelial cells (Tian et al. 1997; Jain et al. 1998; Wiesener 2003; Simon and Keith 2008). HIF3A, also known as IPAS, acts as a negative regulator of HIF1A and HIF2A (Makino et al. 2001 and reviewed in Yang et al. 2015).

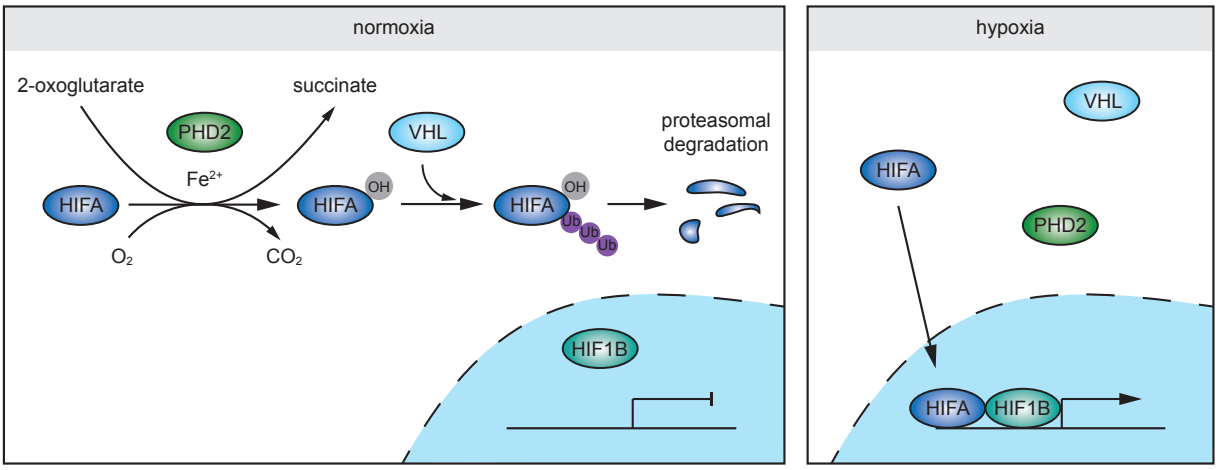

Figure 1.9. Hypoxia response pathway. During normoxia (left), prolyl residues in the oxygen dependent degradation (ODD) domain of HIFA proteins are hydroxylated by PHD2, an iron and 2-oxoglutarate dependent dioxygenase. Hydroxylation of HIFA increases its affinity for the E3 ubiquitin ligase VHL which promotes subsequent proteasomal degradation. During hypoxic conditions (right), HIFA hydroxylation is prevented and stabilised HIFA enters the nucleus to form a heterodimeric transcription factor complex with constitutive HIF1B and alter gene expression.

1.6.3 Hypoxia and HIFA during cancer progression

Given the various roles of hypoxia and hypoxia inducible factors in development and physiology, their significance in disease, most prominently in cardiovascular disease and cancer, is not surprising. Mutations in *HIF2A* are associated with polycythaemia (Percy et al. 2008b; Percy et al. 2008a) and the activation of HIF1A and HIF2A protects ischaemic tissues from injury (Jurgensen 2004; Loor and Schumacker 2008). One of the most striking correlations of hypoxia and disease was perhaps the finding that tumour hypoxia slows growth and can induce necrosis (Barach and Bickerman 1954; Thomlinson 1977). Hypoxic areas are characteristic of tumours and detectable once they outgrow the oxygen diffusion limit of 100-200 µm or 10-20 cell layers (Thomlinson and Gray 1955; Thomlinson 1965). It was in 1956, when Otto Warburg first described the upregulation of glucose transporters, glycolytic enzymes or energetic and metabolic intermediates associated with glycolysis in an aerobic environment, a paradoxical phenomenon known as “Warburg effect” (Warburg 1956; Denko 2008). The clinical importance of tumour hypoxia came into focus with the observation of resistance to radiotherapy and chemotherapy, which rely on the presence of mole-

cular oxygen and a functional vascularisation (Gray et al. 1953; Davidson et al. 1955; Deschner and Gray 1959; Teicher et al. 1981; Teicher 1994; Shannon et al. 2003; Overgaard 2007). Typical tumorigenic features including angiogenesis (Blumenson and Bross 1976), metastatic potential (van den Brenk et al. 1972; Young et al. 1988) and DNA replication (Young and Hill 1990) were ascribed to insufficient oxygenation within the tissue and became predictive of poor patient survival. Treatment resistance and systemic metastases have been described for prostate, cervix, breast or head and neck cancer (Brizel 1996; Chaudary and Hill 2007; Vaupel and Mayer 2007; Chan et al. 2007). Limited success has been made with tumour oxygenation during radiotherapy or by the administration of hypoxia-activated pro-drugs (Rischin et al. 2005; Overgaard 2007). However, treatment can be further complicated by hypoxia promoted expression of the multidrug resistance gene *MDR1* which regulates efflux of chemotherapeutic drugs (Comerford 2002).

Tumours experience both chronic hypoxia due to diffusion limitation and acute hypoxia as a result of transient changes in blood flow through the disorganised vasculature of large tumours (Chaplin et al. 1986; Dewhirst et al. 2008). Hypoxia-reoxygenation cycles are believed to enhance the occurrence of DNA strand breaks (DSB) and mutagenesis through the action of ROS (Cairns and Hill 2004; Klein et al. 2006), thereby contributing to genetic instability commonly associated with cancer. Although hypoxia induces p53 to promote apoptosis, the selection of cells defective in apoptotic pathway components leads to increased resistance to apoptosis (Graeber 1994; Graeber et al. 1996; Zhang and Hill 2004). Furthermore, chronically hypoxic tumour cells downregulate DNA repair pathways, which increases the mutational potential on the one hand, but also enhances their sensitivity to radiotherapy (Blais et al. 2006; Chan et al. 2008).

Finally, HIFA and VHL are directly implicated in several malignancies (Maxwell et al. 1999; Koukourakis et al. 2002; Semenza 2003; Holmquist-Mengelbier et al. 2006). The activation of oncogenes (e.g. *SRC, HRAS*) or loss of tumour suppressor genes (e.g. *VHL* (see below) or *PTEN*) lead to the accumulation and activation of HIF1A even in normoxia (Semenza 2003; Denko 2008). HIF1A has been associated with poor patient survival in cervical, breast or ovarian cancer (Birner 2000; Birner et al. 2001; Bos et al. 2001; Schindl 2002) and activated HIF2A correlates with mortality in the case of neuroblastoma (Holmquist-Mengelbier et al. 2006) or head and neck squamous cell carcinoma (Koukourakis et al. 2002). Inhibition of HIF1A in human breast and colon cancer cells reduced tumour growth in mice (Livingston et al. 2000) while the absence of Hif1a in a mouse transgenic breast cancer model suppressed the potential to metastasise into the lung (Liao et al. 2007). Therefore, drugs to block HIF1 or HIF1 target genes as well as anaerobic bacteriolytic therapies are subject to cancer treatment evaluation (Dang et al. 2001; Giaccia et al. 2003; Semenza 2007). However, the role of hypoxia-inducible factors in cancer progression appears more complex than initially anticipated, since the inhibition of HIF2A in renal cell carcinoma indeed resulted in decreased tumour mass in mice while the suppression of HIF1A increased tumour mass (Raval et al. 2005). Mutations in *VHL* are common to sporadic kidney cancer and renal cell carcinoma cells (Maxwell et al. 1999). The “von Hippel-Lindau (VHL) disease” is a human hereditary cancer syndrome characterised by germline mutations in *VHL*

that exhibit a greatly enhanced susceptibility to highly vascularised tumours (Mandriota et al. 2002; Raval et al. 2005). Renal cell carcinoma (RCC) commonly originates from loss of VHL function but not exclusively through consequent HIFA stabilisation. Although both HIF1A and HIF2A have been implicated in this type of cancer (though apparently opposing each other) (Raval et al. 2005), a role of insufficient ß-catenin degradation in *VHL*$^{-/-}$ renal carcinoma cell lines as well as defects in extracellular matrix formation and a decreased induction of apoptosis upon loss of VHL have been proposed to contribute to a tumorigenic potential (Bishop et al. 2004; Kurban et al. 2006; Roe et al. 2006; Peruzzi et al. 2006).

1.7 Quantitative genetics and disease

Phenotypic traits can be discrete, i.e. they are either present or absent and are inherited in a Mendelian pattern. Quantitative genetics refers to continuous phenotypes that are not brought about by this textbook pattern of inheritance but rather by a number of genes that collectively and quantitatively influence the trait in interaction with the environment (Hill and Mulder 2011). Examples of such complex traits are the colour and shape of fruit, the height or size of organisms as well as diseases like diabetes (Donnelly 2008), schizophrenia (Purcell et al. 2009) and cancer (Vazquez et al. 2012). The function and activity of the genes that influence a given phenotype is further dependent on natural variation that introduces single nucleotide polymorphisms (SNPs) or small insertions or deletions (InDels) into genes or non-coding DNA. Genome-wide association studies (GWAS) aim at comparing the genomes of individuals to correlate the presence of SNPs within genes with a specific phenotype and in this manner define risk factors or susceptibility genes in disease (Illig et al. 2009; Soto-Ortolaza et al. 2013). Risk factors have been described and include the *BRCA1* gene for breast cancer (Neuhausen et al. 1994; Williams et al. 2005), *MLH1* in colorectal cancer (Papadopoulos et al. 1994), *SNCA* in Parkinson's disease (Warner and Schapira 2003; Mueller et al. 2005) and *MYO18B* in schizophrenia (Purcell et al. 2009) to name only a few within this field of ongoing research (a detailed catalogue of GWAS studies is available from the National Human Genome Research Institute). With a better knowledge of risk factors, disease progress and outcome is more predictable and treatments can be designed more effectively.

1.7.1 Mapping of QTLs

Quantitative trait loci (QTLs) are genomic regions which contain susceptibility genes and are distributed over the genome (Collard et al. 2005). They can be identified because they segregate with a trait of interest. In GWAS, QTLs are described by the over-representation of the same genomic regions containing genetic variants, or in other words by the linkage to a phenotype

(Daniels et al. 1996; Chung et al. 2014). Since the sample number in genome-wide association studies is limiting (Almasy and Blangero 2008), model organisms with a relatively short life cycle are powerful tools to not only identify QTLs, but also to characterise the genes within a given QTL in respect to a genetically complex phenotype of interest. QTL mapping has been performed in plants (Young 1996), *Drosophila melanogaster* (Leips and Mackay 2000; Pasyukova et al. 2000; Edwards and Mackay 2009), yeast (Katou et al. 2009; Liti and Louis 2012) or *C. elegans* (Ayyadevara et al. 2003; Green et al. 2013; Andersen et al. 2015) and resulted in the description of behavioural as well as disease related traits. Basically, wild isolates that are sufficiently diverse on a genomic level, are crossed, and recombinant inbred lines (RILs) are obtained via backcrossing (Takuno et al. 2012; Mulualem and Bekeko 2016). With the help of molecular markers such as fragment-length polymorphisms (FLPs), the parental sequence origin is determined and tracked (Zipperlen et al. 2005). The set of RILs is compared to the original isolate to establish genome-wide genotype-phenotype maps and identify linkage disequilibria, i.e. loci that are associated with the trait of interest. This straight-forward strategy has helped in gaining a deeper understanding in the complex nature of disease.

Aim of this thesis

2

As of February 2017, the World Health Organisation describes cancer as the second leading cause of death globally, after ischaemic heart disease and stroke (http://www.who.int/cancer/). Hereby, the most common types of cancer concern the lung, liver, colon, stomach and breast. Cancer is a disease during which cells divide in an uncontrolled manner so that tissues grow abnormally to give rise to so called “tumours” that compromise organ function. Cells altered in such a way can spread to other parts of the body and build new colonies known as “metastases”, which are the major cause of death from cancer. The transformation of normal cells into tumour cells occurs through carcinogens, among which radiation (UV, ionising), tobacco smoke or aflatoxins (e.g. present in raw mushrooms) as well as viral and bacterial infections. Cell transformation is the process of DNA alterations (mutations) with consequent changes in protein activity or function. Progress in research has helped in gaining insight into the contribution of basic cellular signalling pathways involved in the normal development of higher organisms during cancer. Prominent examples comprise the highly conserved WNT, EGFR/RAS/MAPK and NOTCH pathways (Reya and Clevers 2005; Fernandez-Medarde and Santos 2011; Takebe et al. 2013). However, while deviations in these signalling pathways can initiate cell transformation and cancer development, the combination and interaction of further genes or “risk factors” present within an individual genome (the entirety of genes) greatly determines the speed of disease progression, response to treatment and thus prognosis (Stessman et al. 2014). Risk factors contribute to a disease through not necessarily obvious processes when they exhibit a specific DNA composition brought about by spontaneous mutations. Such spontaneous mutations (polymorphisms) occur naturally and are the origin of evolution, since they change gene sequences and affect protein function. Therefore, a deeper understanding of the effect of polymorphisms on the function of risk factors and thus disease outcome is of great importance. In genome-wide association studies (GWAS), the DNA sequence of disease patients is compared to discover risk factors, i.e. genes in which mutations occur with increased frequency (Soto-Ortolaza et al. 2013). Although such studies have helped in describing risk factors, they suffer from a limited sample number and the lack of further functional studies. Therefore, the application of simple organisms like the nematode *C. elegans* is preferred, since basic signalling pathways are conserved (Spradling et al. 2006). During the development of the *C. elegans* egg-laying organ (vulva), the WNT, RAS/MAPK and NOTCH signalling pathways play crucial roles and mis-regulated signalling results in visible quantifiable changes (pheno-

types) (Sternberg 2005). Thus, it is a feasible system to identify risk factors (also called modifiers) and study their effect on these signalling pathways.

The aim was to simulate a simplified cancerous environment by employing mutated *C. elegans* lines that exhibit impaired function of ß-catenin, the master regulator of WNT signalling or an overactive form of RAS that is frequently found in cancer tissues (Fernandez-Medarde and Santos 2011; Clevers and Nusse 2012). Further, to mimic the natural variation in the human population, we employed the two worm strains N2 and CB4856 that are diverse on a genomic level, mixed their genomes to obtain a range of mutation included introgression lines (milLs) carrying different genomic parts of N2 and CB4856 (Doroszuk et al. 2009) and aimed at verifying previously predicted quantitative trait loci (QTLs) that contain modifiers of the signalling pathways (Schmid et al. 2015). By assessing the effect of defined CB4856 and N2 genomic regions or the knockdown of selected genes respectively on the outcome of the mutant phenotype, we expected to find a number of modifiers of the WNT and RAS/MAPK pathways, which we could then describe in more detail and in that contribute another tiny piece of understanding to the vast and incomplete field of cancer research.

Projects

3

3.1 Quantitative trait loci on chromosome I affect Wnt and RAS/MAPK signalling during vulval induction

3.1.1 Abstract

A number of studies have aimed at investigating the origin and potential treatment of monogenic diseases. However, polygenic diseases arising from an interplay between several malfunctioning signalling pathways are the predominant cause of up to 60% of deaths in the human population. Quantitative genetic approaches provide a powerful tool to elucidate genetic risk factors underlying such complex diseases.

We have used two isolates of *C. elegans*, N2 Bristol and CB4856 Hawaii, to study the influence of naturally occurring polymorphisms on mutant genetic backgrounds well-known to promote diseases such as cancer. We chose the development of the *C. elegans* vulva as the phenotypic readout for WNT and EGFR/RAS/MAPK signalling activity, where changes in signalling result in either a Multivulva or Vulvaless phenotype that can be quantified at single-cell resolution.

Previous work has established comprehensive QTL maps spanning the entire genome. The maps were generated by comparing an N2 strain carrying a mutation in *let-60/RAS* or *bar-1/ß-catenin* to animals carrying the *let-60* or *bar-1* mutation in a mixed N2/CB4856 background (so called mutation included recombinant inbred lines, miRILs). We narrowed down the genomic regions containing a QTL by generating N2 strains mutant for *bar-1* or *let-60* and carrying well-defined CB4856 introgressions (miILs). Subsequently, we identified candidate polymorphic modifier genes of the two pathways by performing RNAi and continued by verifying the candidates with the use of mutants. Further studies will be necessary to study the relation between the candidate genes and RAS/MAPK or WNT signalling in more detail.

3.1.2 Introduction

Quantitative genetics describes phenotypes that are not brought about by the textbook Mendelian pattern of inheritance, during which one gene gives rise to a phenotype. It is more often the case that a number of genes influence a trait quantitatively and in interaction with the environment (Hill and Mulder 2011). Many diseases, such as diabetes (Donnelly 2008), schizophrenia (Purcell et al. 2009) and cancer (Vazquez et al. 2012) are based on such complex traits. A number of studies aim at identifying these complex traits or risk factors to predict the progress and outcome of diseases and to design more effective treatments. Quantitative trait loci (QTLs) are genomic regions that contribute such factors and they can be dispersed over an entire genome. The mapping of QTLs has helped scientists in finding and characterising genes which contribute to diseases (Fisher 1918; Wright 1921; Paterson et al. 1988).

In this project, we have used the development of the *C. elegans* vulva as a model to discover QTLs influencing the WNT and RAS/MAPK signalling pathways. We employed previously published approaches to study natural variation as follows (Doroszuk et al. 2009; Schmid et al. 2015). The two strongly diverging wild isolates of *C. elegans,* N2 Bristol and CB4856 Hawaii differ by one single nucleotide polymorphism (SNP) every 412 bp (Thompson et al. 2013), thus allowing a thorough functional analysis of naturally occurring polymorphisms. In order to analyse polymorphic modifiers of a signalling pathway, the N2 isolate carrying a mutant allele of a gene acting in this signalling pathway is crossed with the CB4856 Hawaiian isolate to generate mutation included recombinant inbred lines (miRILs) (**Fig. 3.1**). The animals are allowed to self-fertilise to enrich for homozygous lines, before the genomic constitution is determined by FLP mapping and established genomic markers (Zipperlen et al. 2005). The CB4856 Hawaiian genomic regions that alter the mutant phenotype as compared to the N2 Bristol background are selected for further analysis. These regions are verified and narrowed to a smaller region with the help of introgression lines (Doroszuk et al. 2009). Since both the N2 Bristol and CB4856 Hawaiian genome have been sequenced (Thompson et al. 2015), polymorphic and/or (partially) deleted genes (Maydan et al. 2010) within the region are determined and analysed by RNAi and subsequent mutant analysis.

3.1.2.1 QTLs in the *let-60(n1046gf) / RAS(gf)* mutant background

Schmid et al. 2015 performed QTL mapping as described above to identify three QTLs containing modifiers of RAS/MAPK signalling: for QTL1 on chromosome 1 the Bristol background caused reduced RAS/MAPK activity while the opposite is true for QTL2 on chromosome 2 and QTL3 on chromosome V. The QTLs were verified using appropriate introgression lines (ewIR2, 5, 7, 9, 10, 11 and 17) (Doroszuk et al. 2009) and the QTL found on chromosome I could be subdivided into two smaller regions, QTL1a and QTL1b. While QTL1a has not been studied, 107 of the 142 candidate genes within the smaller QTL1b region were subjected to RNAi to find effects on vulval

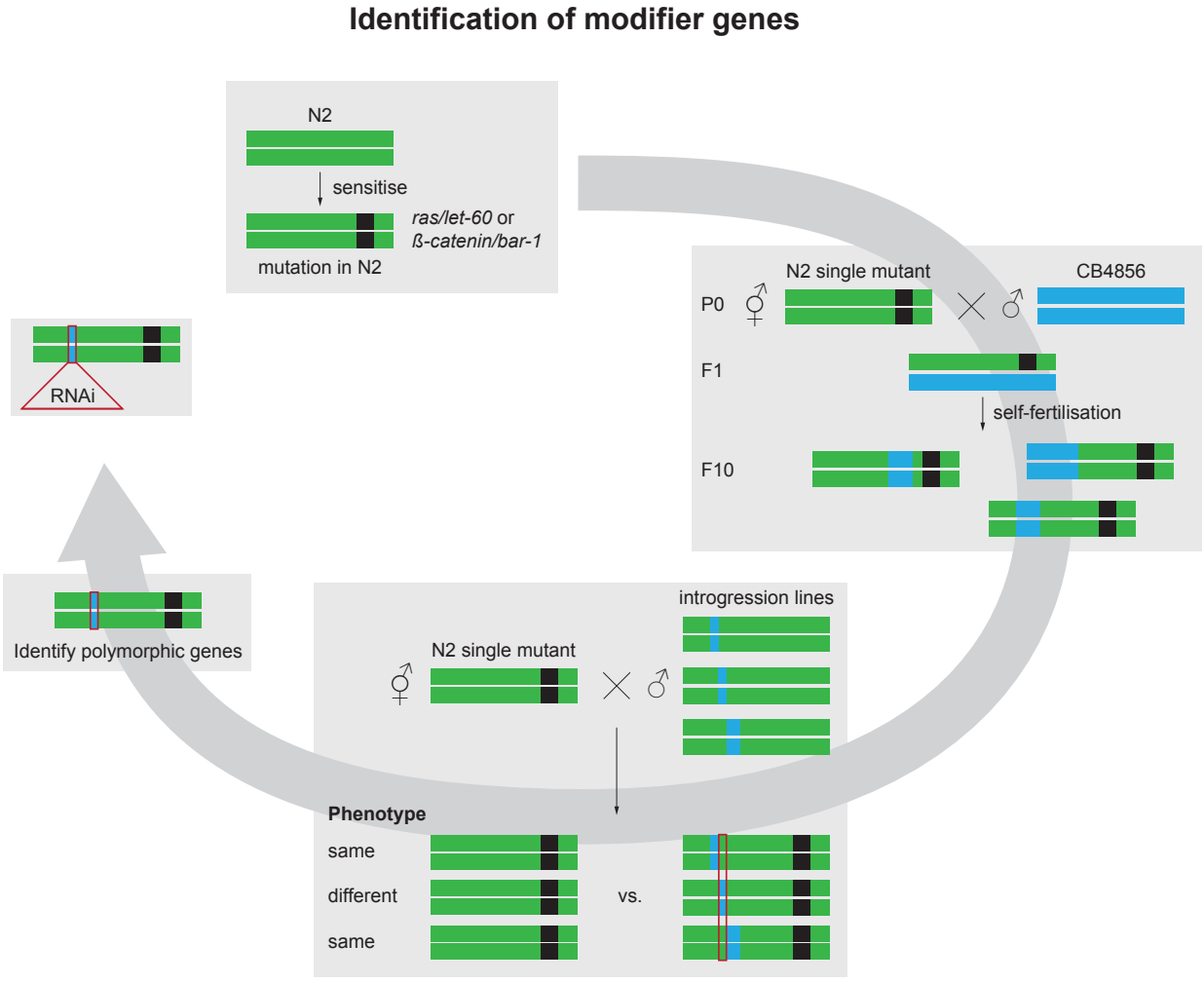

Figure 3.1. Strategy of QTL mapping. 1) Modifier genes of a selectable trait (e.g. *let-60 / RAS* or *bar-1 / ß-catenin*) are analysed. 2) The region contributing to the phenotype is determined by crossing the sensitised N2 Bristol strain with CB4856 Hawaii to create mutation included recombinant inbred lines (miRILs). QTLs are predicted via genotype-phenotype associations. 3) The predicted QTL is verified and narrowed by using lines carrying defined CB4856 Hawaiian introgressions in an otherwise N2 Bristol background. A modifier is contained within the genomic region shared among miILs that differ in phenotype from the 'pure' N2 Bristol background. 4) Polymorphic genes exhibiting coding SNPs between CB4856 and N2 as well as (partially) deleted genes are identified within the QTL region. 5) These genes are studied via RNAi, over-expression and mutant analysis and correlated with the trait of interest.

induction in both the "pure" N2 and CB4856 introgressed line (general RAS/MAPK modifiers) or one of the strains only (isolate-specific modifier). For further experiments, the focus was set on the 15 polymorphic modifiers found (Schmid et al. 2015), i.e. genes affecting RAS/MAPK signalling either in the N2 or the CB4856 variant and thereby suggesting functional difference between the two isolates. Schmid et al. (2015) extensively studied the polymorphic modifier AMX-2, a monoamine oxidase which regulates RAS/MAPK signalling through serotonin metabolism.

3.1.2.2 QTL map in the *bar-1(ga80lf) / ß-catenin(lf)* mutant background

Analogous to the studies on polymorphic RAS/MAPK modifiers mentioned above, linkage disequilibria had been found in the *bar-1(ga80lf) / ß-catenin(lf)* mutant background and two QTLs affecting vulval induction were predicted for chromosome I and II (**Fig. 3.2**). We continued our analysis on the QTL on chromosome I while the Kammenga group investigated both QTLs in more detail and verified the second QTL with the introgression lines ewIR21 and ewIR23 (J. Kammenga, personal communication).

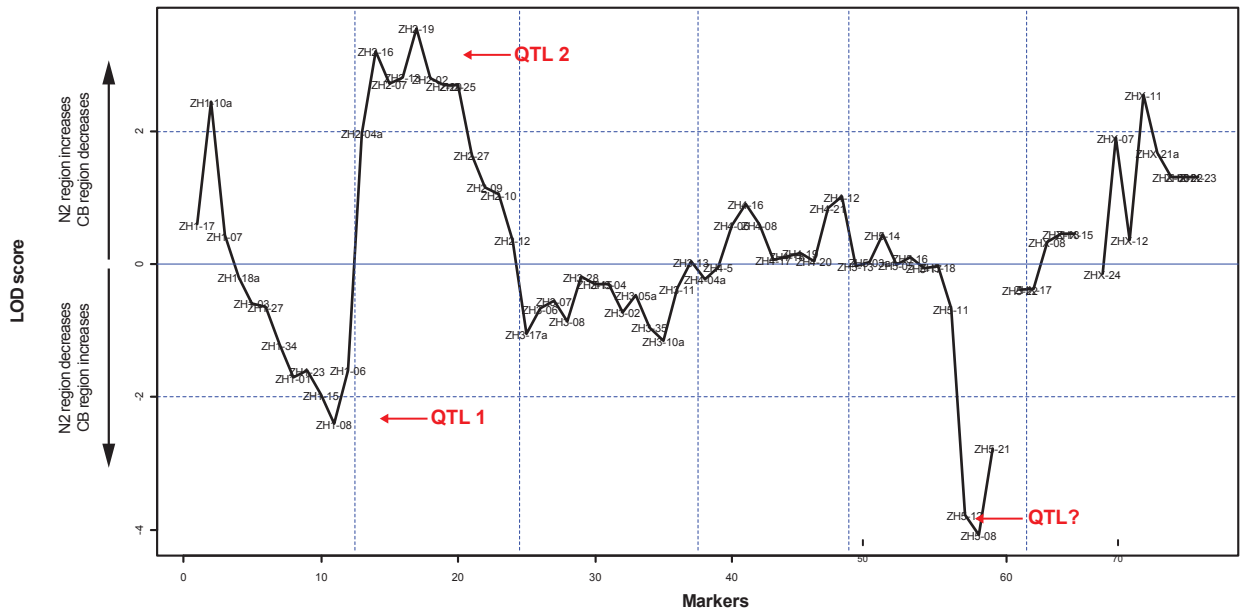

Figure 3.2. QTL map in the *bar-1(ga80)* mutant background. By using *bar-1(ga80)* sensitised RILs, two QTLs affecting Wnt signaling during vulval development were identified. These are localised to the far end of chromosome I and centrally on chromosome II. The presumptive QTL on chromosome IV requires more detailed analysis. Note the absence of information on chromosome X in close proximity to the *bar-1* locus, where no recombination took place. The x-axis indicates the position of genetic markers and the y-axis shows the likelihood of disequilibrium (LOD) score * significance. Graph adapted from T. Schmid, L.B. Snoek.

3.1.3 Local refinement of the QTL1 in the *bar-1(ga80)* background

To find modifiers of WNT signalling during vulval development, we continued to focus on the QTL on chromosome I, since it partially overlaps with the QTL that was found in the *let-60(n1046gf)* mutant background (Schmid et al. 2015 and **Fig. 3.2**). To locally refine the QTL found in the region around the fragment length polymorphism marker ZH1-08 (I: 12297522) (**Fig. 3.2** and T. Schmid, personal communication) we chose to use the introgression lines ewIR9 (CB4856 region I: 9135001-11315000, markers ZH1-22-egPO105), ewIR10 (CB4856 region I: 8654362-14162928, markers ZH1-22-ZH1-06 and III: 6444001-11217000, markers

pkP3100-pkP3059), and ewIR17 (CB4856 region I: 12433001-15059000, markers pkP1070-pkP1072) (Zipperlen et al. 2005; Doroszuk et al. 2009; Thompson et al. 2015) that generously span the region (**Fig. 3.2** and **3.3**). In parallel, the Kammenga group employed ewIR13 (positioned around the marker egPN104) and ewIR14 (markers egPN104-egPO105) (Doroszuk et al. 2009). Note that the sequence positions correspond to the Bristol N2 genome (WormBase WS195). We crossed the introgression lines into the *bar-1(ga80)* mutant and determined their genotype by PCR and sequencing (*bar-1* locus) as well as FLP mapping as described in Zipperlen et al. (2005) to determine the presence of introgressed sequences. As controls, we included “pure” N2 Bristol and CB4856 animals into the mapping analysis. Since the ewIR10 introgression line carries genomic regions of CB4856 on chromosome I and III, we performed FLP mapping for both regions. We discarded any *bar-1(ga80)* mutation including ewIR10 introgression line (miIL) carrying CB4856 genomic sequences on chromosome III. From each cross between EW15 (*bar-1(ga80)* mutant) and ewIR9, ewIR10 and ewIR17, we analysed 48 lines (**Tables 3.1, 3.2** and **3.3**). Strain numbers are indicated for lines stored at -80 °C. Where sequencing gave ambiguous or no results, regions are marked in blue (“heterozygous”) or white (no data).

During the cloning of progeny from ewIR10 miILs, meiotic recombination events in meiosis resulted in the diminution and segmentation of the CB4856 region and we obtained a range of lines with a combination of smaller introgressed regions (**Table 3.2**). No recombination took place in the progeny of ewIR9 or ewIR17 miILs.

Lysate	Genomic location								Strain
	ZH1-03	ZH1-27	ZH1-34	ZH1-01	ZH1-23	ZH1-15	ZH1-08	ZH1-06	
CB	Hawaii	Hawaii	Hawaii	Hawaii	Hawaii	Hawaii	Hawaii	Hawaii	
N2	Bristol	Bristol	Bristol	Bristol	Bristol	Bristol	Bristol	Bristol	
ewIR9	Bristol	Bristol	Bristol	Bristol	Hawaii	Hawaii	Bristol	Bristol	
1	Bristol		Bristol	Bristol		Hawaii	Bristol	Bristol	
2	Bristol			Bristol		Bristol	Bristol	Bristol	
3	Bristol		Bristol	Bristol		Hawaii	Bristol	Bristol	
4	Bristol	Bristol		Bristol	Hawaii	Hawaii	Bristol	Bristol	AH3382
5	Bristol	Bristol		Bristol		Bristol	Bristol	Bristol	AH3333
6	Bristol	Bristol	Bristol	Bristol		Hawaii	Bristol	Bristol	
7	Bristol			Bristol		Hawaii	Bristol	Bristol	
8	Bristol	Bristol	Bristol	Bristol		Bristol	Bristol	Bristol	AH3370
9	Bristol			Bristol	Bristol	Bristol	Bristol	Bristol	
10	Bristol	Bristol		Bristol	Hawaii	Hawaii	Bristol	Bristol	AH3383
11		Bristol	Bristol	Bristol	Hawaii	Hawaii	Bristol	Bristol	AH3334
12	Bristol	Bristol		Bristol	Hawaii	Hawaii	Bristol	Bristol	
13	Bristol	Bristol		Bristol	Bristol	Bristol	Bristol	Bristol	
14	Bristol	Bristol		Bristol		Bristol	Bristol	Bristol	
15	Bristol	Bristol		Bristol	Hawaii	Hawaii	Bristol	Bristol	
16		Bristol	Bristol	Bristol	Hawaii	Hawaii	Bristol	Bristol	
17	Bristol		Bristol	Bristol	Bristol	Bristol	Bristol	Bristol	
18	Bristol			Bristol		Bristol	Bristol	Bristol	
19	Bristol		Bristol	Bristol		Hawaii	Bristol	Bristol	
20	Bristol			Bristol		Bristol		Bristol	
21		Bristol	Bristol	Bristol	Bristol	Bristol	Bristol	Bristol	
22		Bristol		Bristol		het	Bristol	Bristol	
23	Bristol	Bristol		Bristol	Hawaii	Hawaii	Bristol	Bristol	
24		Bristol		Bristol		Hawaii	Bristol	Bristol	
25	Bristol	Bristol	Bristol	Bristol	Hawaii	Hawaii	Bristol	Bristol	
26	Bristol			Bristol		Bristol	Bristol	Bristol	
27	Bristol	Bristol	Bristol	Bristol	Hawaii	Hawaii	Bristol	Bristol	
28	Bristol	Bristol		Bristol		Bristol	Bristol	Bristol	
29		Bristol	Bristol	Bristol		Hawaii	Bristol	Bristol	
30	Bristol	Bristol	Bristol	Bristol		Bristol	Bristol	Bristol	
31		Bristol		Bristol		Bristol	Bristol	Bristol	
32	Bristol	Bristol	Bristol	Bristol	Bristol	Bristol	Bristol	Bristol	AH3335
33	Bristol	Bristol		Bristol		Hawaii	Bristol	Bristol	
34		Bristol	Bristol	Bristol		Hawaii	Bristol	Bristol	
35		Bristol	Bristol	Bristol		Bristol	Bristol	Bristol	
36	Bristol	Bristol	Bristol	Bristol		Bristol	Bristol	Bristol	
37		Bristol	Bristol	Bristol		Bristol	Bristol	Bristol	
38		Bristol	Bristol	Bristol		Hawaii	Bristol	Bristol	
39	Bristol	Bristol	Bristol	Bristol	Bristol	Bristol	Bristol	Bristol	
40	Bristol	Bristol	Bristol	Bristol	Hawaii	Hawaii	Bristol	Bristol	
41	Bristol			Bristol		Hawaii	Bristol	Bristol	
42	Bristol			Bristol		Hawaii	Bristol	Bristol	
43	Bristol			Bristol		Hawaii	Bristol	Bristol	
44	Bristol			Bristol		Hawaii	Bristol	Bristol	
45	Bristol	Bristol		Bristol		Bristol	Bristol	Bristol	
46		Bristol	Bristol	Bristol		Bristol	Bristol	Bristol	
47	Bristol	Bristol		Bristol		Hawaii	Bristol	Bristol	
48	het	Bristol	Bristol	Bristol		Hawaii	Bristol	Bristol	

Table 3.1. Genetic constitution of *bar-1(ga80)* mutants introgressed with ewIR9 (chromosome I). The genomic location is defined by FLP marker positions and the constitution of ewIR9 is indicated as a reference. 48 lysates were mapped and stored strains are named. Black indicates Hawaiian sequence and grey indicates N2 Bristol sequence. Blue bars indicate heterozygousity (double peak in the sequence) and white bars indicate inconclusive sequencing results.

Lysate	Genomic location								Strain
	ZH1-01	ZH1-22	ZH1-23	ZH1-15	ZH1-05	ZH1-08	ZH1-09	ZH1-06	
CB	Hawaii	Hawaii	Hawaii	Hawaii	Hawaii	Hawaii	Hawaii	Hawaii	
N2	Bristol	Bristol	Bristol	Bristol	Bristol	Bristol	Bristol	Bristol	
ewIR10	Bristol	Hawaii	Hawaii	Hawaii	Hawaii	Hawaii	Hawaii	Hawaii	
1	Bristol	het		het		het	het	Bristol	
2	Bristol	Bristol	Bristol	Bristol	Bristol	Bristol	Bristol	Bristol	
3	Bristol	Hawaii		Hawaii	Hawaii	Hawaii	Hawaii	Hawaii	AH3378
4	Bristol	Bristol	Bristol	Bristol	Bristol	Bristol	Bristol	Bristol	
5	Bristol	Bristol		Bristol	Bristol	Bristol	Bristol	Hawaii	AH3331
6	Bristol	Bristol		Bristol		Bristol	Bristol	Bristol	
7	Bristol	Hawaii		Hawaii	Hawaii	Hawaii	Hawaii	Hawaii	
8	Bristol	Bristol		Bristol	Bristol	Bristol	Bristol	Bristol	
9	Bristol	Hawaii	Hawaii	Bristol	Bristol	Bristol	Bristol	Bristol	AH3364
10	Bristol	Bristol	Bristol	Bristol	Bristol	Bristol	Bristol	Bristol	
11	Bristol	Bristol	Bristol	Bristol	Bristol	Bristol	Bristol	Hawaii	
12	Bristol	Hawaii		Hawaii	Hawaii	Hawaii	Hawaii	Hawaii	
13	Bristol	Hawaii		Hawaii	Hawaii	Hawaii	Hawaii	Hawaii	
14	Bristol	Hawaii		Hawaii	Hawaii	Hawaii	Hawaii	Hawaii	
15	Bristol	Hawaii		Hawaii	Hawaii	Hawaii	Hawaii	Hawaii	
16	Bristol	Hawaii		Hawaii	Hawaii	Hawaii	Hawaii	Hawaii	
17	Bristol	Bristol		Bristol	Bristol	Bristol	Bristol	Bristol	
18	Bristol	Bristol	Bristol	Bristol	Bristol	Bristol	Hawaii	Hawaii	AH3415
19	Bristol	Bristol	Bristol	Bristol	Bristol	Bristol	Bristol	Bristol	
20	Bristol	Bristol		Bristol	Bristol	Bristol	Bristol	Bristol	
21	Bristol	Bristol		Bristol	Bristol	Bristol	Bristol	Bristol	
22	Bristol	Bristol		Bristol	Bristol	Bristol	Bristol	Bristol	
23	Bristol	Bristol		Bristol	Bristol	Bristol	Bristol	Bristol	
24	Bristol	Hawaii		Hawaii	Hawaii	Bristol	Bristol	Bristol	AH3417
25	Bristol	Hawaii		Hawaii	Bristol	Bristol	Bristol	Hawaii	AH3367
26	Bristol	Bristol		Bristol	Bristol	Bristol	Bristol	Bristol	
27		Bristol	Bristol		Bristol	Bristol	Bristol	Bristol	
28	Bristol	Bristol		Bristol	Bristol	het	het	het	
29	Bristol	Bristol		Bristol	Bristol	Bristol	Bristol	Bristol	
30	Bristol	Hawaii		Hawaii	Hawaii	Hawaii	Hawaii	Hawaii	AH3379
31	Bristol	Bristol		Bristol	Bristol	Bristol	Bristol	Bristol	
32	Bristol	Bristol		Bristol	Bristol	Bristol	Bristol	Bristol	AH3381
33	Bristol	Bristol			Bristol	Bristol	Bristol	Bristol	
34	Bristol	Bristol	Bristol		Bristol	Bristol	Bristol	Hawaii	
35	Bristol	Hawaii		Hawaii	Hawaii	Hawaii	Hawaii	Hawaii	AH3380
36	Bristol	Bristol			Bristol	Bristol	Bristol	Bristol	
37	Bristol	Hawaii		Hawaii	Hawaii	Hawaii	Hawaii	Hawaii	
38	Bristol	Hawaii		Hawaii	Hawaii	Hawaii	Hawaii	Hawaii	
39							Hawaii		
40	Bristol	Bristol				het	Hawaii	het	
41	Bristol	Hawaii	het	Hawaii	Hawaii	Hawaii	Hawaii	Hawaii	
42	Bristol	Hawaii		Hawaii	Hawaii	Hawaii	Hawaii	Hawaii	
43	Bristol	Bristol		Bristol	Bristol	Bristol	Bristol	Bristol	AH3418
44	Bristol	Hawaii		Hawaii	Bristol	Bristol	Bristol	Bristol	
45	Bristol	Hawaii		Bristol	Bristol	Bristol	Bristol	Bristol	
46	Bristol	Hawaii		Hawaii		Hawaii	Hawaii	Hawaii	
47	Bristol	Bristol		Bristol	Bristol	Bristol	Bristol	Bristol	AH3332
48	Bristol	Hawaii		Hawaii	Hawaii	Hawaii	Hawaii	Hawaii	

Table 3.2. Genetic constitution of *bar-1(ga80)* mutants introgressed with ewIR10 (chromosome I). The genomic location is defined by FLP marker positions and the constitution of ewIR10 is indicated as a reference. 48 lysates were mapped and stored strains are named. Black indicates Hawaiian sequence and grey indicates N2 Bristol sequence. Blue bars indicate heterozygousity (double peak in the sequence) and white bars indicate inconclusive sequencing results.

	Genomic location								
	ZH1-03	ZH1-27	ZH1-34	ZH1-01	ZH1-23	ZH1-15	ZH1-08	ZH1-06	
CB	Hawaii	Hawaii	Hawaii	Hawaii	Hawaii	Hawaii	Hawaii	Hawaii	
N2	Bristol	Bristol	Bristol	Bristol	Bristol	Bristol	Bristol	Bristol	
ewIR17	Bristol	Bristol	Bristol	Bristol	Bristol	Bristol	Bristol	Hawaii	
1	Bristol			Bristol	Bristol	Bristol	Bristol	Hawaii	
2	Bristol			Bristol			Bristol		
3	Bristol		Bristol	Bristol		Bristol	Bristol	Hawaii	
4	Bristol		Bristol	Bristol		Bristol	Bristol	Bristol	
5	Bristol					Bristol	Bristol	Bristol	AH3377
6	Bristol			Bristol	Bristol	Bristol	Bristol	Hawaii	
7	Bristol		Bristol	Bristol	Bristol	Bristol	Bristol	Hawaii	
8	Bristol			Bristol		Bristol	Bristol	Hawaii	
9	Bristol		Bristol	Bristol		Bristol	Bristol	Hawaii	
10	Bristol			Bristol		Bristol	Bristol	Hawaii	
11	Bristol		Bristol	Bristol		Bristol	Bristol	Bristol	
12	Bristol	Bristol		Bristol		Bristol	Bristol	Hawaii	
13	Bristol			Bristol		Bristol	Bristol	Bristol	
14	Bristol			Bristol	Bristol	Bristol	Bristol	Hawaii	
15	Bristol		Bristol	Bristol	Bristol	Bristol	Bristol	Bristol	
16	Bristol			Bristol	Bristol	Bristol	Bristol	Bristol	AH3327
17	Bristol		Bristol	Bristol		Bristol	Bristol	Bristol	
18	Bristol			Bristol	Bristol	Bristol	Bristol	Bristol	
19	Bristol		Bristol	Bristol		Bristol	Bristol	Hawaii	AH3328
20	Bristol			Bristol		Bristol	Bristol	Hawaii	
21	Bristol		Bristol	Bristol		Bristol	Bristol	Bristol	
22	Bristol			Bristol		Bristol	Bristol	Bristol	
23	Bristol		Bristol	Bristol		Bristol	Bristol	Hawaii	AH3330
24	Bristol			Bristol		Bristol	Bristol	Bristol	
25	Bristol		Bristol	Bristol	Bristol	Bristol	Bristol	Hawaii	
26	Bristol			Bristol	Bristol	Bristol	Bristol	Hawaii	
27	Bristol	Bristol				Bristol	Bristol	Hawaii	
28	Bristol	Bristol	Bristol	Bristol		Bristol	Bristol	Hawaii	
29	Bristol		Bristol	Bristol	Bristol	Bristol	Bristol	Bristol	AH3329
30	Bristol			Bristol	Bristol	Bristol	Bristol	Bristol	
31	Bristol	Bristol		Bristol		Bristol	Bristol	Bristol	
32	Bristol	Bristol		Bristol		Bristol	Bristol	Bristol	
33	Bristol		Bristol	Bristol	Bristol	Bristol	Bristol	Hawaii	
34	Bristol			Bristol		Bristol	Bristol	Bristol	
35	Bristol	Bristol	Bristol	Bristol	Bristol	Bristol	Bristol	Bristol	
36	Bristol		Bristol	Bristol		Bristol	Bristol	Hawaii	
37	Bristol			Bristol	Bristol	Bristol	Bristol	Hawaii	
38	Bristol			Bristol	Bristol	Bristol	Bristol	Hawaii	
39	Bristol			Bristol		Bristol	Bristol	Hawaii	
40	Bristol			Bristol		Bristol	Bristol	Bristol	
41	Bristol				Bristol	Bristol	Bristol	Bristol	
42	Bristol			Bristol	Bristol	Bristol	Bristol	Hawaii	
43	Bristol	Bristol		Bristol		Bristol	Bristol	Hawaii	
44	Bristol		Bristol	Bristol		Bristol	Bristol	Bristol	
45	Bristol			Bristol		Bristol	Bristol	Hawaii	
46	Bristol			Bristol	Bristol	Bristol	Bristol	Bristol	
47	Bristol			Bristol	Bristol	Bristol	Bristol	Hawaii	
48	Bristol			Bristol		Bristol	Bristol	Bristol	

Lysate

Strain

Table 3.3. Genetic constitution of *bar-1(ga80)* mutants introgressed with ewIR17 (chromosome I). The genomic location is defined by FLP marker positions and the constitution of ewIR17 is indicated as a reference. 48 lysates were mapped and stored strains are named. Black indicates Hawaiian sequence and grey indicates N2 Bristol sequence. White bars indicate inconclusive sequencing results.

3.1.4 Two QTLs on chromosome I affect WNT signalling

We continued our analysis by determining the vulval induction index of selected strains to verify and locally restrict the QTL on chromosome I. We counted vulval induction of several lines, since we expected the presence of background mutations we had not genotyped for and that may influence induction. As expected, we observed a range of vulval induction indexes for both the outcrossed and the introgressed lines (**Tables 3.4, 3.5, 3.6**). With the assumption that analysing a number of lines balances the effect of background mutations, we found that the VI of *bar-1(ga80)* mutant animals was increased when the CB4856 introgressions of ewIR9, ewIR10 and ewIR17 were fully present. However, a small CB4856 genomic region at the marker position ZH1-06 only (obtained from recombination in ewIR10) did not change the VI (line #34 and AH3331). Interestingly, a complex introgression in AH3367 (**Table 3.2**, CB4856 sequence at positions ZH1-22, possibly ZH1-23, ZH1-15 and ZH1-06 and N2 Bristol sequence at position ZH1-05, ZH1-08 and ZH1-09) suppressed vulval induction compared to the outcrossed *bar-1(ga80)* mutant lines, thereby contradicting our previous finding. However, we did not consider the result of this line as we had no supportive data from similar lines at this point. At the same time, the Kammenga group found a significant contribution to the change in WNT signalling strength by the introgressions provided by ewIR13 and ewIR14 (J. Kammenga, personal communication).

	Line / Strain	Mean VI	95% C.I.
***bar-1(ga80)* mutant siblings without introgression**	AH3335	2.25	2.04 - 2.47
	Line #9	2.26	2.01 - 2.48
	Line #13	2.59	2.40 - 2.76
	AH3333	2.68	2.50 - 2.83
	Line #17	2.70	2.56 - 2.81
	AH3370	2.80	2.66 - 2.92
	average of all	**2.52**	**2.43 - 2.59**
ewIR9; *bar-1(ga80)*	Line #25	2.36	1.92 - 2.76
	Line #23	2.75	2.55 - 2.93
	AH3383	2.78	2.57 - 2.93
	AH3334	2.78	2.68 - 2.88
	AH3382	2.79	2.68 - 2.89
	Line #15	2.86	2.64 - 3.00
	Line #16	2.86	2.76 - 2.94
	Line #40	2.88	2.70 - 3.00
	Line #27	2.92	2.81 - 3.00
	average of all	**2.78*** **	**2.71 - 2.84**

Table 3.4. Mean VI and 95% confidence intervals of *bar-1(ga80)* mutants with and without the ewIR9 introgression. The values were derived from bootstrapping 1000 samples. *** indicates $p < 0.001$.

These findings indicate the presence of two rather than one QTL affecting vulval induction of *bar-1(ga80)* mutant animals: The Hawaiian sequence at position ZH1-06, which is located distally to the ewIR9 introgression and within the ewIR17 (beginning) and ewIR10 (end) introgressions, did not contribute to the phenotype. Furthermore, the ewIR13 and ewIR14 introgressions are located within the ewIR9 introgression and both changed vulval induction (J. Kammenga, personal communication). Thus, we suspect a larger QTL of 1.52 Mb (I: 9569913-11085294) covered by ewIR13 and a smaller QTL of 0.9 Mb (I: 14162929 – 15059001) within ewIR17 (**Fig. 3.3**). Furthermore, these results suggest that the QTL regions found in the *let-60(n1046)* and *bar-1(ga80)* backgrounds do not overlap.

		Line / Strain	Mean VI	95% C.I.
***bar-1(ga80)* mutant siblings without introgression**		AH3381	1.84	1.36 - 2.30
		AH3332	1.90	1.52 - 2.24
		AH3418	2.01	1.69 - 2.31
		Line #8	2.02	1.61 - 2.41
		Line #10	2.48	2.23 - 2.71
		Line #17	2.59	2.37 - 2.78
		Line #19	2.76	2.64 - 2.86
		average of all	**2.24**	**2.12 - 2.37**
ewIR10; bar-1(ga80)	small introgression	AH3367	1.53	1.18 - 1.89
		Line #34	2.34	2.00 - 2.62
		AH3331	2.35	2.10 - 2.57
		average of all	**2.16**	**1.99 - 2.33**
	entire introgression	AH3378	2.61	2.46 - 2.75
		Line #37	2.73	2.59 - 2.84
		Line #42	2.83	2.70 - 2.94
		AH3380	2.88	2.77 - 2.97
		average of all	**2.73*** **	**2.66 - 2.80**

Table 3.5. Mean VI and 95% confidence intervals of *bar-1(ga80)* mutants with and without the ewIR10 introgression (full and partial). The values were derived from bootstrapping 1000 samples. *** indicates $p < 0.001$.

	Line / Strain	Mean VI	95% C.I.
***bar-1(ga80)* mutant siblings without introgression**	Line #30	2.16	1.90 - 2.43
	AH3377	2.18	1.90 - 2.44
	Line #4	2.52	2.21 - 2.76
	Line #35	2.66	2.49 - 2.82
	AH3329	2.74	2.57 - 2.87
	average of all	**2.46**	**2.36 - 2.56**
ewIR17; *bar-1(ga80)*	Line #25	2.17	1.92 - 2.44
	Line #33	2.18	1.92 - 2.42
	AH3328	2.43	2.08 - 2.73
	Line #14	2.82	2.60 - 2.98
	AH3330	2.86	2.76 - 2.95
	Line #25	2.86	2.75 - 2.95
	Line #1	2.90	2.77 - 2.99
	average of all	**2.74*** **	**2.66 - 2.80**

Table 3.6. Mean VI and 95% confidence intervals of *bar-1(ga80)* mutants with and without the ewIR17 introgression. The values were derived from bootstrapping 1000 samples. *** indicates $p < 0.001$.

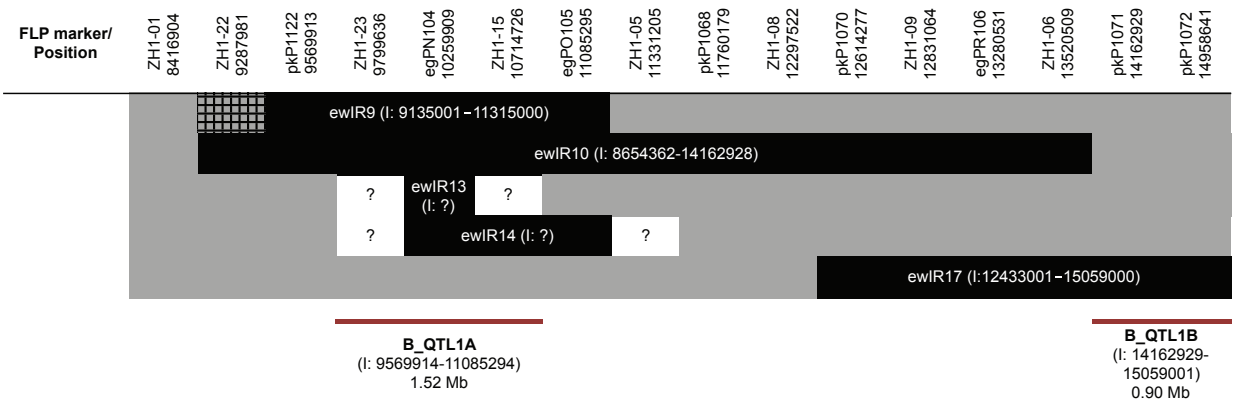

Figure 3.3. Local refinement of the QTL1 in the *bar-1(ga80)* mutant background. Introgression line analysis revealed two smaller QTLs where vulval induction is increased by the CB4856 sequence. B_QTL1A spans 1.52 Mb while B_QTL1B comprises 0.9 Mb. Black – CB4856 introgression, grey – N2 Bristol genomic region. Sequencing and FLP mapping information in the strains ewIR13 and ewIR14 were not fully available at the time of analysis (marked with "?"). We did not genotype the ewIR9 strain at the position ZH1-22 but expect the presence of the CB4856 region according to the WGS data (shaded rectangle).

3.1.5 RNAi screen of polymorphic genes within the B_QTL1B region

To identify polymorphic genes that modify vulval induction in *bar-1(ga80)* mutant animals, we performed RNAi against genes that either contain coding SNPs (Thompson et al. 2015) or are (partially) deleted between CB4856 and N2 (Maydan et al. 2010). The smaller B_QTL1B (0.9 Mb) region contains 45 such genes (**Table 3.7**) while we identified 55 polymorphic genes within the B_QTL1A region (**Table 7.1**, Appendix). The amino acid changes caused by the SNP are indicated in brackets, if several isoforms are affected. We started our RNAi analysis with the smaller QTL and used bacterial clones from commercially available RNAi libraries (Reboul et al. 2001; Rual et al. 2004) that we verified by sequencing. We knocked down the candidate genes in AH3330 (miIL) and AH3377 (*bar-1(ga80)* sibling mutant line without introgression). Thirteen genes were not analysed, either due to the lack of corresponding RNAi clones or because the gene sequence could not be verified by sequencing (see **Table 3.7** for details).

Table 3.7. List of polymorphic genes within the QTL1B region in the *bar-1(ga80)* mutant background. Brackets indicate that several isoforms are affected by the SNP.

Gene	Sequence name	Amino acid change	RNAi
-	*C37A5.11*[1)]	Thr15Ala	-
-	*C37A5.7*	[Arg147Gly, Arg147Gly]	no change / n.a.
pry-1	*C37A5.9*	Glu229Gly, Met233Val	diff. change
pes-7	*F09C3.1*[2)]	Leu372Gln	n.a.
fbxa-103	*F09C3.4*	Gln44Lys, Gly285Cys	no change
-	*F11C3.1*	Phe283Cys, Phe283Val	no change
unc-122	*F11C3.2*[2)]	Ile503Ser, Leu15Arg	n.a.
-	*F21F12.1*	[Ala88Pro, Ala88Pro]	no change
-	*F31C3.3*	Gln526Lys, Met1581Val, Thr758Ala, Val89Leu	no change
-	*F31C3.6*	Tyr25Ser	no change
maph-1.1	*F32A7.5*	[Gly663Val, Gly535Val, Gly663Val]	no change
str-245	*F32A7.7*	Ala141Thr	no change
-	*F33H2.2*	Ser398Cys	no change / n.a.
set-10	*F33H2.7*	Leu52Met	no change
sur-2	*F39B2.4*[2)]	[Ile1486Met, Ile1488Met]	n.a.
mtcu-1	*F39B2.7*	[Glu53Asp, Glu53Asp], [Ser24Pro, Ser24Pro]	diff. change
-	*F49B2.3*	Thr88Ala	diff. change
-	*F49B2.7*[1)]	Arg58Gln, Asp201Gly, Phe188Leu, Ser232Arg, Val-39Leu	n.a.
clec-116	*K04H8.1*	Cys104Arg, Gln223Lys	no change
-	*K04H8.2*[2)]	Ala203Glu, Asn150Asp	n.a.

-	*K05C4.2*	[Val22Ile, Val22Ile, Val22Ile]	no change
-	*K05C4.3*	Gly319Glu, Ile114Leu, Lys107Asn, Met473Thr	no change
-	*K05C4.4*[2)]	Arg36His, Glu159Asp	n.a.
-	*K05C4.7*	[Ala267Thr, Ala267Thr]	no change / n.a.
-	*K05C4.8*[2)]	Gly32Glu, Phe95Leu	n.a.
-	*K05C4.9*	deletion	diff. change
hpo-13	*Y105E8A.10*[2)]	[His947Gln, His918Gln, His910Gln, His910Gln, His-910Gln]	n.a.
-	*Y105E8A.13*[1)]	Ala237Pro	n.a.
yars-1	*Y105E8A.19*	Leu213Val	developmental arrest
-	*Y105E8A.20*	[Glu396Val, Glu278Val, Glu278Val], [Phe503Leu, Phe385Leu, Phe385Leu]	no change
-	*Y105E8A.21*	[Arg720Ser, Arg720Ser]	no change
rpom-1	*Y105E8A.23*	[Asp216Asn, Asp216Asn], [Val56Ile, Val56Ile]	no change / n.a.
-	*Y105E8A.25*	Met7Ile	diff. change
eat-18	*Y105E8A.7*	[Gly688Ser, Gly688Ser]	no change
-	*Y105E8A.8*[2)]	Thr262Ile	n.a.
ttm-5	*Y54E5A.1*	Ile191Val	no change
-	*Y54E5A.2*	Ile57Leu, Ser14Pro, Tyr48Phe	no change
npp-4	*Y54E5A.4*	[Thr354Ser, Thr354Ser]	developmental arrest
smp-1	*Y54E5B.1*	Ile666Met	no change
frm-1	*ZK270.2*	[Gly3386Trp, Gly3375Trp, Gly3375Trp, Gly3375Trp, Gly3375Trp], [Leu645Pro, Leu634Pro, Leu634Pro, Leu634Pro, Leu634Pro], [Ser3949Pro, Ser3938Pro, Ser3938Pro, Ser3938Pro, Ser3938Pro], [Tyr3704Ser, Tyr3693Ser, Tyr3693Ser, Tyr3693Ser, Tyr3693Ser]	no change
tep-1	*ZK337.1*	[Arg112Gly, Arg112Gly, Arg112Gly, Arg112Gly, Arg-112Gly, Arg112Gly]	no change / n.a.
-	*ZK849.1*	Cys313Arg	no change
best-25	*ZK849.4*[2)]	Leu519Pro	n.a.
best-26	*ZK849.5*	Ser58Arg	diff. change
-	*ZK849.6*[1)]	Asn58Ser, Ser28Tyr	n.a.

[1)] Gene was not analysed due to the lack of a corresponding RNAi clone.

[2)] Gene was not analysed since the sequence of the RNAi clone could not be verified by Sanger sequencing.

The knock-down of *C37A5.7, F33H2.2, ZK337.1, K05C4.7* and *Y105E8A.23* was not analysed, partially due to a bacterial contamination. We observed a developmental arrest in worms when we knocked down *Y105E8A.19 (yars-1)* or *Y54E5A.4 (npp-4)* in either strain, so that vulval induction could not be scored. We screened further genes and found no difference in vulval induction compared to the empty vector control when we knocked down the genes *F09C3.4 (fbxa-103), F11C3.1, F21F12.1, F31C3.3, F31C3.6, F32A7.5 (maph-1.1), F32A7.7 (str-245), F33H2.7, K04H8.1 (clec-116), K05C4.2, K05C4.3, Y105E8A.20, Y105E8A.21, Y105E8A.7 (eat-18), Y54E5A.1 (ttm-5), Y54E5A.2, ZK270.2 (frm-1), ZK849.1* or *Y54E5B.1 (smp-1)*. The silencing of *C37A5.9 (pry-1), F39B2.7 (mtcu-1), F49B2.3, K05C4.9, Y105E8A.29* and *ZK849.5* resulted in significant changes in vulval induction in either AH3330 or AH3377 (**Table 3.8** and **Fig. 3.4**). Changes in the VI of both strains upon RNAi were not observed.

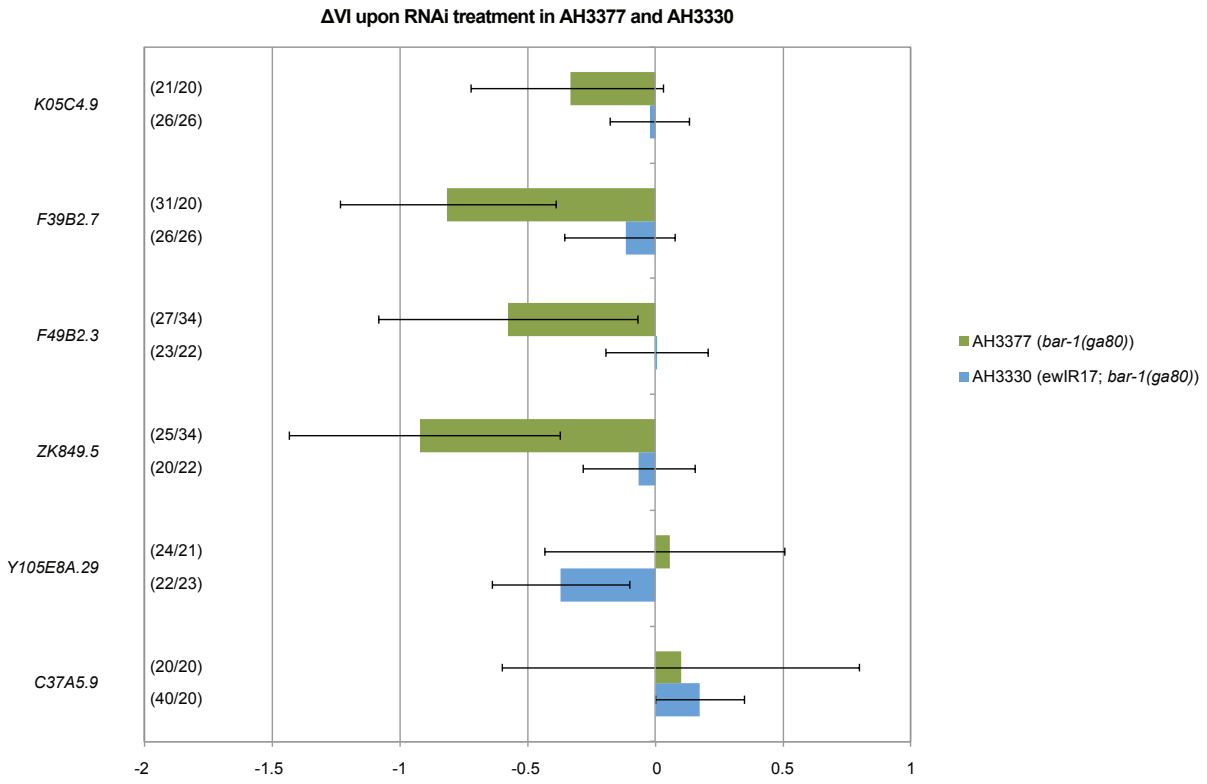

Figure 3.4. The knock-down of polymorphic genes affects Wnt signalling in either *bar-1(ga80)* (AH3377) or *ewIR17; bar-1(ga80)* (AH3330) animals (genome-specific modifiers). The difference in VI as compared to the respective empty vector controls is shown. Values were derived from bootstrapping 1000 samples. The number of animals analysed is indicated in brackets (RNAi clone/eV). Error bars indicate the 95% confidence interval.

Table 3.8. Differential change in the vulval induction index of AH3330 and AH3377 upon RNAi.

		Mean	95% C.I.	P	% Vul	n
Y105E8A.29	*ewIR17; bar-1(ga80)*[1)]	2.53	2.25 - 2.80	0.008	40.9	22
	bar-1(ga80)[1)]	1.75	1.38 - 2.10	0.403	83.3	24
C37A5.9	*ewIR17; bar-1(ga80)*[2)]	2.97	2.92 - 3.00	0.009	2.5	40
	bar-1(ga80)[2)]	1.91	1.42 - 2.35	0.183	85.0	20
ZK849.5	*ewIR17; bar-1(ga80)*[3)]	2.77	2.60 - 2.93	0.762	35.0	20
	bar-1(ga80)[3)]	1.14	0.74 - 1.54	0.001	84.0	25
F49B2.3	*ewIR17; bar-1(ga80)*[3)]	2.85	2.71 - 2.96	0.463	21.7	23
	bar-1(ga80)[3)]	1.48	1.07 - 1.90	0.016	85.2	27
F39B2.7	*ewIR17; bar-1(ga80)*[4)]	2.79	2.57 - 2.95	0.839	23.1	21
	bar-1(ga80)[4)]	1.88	1.53 - 2.24	0.001	58.3	31
K05C4.9	*ewIR17; bar-1(ga80)*[5)]	2.86	2.73 - 2.96	0.562	11.5	26
	bar-1(ga80)[4)]	2.31	2.00 - 2.60	0.021	33.3	21
eV[1)]	*ewIR17; bar-1(ga80)*	2.89	2.76 - 3.00	-	13.0	23
	bar-1(ga80)	1.70	1.36 - 2.00	-	85.7	21
eV[2)]	*ewIR17; bar-1(ga80)*	2.80	2.60 - 2.95	-	20.0	20
	bar-1(ga80)	1.57	1.10 - 2.08	-	80.0	20
eV[3)]	*ewIR17; bar-1(ga80)*	2.84	2.68 - 2.98	-	18.2	22
	bar-1(ga80)	2.05	1.72 - 2.38	-	64.7	34
eV[4)]	*ewIR17; bar-1(ga80)*	2.90	2.80 - 2.98	-	20.0	20
	bar-1(ga80)	2.70	2.50 - 2.90	-	35.0	20
eV[5)]	*ewIR17; bar-1(ga80)*	2.89	2.77 - 3.00	-	11.5	26
	bar-1(ga80)	-	-	-	-	-

3.1.6 Identification of candidate genes within QTL1a affecting RAS/MAPK signalling

The QTL1a region affecting RAS/MAPK signalling had been previously restricted to the genomic introgression provided by ewIR5 (I: 6280001-10873000) without the overlapping region from ewIR2 and ewIR9 (Schmid et al. 2015 and **Fig. 3.5**). Since the *let-60(n1046)* mutant strain that had carried the introgression of ewIR5 was not available anymore, we re-created the milL and verified it via PCR and sequencing (in terms of the *let-60* locus) as well as FLP mapping as explained above. Similarly, recombination during the crossing resulted in lines that carry smaller parts of the introgressed region present in ewIR5 (**Table 3.9** and **Fig. 3.5**).

Lysate	Genomic location								Strain
	ZH1-18a	ZH1-03	ZH1-27	ZH1-34	ZH1-01	ZH1-22	ZH1-23	ZH1-15	
CB	Hawaii	Hawaii	Hawaii	Hawaii	Hawaii	Hawaii	Hawaii	Hawaii	
N2	Bristol	Bristol	Bristol	Bristol	Bristol	Bristol	Bristol	Bristol	
ewIR5	Bristol	Bristol	Bristol	Hawaii	Hawaii	Hawaii	Hawaii	Hawaii	
1	Bristol	Bristol		Bristol	Bristol	Bristol	Bristol	Bristol	AH3323
2	Bristol	Bristol	Bristol		Hawaii	Hawaii	Hawaii	Hawaii	
3	Bristol	Bristol			Hawaii	Hawaii	Hawaii	Hawaii	
4	Bristol	Bristol		Bristol	Bristol		Bristol	Bristol	
5	Bristol	Bristol			Bristol	Bristol	Bristol	Bristol	
6	Bristol	Bristol		Hawaii	Hawaii	Hawaii	Hawaii	Bristol	AH3321
7	Bristol	Bristol		Hawaii	Hawaii	Hawaii	Hawaii	Hawaii	
8	Bristol	Bristol		Bristol	Bristol	Bristol	Bristol	Bristol	
9	Bristol	Bristol			Bristol	Bristol	Bristol	Bristol	
10	Bristol	Bristol	Bristol		Bristol	Bristol	Bristol	Bristol	
11	Bristol	Bristol			Hawaii	Hawaii	Hawaii	Hawaii	
12	Bristol	Bristol			Bristol	Bristol	Bristol	Bristol	
13	Bristol	Bristol	Bristol	Hawaii	Hawaii	Hawaii	Hawaii	Hawaii	AH3363
14	Bristol	Bristol			Bristol	Bristol	Bristol	Bristol	
15	Bristol	Bristol		Bristol	Bristol	Bristol		Bristol	
16	Bristol	Bristol	Bristol	Hawaii	Hawaii	Hawaii	Hawaii	Hawaii	AH3322
17	Bristol	Bristol			Hawaii	Hawaii	Hawaii	Hawaii	
18	Bristol	Bristol	Bristol		Bristol	Bristol	Bristol	Bristol	
19	Bristol	Bristol			Bristol	Bristol	Bristol	Bristol	
20	Bristol	Bristol			Hawaii	Hawaii	Hawaii	Hawaii	
21	Bristol	Bristol	Bristol	Hawaii	Hawaii	Hawaii	Hawaii	Hawaii	AH3320
22	Bristol	Bristol			Hawaii	Hawaii	Hawaii	Bristol	
23	Bristol	Bristol			Hawaii	Hawaii	Hawaii	Hawaii	
24	Bristol	Bristol			het	het	het	het	
25	Bristol	Bristol	Bristol		Hawaii	Hawaii	Hawaii	Hawaii	
26	Bristol	Bristol	Bristol		Hawaii	Hawaii	Hawaii	Hawaii	
27	Bristol	Bristol			Bristol	Bristol	Bristol	Bristol	
28	Bristol	Bristol			Bristol	Bristol	Bristol	Bristol	
29	Bristol	Bristol		Bristol	Bristol	Bristol	Bristol	Bristol	
30	Bristol	Bristol			Hawaii	Hawaii	Hawaii	Bristol	
31	Bristol	Bristol			Hawaii	Hawaii	Hawaii	Hawaii	
32	Bristol	Bristol		Bristol	Bristol	Bristol	Bristol	Bristol	
33	Bristol	Bristol	Bristol		Bristol	Bristol	Bristol	Bristol	
34	Bristol	Bristol	Bristol		Hawaii	Bristol	Bristol	Bristol	AH3319
35	Bristol	Bristol			Bristol	Bristol	Bristol	Bristol	
36	Bristol	Bristol			Bristol	Bristol	Bristol	Bristol	
37	Bristol	Bristol		Bristol	Bristol	Bristol	Bristol	Bristol	
38	Bristol	Bristol		Bristol	Bristol	Bristol	Bristol	Hawaii	AH3325
39	Bristol	Bristol		Bristol	Bristol	Bristol	Bristol	Bristol	AH3362
40	Bristol	Bristol	Bristol	Bristol	Bristol	Bristol	Bristol	Bristol	AH3326
41	Bristol	Bristol	Bristol		Bristol	Bristol	Bristol	Bristol	
42	Bristol	Bristol	Bristol		Bristol	Bristol	Bristol	Bristol	
43	Bristol	Bristol			Bristol	Bristol	Bristol	Bristol	
44	Bristol	Bristol		Hawaii	Hawaii	Hawaii	Hawaii	het	
45	Bristol	Bristol		Hawaii	Hawaii	Hawaii	Bristol	Bristol	AH3324
46	Bristol	Bristol			Bristol	Bristol	Bristol	Bristol	
47	Bristol	Bristol			Bristol	Bristol	Bristol	Bristol	
48	Bristol	Bristol		Bristol	Bristol	Bristol	Bristol	Bristol	

Table 3.9. Genetic constitution of *let-60(n1046)* mutants introgressed with ewIR5 (chromosome I). The genomic location is defined by FLP marker positions and the constitution of ewIR5 is indicated as a reference. 48 lysates were mapped and stored strains are named. Black indicates Hawaiian sequence and grey indicates N2 Bristol sequence. Blue bars indicate heterozygousity (double peak in the sequence) and white bars indicate inconclusive sequencing results.

We determined the vulval induction index of selected lines and verified the increase in vulval induction by the full CB4856 introgression provided by ewIR5 (**Table 3.10** and **Fig. 3.5**). Furthermore, vulval induction of *let-60(n1046)* mutant animals was increased significantly in lines carrying the CB4856 sequence at the marker positions ZH1-34, ZH1-01, ZH1-22 and ZH1-23 (e.g. AH3321). RAS/MAPK signalling was still enhanced when the CB4856 sequence was present at ZH1-34, ZH1-01 and ZH1-22 only (AH3324). Finally, the vulval induction index was unchanged in *let-60(n1046)* mutant lines positive for the Hawaiian sequence at positions ZH1-34 and ZH1-01 (AH3319) or ZH1-15 only (AH3325) (**Table 3.10** and **Fig. 3.5**) (Note that in AH3319, the genotyping was inconclusive at the marker position ZH1-34, but we assumed the presence of CB4856 sequence since double recombination seemed unlikely). These findings suggest that modifiers of RAS/MAPK signalling are present at and closely around the ZH1-22 marker position. Since previous analyses had excluded a contribution by the ewIR2 and ewIR9 introgressions (Schmid et al. 2015), the QTL1a region containing modifiers could be placed at I: 8416905-9135000, thus spanning 0.7 Mb (**Fig. 3.5**).

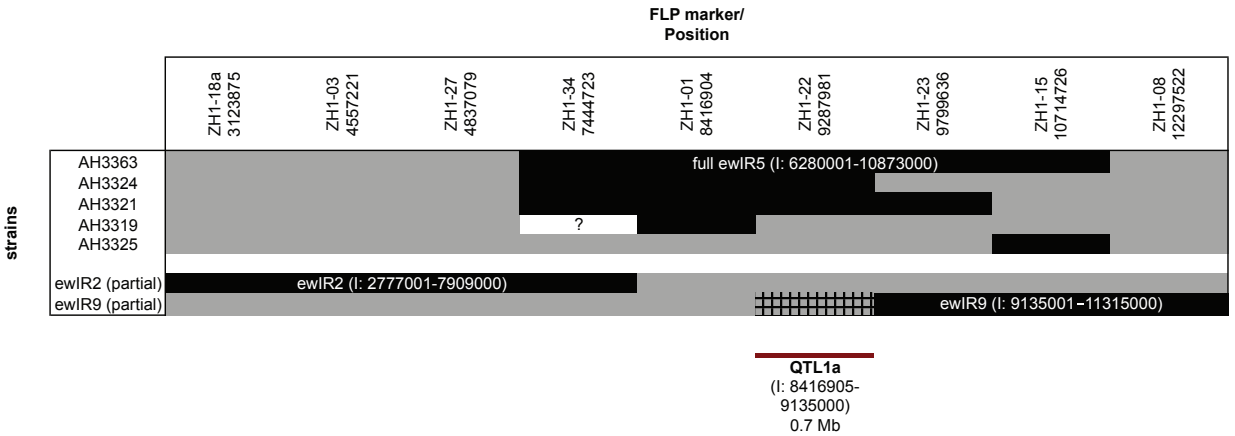

Figure 3.5. Local refinement of the QTL1a in the *let-60(n1046)* mutant background. Introgression line analysis revealed a smaller QTL where vulval induction is increased by the CB4856 sequence. The QTL1a spans 0.7 Mb. Black – CB4856 introgression, grey – N2 Bristol genomic region. The sequencing and FLP mapping information at the marker position ZH1-34 in AH3319 was inconclusive and is marked with „?“. We did not genotype the ewIR9 strain at the position ZH1-22 but expect the presence of the CB4856 region according to the WGS data (shaded rectangle).

	Line / Strain	Mean VI	95% C.I.
***let-60(n1046)* mutant siblings without introgression**	Line #37	3.37	3.17 - 3.56
	AH3362	4.24	3.86 - 4.62
	Line #10	3.29	3.12 - 3.48
	AH3323	3.52	3.25 - 3.83
	AH3326	3.76	3.50 - 4.02
	Line #42	3.47	3.28 - 3.67
	Line #29	3.50	3.23 - 3.83
	average of all	**3.57**	**3.47 - 3.67**
ewIR5; *let-60(n1046)* entire introgression	AH3363	4.31	4.02 - 4.62
	Line #7	3.96	3.66 - 4.28
	Line #2	3.48	3.25 - 3.70
	Line #3	3.69	3.40 - 3.98
	AH3320	4.24	3.94 - 4.52
	AH3322	3.92	3.61 - 4.30
	average of all	**3.97*** **	**3.84 - 4.10**
***ewIR5; let-60(n1046)* partial introgression**	AH3319	3.65	3.43 - 3.87
	AH3325	3.50	3.28 - 3.73
	Line #22	3.59	3.40 - 3.79
	Line #30	3.50	3.28 - 3.75
	AH3324	3.95**	3.67 - 4.23
	AH3321	3.98***	3.79 - 4.19

Table 3.10. Mean VI and 95% confidence intervals of *let-60(n1046)* mutants with and without the ewIR5 introgression (full or partial). The values were derived from bootstrapping 1000 samples. *** indicates $p < 0.001$ and ** $p < 0.01$.

We looked for polymorphic genes in this region and found 47 genes carrying coding SNPs between the N2 Bristol and CB4856 Hawaiian genomes (Thompson et al. 2015) (**Table 3.11**). We performed RNAi against 41 genes of which i) clones were available and ii) the sequences could be verified by sequencing (see **Table 3.11** for details). We employed AH3326 (*let-60(n1046)* in the “pure” N2 Bristol background) and AH3363 (*let-60(n1046)* miIL). As we had expected, we found candidates affecting RAS/MAPK signalling in one background only (**Table 3.12** and **Fig. 3.6**) or in both backgrounds (**Table 3.13** and **Fig. 3.7**).

Table 3.11. List of polymorphic genes within the QTL1a region in the *let-60(n1046)* mutant background. Brackets indicate that several isoforms are affected by the SNP.

Gene	Sequence name	Amino acid change	RNAi
-	*C31H5.1*	Ala112Val	no change
-	*C36B1.9*[1)]	Ile107Thr	n.a.
ceh-6	*K02B12.1*	Ser167Asn, Pro341Leu	diff. change
cle-1	*C36B1.1*	[Val240Asp, Val240Asp]	no change
cutl-7	*F53B6.6*	Lys562Thr	no change
-	*D1081.10*[1)]	Val182Leu, Asn105His, Glu179Lys	n.a.
-	*D1081.4*	Asn150Asp	no change
-	*D1081.5*	Leu269Ser	change in both
-	*D1081.9*	Ile178Leu	no change
-	*F25H5.7*	Val149Asp	no change
-	*F29D10.3*	Gly300Cys	change in both
-	*F32H2.10*	Phe84Ser	diff. change
-	*F32H2.6*	Ser142Leu	developmental arrest
-	*F32H2.7*	Glu247Gly	no change
-	*F36A2.13*	[Ala1848Val, Ala1848Val], [Asn2045Ser, Asn2045Ser], [Ser2639Thr, Ser2639Thr], [Val-2627Gly, Val2627Gly]	no change
-	*F36A2.2*	Asn398Asp	change in both
-	*F39H11.1*	[Lys24Gln, Lys24Gln]	no change
-	*F43G9.12*	Phe478Ile	sterility
-	*F43G9.3*	Gln163Arg	no change
-	*F53B6.4*	Thr120Lys	no change
-	*F55H12.3*	Glu1733Asp, Phe2921Val, Cys973Phe, Asn-2941His, Gln580Lys	diff. change
fasn-1	*F32H2.5*	Pro420Leu	death at L1/L2
fcp-1	*F36F2.6*	Val654Ala	diff. change
fer-1	*F43G9.6*	[Gly1454Asp, Gly1327Asp, Gly1327Asp], [Gln-1317Lys, Gln1190Lys, Gln1190Lys], [Gln1919His, Gln1792His, Gln1792His]	diff. change
gls-1	*C36B1.8*	[Pro708Ser, Pro708Ser, Pro664Ser]	no change
gon-2	*T01H8.5*	[Ala1115Val, Ala1176Val, Ala1075Val, Ala770Val], [Met668Leu, Met729Leu, Met628Leu, Met323Leu]	diff. change
-	*K02B12.2*	Ala85Glu	no change
-	*K02B12.5*	Leu569Arg	no change

-	*K07A12.1*	[Arg154His, Arg154His]	change in both
mrps-15	*K07A12.7*	Thr95Ile	sterility
mrt-1	*F39H2.5*[1)]	[Ser527Tyr, Ser527Tyr]	n.a.
pqn-26	*DY3.5*	Leu22Ser	diff. change
prmt-7	*W06D4.4*	[Thr617Ile, Thr617Ile]	no change
-	*R05D11.5*[2)]	[Leu158Met, Leu158Met]	n.a.
-	*R05D11.9*[1)]	Ala301Val	n.a.
rad-54	*W06D4.6*	Ala127Thr	diff. change
rskn-1	*T01H8.1*	[Ala439Ser, Ala445Ser, Ala406Ser, Ala388Ser, Ala426Ser, Ala426Ser]	change in both
sec-12	*K02B12.3*	Glu17Asp	death at L1/L2
sup-17	*DY3.7*	[Phe195Leu, Phe195Leu]	change in both
syx-7	*F36F2.4*[2)]	[Ala127Ser, Ala127Ser]	n.a.
-	*T08G11.1*	[Pro1704Gln, Pro1704Gln, Pro1704Gln], [Val2807Ala, Val2807Ala, Val2834Ala]	no change
-	*T08G11.2*	Leu131Ser	no change
-	*T08G11.3*	His491Gln	no change
-	*W06D4.3*	Cys147Phe, Cys147Ser	change in both
-	*ZK858.5*	Glu384Gln	diff. change
-	*ZK858.6*	[Pro181Leu, Pro181Leu, Pro218Leu]	no change
-	*ZK858.7*	Val297Ala	change in both

[1)] Gene was not analysed due to the lack of a corresponding RNAi clone.

[2)] Gene was not analysed since the sequence of the RNAi clone could not be verified by Sanger sequencing.

RNA interference of *F32H2.6, F43G9.12, F32H2.5 (fasn-1), F36F2.6 (fcp-1)* and *K02B12.3 (sec-12)* caused developmental defects and vulval induction could not be scored. The knockdown of *F43G9.12* and *K07A12.7 (mrps-15)* led to sterility of the P0 generation and no progeny while worms subjected to on *F32H2.5 (fasn-1)* or *K02B12.3 (sec-12)* RNAi died at the L1/L2 stage. Interestingly, the non-introgressed *let-60(n1046)* mutant strain AH3326 died as embryos on *F32H2.6* RNAi, whereas the introgressed worms (AH3363) hatched and lived but arrested soon thereafter. Moreover, the reduction of *F36F2.6 (fcp-1)* resulted in a developmental delay of approx. one day for the non-introgressed line and a 1.5 – 2 days delay for the introgressed line as well as an overall sick appearance of both strains. Nevertheless, vulval induction was scored and was affected in AH3363 but not AH3326 (**Table 3.12** and **Fig. 3.6**). A genomic background specific change in vulval induction was furthermore discovered when *K02B12.1 (ceh-6), T01H8.5 (gon-2), F32H2.10, F55H12.3, F43G9.6 (fer-1), W06D4.6 (rad-54)* or *ZK858.5* were knocked down.

Table 3.12. Differential change in the vulval induction index of AH3326 and AH3363 upon RNAi.

		Mean	95% C.I.	P	% Muv	n
K02B12.1	*ewIR5; let-60(n1046)*[1)]	4.99	4.65 - 5.33	0.942	100.0	20
	let-60(n1046)[1)]	5.15	4.91 - 5.40	0.000	100.0	29
T01H8.5	*ewIR5; let-60(n1046)*[1)]	4.49	4.12 - 4.86	0.310	85.7	21
	let-60(n1046)[1)]	4.87	4.59 - 5.13	0.013	96.4	28
F32H2.10	*ewIR5; let-60(n1046)*[2)]	4.08	3.75 - 4.40	0.539	71.9	32
	let-60(n1046)[2)]	4.52	4.23 - 4.82	0.000	93.3	30
F36F2.6	*ewIR5; let-60(n1046)*[2)]	3.22	3.06 - 3.42	0.000	27.8	18
	let-60(n1046)[2)]	3.60	3.29 - 3.95	0.272	42.9	21
F55H12.3	*ewIR5; let-60(n1046)*[3)]	4.79	4.48 - 5.08	0.313	91.7	24
	let-60(n1046)[3)]	5.19	4.95 - 5.40	0.003	100.0	29
F43G9.6	*ewIR5; let-60(n1046)*[4)]	3.81	3.48 - 4.09	0.001	57.6	33
	let-60(n1046)[4)]	3.83	3.52 - 4.16	0.365	60.0	25
W06D4.6	*ewIR5; let-60(n1046)*[5)]	4.93	4.64 - 5.23	0.829	100.0	22
	let-60(n1046)[5)]	5.13	4.89 - 5.35	0.000	100.0	27
ZK858.5	*ewIR5; let-60(n1046)*[6)]	4.80	4.52 - 5.07	0.230	91.3	23
	let-60(n1046)[6)]	4.34	4.10 - 4.58	0.001	92.0	25
eV[1)]	*ewIR5; let-60(n1046)*	4.62	4.32 - 4.89	-	95.5	22
	let-60(n1046)	4.40	4.13 - 4.69	-	90.3	31
eV[2)]	*ewIR5; let-60(n1046)*	4.06	3.73 - 4.42	-	74.2	31
	let-60(n1046)	3.71	3.45 - 3.97	-	63.3	30
eV[3)]	*ewIR5; let-60(n1046)*	4.88	4.67 - 5.07	-	96.6	29
	let-60(n1046)	4.67	4.42 - 4.93	-	96.7	30
eV[4)]	*ewIR5; let-60(n1046)*	4.35	4.14 - 4.54	-	88.6	35
	let-60(n1046)	3.90	3.66 - 4.14	-	74.3	35
eV[5)]	*ewIR5; let-60(n1046)*	4.74	4.46 - 5.02	-	96.3	27
	let-60(n1046)	4.50	4.21 - 4.79	-	89.7	29
eV[6)]	*ewIR5; let-60(n1046)*	4.94	4.64 - 5.20	-	96.0	25
	let-60(n1046)	4.83	4.60 - 5.08	-	100.0	24

RNA interference of *ZK858.7, DY3.5 (pqn-26), D1081.5, T01H8.1, W06D4.3, K07A12.1*, *F29D10.3, DY3.7* and *F36A2.2* altered the VI of both AH3363 and AH3326 (**Table 3.13** and **Fig. 3.7**). Note that the knockdown of *ZK858.7* reduced vulval induction to almost wild-type levels in both strains. No change was observed when *C31H5.1, C36B1.1 (cle-1), F53B6.6*

Table 3.13. Changes in the vulval induction index of AH3326 and AH3363 upon RNAi.

		Mean	95% C.I.	P	% Muv	n
T01H8.1	*ewIR5; let-60(n1046)*[1)]	5.10	4.87 - 5.28	0.010	100.0	27
	let-60(n1046)[1)]	5.02	4.79 - 5.23	0.000	100.0	28
W06D4.3	*ewIR5; let-60(n1046)*[2)]	3.00	3.00 - 3.00	0.000	0.0	40
	let-60(n1046)[2)]	3.00	3.00 - 3.00	0.000	0.0	40
K07A12.1	*ewIR5; let-60(n1046)*[3)]	3.34	3.15 - 3.58	0.000	45.0	20
	let-60(n1046)[3)]	3.20	3.10 - 3.37	0.000	33.3	15
F29D10.3	*ewIR5; let-60(n1046)*[4)]	3.80	3.56 - 4.03	0.000	71.9	32
	let-60(n1046)[4)]	4.10	3.82 - 4.38	0.004	86.7	30
D1081.5	*ewIR5; let-60(n1046)*[4)]	3.99	3.77 - 4.12	0.000	86.7	30
	let-60(n1046)[4)]	3.76	3.53 - 4.02	0.000	63.3	30
DY3.7	*ewIR5; let-60(n1046)*[4)]	3.83	3.61 - 4.06	0.000	74.3	35
	let-60(n1046)[4)]	3.63	3.42 - 3.83	0.000	66.7	30
F36A2.2	*ewIR5; let-60(n1046)*[4)]	3.90	3.48 - 4.35	0.000	65.0	20
	let-60(n1046)[4)]	3.93	3.69 - 4.17	0.000	76.9	26
DY3.5	*ewIR5; let-60(n1046)*[5)]	4.64	4.39 - 4.89	0.037	96.4	28
	let-60(n1046)[5)]	4.34	4.08 - 4.62	0.006	88.5	26
ZK858.7	*ewIR5; let-60(n1046)*[6)]	3.03	3.00 - 3.10	0.000	3.2	31
	let-60(n1046)[6)]	3.03	3.00 - 3.10	0.000	3.3	30
eV[1)]	*ewIR5; let-60(n1046)*	4.61	4.32 - 4.90	-	95.5	22
	let-60(n1046)	4.41	4.12 - 4.69	-	90.3	31
eV[2)]	*ewIR5; let-60(n1046)*	4.74	4.48 - 4.98	-	96.3	27
	let-60(n1046)	4.50	4.22 - 4.78	-	89.7	29
eV[3)]	*ewIR5; let-60(n1046)*	4.34	4.24 - 4.54	-	88.6	35
	let-60(n1046)	3.89	3.67 - 4.13	-	74.3	35
eV[4)]	*ewIR5; let-60(n1046)*	4.82	4.62 - 5.03	-	100.0	30
	let-60(n1046)	4.53	4.27 - 4.79	-	91.4	35
eV[5)]	*ewIR5; let-60(n1046)*	4.34	4.11 - 4.54	-	88.6	35
	let-60(n1046)	3.90	3.67 - 4.12	-	77.1	35
eV[6)]	*ewIR5; let-60(n1046)*	4.06	3.76 - 4.40	-	74.2	31
	let-60(n1046)	3.72	3.47 - 3.97	-	63.3	30

(cutl-7), D1081.4, D1081.9, F25H5.7, F32H2.7, F36A2.13, F39H11.1, F43G9.3, F53B6.4, *C36B1.8 (gls-1), K02B12.2, K02B12.5, W06D4.4 (prmt-7), T08G11.1, T08G11.2, T08G11.3* or *ZK858.6* were knocked down.

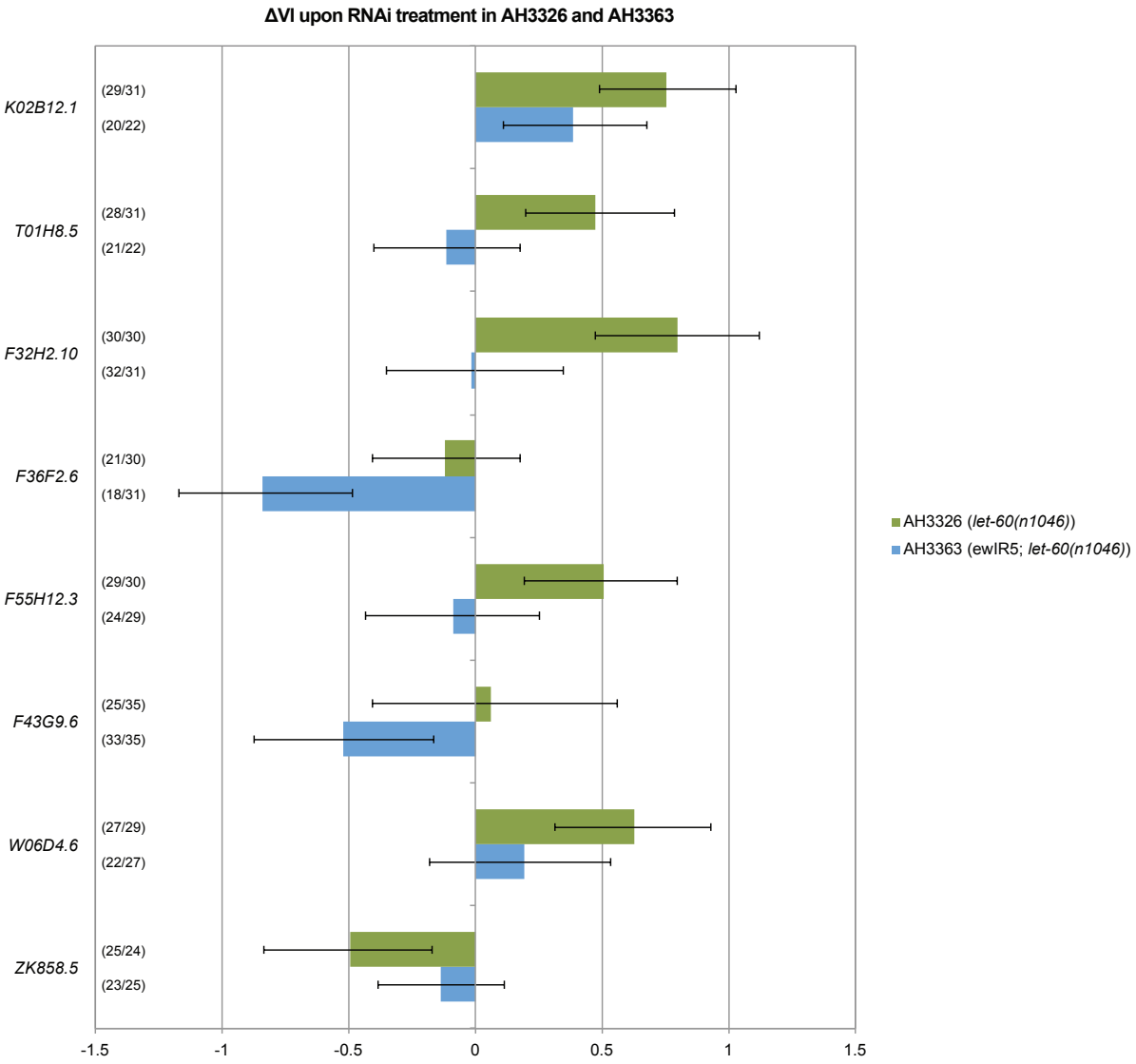

Figure 3.6. The knockdown of polymorphic genes affects RAS/MAPK signalling in either *let-60(n1046)* (AH3326) or *ewIR5; let-60(n1046)* (AH3363) animals (genome-specific modifiers). The difference in VI as compared to the respective empty vector controls is shown. Values were derived from bootstrapping 1000 samples. The number of animals analysed is indicated in brackets (RNAi clone/eV). Error bars indicate the 95% confidence interval.

We have started the verification of the RNAi results by using corresponding mutants. Here, we focused on the modifiers that exhibited genome-specific, “differential” effects (i.e. where either the CB4856 Hawaiian or the N2 Bristol allele showed altered vulval induction upon RNAi) and have human orthologues. We have crossed balanced mutants carrying a deletion in *gon-2* (VC1463) or *ceh-6* (VC2666) to the *let-60(n1046)* mutant animals, but have not had the time to analyse their VI. Further mutants of *fer-1, fcp-1, ZK858.5* and *rad-54* exist but have not been crossed. The verification of *F55H12.3* and *F32H2.10* would include prior mutagenesis (e.g. via CRISPR) to obtain an appropriate mutant.

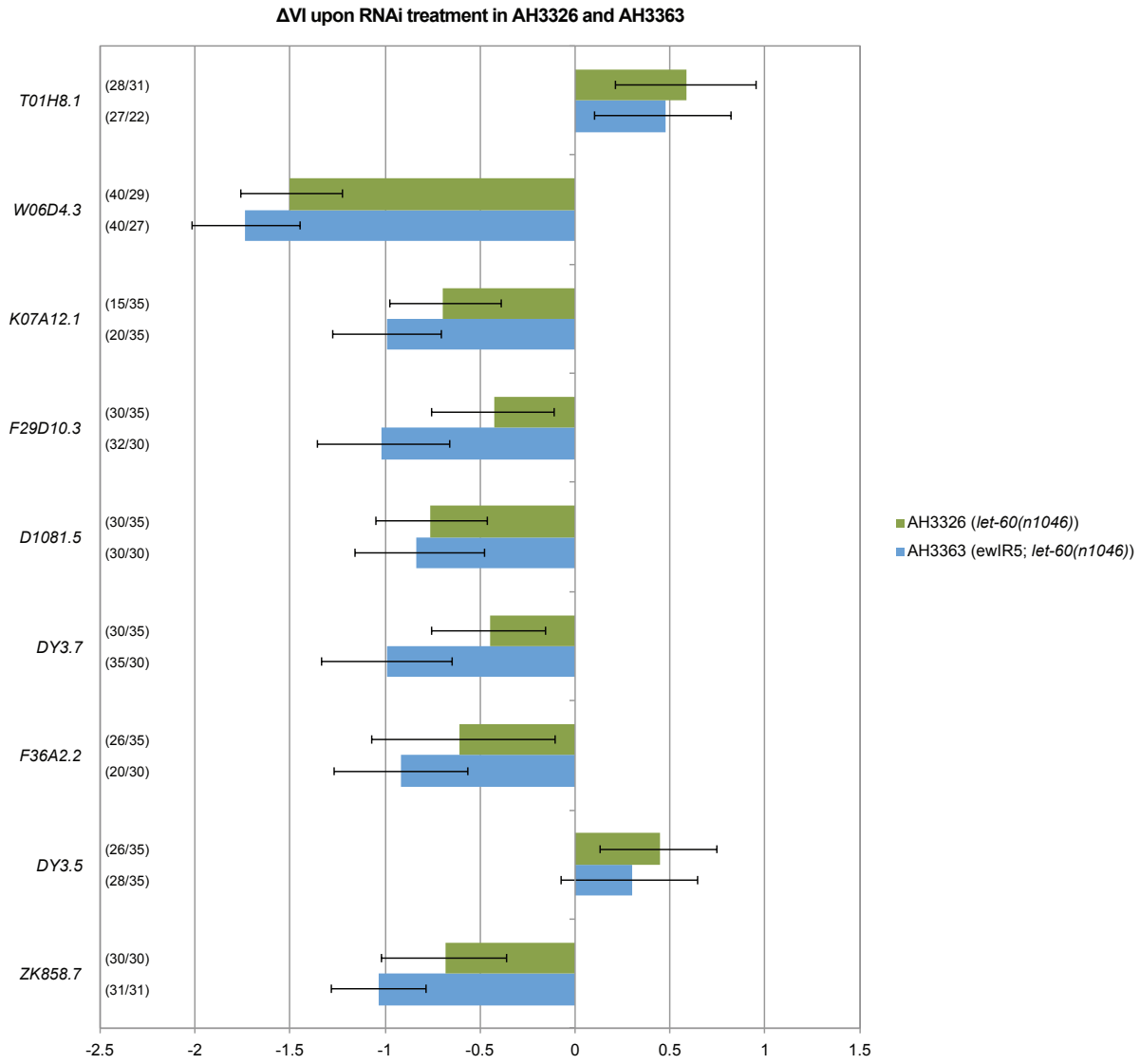

Figure 3.7. The knockdown of polymorphic genes affects RAS/MAPK signalling in both *let-60(n1046)* (AH3326) and *ewIR5; let-60(n1046)* (AH3363) animals (general modifiers). The difference in VI as compared to the respective empty vector controls is shown. Values were derived from bootstrapping 1000 samples. The number of animals analysed is indicated in brackets (RNAi clone/eV). Error bars indicate the 95% confidence interval.

3.1.7 Discussion

Previous studies have helped in gaining insight into how mis-regulated signalling pathways such as WNT and RAS/MAPK predispose to or initiate a certain disease (Giles et al. 2003; Prior et al. 2012) and thereby represent basic pathological determinants. However, little is known about the contribution of so called „modifier genes“ that influence signalling strength, networks and modes of crosstalk (Eichler et al. 2010; Stessman et al. 2014). In this project, we have continued the work described by Schmid et al. (2015) to identify such modifier genes affecting the WNT and RAS/MAPK signalling pathways. Their previous efforts resulted in the prediction of three QTLs (chromosome I, II and V) that modify RAS/MAPK signalling (Schmid et al. 2015) and two QTLs (chromosome I and II) containing modifiers of WNT signalling (Schmid et al., unpublished data). Using selected lines of an introgressed N2 Bristol / CB4856 collection that covers the entire genome (Doroszuk et al. 2009) we were able to not only verify the predicted QTLs on the first chromosome, both in terms of WNT and RAS/MAPK signalling, but also to narrow the regions (**Tables 3.9, 3.10**) and subdivide the QTL in the *bar-1(ga80)* background (**Fig. 3.3**). By performing RNA interference on animals carrying the *bar-1(ga80)* or *let-60(n1046)* mutation in the “pure” N2 Bristol or the N2 Bristol / CB4856 introgressed background, we identified a number of modifiers that appear to be either general modifiers of the signalling pathway analysed, i.e. induction was affected upon RNAi in both strains, or background specific modifiers, i.e. induction was affected upon RNAi in either the introgressed or non-introgressed strain. Further analysis of these candidate genes by mutant analysis, fluorescent reporter constructs, epistasis or tissue-specificity will verify the RNAi data and help discovering a mechanistic link to the pathway affected.

3.1.7.1 RNAi is partially limited to the analysis of non-synonymous SNPs

Thompson et al. (2013) identified on average one polymorphism every 412 bp between CB4856 and N2 Bristol. It is plausible that these SNPs are not confined to coding, exonic regions of genes but also dispersed across 5’ or 3’ untranslated regions, regulatory elements (e.g. enhancers) or noncoding RNA. Although RNA interference with noncoding RNA is not impossible, it is complicated by secondary structures or nuclear localisation of the RNA (Gutschner et al. 2011). The analysis of untranscribed DNA stretches by RNAi on the other hand is impossible due to obvious reasons. As a consequence, we limited our analysis to non-synonymous SNPs with the notion that protein function is altered between isolates and can be assessed by RNAi. However, the regulatory nature of untranslated DNA should not be underestimated as it contributes to translational control, mRNA stability, splicing, localisation or post-transcriptional regulation by miRNAs (Mignone et al. 2002). Transcription factor binding sites within promoter, 3’ UTR or intronic regions determine temporal and spatial gene expression patterns (Beck et al. 1991; Choi et al. 2012). Indeed, a great fraction of the SNPs identified between CB4856 and N2 maps to such untranslated regions (Thompson et al. 2015). An analysis of such synonymous SNPs went beyond the scope of

this thesis but could be incorporated in future studies by including expression QTL analyses (eQTLs). Especially during the detailed analysis of candidate genes identified by RNAi, the relative importance of non-coding SNPs within the candidate gene sequence should be interrogated, e.g. via CRISPR/Cas9 mediated modification.

3.1.7.2 Functional polymorphisms can give rise to background specific modifiers

The presence of the N2 Bristol background at the position of QTL1 in both *let-60(n1046)* and *bar-1(ga80)* decreased signalling strength and vice versa, the CB4856 region enhanced signalling (Schmid et al. 2015 and **Fig. 3.2**), which supports previous findings on natural variation during vulval development (Milloz et al. 2008). We had expected to encounter one or several of four scenarios upon knockdown of polymorphic candidate genes. Firstly, the knockdown of an inhibitor present in the N2 background but not or less active in CB4856 would enhance the VI of non-introgressed mutants. Conversely, the inactivation of an inhibitor present in CB4856 but absent or less active in N2 should increase induction in Hawaii but not Bristol. Thirdly, the suppression of an enhancer acting in N2 but not (or less) in CB4856 is expected to lower the vulval induction of non-introgressed but not introgressed lines and finally, the opposite should occur for a CB4856 specific enhancer. We discovered candidates for N2 Bristol specific inhibitors (*K02B12.1 (ceh-6), T01H8.5 (gon-2), F32H2.10, F55H12.3* and *W06D4.6 (rad-54)*), N2 specific enhancers (*ZK858.5, ZK849.5 (best-26), F49B2.3, F39B2.7 (mtcu-1)* and *K05C4.9*) and CB4856 specific enhancers (*F36F2.6 (fcp-1), F43G9.6 (fer-1)* and *Y105E8A.29*) (**Tables 3.8, 3.12** and **Fig. 3.4, 3.6**). The knockdown of *C37A5.9 (pry-1)* increased vulval induction in the introgressed *bar-1(ga80)* mutant strain AH3330 but not AH3377 suggesting it encodes a CB4856 specific inhibitor. However, our RNAi experiments with *bar-1(ga80)* introgressed and non-introgressed animals generally exhibited a considerable variability in vulval induction indexes so that the results request cautious interpretation. PRY-1 is the worm Axin (Korswagen 2002) and it is therefore likely that loss of the protein increases WNT signalling strength in both introgressed and non-introgressed lines.

3.1.7.3 Polymorphic genes can affect RAS/MAPK signalling irrespective of the genomic background

In addition to polymorphic genes that act differently depending on the genomic background they are placed in, we discovered more general modifiers of RAS/MAPK signalling (*T01H8.1 (rskn-1)*, *W06D4.3, K07A12.1, F29D10.3, D1081.5, DY3.7 (sup-17), F36A2.2, DY3.5 (pqn-26)* and *ZK858.7*), i.e. RNA interference caused a change in vulval induction in both the introgressed and non-introgressed strain (**Table 3.13** and **Fig. 3.7**). A direct involvement in RAS/MAPK signalling of RSKN-1 and SUP-17 is likely. RSKN-1 has been described as a critical downstream effector of RAS/MAPK signalling (Cha et al. 2012) and encodes a member of the RSK (ribosomal

S6 kinase) family of serine/threonine kinases which are targets of RAS/MAPK-ERK (Frödin and Gammeltoft 1999) and themselves negatively feed back on the cascade (Saha et al. 2012). SUP-17 is an ADAM protein, which is a metalloproteinase involved in Notch receptor cleavage and signalling (Wen et al. 1997) that strongly interacts with RAS/MAPK signalling during vulval development (Yoo et al. 2004). The product of *ZK858.7* appeared to play a central role during RAS/MAPK signalling, since its knockdown reduced the VI to levels comparable with the wild-type. *ZK858.7* is orthologous to human tRNA methyltransferase 6 that has been implicated in 1-methyladenosine modification on mitochondrial tRNAs (Chujo and Suzuki 2012) and frameshift mutations have been discovered in colon cancer (Yeon et al. 2017).

3.1.7.4 Some caveats for the comparative study of different strains

Our findings support the feasibility of using natural wild isolates and introgression lines obtained thereof to investigate modifiers of well-known signalling pathways. However, one might argue that an obvious disadvantage of this approach is the combination of different genomic backgrounds that have evolved in the introgression lines, the N2 Bristol and mutant lines. This seems disturbing, since the aim is in fact to find modifiers rather than to introduce them into the system. Indeed, the introgression lines were obtained from crosses between N2 Bristol and CB4856 (Doroszuk et al. 2009) and were subsequently used in crosses to include the introgression into yet another *C. elegans* strain containing a sensitising mutation. Thus, the genomic backgrounds of at least three *C. elegans* lines exposed to individual natural selection were combined to obtain the final experimental strain and to study natural polymorphisms. With the rapid progress and dropping costs in whole genome sequencing it becomes clear that strains differ more strongly in their genetic constitution than anticipated (Thompson et al. 2013 and T. Schmid, doctoral thesis). The MT2124 strain commonly used to study the *let-60(n1046)* mutation is a good example for a strong deviation from the wild-type situation, since it contains several SNPs in core components of the RAS/MAPK pathway itself (e.g. *let-23, age-1* or *gap-1*). It is thus important to be aware of this issue when the effect of polymorphisms on a given mutant background and within a defined environment is studied. Clearer conclusions of the relative effect of a modifier can be drawn by performing allele swapping experiments using established methods like MosSCI (Frøkjær-Jensen et al. 2008) or CRISPR/Cas9 for endogenous gene modification (Jinek et al. 2012).
In summary, the approach proposed by Schmid et al. (2015) and others is promising in defining new modifiers of well-described signalling pathways and in uncovering their contribution to disease development. Especially by using simple short-lived model organisms, the generation of genetically mixed backgrounds is feasible and allows the generation of an immense amount of data within a relatively short period of time. In the current project, we have superficially analysed the effect of polymorphisms on protein function. However, the use of introgression lines can be and is extended to the field of genetical genomics to interrogate mRNA or protein expression level variation (Breitlin et al. 2008), which exemplifies the value of studying natural variation.

3.1.8 Acknowledgements

We wish to thank all present and past members of the Hajnal laboratory as well as Jan Kammenga, L. Basten Snoek, Miriam Rodriguez and Tobias Schmid for critical input and extensive support in this project. Further thanks go to Fabienne Largey, Leontien van der Bent, Katharina Jovic and Kateřina Apolínová for their work on the verification of the QTLs and the RNAi screens. We thank J. Ahringer and J. Reboul for RNAi clones, the *Caenorhabditis elegans* Genetic Center for strains. This work was supported by grants from the Swiss National fond SNF to A.H. and the Kanton Zürich.

3.2 Manuscript draft

Submitted Manuscript: Confidential

Title:

Cross-talk between the NOTCH and Hypoxia pathways modulates RAS/MAPK-mediated cell fate decisions in *C. elegans*

Authors: Sabrina Maxeiner[1,2], Judith Grolleman[1,3], Tobias Schmid[1], Jan Kammenga[4] and Alex Hajnal[1,*]

Affiliations:

[1]University of Zurich, Institute of Molecular Life Sciences, Winterthurerstrasse 190, Zurich CH-8057, Switzerland.

[2]PhD Program in Molecular Life Science

[3]Current address: Radboud University Nijmegen Medical Centre, Department of Human Genetics, Nijmegen, The Netherlands

[4]Laboratory of Nematology, Wageningen University, Wageningen, The Netherlands

*Correspondence to: alex.hajnal@imls.uzh.ch

One Sentence Summary:

Atmospheric oxygen levels modulate the RAS/MAPK signaling pathway in the Nematode *C. elegans* through a cross-talk between the DELTA/NOTCH and Hypoxia signaling pathways.

Maxeiner et al.

Abstract:

Animals need to adjust many cellular functions to oxygen availability. We show that the Nematode *C. elegans* adapts the activity of the conserved RAS/MAPK pathway, a key regulator of various functions during development and adulthood, to changes in atmospheric oxygen concentration. Hypoxia inhibits the cellular responses to RAS/MAPK activation via the hypoxia-inducible factor HIF-1, which induces the nuclear hormone receptor NHR-57 to counteract MAPK signaling. Furthermore, cross-talk between the NOTCH and hypoxia pathways modulates the sensitivity of the RAS/MAPK pathway to hypoxia. Lateral NOTCH signaling induces the prolyl-hydroxylase EGL-9, which promotes HIF-1 degradation in uncommitted precursor cells, thereby allowing RAS/MAPK-induced differentiation. By inducing DELTA family NOTCH ligands, RAS/MAPK signaling creates a positive feedback loop that keeps precursor cells competent to respond to inductive signals. This regulatory network between the NOTCH, Hypoxia and RAS/MAPK pathways permits adaptation of developmental processes to variations in oxygen concentration.

Main Text:

The RAS/MAPK pathway regulates cell growth, differentiation, proliferation, apoptosis and migration in all metazoans (*1*). Moreover, constitutively activating mutations in HRAS, NRAS or KRAS are among the most frequent tumor initiating mutations in human cancer (*2*). In *C. elegans,* RAS/MAPK signaling is involved in several developmental processes, such as the specification of the excretory duct cell precursor, the differentiation and maturation of meiotic germ cells or the development of the hermaphrodite vulva (*3-5*). During vulval development, an EGF-like ligand (LIN-3) is secreted from the gonadal anchor cell (AC) to activate RAS/MAPK signaling in the adjacent vulval precursor cells (VPCs) through an EGF receptor family tyrosine kinase (**Fig. 1A**). Activation of RAS/MAPK signaling in the proximal VPCs that are near the AC (P5.p, P6.p & P7.p) induces the expression of Delta-like DSL ligands, which activate DELTA/NOTCH signaling between adjacent VPCs. NOTCH performs two distinct functions during vulval induction. First, NOTCH maintains the VPCs competent to respond to the inductive AC signal and differentiate (*6*). After the VPC closest to the AC, P6.p, has reached the highest RAS/MAPK activity and adopted the primary (1°) fate, strong activation of the NOTCH pathway in the neighboring VPCs P5.p and P7.p inhibits MAPK signaling and specifies the secondary (2°) fate in these cells (*6*, *7*). The distal VPCs (P3.p, P4.p and P8.p), which receive neither the RAS/MAPK nor NOTCH signal, adopt the tertiary (3°), uninduced fate. This results in the induction of the three proximal VPCs and establishes a robust 3°-3°-2°-1°-2°-3° pattern of vulval cell fates (*7*). Activating mutations in the RAS/MAPK pathway lead to the induction of more than three VPCs and a Multivulva (Muv) phenotype, while loss-of-function mutations in components of the RAS/MAPK pathway cause a Vulvaless (Vul) phenotype. Thus, the average

number of induced VPCs, termed the vulval induction index (VI), is used to quantify signaling strength (e.g. VI>3 indicates hyperinduction).

Animals have evolved cellular and behavioral responses to adapt to variations in oxygen concentration. At the cellular level, the hypoxia-response pathway mediates the adaptation to low oxygen conditions and a switch from aerobic to anaerobic metabolism (*8*). In ambient oxygen, the *C. elegans* hypoxia-inducible factor α HIF-1 is hydroxylated at a specific proline residue within the degradation domain by the prolyl hydroxylase EGL-9 (**Fig. 2A**). Hydroxylated HIF-1 interacts with the von Hippel-Lindau E3 ubiquitin ligase VHL-1 complex and is degraded by the 26S proteasome (*9*). HIF-1 is stabilized in low oxygen and forms a complex with the constitutively expressed HIFß subunit AHA-1 to promote the expression of specific target genes.

We have previously used quantitative genetics to identify modifiers of the RAS/MAPK pathway by comparing two highly polymorphic *C. elegans* strains, N2 Bristol and CB4856 Hawaii (*10*). Notably, CB4856 Hawaii exhibits an overall elevated activity of the RAS/MAPK pathway compared to the N2 Bristol reference strain. Among the RAS/MAPK modifiers identified were *F44F1.1,* a calpain paralog (*F44F1.3*) and *pfd-3*, a prefoldin orthologous to human VHL binding protein 1 (*10*). Both genes had been identified in a screen for suppressors of the *egl-9* prolyl hydroxylase egg-laying-defective phenotype (*11*). Together, these findings suggested that genetic variation of the hypoxia-response pathway might account for differences in RAS/MAPK signaling activity in different *C. elegans* isolates.

To test this hypothesis, we used CRISPR/CAS9 editing to introduce the activating G13E *let-60 ras* mutation (*12*) into the CB4856 Hawaii *(zh122)* and N2 Bristol *(zh121)* backgrounds and determined the VI of animals raised at different oxygen concentrations. CB4856 animals carrying the G13E mutation exhibited a higher VI than N2 animals carrying the same mutation

when raised between 21% (normoxia) and 3% O_2 (mild hypoxia) (**Fig. 1B,C**). At 1% O_2 the VI decreased in the CB4856 background, and at 0.5% O_2 the VI was reduced to the same level in both strains. Thus, the difference in RAS/MAPK pathway activity between CB4856 and N2 may be due to differences in their oxygen sensitivity. Besides the canonical *let-60* G13E allele *(n1046)*, hypoxia (0.5% O_2) also reduced the VI in animals carrying *rf* mutations in *let-23 egfr*, *let-60 ras* or *lin-45 raf* and an activated MAPK transgene *mpk-1(gaIs37gf)* (**Fig. 1D**). However, the VI of *lin-1(lf)*, which encodes an Ets transcription factor that represses vulval induction downstream of MPK-1, was not affected by hypoxia. In addition to vulval development, hypoxia also reduced RAS/MAPK signaling in germ cells and during excretory duct cell specification. The germ cells of *let-60 ras(ga89gf)* mutants raised at the restrictive temperature exit the pachytene stage at an accelerated rate (*4*), which results in the proximal stacking of immature oocytes (**Fig. 1E**), while *let-60 ras(n1046gf)* animals often exhibit duplications of the duct cell (*3*) (**Fig. 1F**). Hypoxia partially suppressed both *let-60(gf)* phenotypes (**Fig. 1E,F**).

The abrupt rather than gradual reduction in RAS/MAPK activity under hypoxia (**Fig. 1C**) suggested the existence of a regulatory switch activated at a threshold oxygen concentration, rather than a metabolic effect of hypoxia. We thus examined the genetic interaction between mutants in the RAS/MAPK and hypoxia-response pathways. The VI of *let-60(n1046gf)* mutants was reduced by *lf* mutations in *egl-9* (*13*) or *vhl-1* (*14*), while the *hif-1(ia04)* deletion allele (*15*) increased the VI (**Fig. 2B,C**). The larger *hif-1* deletion *zh111* that likely represents a null allele (**Fig. S1**) caused an even greater increase in the VI. Moreover, *let-60(gf); egl-9(lf) hif-1(ia04)* triple mutants exhibited the same increase in VI as *let-60(gf); hif-1(ia04)* double mutants, indicating that *hif-1* inhibits RAS/MAPK signaling downstream of *egl-9* prolyl hydroxylase (**Fig. 2A-C**). *egl-9(lf)* also reduced the VI of mutants in other RAS/MAPK pathway components, such

as the guanine nucleotide exchange factor *sos-1* or the *raf* homolog *lin-45*. Though, mutations in EGF *lin-3*, the EGF receptor *let-23* or its adaptors were insensitive to *egl-9(lf)* (**Fig. S2**). A wild-type but not a hydroxylase-deficient *egl-9::gfp* transgene (*16*) rescued the reduced VI of *let-60(n1046gf); egl-9(sa307lf)* mutants (**Fig. 2D**). Interestingly, the wild-type *egl-9::gfp* transgene further increased the VI of *let-60(n1046gf)* single mutants, indicating that enzymatic EGL-9 activity is rate-limiting in HIF-1 degradation under normoxia.

Surprisingly, hypoxia reduced the VI of *let-60(n1046gf); hif-1(zh111lf)* mutant*s*, while *let-60(n1046gf); egl-9(sa307lf)* mutants were insensitive to hypoxia (**Fig. 2E**). Thus, HIF-1 mediates only part of the hypoxic regulation of RAS/MAPK signaling. Under hypoxia, the monoamine oxidase *amx-2* is up-regulated in the intestinal cells, where it catalyzes the oxidation of serotonin (*10*, *11*). The serotonin oxidation product 5-hydroxyindoleaceticacid (5-HIAA) systemically inhibits RAS/MAPK signaling by antagonizing signaling through the SER-1 serotonin receptor pathway. Since the VI of *amx-2(lf); let-60(n1046gf)* mutants was not reduced under hypoxia (**Fig. 2E**), the inhibition of the SER-1 pathway by 5-HIAA possibly mediates the HIF-1-independent effect of hypoxia on RAS/MAPK signaling.

Although the expression of a translational *hif-1::gfp* reporter was undetectable under normoxia, in *egl-9(sa307lf)* or *vhl-1(ok161)* mutants HIF-1::GFP was expressed in all VPCs (**Fig. 3A**). To test if HIF-1 acts in the VPCs or intestine, we performed Pn.p- and intestine-specific RNAi (*17*, *18*). Only Pn.p cell-specific *hif-1* RNAi increased the VI of *let-60(n1046gf)* (**Fig. 3B**). Thus, EGL-9 and VHL-1 induce HIF-1 degradation in the VPCs to positively regulate RAS/MAPK signaling. The functional *egl-9::gfp* reporter was initially expressed in mid L2 larvae in the three proximal VPCs that are induced to adopt vulval cell fates (**Fig. 3C**). After vulval induction in early L3 larvae, EGL-9::GFP expression faded in the 1° P6.p descendants and increased in the 2°

P5.p and P7.p descendants (**Fig. 3C,D**). This pattern suggested that either RAS/MAPK signaling inhibits or lateral DELTA/NOTCH signaling activates EGL-9::GFP expression in the VPCs. Since EGL-9::GFP expression was reduced in *let-60(rf)* mutants, RAS/MAPK signaling promotes rather than inhibits *egl-9* expression (**Fig. 3C,E**). Furthermore, EGL-9::GFP expression was lost in the VPCs of *lin-12 notch(lf)* mutants, while *lin-12(n137gf)* mutants showed equally strong expression in all VPCs (**Fig. 3C,F,G**). Thus, *egl-9* is a target of the LIN-12 NOTCH pathway. Since RAS/MAPK signaling induces the expression of the DSL NOTCH ligands (**Fig. 1A**), reducing RAS/MAPK signaling likely represses EGL-9::GFP expression indirectly. In contrast to RAS/MAPK pathway mutants, *egl-9(lf)* did not affect the vulval phenotypes of *lin-12 gf* or *rf* mutants (**Fig. S3**).

To identify gene(s) downstream of HIF-1 that mediate the repression of RAS/MAPK signaling, we screened genes exhibiting an at least two-fold HIF-1 dependent induction (*19*, *20*) in a *let-60(n1046gf); egl-9(sa307lf)* and a *let-60(n1046gf); hif-1(zh111lf)* background by RNAi (**Tables S1,S2**). Knock-down of a HIF-1 target that inhibits RAS/MAPK signaling should increase the VI in the *egl-9(sa307lf)* but not the *hif-1(zh111lf)* background. This approach identified *nhr-57* as a negative regulator of RAS/MAPK signaling (**Fig. 4A, Table S1**). *nhr-57* encodes a nuclear hormone receptor similar to the *Drosophila* estrogen-related receptor ERR2 and vertebrate glucocorticoid hormone receptors. The increased VI in *nhr-57(tm4533lf)* deletion mutants confirmed NHR-57 as a negative regulator of RAS/MAPK signaling (**Fig. 4B**). Before vulval induction, a translational *nhr-57::gfp* reporter was not detectable in the VPCs, but expressed in the distal, uninduced VPCs after vulval induction (**Fig. 4D, E**). NHR-57::GFP expression was absent in the descendants of the induced proximal VPCs until they had completed their last round of divisions and terminally differentiated. Consistent with its role as a HIF-1 target, NHR-

57::GFP expression was up-regulated in *egl-9(lf)* mutants (**Fig. 4D**). Unlike *hif-1(zh111lf)*, the VI of *let-60(n1046gf); nhr-57(tm4533lf)* mutants did not significantly change under hypoxia (**Fig. 4C**). Therefore, NHR-57 mediates both the HIF-1 dependent and independent regulation of RAS/MAPK signaling by oxygen (*21*).

The hypoxia-response pathway thus sets a baseline for the cellular sensitivity to RAS/MAPK signaling when oxygen becomes limiting. However, since the activity of the prolyl hydroxylase EGL-9 is limiting even under normoxia, the hypoxia-response pathway exerts its inhibitory effect even under normoxia. Epistasis analysis indicates that the nuclear hormone receptor NHR-57, the downstream integrator of the hypoxic response, functions at the level of or in parallel with the ETS family transcription factor LIN-1 (*22*) (**Fig. 4E**). Likewise, interactions of mammalian ETS family transcription factors with steroid receptors have been reported (*23-26*). By linking the HIF-1 degradation pathway via EGL-9 expression to DELTA/NOTCH signaling, the VPCs modulate their sensitivity towards the inductive RAS/MAPK signal according to their spatial position and differentiate depending on oxygen availability. To our knowledge, prolyl hydroxylases have so far not been implicated in DELTA/NOTCH-regulated developmental processes in other animals, though a dependence of the mammalian prolyl hydroxylase EGLN3 on transcription downstream of NOTCH has been reported (*27*, *28*). By inducing the expression of multiple DELTA family NOTCH ligands, RAS/MAPK signaling creates a positive feedback loop that maintains low NHR-57 levels in the proximal VPCs to keep them competent to respond to inductive signals. Connecting the hypoxia-response to developmental signaling pathways thus permits the animals to adapt their development to changing environmental conditions, resulting in developmental robustness and flexibility.

References and Notes:

1. L. Santarpia, S. M. Lippman, A. K. El-Naggar, Targeting the MAPK-RAS-RAF signaling pathway in cancer therapy. *Expert Opinion on Therapeutic Targets*. **16**, 103–119 (2012).

2. L. E. Goldfinger, J. V. Michael, Regulation of Ras signaling and function by plasma membrane microdomains. *Biosci Trends*. **11**, 23–40 (2017).

3. I. Abdus-Saboor *et al.*, Notch and Ras promote sequential steps of excretory tube development in *C. elegans*. *Development*. **138**, 3545–3555 (2011).

4. D. L. Church, K. L. Guan, E. J. Lambie, Three genes of the MAP kinase cascade, *mek-2, mpk-1/sur-1* and *let-60 ras*, are required for meiotic cell cycle progression in *Caenorhabditis elegans*. *Development*. **121**, 2525–2535 (1995).

5. K. Kornfeld, Vulval development in *Caenorhabditis elegans*. *Trends Genet.* **13**, 55–61 (1997).

6. M. Wang, P. W. Sternberg, Competence and Commitment of *Caenorhabditis elegans* Vulval Precursor Cells. *Developmental Biology*. **212**, 12–24 (1999).

7. A. S. Yoo, C. Bais, I. Greenwald, Crosstalk between the EGFR and LIN-12/Notch pathways in *C. elegans* vulval development. *Science*. **303**, 663–666 (2004).

8. G. L. Semenza, Hypoxia-inducible factor 1: oxygen homeostasis and disease pathophysiology. *Trends in Molecular Medicine*. **7**, 345–350 (2001).

9. Z. Zhang, J. Yan, Y. Chang, S. ShiDu Yan, H. Shi, Hypoxia inducible factor-1 as a target for neurodegenerative diseases. *Curr. Med. Chem.* **18**, 4335–4343 (2011).

10. T. Schmid *et al.*, Systemic Regulation of RAS/MAPK Signaling by the Serotonin Metabolite 5-HIAA. *PLoS Genet*. **11**, e1005236 (2015).

11. E. H. Gort *et al.*, The TWIST1 oncogene is a direct target of hypoxia-inducible factor-2α. *Oncogene*. **27**, 1501–1510 (2007).

12. G. J. Beitel, S. G. Clark, H. R. Horvitz, *Caenorhabditis elegans ras* gene *let-60* acts as a switch in the pathway of vulval induction. *Nature*. **348**, 503–509 (1990).

13. C. Darby, C. L. Cosma, J. H. Thomas, C. Manoil, Lethal paralysis of *Caenorhabditis elegans* by *Pseudomonas aeruginosa*. *Proc. Natl. Acad. Sci. U.S.A.* **96**, 15202–15207 (1999).

14. A. C. Epstein *et al.*, *C. elegans* EGL-9 and mammalian homologs define a family of dioxygenases that regulate HIF by prolyl hydroxylation. *Cell*. **107**, 43–54 (2001).

15. H. Jiang, R. Guo, J. A. Powell-Coffman, The *Caenorhabditis elegans hif-1* gene encodes a bHLH-PAS protein that is required for adaptation to hypoxia. *Proc. Natl. Acad. Sci. U.S.A.* **98**, 7916–7921 (2001).

16. Z. Shao, Y. Zhang, J. A. Powell-Coffman, Two Distinct Roles for EGL-9 in the Regulation of HIF-1-Mediated Gene Expression in *Caenorhabditis elegans*. *Genetics*. **183**, 821–829 (2009).

17. J. Pilipiuk, C. Lefebvre, T. Wiesenfahrt, R. Legouis, O. Bossinger, Increased IP3/Ca2+ signaling compensates depletion of LET-413/DLG-1 in *C. elegans* epithelial junction assembly. *Developmental Biology*. **327**, 34–47 (2009).

18. H. Qadota *et al.*, Establishment of a tissue-specific RNAi system in *C. elegans. Gene*. **400**, 166–173 (2007).

19. T. Bishop *et al.*, Genetic Analysis of Pathways Regulated by the von Hippel-Lindau Tumor Suppressor in *Caenorhabditis elegans*. *PLoS Biol.* **2**, e289 (2004).

20. C. Shen, D. Nettleton, M. Jiang, S. K. Kim, J. A. Powell-Coffman, Roles of the HIF-1 hypoxia-inducible factor during Hypoxia Response in *Caenorhabditis elegans*. *J. Biol. Chem.* **280**, 20580–20588 (2005).

21. Y. Li *et al.*, HIF- and Non-HIF-Regulated Hypoxic Responses Require the Estrogen-Related Receptor in *Drosophila melanogaster*. *PLoS Genet*. **9**, e1003230 (2013).

22. G. J. Beitel, S. Tuck, I. Greenwald, H. R. Horvitz, The *Caenorhabditis elegans* gene *lin-1* encodes an ETS-domain protein and defines a branch of the vulval induction pathway. *Genes & Development*. **9**, 3149–3162 (1995).

23. J. Mullick *et al.*, Physical Interaction and Functional Synergy between Glucocorticoid Receptor and Ets2 Proteins for Transcription Activation of the Rat Cytochrome P-450c27 Promoter. *J. Biol. Chem.* **276**, 18007–18017 (2001).

24. P. Cao *et al.*, Estrogen receptor α enhances the transcriptional activity of ETS-1 and promotes the proliferation, migration and invasion of neuroblastoma cell in a ligand dependent manner. *BMC Cancer 2015 15:1*. **15**, 491 (2015).

25. C.-D. Geng, W. V. Vedeckis, c-Myb and members of the c-Ets family of transcription factors act as molecular switches to mediate opposite steroid regulation of the human glucocorticoid receptor 1A promoter. *J. Biol. Chem.* **280**, 43264–43271 (2005).

26. B. T. Kalet *et al.*, Transcription factor Ets1 cooperates with estrogen receptor α to stimulate estradiol-dependent growth in breast cancer cells and tumors. *PLoS ONE*. **8**, e68815 (2013).

27. Y. Li, M. A. Hibbs, A. L. Gard, N. A. Shylo, K. Yun, Genome-Wide Analysis of N1ICD/RBPJ Targets In Vivo Reveals Direct Transcriptional Regulation of Wnt, SHH, and Hippo Pathway Effectors by Notch1. *STEM CELLS*. **30**, 741–752 (2012).

28. S. Ohashi *et al.*, A NOTCH3-Mediated Squamous Cell Differentiation Program Limits Expansion of EMT-Competent Cells That Express the ZEB Transcription Factors. *Cancer Research*. **71**, 6836–6847 (2011).

Acknowledgments

We wish to thank the members of the Hajnal laboratory, Jan Kammenga, Beatrice Beck-Schimmer and Konrad Basler for critical discussion and comments on the manuscript, and R. Maier and D. Schnarwiler for their help in designing and manufacturing the hypoxic chambers. We are also grateful to the *C. elegans* Genetic Center and the Mitani lab for providing strains, Andrew Fire for GFP vectors and J. Ahringer for RNAi clones. This work was supported by a grant from the Swiss National Science Foundation to A.H. no. 31003A-166580 and the Kanton of Zürich. Materials and Methods used are described in the Supplementary online Materials.

Maxeiner et al.

Figures

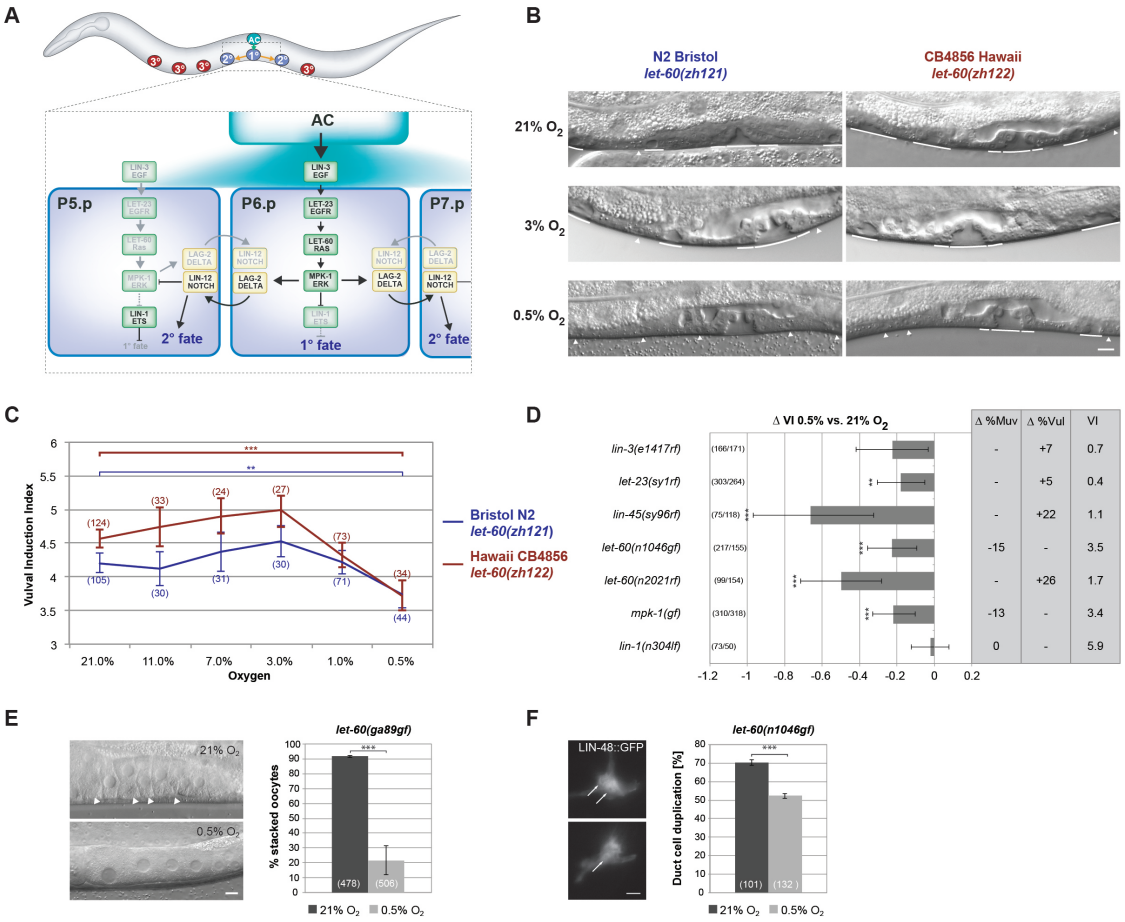

Figure 1. Hypoxia suppresses RAS/MAPK signaling in different tissues.

(A) Overview of vulval development showing the known interactions between the RAS/MAPK and DELTA/NOTCH pathways. **(B)** Vulval phenotypes of the *let-60 ras* G13E mutation in the N2 Bristol (left) and CB4856 Hawaii (right) background with varying oxygen concentrations. Solid lines indicate induced 1° and 2° and arrowheads uninduced 3° VPCs in L4 larvae. **(C)** VI of N2 Bristol and CB4856 Hawaii *let-60 ras* G13E mutants raised in varying oxygen concentrations. **(D)** Effect of hypoxia on different RTK/RAS/MAPK pathway mutants. ΔVI indicates the change in VI of animals raised in 0.5% compared to controls grown in 21% oxygen.

Δ%Muv and Δ%Vul indicate the change in the percentage of animals with VI>3 and VI<3, respectively. The absolute VIs in 0.5% oxygen are shown in the rightmost column. **(E)** Suppression of the stacked oocyte phenotype in *let-60(ga89gf)* animals by hypoxia. Arrowheads point at the stacked oocytes formed in the proximal gonad under normoxia. **(F)** Suppression of the duct cell duplication phenotype in *let-60(n1046gf)* mutants by hypoxia. Arrows point at the two duct cell nuclei formed under normoxia. Error bars in **(C)** and **(D)** indicate the 95% confidence intervals, and p-values, indicated with *** $p < 0.001$ and ** $p < 0.01$, were derived by bootstrapping 1000 samples. In **(E)** and **(F),** error bars indicate the standard error of the mean, and p-values were calculated with a Fisher's exact test. The numbers of animals scored are indicated in brackets. The scale bars are 5 μm.

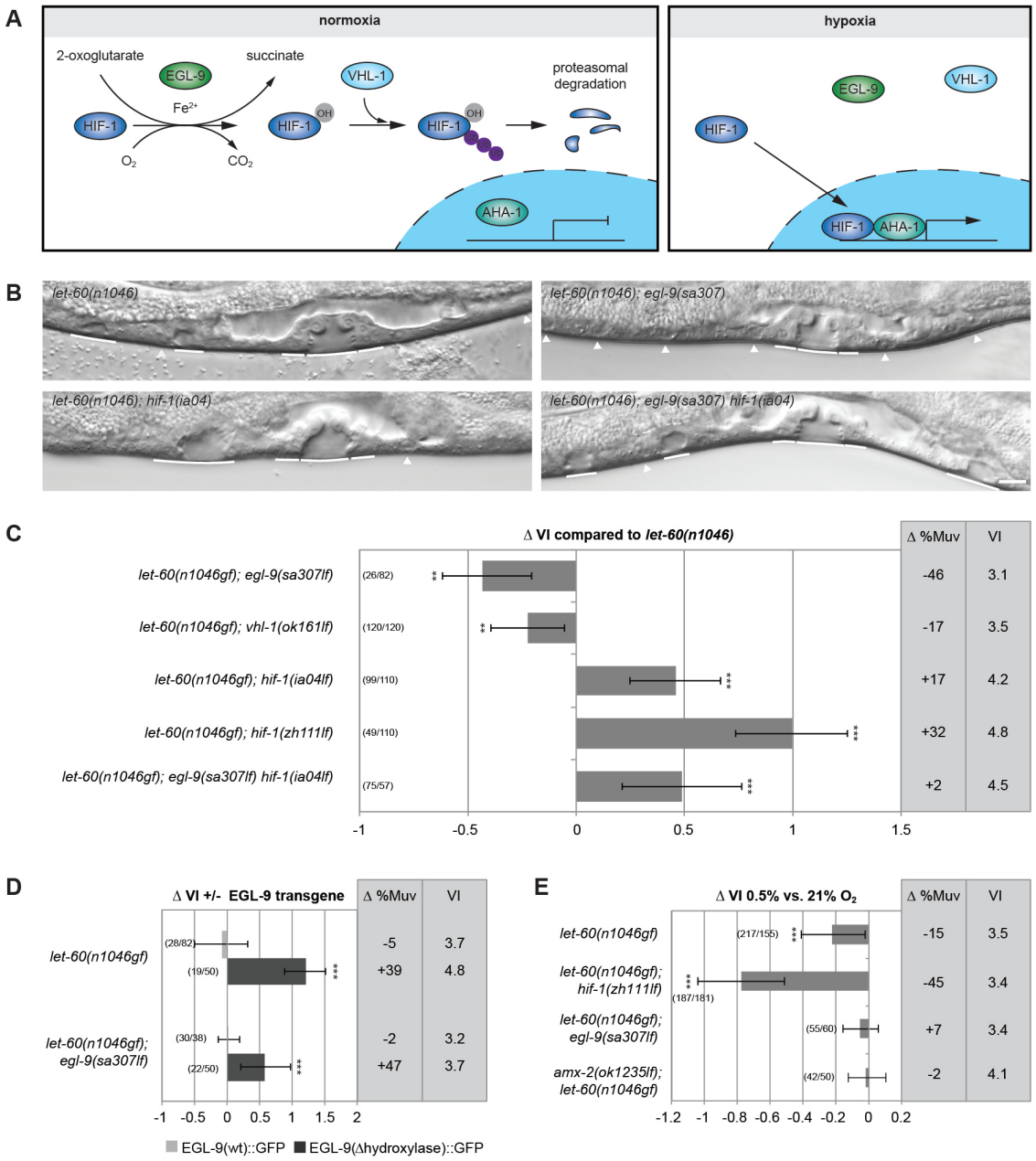

Figure 2. The hypoxia-response pathway negatively regulates RAS/MAPK signaling under normoxia.

(A) Schematic overview of the hypoxia response pathway. (**B**) Vulval phenotypes of double and triple mutants between *let-60(n1046gf)* and components of the hypoxia-response pathway under

normoxia. Solid lines indicate induced 1° and 2° and arrowheads uninduced 3° VPCs in the L4 larvae. **(C)** Mutations in the hypoxia pathway change the VI of *let-60(n1046gf)* mutants. ΔVI indicates the change in VI of the indicated genotypes relative to *let-60(n1046gf)* single mutant siblings obtained from the crosses. Δ%Muv indicates the change in the percentage of animals with VI>3. The absolute VIs are shown in the rightmost column. **(D**) Overexpression of *egl-9::gfp* increases the VI. ΔVI indicates the change in VI of animals carrying a wild-type (grey bars) or hydroxylase deficient (black bar) multi-copy *egl-9::gfp* array compared to siblings without array. **(E)** Hypoxia reduces the VI in *hif-1* but not in *egl-9* or *amx-2* mutants. ΔVI indicates the change in VI of animals grown under hypoxia versus normoxia. Error bars indicate the 95% confidence intervals. p-values, indicated with *** $p < 0.001$ and ** $p < 0.01$, were derived by bootstrapping 1000 samples. The numbers of animals scored are indicated in brackets. The scale bar indicates 5 μm.

Maxeiner et al.

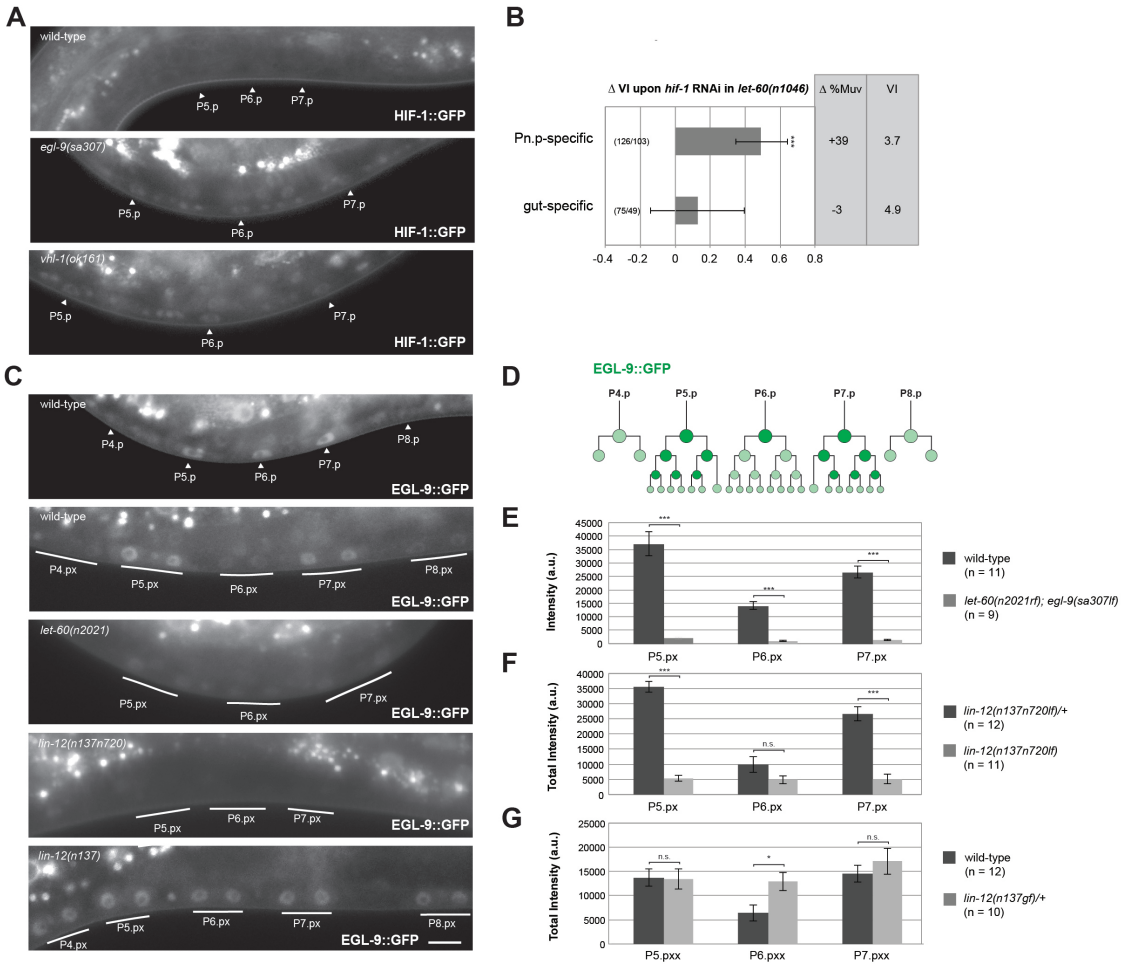

Figure 3. *egl-9* is a NOTCH target that promotes HIF-1 degradation in the induced VPCs.

(A) HIF-1::GFP expression in wild-type, *egl-9(sa307lf)* and *vhl-1(ok161lf)* larvae before vulval induction. Arrowheads point at the nuclei of the three proximal VPCs. **(B)** Pn.p cell- and gut-specific *hif-1* RNAi (see supplementary information). ΔVI indicates the change in VI in *hif-1* RNAi compared to empty vector treated control animals. Error bars indicate the 95% confidence interval, and p-values were derived by bootstrapping 1000 samples. **(C)** EGL-9::GFP expression in the wild-type before (mid L2, top panel) and after induction (early L3, second panel), and in *let-60 ras(rf)*, *lin-12 notch(lf)* and *lin-12 notch(gf)* mutants after induction. Induced VPCs are underlined. The scale bar is 5 µm. **(D)** Schematic representation of the wild-type EGL-9::GFP

pattern during vulval development. **(E-G)** Quantification of EGL-9::GFP expression in the four genotypes shown in **(C)** after vulval induction (early L3). Error bars indicate the standard error of the mean, and p-values, indicated with *** $p < 0.001$, ** $p < 0.01$ and * $p < 0.05$, were calculated in a two-tailed Student's t-test. The numbers of animals scored are indicated in brackets.

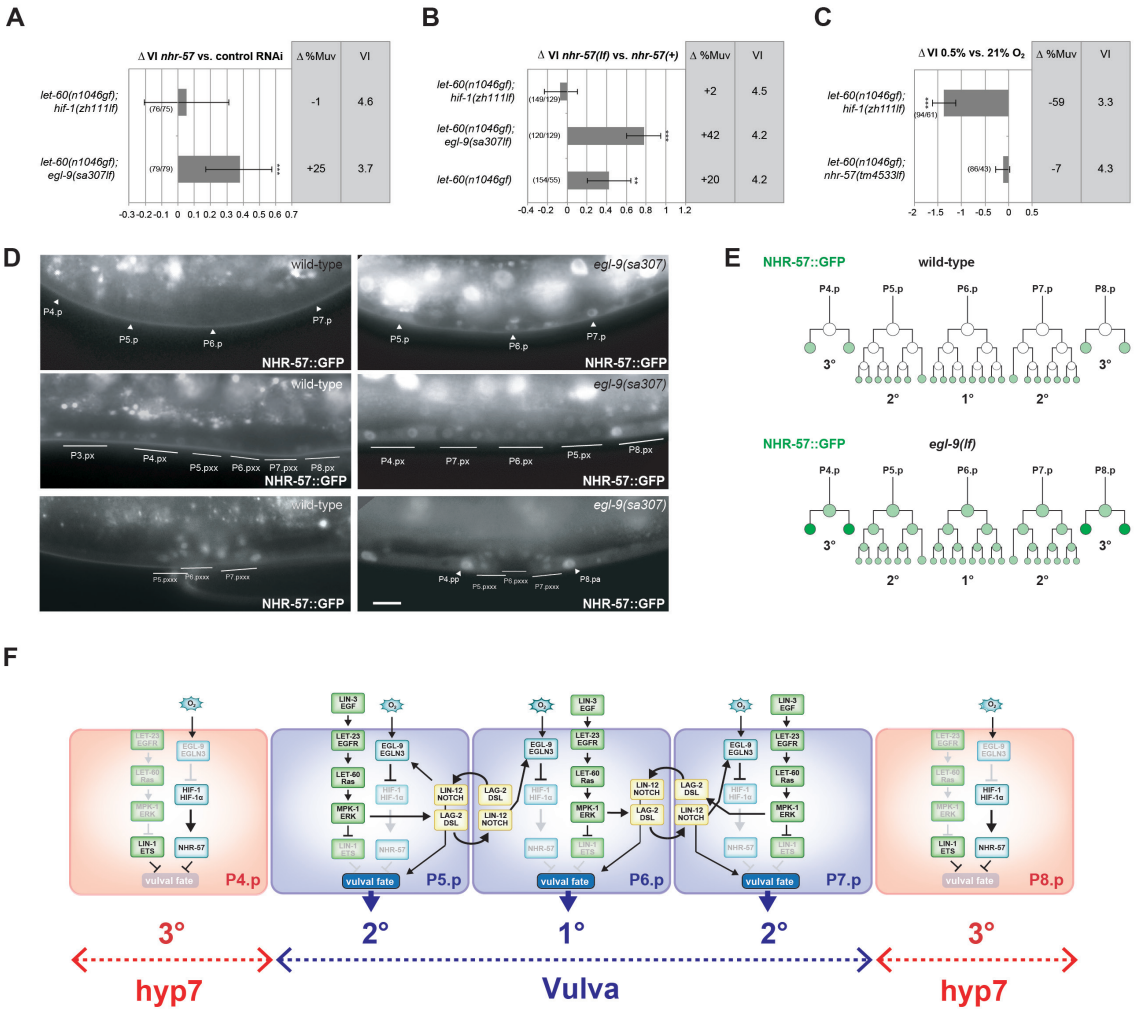

Figure 4. The HIF-1 target NHR-57 inhibits RAS/MAPK signaling through a DELTA/NOTCH-induced negative feedback loop.

(A) Knock-down of *nhr-57* increases the VI in an *egl-9(lf)* but not a *hif-1(lf)* background. ΔVI and Δ%Muv indicate the changes in VI and percentage of animals with VI>3 after *nhr-57* RNAi compared to empty vector treated control animals. **(B)** The *nhr-57(tm4533)* deletion allele increases the VI of *let-60(n1046gf)* single and *let-60(n1046gf); egl-9(sa307lf)* double mutants but has no effect in a *hif-1(zh111lf)* background. ΔVI and Δ%Muv indicate the changes in VI and

percentage of animals with VI>3 compared to *nhr-57(+)* control siblings. **(C)** Hypoxic treatment decreases the VI in the *hif-1(zh111)* but not the *nhr-57(tm4533)* background. ΔVI and Δ%Muv indicate the changes in VI and percentage of animals with VI>3 raised in hypoxia compared to normoxia. Error bars indicate the 95% confidence intervals, and p-values, indicated with *** $p < 0.001$ and ** $p < 0.01$, were derived by bootstrapping 1000 samples. The numbers of animals scored are indicated in brackets. **(D)** NHR-57::GFP expression pattern in the wild-type (left panels) and *egl-9(lf)* (right panels) background before (top panels) and after induction (middle panels), and at the end of vulval differentiation (bottom panels). Arrowheads and solid lines point at the nuclei of the induced or uninduced VPCs and their descendants, respectively. The scale bar is 5 µm. **(E)** Schematic representation of the NHR-57::GFP pattern during vulval development in the wild-type (top) and in an *egl-9(lf)* background (bottom). **(F)** Model illustrating the cross-talk of the hypoxia-response, DELTA/NOTCH and RAS/MAPK pathways during vulval induction. Lateral DELTA/NOTCH signaling between the proximal VPCs induces EGL-9 expression to maintain low HIF-1 and NHR-57 levels, thereby keeping the VPCs competent to respond to RAS/MAPK signaling, which in turn maintains expression of the DELTA family NOTCH ligands. Distal VPCs loose their competence due to higher NHR-57 levels and adopt the 3° fate.

Supplementary Materials for

Cross-talk between the NOTCH and Hypoxia pathways modulates RAS/MAPK-mediated cell fate decisions in *C. elegans*

Sabrina Maxeiner[1,2], Judith Grolleman[1,3], Tobias Schmid[1], Jan Kammenga[4] and Alex Hajnal[1,*]

correspondence to: alex.hajnal@imls.uzh.ch

This PDF file includes:

Materials and Methods

C. elegans strains

C. elegans strains were maintained at 20°C using standard procedures (*1*) unless stated differently. *C. elegans* Bristol refers to the wild-type N2 strain and Hawaii to CB4856 (*2*). The transgenic lines were generated as described in
(*3*, *4*). N2 strains carrying *let-60(ga89)* or *egl-9(n586)* were maintained at 20°C and shifted to 25°C for mutant analysis. The following mutations and transgenes were used in this study: **LG III**: *unc-32(e189) lin-12(n137n720)* (*5*), *dpy-19(e1259) lin-12(n137)* (56), *hT2[bli-4(e937) let-?(q782) qIs48]* (I;III) (*6*). **LG IV**: *let-60(n1046)* (*7*), *let-60(zh121)* (this study), *let-60(zh122)* (this study), *let-60(ga89)* (*8*), *let-60(n2021)* (*7*), *lin-1(n304)* (*9*), *lin-3(e1417)* (*10*), *lin-45(sy96)* (*11*). **LG V**: *egl-9(sa307)* (*12*), *hif-1(ia04)* (*13*), *hif-1(zh111)* (this study), *nhr-57(tm4533)* (Mitani lab). **LG X**: *vhl-1(ok161)* (*14*), *rde-1(ne219)* (*15*), **Transgenes**: *gaIs47[lin-31::mpk-1(gf); lin-31::D-mek(gf)]* (*16*), *iaIs38[egl-9p::egl-9::tag + unc-119(+)]* (*17*), *iaEx101[egl-9p::egl-9(H487A)::tag + unc-119(+)]*(*17*), *duIs[P_{elt-2}::rde-1(+); pRF4]* (*18*), *zhEx418[lin-31::rde-1;myo-2::mCherry]* (*19*), *saIS14[lin-48p::gfp]* (*20*), *opIs206[Phif-1::hif-1::gfp::hif-1* 3'UTR + *unc-119(+)]* (*21*), *zhEx605[Pnhr-57::nhr-57::gfp:: nhr-57* 3' UTR + *unc-119(+)]* (this study).

RNAi and microscopy

RNAi was performed as described in Kamath et al. (2002) (*22*). Animals were synchronized by bleaching and raised on bacteria expressing dsRNA. The empty vector plasmid L4440 was used as a negative control and dsRNA against *rpn-6.1* as a positive control. Vulval induction was scored in the F1 generation. Animals were anesthetized in in a drop of 5mM tetramisole and analysed using differential interference contrast (DIC) and fluorescence microscopy.

Hypoxic treatment

Hypoxic chambers were adapted from Fawcett et al. (2002) (*23*). Briefly, a glass bowl with flange served as container for small NGM plates. A customized lid was made, which consists of an acrylic glass plate surrounded by a metal ring equipped with an immersion to fit in an O-ring. Two holes in the acrylic glass served as the gas in- and output apertures. A third larger hole accommodates an oxygen measuring device (GOX 100). A hypoxic environment was generated via oxygen replacement by N_2 until the desired O_2 concentration was obtained. NGM plates containing mixed stage *C. elegans* were incubated for three to five days and analyzed at the microscope.

Generation of *hif-1(zh111)*

Co-CRISPR was employed as described in Arribere et al. (2014) (*24*). 25 ng/µl *dpy-10* sgRNA pJA58 was co-injected into N2 Bristol animals with 25 ng/µl of a sgRNA targeting *hif-1*, GAT AGA AAA GTG AGT CCT AA, 500 nM of *dpy-10(cn64)* repair template AF-ZF-827 and 50 ng/µl of pDD162. Candidate worms were selected from plates harboring a large number of Rol progeny and analyzed by PCR. The *zh111* deletion spans 2464 bp and removes exons three to five (region upstream: ATT TCA AAA AAT TTT TGA CA. Region downstream: CTA AGT TAA AAA AAC AAC AG).

Generation of *let-60(zh121)* and *let-60(zh122)*
CRISPR/Cas9 was employed as described in Friedland et al. (2013) (*25*). The sgRNA sequence AAT GAC GGA GTA CAA GCT TG was inserted into plasmid #46169 (PU6::unc-119_sgRNA) via site-directed mutagenesis. The *let-60* genomic locus was partially amplified using the primers AAG GAG CAA ATC GAA CAG AC and ATC CAT TTT ATT AGG CAC GCA C and cloned into p-GEM®-T easy. The silently mutated PAM and the G13E mutation were obtained using the primers TGA GTG CTG ATT TAC CAA CTC CTC CAT CTC CAA CTA CCA CAA GCT TGT ACT CCG TC and AAG CTT GTG GTA GTT GGA GAT GGA GGA GTT GGT AA ATC AGC ACT CAC CAT TCA ACT CAT C. N2 Bristol or CB4856 Hawaii animals were injected with 50 ng/µl sgRNA plasmid, 50 ng/µl pDD162, 50 ng/µl repair template and 5 ng/µl pCFJ104. The progeny was screened for the Multivulva phenotype and candidate animals were verified by PCR and sequencing.

Translational *nhr-57* reporter
A 1206 bp fragment upstream of the *nhr-57* transcriptional start site was amplified together with the coding genomic region (without the stop codon) using the primers cta aca act tgg aaa tga aat CAC CAA CAC CTT CTA CAC AGC TGC and gtt ctt ctc ctt tac tca tTT GTC CAT CAA TGA TTT TAT AGA TTT TGT CG. The *gfp* sequence was amplified from pPD95.75 using the primers ATG AGT AAA GGA GAA GAA C and gag atc tgg ttc aaa tag CTA TTT GTA TAG TTC ATC CAT GC. 459 bp of the *nhr-57* 3' UTR were amplified using the primers GCT ATT TGA ACC AGA TCT CTT C and cag tac ggc cga cta gta gGA ATA AAT CAT CCC AAA GCC GTT TTT G. A vector backbone containing a *CB-unc-119(+)* rescue as well as the *AmpR* gene was amplified using the primers ATT TCA TTT CCA AGT TGT TAG CG and CTA CTA GTC GGC CGT ACT GAG GTG TTG TCG CTT TTA TTG GG. The four fragments were combined into a 10.170 kb plasmid (pSMa32) using Gibson Assembly®. N2 animals were injected (due to a mutation in the *CB-unc-119(+)* gene) with 5 ng/µl pSMa32, 2.5 ng/µl pCFJ104 and 100 ng/µl pBS. Transformants were isolated based on the presence of the co-injection marker.

References to Supplementary Materials

1. S. Brenner, The Genetics of *Caenorhabditis elegans*. *Genetics*. **77**, 71–94 (1974).

2. E. C. Andersen *et al.*, A Powerful New Quantitative Genetics Platform, Combining *Caenorhabditis elegans* High-Throughput Fitness Assays with a Large Collection of Recombinant Strains. *G3: Genes, Genomes, Genetics*. **5**, 911–920 (2015).

3. P. B. Tan, M. R. Lackner, S. K. Kim, MAP Kinase Signaling Specificity Mediated by the LIN-1 Ets/LIN-31 WH Transcription Factor Complex during *C. elegans* Vulval Induction. *Cell*. **93**, 569–580 (1998).

4. C. C. Mello, J. M. Kramer, D. Stinchcomb, V. Ambros, Efficient gene transfer in *C.elegans*: extrachromosomal maintenance and integration of transforming sequences. *EMBO J*. **10**, 3959–3970 (1991).

5. I. Greenwald, G. Seydoux, Analysis of gain-of-function mutations of the *lin-12* gene of *Caenorhabditis elegans*. *Nature*. **346**, 197–199 (1990).

6. K. S. McKim, K. Peters, A. M. Rose, Two types of sites required for meiotic chromosome pairing in *Caenorhabditis elegans*. *Genetics*. **134**, 749–768 (1993).

7. G. J. Beitel, S. G. Clark, H. R. Horvitz, *Caenorhabditis elegans ras* gene *let-60* acts as a switch in the pathway of vulval induction. *Nature*. **348**, 503–509 (1990).

8. D. M. Eisenmann, S. K. Kim, Mechanism of Activation of the *Caenorhabditis Elegans* Ras Homologue Let-60 by a Novel, Temperature-Sensitive, Gain-of-Function Mutation. *Genetics*. **146**, 553–565 (1997).

9. G. J. Beitel, S. Tuck, I. Greenwald, H. R. Horvitz, The *Caenorhabditis elegans* gene *lin-1* encodes an ETS-domain protein and defines a branch of the vulval induction pathway. *Genes & Development*. **9**, 3149–3162 (1995).

10. B. J. Hwang, A cell-specific enhancer that specifies *lin-3* expression in the *C. elegans* anchor cell for vulval development. *Development*. **131**, 143–151 (2004).

11. P. W. Sternberg, A. Golden, M. Han, Role of a *raf* Proto-Oncogene during *Caenorhabditis elegans* Vulval Development. *Philosophical Transactions of the Royal Society B: Biological Sciences*. **340**, 259–265 (1993).

12. C. Darby, C. L. Cosma, J. H. Thomas, C. Manoil, Lethal paralysis of *Caenorhabditis elegans* by *Pseudomonas aeruginosa*. *Proc. Natl. Acad. Sci. U.S.A.* **96**, 15202–15207 (1999).

13. H. Jiang, R. Guo, J. A. Powell-Coffman, The *Caenorhabditis elegans hif-1* gene encodes a bHLH-PAS protein that is required for adaptation to hypoxia. *Proc. Natl. Acad. Sci. U.S.A.* **98**, 7916–7921 (2001).

14. A. C. Epstein *et al.*, *C. elegans* EGL-9 and mammalian homologs define a family of dioxygenases that regulate HIF by prolyl hydroxylation. *Cell*. **107**, 43–54 (2001).

15. H. Qadota *et al.*, Establishment of a tissue-specific RNAi system in *C. elegans*. *Gene*. **400**, 166–173 (2007).

16. M. R. Lackner, S. K. Kim, Genetic analysis of the *Caenorhabditis elegans* MAP kinase gene *mpk-1*. *Genetics*. **150**, 103 (1998).

17. Z. Shao, Y. Zhang, J. A. Powell-Coffman, Two Distinct Roles for EGL-9 in the Regulation of HIF-1-Mediated Gene Expression in *Caenorhabditis elegans*. *Genetics*. **183**, 821–829 (2009).

18. J. Pilipiuk, C. Lefebvre, T. Wiesenfahrt, R. Legouis, O. Bossinger, Increased IP3/Ca2+ signaling compensates depletion of LET-413/DLG-1 in *C. elegans* epithelial junction assembly. *Developmental Biology*. **327**, 34–47 (2009).

19. A. Haag *et al.*, An In Vivo EGF Receptor Localization Screen in *C. elegans* Identifies the Ezrin Homolog ERM-1 as a Temporal Regulator of Signaling. *PLoS Genet*. **10**,

e1004341 (2014).

20. T. A. Berset, The *C. elegans* homolog of the mammalian tumor suppressor Dep-1/Scc1 inhibits EGFR signaling to regulate binary cell fate decisions. *Genes & Development*. **19**, 1328–1340 (2005).

21. A. Sendoel, I. Kohler, C. Fellmann, S. W. Lowe, M. O. Hengartner, HIF-1 antagonizes p53-mediated apoptosis through a secreted neuronal tyrosinase. *Nature*. **465**, 577–583 (2010).

22. R. S. Kamath *et al.*, Systematic functional analysis of the *Caenorhabditis elegans* genome using RNAi. *Nature*. **421**, 231–237 (2003).

23. E. M. Fawcett, J. W. Horsman, D. L. Miller, Creating Defined Gaseous Environments to Study the Effects of Hypoxia on *C. elegans*. *JoVE* (2012), doi:10.3791/4088.

24. J. A. Arribere *et al.*, Efficient marker-free recovery of custom genetic modifications with CRISPR/Cas9 in *Caenorhabditis elegans. Genetics*. **198**, 837–846 (2014).

25. A. E. Friedland *et al.*, Heritable genome editing in *C. elegans* via a CRISPR-Cas9 system. *Nat. Methods*. **10**, 741–743 (2013).

Supplementary Figures

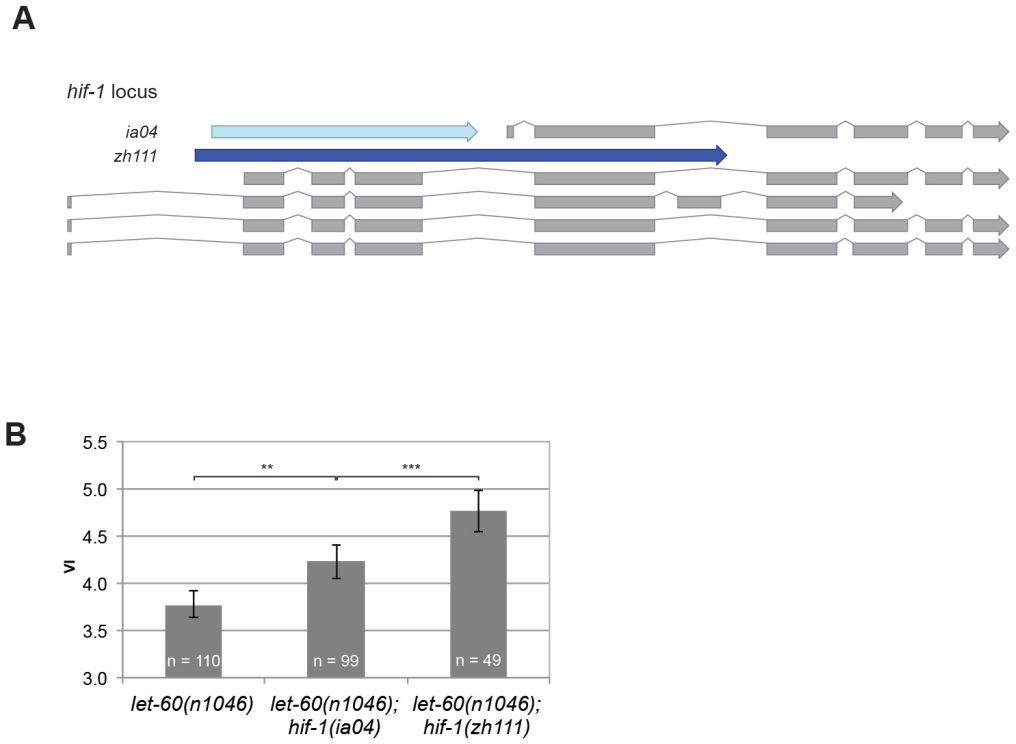

Fig. S1. Comparison of the *zh111* and *ia04* deletions in the *hif-1* locus.

(**A**) Schematic representation of the *hif-1* locus with the five isoforms shown in grey. The canonical deletion allele *ia04* is depicted in light blue and the larger *zh111* deletion is shown in dark blue. Note that the *zh111* deletion affects all isoforms. (**B**) The *zh111* allele has a stronger effect on the VI in the *let-60(n1046)* background than *ia04*. Error bars in **(B)** indicate the 95% confidence intervals, and p-values, indicated with *** $p < 0.001$ and ** $p < 0.01$, were derived by bootstrapping 1000 samples.

Maxeiner et al.

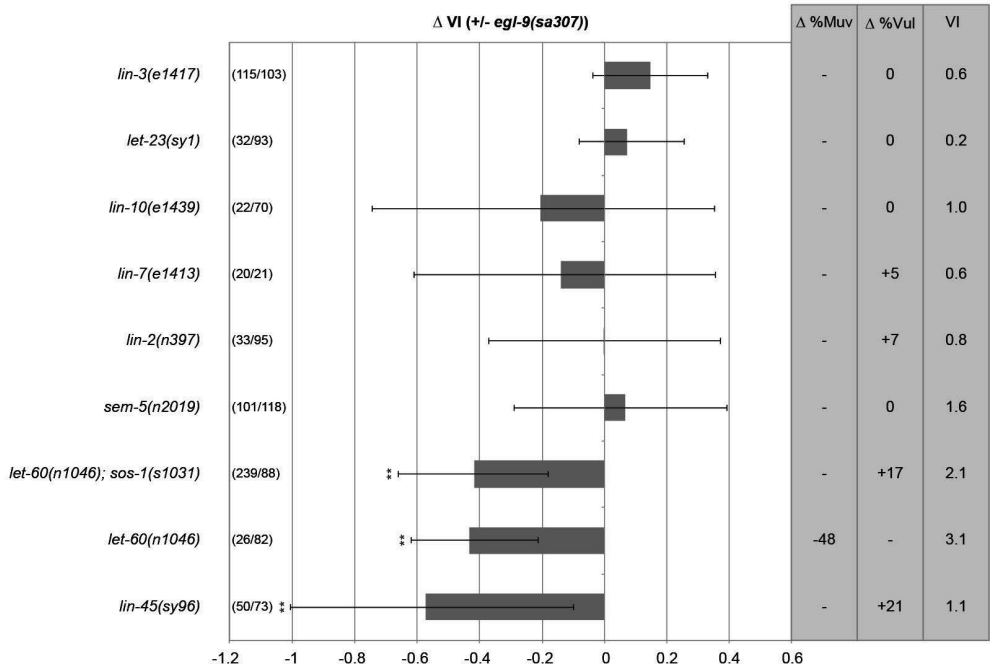

Fig. S2. Genetic interaction between *egl-9(lf)* and RAS/MAPK pathway mutations.

ΔVI indicates the change in VI of the indicated genotypes in the *egl-9(lf)* background compared to single (or double) mutant siblings obtained from the crosses. Δ%Muv and Δ%Vul indicate the changes in the percentage of animals with VI>3 and VI<3, respectively. The absolute Vis of the double (or triple) mutants are shown in the rightmost column. Error bars indicate the 95% confidence intervals. p-values, indicated with ** $p < 0.01$, were derived by bootstrapping 1000 samples. The numbers of animals scored are indicated in brackets.

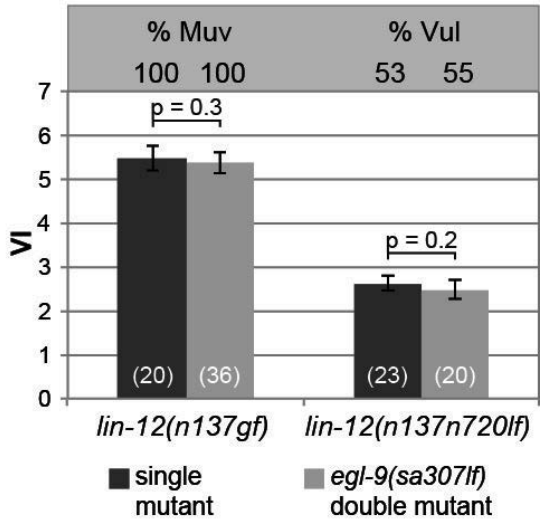

Fig. S3. Genetic interaction between *egl-9(lf)* and *lin-12 notch* mutations.

The absolute VIs of *lin-12(gf)* and *lin-12(lf)* mutants in the *egl-9(lf)* background compared to *egl-9(+)* single mutant siblings obtained from the crosses are shown. %Muv and %Vul indicate the percentage of animals with VI>3 and VI<3, respectively. Error bars indicate the 95% confidence intervals. p-values were derived by bootstrapping 1000 samples. The numbers of animals scored are indicated in brackets.

Sequence Name	Gene Name	Genotype	VI	95% C.I.	P	% Muv	n
K10H10.4	-	*let-60(n1046); egl-9(sa307)*[1]	3.09	3.00 - 3.20	0.005	14	22
		let-60(n1046); hif-1(zh111)[1]	4.28	4.10 - 4.51	0.650	90	44
W07A12.6	*oac-54*	*let-60(n1046); egl-9(sa307)*[1]	3.20	3.10 - 3.35	0.102	30	20
		let-60(n1046); hif-1(zh111)[1]	n.a.	n.a.	n.a.	n.a.	n.a.
Y44A6C.1	-	*let-60(n1046); egl-9(sa307)*[1]	3.18	3.05 - 3.34	0.072	23	22
		let-60(n1046); hif-1(zh111)	n.a.	n.a.	n.a.	n.a.	n.a.
T05B4.2	*nhr-57*	*let-60(n1046); egl-9(sa307)*[3]	3.58	3.38 - 3.77	0.000	69	26
		let-60(n1046); hif-1(zh111)[3]	4.70	4.47 - 4.94	0.901	100	32
T25E12.4	*dkf-2*	*let-60(n1046); egl-9(sa307)*[1]	3.28	3.11 - 3.46	0.199	33	27
		let-60(n1046); hif-1(zh111)	n.a.	n.a.	n.a.	n.a.	n.a.
M01H9.3	-	*let-60(n1046); egl-9(sa307)*[1]	3.27	3.05 - 3.55	0.236	25	20
		let-60(n1046); hif-1(zh111)	n.a.	n.a.	n.a.	n.a.	n.a.
C56E6.2	-	*let-60(n1046); egl-9(sa307)*[1]	3.11	3.00 - 3.24	0.014	13	23
		let-60(n1046); hif-1(zh111)[1]	4.03	3.65 - 4.45	0.302	70	20
F22B5.7	*zyg-9*	*let-60(n1046); egl-9(sa307)*[1]	3.08	3.00 - 3.22	0.006	9	23
		let-60(n1046); hif-1(zh111)	n.a.	n.a.	n.a.	n.a.	n.a.
C01B4.1	*str-257*	*let-60(n1046); egl-9(sa307)*[1]	3.10	3.03 - 3.21	0.008	21	19
		let-60(n1046); hif-1(zh111)	n.a.	n.a.	n.a.	n.a.	n.a.
C29F9.5	-	*let-60(n1046); egl-9(sa307)*[1]	3.04	3.00 - 3.11	0.000	9	23
		let-60(n1046); hif-1(zh111)[1]	4.46	4.07 - 4.86	0.797	86	22
C36A4.9	*acs-19*	*let-60(n1046); egl-9(sa307)*[1]	3.12	3.00 - 3.28	0.034	10	20
		let-60(n1046); hif-1(zh111)[1]	4.10	3.73 - 4.45	0.430	80	20
F45D11.16	-	*let-60(n1046); egl-9(sa307)*[2]	3.17	3.05 - 3.33	0.028	19	21
		let-60(n1046); hif-1(zh111)	n.a.	n.a.	n.a.	n.a.	n.a.
W04E12.4	-	*let-60(n1046); egl-9(sa307)*[2]	3.51	3.33 - 3.71	0.838	55	29
		let-60(n1046); hif-1(zh111)[2]	4.22	3.95 - 4.48	0.007	87	30
F53F4.5a	*fmo-4*	*let-60(n1046); egl-9(sa307)*[2]	3.31	3.14 - 3.52	0.243	38	21
		let-60(n1046); hif-1(zh111)	n.a.	n.a.	n.a.	n.a.	n.a.
K08E3.1	*tyr-2*	*let-60(n1046); egl-9(sa307)*[3]	3.04	3.00 - 3.13	0.281	4	23
		let-60(n1046); hif-1(zh111)[3]	3.96	3.74 - 4.19	0.002	67	55
C01B12.1	*sqt-2*	*let-60(n1046); egl-9(sa307)*[3]	3.20	3.10 - 3.30	0.049	40	20
		let-60(n1046); hif-1(zh111)[3]	4.32	4.08 - 4.55	0.184	95	20
C04F2.1	*srh-79*	*let-60(n1046); egl-9(sa307)*[2]	3.50	3.28 - 3.77	0.756	47	32
		let-60(n1046); hif-1(zh111)[2]	4.61	4.31 - 4.90	0.412	92	26
C13D9.4	*srsx-11*	*let-60(n1046); egl-9(sa307)*[2]	3.45	3.27 - 3.64	0.683	50	28
		let-60(n1046); hif-1(zh111)[2]	4.51	4.09 - 4.89	0.286	86	22
C14E2.5	-	*let-60(n1046); egl-9(sa307)*[2]	3.47	3.18 - 3.80	0.676	36	25
		let-60(n1046); hif-1(zh111)	n.a.	n.a.	n.a.	n.a.	n.a.
C28H8.8	-	*let-60(n1046); egl-9(sa307)*[3]	3.16	3.00 - 3.36	0.784	14	22
		let-60(n1046); hif-1(zh111)[3]	4.35	4.12 - 4.62	0.244	96	26
C50E3.9	-	*let-60(n1046); egl-9(sa307)*[2]	3.48	3.33 - 3.65	0.822	61	33
		let-60(n1046); hif-1(zh111)[2]	4.65	4.31 - 4.98	0.480	90	29
F13B9.6	*cutl-29*	*let-60(n1046); egl-9(sa307)*[2]	3.55	3.33 - 3.79	0.882	57	21
		let-60(n1046); hif-1(zh111)	n.a.	n.a.	n.a.	n.a.	n.a.
F56C3.3	-	*let-60(n1046); egl-9(sa307)*[2]	3.31	3.15 - 3.52	0.262	35	31
		let-60(n1046); hif-1(zh111)[2]	4.35	3.98 - 4.72	0.084	83	23
K02F6.1	-	*let-60(n1046); egl-9(sa307)*[4]	3.03	3.00 - 3.08	0.000	5	20
		let-60(n1046); hif-1(zh111)[4]	4.14	3.91 - 4.34	0.005	86	29
R04D3.1	*cyp-14A4*	*let-60(n1046); egl-9(sa307)*[2]	3.49	3.33 - 3.66	0.794	61	38
		let-60(n1046); hif-1(zh111)[2]	4.98	4.72 - 5.25	0.027	97	30
R52.2	-	*let-60(n1046); egl-9(sa307)*[4]	3.58	3.38 - 3.83	0.050	58	26
		let-60(n1046); hif-1(zh111)[4]	4.93	4.64 - 5.24	0.902	97	29
T05B9.2	-	*let-60(n1046); egl-9(sa307)*[2]	3.07	3.00 - 3.17	0.000	11	27
		let-60(n1046); hif-1(zh111)[2]	4.71	4.40 - 4.98	0.627	97	30
T06G6.2	*sra-24*	*let-60(n1046); egl-9(sa307)*[4]	3.52	3.30 - 3.80	0.870	41	27
		let-60(n1046); hif-1(zh111)[4]	5.15	4.89 - 5.39	0.005	100	23
T07H3.4	*clec-21*	*let-60(n1046); egl-9(sa307)*[2]	3.29	3.11 - 3.52	0.241	28	32
		let-60(n1046); hif-1(zh111)[2]	4.23	3.95 - 4.55	0.008	83	29
Y38C1BA.3	*col-109*	*let-60(n1046); egl-9(sa307)*[2]	3.51	3.31 - 3.73	0.806	46	39
		let-60(n1046); hif-1(zh111)[2]	4.80	4.43 - 5.15	0.757	90	20
Y38H6C.2	*srw-65*	*let-60(n1046); egl-9(sa307)*[2]	3.38	3.22 - 3.58	0.475	44	25
		let-60(n1046); hif-1(zh111)[2]	4.69	4.42 - 4.95	0.576	97	31
CC8.2	-	*let-60(n1046); egl-9(sa307)*	n.a.	n.a.	n.a.	n.a.	n.a.
		let-60(n1046); hif-1(zh111)	n.a.	n.a.	n.a.	n.a.	n.a.
eV	-	*let-60(n1046); egl-9(sa307)*[1]	3.40	3.14 - 3.67	-	38	21
		let-60(n1046); hif-1(zh111)[1]	4.17	3.71 - 4.66	-	68	19
eV	-	*let-60(n1046); egl-9(sa307)*[2]	3.39	3.24 - 3.53	-	41	59
		let-60(n1046); hif-1(zh111)[2]	4.65	4.44 - 4.85	-	98	56
eV	-	*let-60(n1046); egl-9(sa307)*[3]	3.08	3.00 - 3.15	-	15	20
		let-60(n1046); hif-1(zh111)[3]	4.48	4.23 - 4.73	-	95	22
eV	-	*let-60(n1046); egl-9(sa307)*[4]	3.34	3.18 - 3.52	-	43	28
		let-60(n1046); hif-1(zh111)[4]	4.64	4.29 - 4.94	-	100	24

Table S1. RNAi screen to identify HIF-1 targets inhibiting vulval development.

Knock-down of selected HIF-1 target genes in *let-60(n1046gf); egl-9(sa307lf)* and *let-60(n1046gf); hif-1(zh111lf)* mutants that had an effect in a primary screen using *let-60n1046gf); egl-9(sa307lf)* mutants only. The empty vector negative controls are shown at the bottom, and for each RNAi experiment the matching control is indicated with the superscript numbers. Note that some genes were not analyzed in the *let-60(n1046gf); hif-1(zh111lf)* strain, since there was no effect in *let-60(n1046gf); egl-9(sa307lf)* mutants. Furthermore, the knock-down of *CC8.2* caused lethality and could not be analyzed. p-values were derived by bootstrapping 1000 samples.

Sequence Name	Gene Name
K08C7.5	fmo-2
F22B5.4	-
F42A10.4a	efk-1
F59B10.4	-
C24B9.9	dod-3
F44B9.1a	dpf-6
C31G12.2	clec-245
Y38E10A.23	-
R10D12.1	-
F56A3.3a	npp-6
C34D4.14	hecd-1
K04H4.2	-
C04A2.1	tbc-6
F02E8.6	npc-1/ncr-1
F45D11.1	-
K02E7.6	-
F16G10.10	-
Y48G8AL.6	smg-2
C01G6.8a	cam-1
F57B9.1	-
F21D12.3	-
T08G3.6	-
Y46G5A.6	-
M05D6.5	-
C34B7.3	cyp-36A1
M03A1.1a	vab-1
Y55F3BR.4	lgc-33
C32D5.12	-
Y19D10A.5	-
C05D12.1	-
C05E4.2	str-20
C10G11.3	srh-51
C42D4.13	-
C42D4.2	-
C50E10.6	sre-54
F20D6.1	-
F25G6.5	stdh-4
F57G8.1	srh-180
H27D07.6	srh-87
R09B5.3	cnc-2
R09E10.2	-
R186.6	mpst-7
T04A11.10	sru-17
T06E4.8	-
T07C5.5	nhr-26
T17H7.1	-
W02A2.3	pqn-74
ZK938.6	chil-9

Table S2. HIF-1 targets without an effect on vulval development.

List of HIF-1 target genes that were knocked down in *let-60(n1046gf); egl-9(sa307lf)* animals and did not change the VI as estimated from the number of Muv animals on the plates.

3.3 Additional experiments not included in the manuscript

3.3.1 Introduction

While the first project focussed on describing regions of quantitative traits positioned on the first chromosome that modify WNT or RAS/MAPK signalling, we investigated in more detail selected candidate genes found during the RNAi screen on QTL1b in the *let-60(n1046)* mutant background within a second project.

The QTL1b region was positioned at I: 12433756-13863711 (N2 Bristol, WormBase WS195) as estimated from the overlapping genomic CB4856 region present in ewIR10 and ewIR17 that had been determined by FLP mapping and partial sequencing (Schmid et al. 2015). The region spans 1.43 Mbp and contains 142 polymorphic modifier genes, of which 107 had been screened by RNAi (Schmid et al. 2015). The knockdown of *W02D9.4, B0019.1 (amx-2), F17B5.4, F44F1.1* and *F44F1.4* increased the VI exclusively in the *let-60(n1046)* background which proposed the presence of negative regulators (more) active in the N2 Bristol but not or less active in the CB4856 background. RNA interference with *C54C8.2 (bgnt-1.8), T07D10.1, T07D10.3, T06G6.9 (pfd-3)*, *W02A11.5 (bath-34), Y18D10A.13 (pad-1), C47B2.6 (gale-1), ZK1225.5, Y40B1B.5 (eif-3.J)* and *K03D10.1 (kal-1)* led to the reduction in VI in the *ewIR17; let-60(n1046)* milL only, suggesting that positive regulators (more) active in the Hawaii background are present. The VI was decreased in both backgrounds upon knockdown of *T26E3.6, F28C12.4 (sra-20), T06G6.7 (srw-88)*, *W02A11.13 (toe-4), Y18D10A.2, Y18D10A.9, F08A8.5, CC4.3 (smu-1), F44F1.6, M01E5.6 (sepa-1), Y40B1A.1, Y6B3B.4, W04A8.6* and *Y36D3A.5 (tfg-1)* indicating more general regulators of RAS/MAPK signalling. To investigate genes exhibiting functional differences due to polymorphisms we focussed our studies on the candidate genes which had an effect in one background only. From the set of genes we decided to start our analysis on *pfd-3* and *F44F1.1* (see **Table 7.2** in the Appendix for polymorphisms).

PFD-3 is a putative prefoldin that is orthologous to human von Hippel-Lindau binding protein 1 (VBP1). The von Hippel-Lindau protein (VHL) acts in the oxygen-sensing pathway and is involved in the proteasomal degradation of hydroxylated hypoxia-inducible factors (HIFs) (Nordstrom-O'Brien et al. 2010). Alterations in the von Hippel-Lindau tumour suppressor (VHL) are associated with the von Hippel-Lindau disease that predisposes to central nervous system haemangioblastomas, renal cysts and renal cell carcinoma (Barontini and Dahia 2010). VBP1 intracellular localisation depends on VHL (Tsuchiya et al. 1996) and the cooperation of VBP1 and VHL was found to be crucial in the efficient poly-ubiquitination and subsequent proteasome-mediated degradation of HIV-1 integrase (Mousnier et al. 2007). These findings suggest the involvement of VBP1 in the VHL pathway, although no correlation with renal tumourigenesis has been observed (Clifford et al. 1999). *F44F1.1* was initially found as a calpain-like sequence (Syntichaki et al. 2002) and was later defined as a pseudogene with reduced or no functionality (WormBase release WS225). *F44F1.1* is paralogous to *F44F1.3*, which is an orthologue of human calpain

15. Calpains are Ca^{2+}-activated regulatory proteases that have been implicated in a number of developmental events, such as cell differentiation, proliferation as well as signal transduction and apoptosis (Sorimachi et al. 1997; Sato and Kawashima 2001), the development of the nervous system, in respiratory diseases, breast cancer and further pathological cases (Huang and Wang 2001). Both polymorphic genes, *F44F1.1* and *pfd-3*, have been identified in a screen for suppression of the egg-laying defective phenotype in the *egl-9* mutant in addition to *lin-10, vhl-1* and *hif-1* (Gort et al. 2007). VHL-1, HIF-1 and EGL-9 are the *C. elegans* homologues of VHL, HIF-1A and EGLN3, respectively, that act in the conserved hypoxia response pathway (Jiang et al. 2001; Epstein et al. 2001). These and the above mentioned findings suggested a functional link between conserved RAS/MAPK and hypoxic signalling events that is influenced by natural variation. Thus, we set out to investigate the interaction of these pathways in more detail.

3.3.2 Verification of candidate genes modulating RAS/MAPK signalling during vulval induction

We started our analysis by verifying the candidate genes *F44F1.1* and *pfd-3* that had been discovered in the RNAi screen performed by Schmid et al. (2015). We crossed the *F44F1.1(ok1765)* allele into the *let-60(n1046)* mutants and found that the deletion in *F44F1.1* decreased vulval induction to an average index of 3.67, 95% CI [3.57, 3.78] (**Fig. 3.8A**) compared to the *let-60(n1046)* single mutant sibling with an average induction of 4.00, 95% CI [3.87, 4.12]. The opposite had been found in the RNAi experiments, where the knockdown of *F44F1.1* had increased vulval induction in the *let-60(n1046)* mutant background (**Fig. 3.8B**). Since *F44F1.1* and *F44F1.3* exhibit some similarity in their genomic sequence as well as their RNAi clone sequences, we performed RNAi against *F44F1.3* and included the *F44F1.3(ok1878)* deletion mutant into our studies. However, RNAi against *F44F1.3* had no effect on either introgressed or non-introgressed lines (**Fig. 3.8C**). Furthermore, we were not able to verify the *ok1878* deletion in the mutant we had obtained from the *Caenorhabditis elegans* Genetic Center (CGC), i.e. there was no deletion in the *F44F1.3* gene (as tested by PCR). Thus, since RNAi frequently shows off-target effects, especially for similar gene sequences, we regarded the data we had obtained using the *F44F1.1(ok1765)* mutant as more relevant for our studies.
The knockdown of *pfd-3* had resulted in the reduced VI in the milL (Schmid et al. 2015). As there was no mutant commercially available, we employed CRISPR/Cas9 in a joined effort with K. Jovic and T. Schmid to obtain a deletion mutant. Following the protocol as described in Friedland et al. (2013), we used four different sgRNAs flanking the *pfd-3* coding sequence (CDS) and a repair template lacking the entire CDS that we had obtained through prior insertion of BglII restriction sites and enzymatic digestion (**Fig. 3.8D**). We obtained mutants harbouring deletions of different sizes that led to sterility when homozygous and that we had lost before we could balance the mutation.

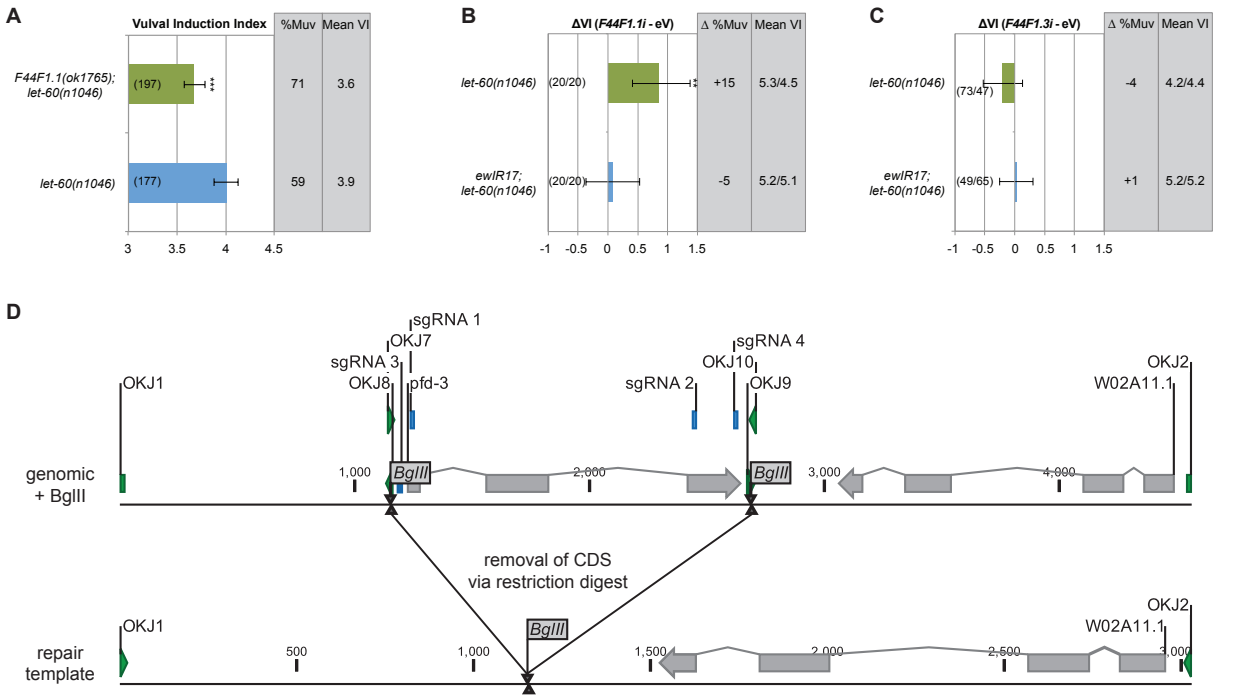

Figure 3.8. (A) A deletion in *F44F1.1* significantly reduces the VI of *let-60(n1046)* mutants. **(B)** The knockdown of *F44F1.1* increases the VI of non-introgressed but not introgressed *let-60(n1046)* mutant lines. The difference in the percentage of Muvs is indicated and the mean VI and number of animals are indicated as RNAi treated / empty vector (eV). **(C)** The knockdown of *F44F1.3* affects neither the VI of introgressed nor the one of non-introgressed animals. The difference in the percentage of Muvs is indicated and the mean VI and number of animals are indicated as RNAi treated / empty vector. p values were derived from from bootstrapping 1000 samples, where *** $p < 0.001$ and ** $p < 0.01$ and the number of animals analysed is indicated in brackets. Error bars indicate the 95% confidence interval. **(D)** Scheme of CRISPR/Cas9 mediated endogenous mutagenesis within the *pfd-3* locus. Via site-directed mutagenesis, two BglII sites were inserted into the repair template to flank the CDS. The CDS was removed via enzymatic restriction digest. OKJ - primers used for cloning, sgRNA - sgRNAs used to cut the genomic sequence, BglII - position of BglII restriction sites.

3.3.3 EGL-9 affects RAS/MAPK signalling at the level or downstream of SEM-5/GRB2 or SOS-1/SOS1

Our results indicating that EGL-9 is a positive regulator of RAS/MAPK signalling in the vulva (see chapter 3.2) were obtained in a *let-60(n1046gf)* mutant background. To exclude allele-specific effects and to study at which step in the RAS/MAPK cascade EGL-9 acts, we performed epistasis experiments. We used the *lin-3(e1417)* (Hwang 2004), *let-23(sy1)* (Aroian and Sternberg 1991), *lin-2(n397)* (Horvitz and Ferguson 1985), *lin-7(e1413)* (Simske et al. 1996), *lin-10(e1439)* (Whitfield et al. 1999), *sem-5(n2019)* (Clark et al. 1992), *sos-1(s1031)* (Chang et al. 2000) and *lin-45(sy96)* (Sternberg et al. 1993) alleles and crossed them to the *egl-9(sa307)* mutant. We found that a loss of EGL-9 decreased the VI of animals mutant for

lin-45 or *let-60* combined with *sos-1* (only the double mutants are viable) but not for any of the other alleles (**Fig. 3.9A**). It is possible that EGL-9 acts at the level of SOS-1 which is however masked by the presence of the *let-60(n1046)* allele. To exclude any allele-specific effects stemming from the *egl-9(sa307)* mutant, we included into our analysis a temperature-sensitive allele of *egl-9*, *n586*. In support of our data we found that the *egl-9(n586)* allele suppressed the VI of *let-60(n1046)* animals with an increase in temperature, most strongly at the restrictive temperature of 25 °C (**Fig. 3.9B**). We conclude that EGL-9 acts either at the level of SEM-5 or SOS-1 or in parallel to promote RAS/MAPK signalling strength in the vulva.

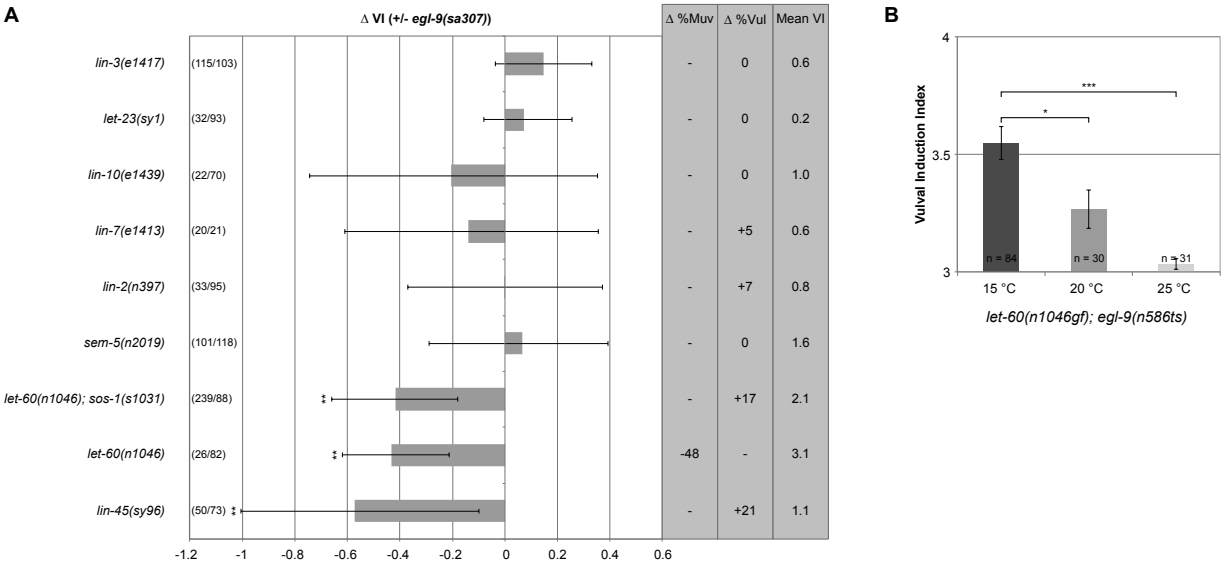

Figure 3.9. Difference in VI values of mutants of the RAS/MAPK pathway with and without the *egl-9(sa307)* or *egl-9(n586ts)* allele. The difference is shown for double mutant animals compared with their respective single mutant siblings. p values were derived from bootstrapping 1000 samples, where *** $p < 0.01$, ** $p < 0.01$ and * $p < 0.05$. **(A)** The mean VI is indicated for the double mutant. The number of animals analysed is indicated in brackets (double mutant / single mutant sibling). Error bars indicate the 95% confidence interval. Note that the *sos-1(s1031)* was analysed in combination with the *let-60(n1046)* allele due to lethality in the single mutant. **(B)** With a rise in temperature, the *egl-9(n586)* allele suppresses the VI of *let-60(n1046)* mutants. The mean values are shown with the 95% confidence intervals as error bars.

3.3.4 EGL-9 and CDK-5 are presumably not involved in the localisation of LET-23

The epistasis analysis indicated that *egl-9* acts at the level or downstream of either SEM-5/GRB2 or SOS-1/SOS1. Others had found that *lin-10* RNAi suppressed the egg-laying defective phenotype of *egl-9* mutants (Gort et al. 2007). Moreover, Park et al. (2012) had described a mechanism, in which EGL-9 competes with CDK-5 for the post-translational modification of LIN-10 to regulate trafficking of the glutamate receptor GLR-1 (**Fig. 3.10A, B**). They proposed that proline hydroxylation of LIN-10 sterically inhibits serine phosphorylation by CDK-5 and thereby

indirectly supports the function of LIN-10 in receptor recycling back to the cell membrane. During hypoxia, when EGL-9 becomes inactive, LIN-10 is phosphorylated and less active in receptor recycling, thus signalling through GLR-1 is decreased. Based on these findings, we asked whether EGL-9 and CDK-5 are similarly involved in LET-23 trafficking by competing for LIN-10 modification in the VPCs (**Fig. 3.10C, D**).

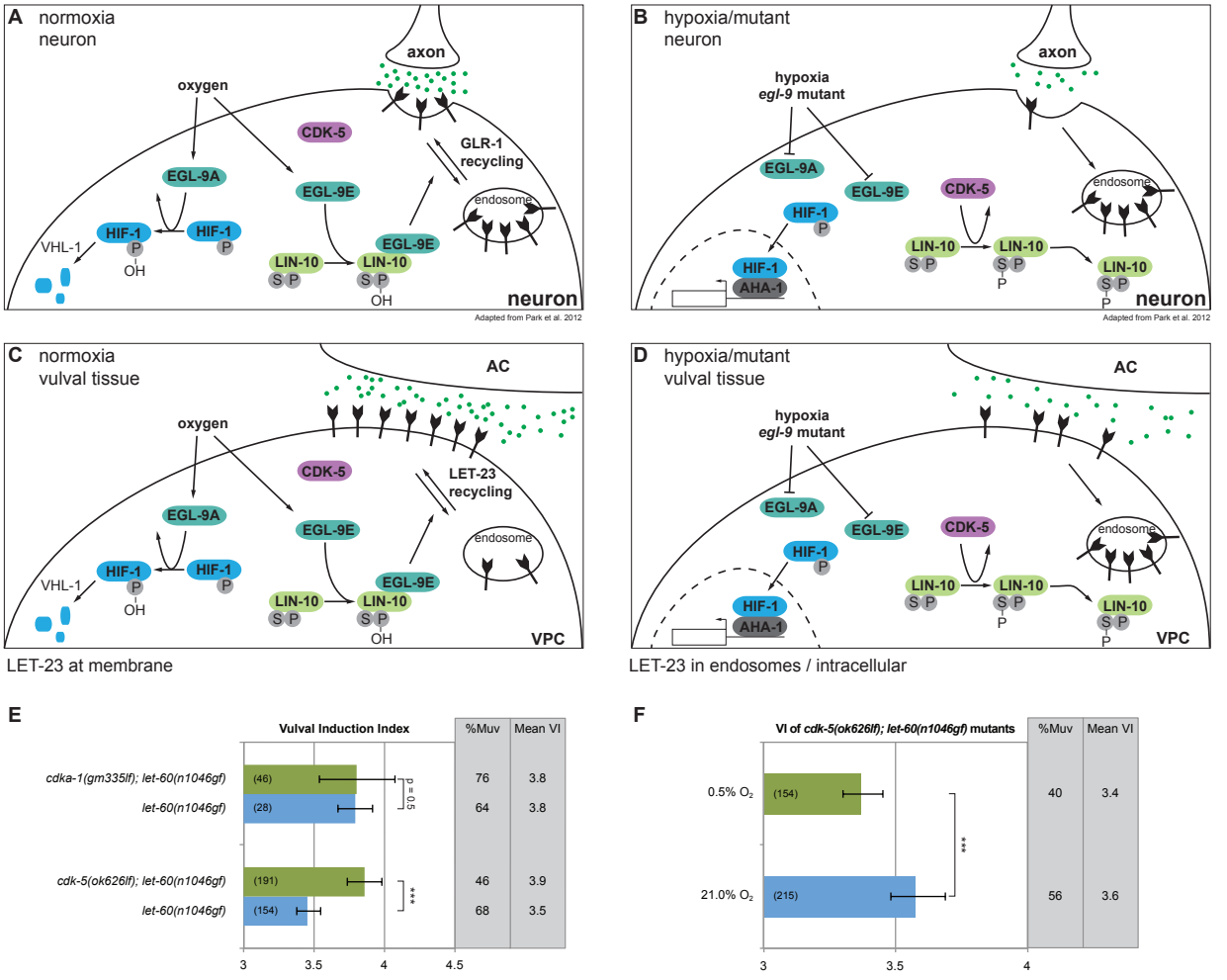

Figure 3.10. Role of EGL-9 in receptor trafficking. In neurons, EGL-9 competes with CDK-5 for LIN-10 post-translational modification in addition to its role in HIF-1 modification. **(A)** In normoxia, prolyl hydroxylation of LIN-10 is thought to promote receptor recycling and signalling. **(B)** In hypoxia, hydroxylation does not take place but LIN-10 is phosphorylated at serine and recycling is diminished. Since LIN-10 localised LET-23 in the VPCs, a similar function of EGL-9 and oxygen could control LET-23 trafficking and signalling. According to the data, EGL-9 would promote LET-23 plasma membrane localisation through LIN-10 modification **(C)** whereas hypoxia reduces signalling through preventing the hydroxylation and allowing CDK-5 mediated phosphorylation of LIN-10 **(D)**. **(E)** The loss of CDKA-1 does not alter RAS/MAPK activity in *let-60(n1046)* mutant animals, whereas loss of CDK-5 increases RAS/MAPK signalling. **(F)** During hypoxia, the VI of animals mutant for *cdk-5* is reduced significantly. p values were derived from bootstrapping 1000 samples, where *** $p < 0.001$. Error bars indicate the 95% confidence interval and the number of animals analysed is indicated in brackets.

We started by crossing the predicted null allele *ok626* of *cdk-5* (Juo et al. 2007) into *let-60(n1046gf)* mutant animals and determining the VI. If CDK-5 is involved in LET-23 trafficking similarly to its function in GLR-1 trafficking, we would expect that vulval induction in the double mutant at normoxia can be increased. Indeed, loss of CDK-5 increased the VI of *let-60(n1046gf)* animals (**Fig. 3.10E**). However, vulval induction of these double mutants was decreased upon hypoxic exposure conflicting the results in neurons, where *cdk-5(ok626lf)* mutants were insensitive to hypoxia (**Fig. 3.10F**) (Park et al. 2012). Finally, a loss of CDKA-1 (also known as p35), the activator of CDK-5 (Juo et al. 2007), had no effect on vulval induction (**Fig. 3.10E**). We continued by introducing a translational LET-23::GFP reporter (Haag et al. 2014) into the *egl-9(sa307lf)* and *cdk-5(ok626lf)* mutant backgrounds and by quantifying fluorescence intensity. In line with the findings in neurons (Juo et al. 2007; Park et al. 2012), there was no visible change in the *cdk-5(ok626lf)* mutant (**Fig. 3.11A**). In *egl-9(sa307lf)* mutants carrying the reporter, we observed a diffuse signal in the VPCs (**Fig. 3.11A**). However, this signal was present also in the *egl-9(sa307lf)* mutant without reporter and seemed dependent on *hif-1*, since there was no such signal in *egl-9(sa307lf) hif-1(ia04)* mutant animals (data not shown). Park et al. (2012) had described that GLR-1 receptor mislocalisation was independent of *hif-1*, thus we expected to see a LET-23 mislocalisation phenotype in *egl-9(sa307lf) hif-1(ia04)* mutant animals, which we did not. Because of the diffuse fluorescence in *egl-9* mutant animals, which we classified as mutant specific auto-fluorescence, we quantified LET-23::GFP by determining the apical to basal ratio as described in Haag et al. (2014). We did not detect any changes in the fluorescence intensity ratio (**Fig. 3.11B**).

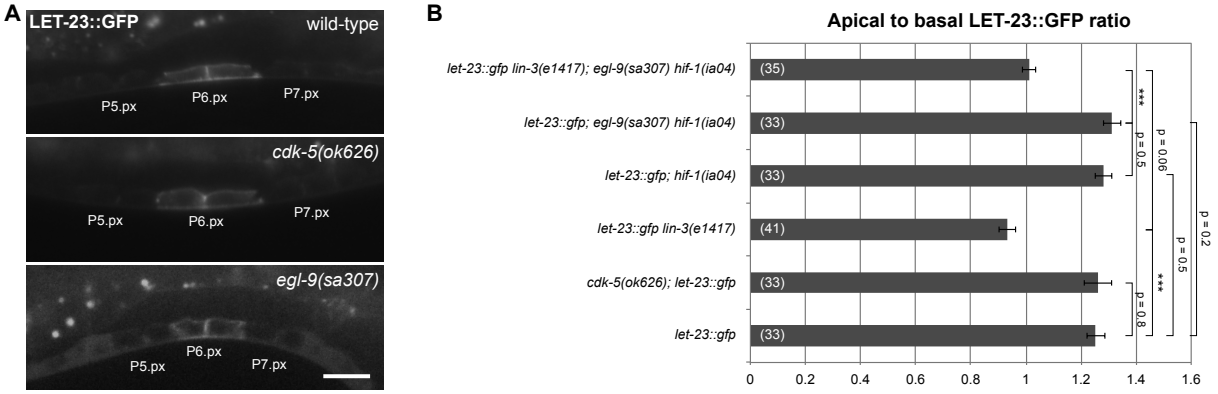

Figure 3.11. Localisation of LET-23::GFP. **(A)** Receptor localisation is prominent at the membrane and unchanged in animals mutant for *cdk-5* or *egl-9.* Note the diffuse fluorescence in *egl-9(sa307)* mutant animals that is specific to the mutant and *hif-1* dependent (see text for details). **(B)** Quantification of apical to basal LET-23::GFP intensity values. Loss of EGL-9, HIF-1 or CDK-5 has not effect on the apical/basal ratio. As a control, intensity was measured in *lin-3(1417)* mutant animals, in which LET-23 internalisation is reduced and the apical/basal ratio similarly reduced (Haag et al. 2014). p values were derived from a two-tailed student's t-test and *** $p < 0.001$. Error bars indicate the standard error of the mean. The number of animals analysed is indicated in brackets. The scale bar indicates 10 µm.

To circumvent the auto-fluorescence and investigate intracellular LET-23 localisation in *egl-9* mutants, we generated animals carrying an extra-chromosomal translational LET-23::mCherry reporter construct. The expression pattern of the reporter was comparable to the GFP version, although accumulation of mCherry in punctae was visible as had also been observed by others (Shcherbo et al. 2007) (**Fig. 3.11A** and **3.12A**). The LET-23::mCherry reporter did not show any intracellular accumulation in the absence of EGL-9 (**Fig. 3.12B**) as opposed to GLR-1 (Park et al. 2012).

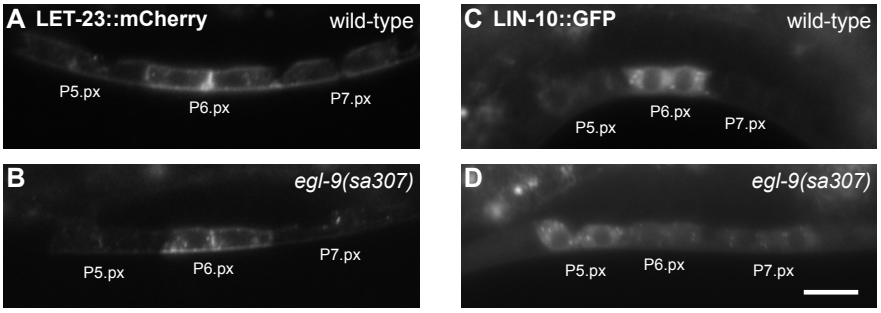

Figure 3.12. Expression of LET-23::mCherry and LIN-10::GFP constructs in the Pn.px stage. Localisation of a LET-23::mCherry construct resembles the expression of LET-23::GFP **(A)**. As for LET-23::GFP, there is no change in localisation in *egl-9(sa307)* mutants **(B)**. In the red fluorescence channel, the autofluorescence is not detectable. A LIN-10::GFP extrachromosomal array is visible in the VPCs intracellularly both in wild-type **(C)** and *egl-9(sa307)* **(D)**. The scale bar indicates 10 µm.

Finally, we analysed the expression of an extra-chromosomal translational LIN-10::GFP reporter that was kindly provided by Rocheleau lab. LIN-10::GFP was present in a punctate pattern throughout the VPC body (**Fig. 3.12C**). Expression was overall variable in intensity and in the number or fate identity of VPCs, e.g. sometimes stronger in P5.p (**Fig. 3.12D**). In the *egl-9(sa307lf)* mutant background, we did not observe any changes in the localisation or intensity of the LIN-10::GFP construct within a given VPC. Note that the more diffuse signal in the mutant does not originate from the reporter but from the auto-fluorescence as explained above. In conclusion, our genetic and fluorescent reporter analyses do not support the model proposed by Park et al. (2012) in terms of vulval development. Rather, hydroxylation seems to actively promote RAS/MAPK signalling in the VPCs without affecting LET-23 receptor trafficking.

3.3.5 Loss of EGL-9 does not impair sex myoblast migration or division

During vulval development, RAS/MAPK signalling downstream of LET-23/EGFR is important to confer vulval cell fates (Sternberg and Horvitz 1986). On the other hand, RAS/MAPK activity downstream of EGL-15/FGFR is involved in the correct formation of the sex muscles that contribute to egg-laying (DeVore et al. 1995; Burdine et al. 1998). The egg-laying system of *C. elegans* is composed of the vulva, sex muscle cells and neurons (White et al. 1976; Sulston and Horvitz 1977) so that defects in egg-laying can be attributed to either component. The hermaphrodite-specific neurons (HSNs) release serotonin to act on the vulval muscles and to stimulate egg-laying (Horvitz et al. 1982) and exogenous serotonin can rescue the egg-laying defects of HSN-ablated defective animals (Waggoner et al. 1998). Animals mutant for *egl-9* do not show any abnormalities in vulval development (present study) and were found to be resistant to exogenous serotonin in terms of egg-laying (Trent et al. 1983), which argues against defects in the neuronal circuit that controls egg-laying behaviour. The sex muscles, i.e. the vulval and uterine muscles, originate from two sex myoblasts that are born at the late L3 stage and migrate towards the developing vulva in response to *egl-17/FGF* (Burdine et al. 1998). Both myoblasts divide three times to produce the 16 descendants giving rise to the sex muscles (eight vulval muscle cells and eight uterine muscle cells) (Corsi et al. 2002). We thus asked, whether the egg-laying defective phenotype of *egl-9* mutants is associated with defects in RAS/MAPK signalling in response to EGL-17/FGF. To this aim, we employed the transcriptional *Phlh-8*::GFP reporter that is expressed in the descendants of the sex myoblasts to monitor division and migration (Harfe et al. 1998). We did not observe any of the severe defects in the migration or division of *Phlh-8*::GFP expressing cells in *egl-9(sa307)* mutant animals (**Fig. 3.13**) as had been described in animals mutant for components of the FGF signalling pathway (Burdine et al. 1998): The two sex myoblasts were positioned correctly close to the vulva and subsequent divisions resulted in 16 daughter cells (eight shown in the focal plane of **Fig. 3.13C, F**). In conclusion, EGL-9 does not seem to be crucial during sex myoblast migration or positioning via FGF and RAS/MAPK activity.

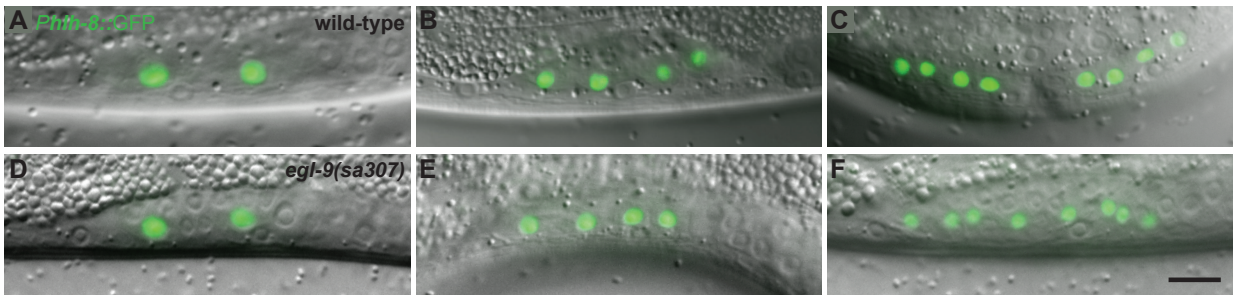

Figure 3.13. Expression of *Phlh-8*::GFP in the migrating sex myoblasts. The sex myoblasts migrate from the tail towards the vulva, undergo three rounds of cell division (two shown here) and produce the sex muscles (**A-C**). Neither migration nor division is impaired in *egl-9(sa307)* mutant animals (**D-F**). The scale bar indicates 10 µm.

3.3.6 A new *hif-1(zh111)* deletion allele is stronger than the *hif-1(ia04)* allele

The *ia04* allele had been described as a null allele, because i) HIF-1 protein was not detectable in the mutant and ii) the 1231 bp deletion was found to cause a frameshift mutation and a premature stop (Jiang et al. 2001; Budde and Roth 2010). (Note that the deletion is annotated incorrectly on Wormbase (WS260) and deletes instead the sequence between 5'-TCCACTGG-CTCCTCCTACTC-3' (upstream) and 5'-AGGATTAGAAAATTGGAGAG-3' (downstream) as we had verified by Sanger sequencing). We and others (M. de Bono, personal communication) are not convinced of the complete loss-of-function nature of the allele for several of the following reasons. The *hif-1* genomic locus encodes five isoforms, one of which is not affected by the *ia04* deletion and had been identified to be expressed (EST information available from the Kohara lab) (**Fig. 3.14A**). This isoform lacks the DNA binding domain but can be regulated by oxygen and comprises one of the PAS domains that interact with HIF-1ß (Jiang et al. 1996) (**Fig. 3.14B**). Furthermore, to detect HIF-1 protein by Western blotting, Budde et al. (2010) had obtained an antibody by using the N-terminus of *C. elegans* HIF-1 that is not present in the shortest isoform, since the transcriptional start site is further downstream in the genomic locus (**Fig. 3.14A**). Additionally, there is a polymorphism in the *hif-1* locus that impairs the first splice donor in this shorter HIF-1 isoform and leads to a truncated protein (72 vs. 503 amino acids) (WormBase, WS260) (**Fig. 3.14A**, black arrowhead). This polymorphism is present in a number of wild isolates, among which CB4856 (Thompson et al. 2013). Based on these observations, we knocked down *hif-1* in the *let-60(n1046gf); hif-1(ia04rf)* mutants and found that vulval induction was slightly but significantly decreased (**Fig. 3.14C**). Next, we employed CRISPR/Cas as described in Arribere et al. (2014) to obtain a larger deletion in *hif-1* as well as to introduce the splice site polymorphism present in CB4856 into the N2 background. While we did not succeed in obtaining the latter strain, we obtained a 2464 bp deletion (*zh111*) that removes parts of all isoforms (**Fig. 3.14A**). We crossed the *hif-1(zh111)* allele to *let-60(n1046gf)* and found that vulval induction was even more increased as by the *hif-1(ia04)* allele (**Fig. 3.14D**), supporting our hypothesis of a residual HIF-1 function in the *hif-1(ia04)*. Unfortunately, we were not able to verify the absence of HIF-1 protein in the mutant as Budde et al. (2010) had proposed, since the commonly used CeHIF-1 antibody was not available anymore.

3.3.7 The canonical hypoxia response pathway affects RAS/MAPK signalling in the vulva during normoxia

Our results indicate that EGL-9 and VHL-1 enhance RAS/MAPK signalling in a sensitised background, whereas HIF-1 inhibits signalling (see also chapter 3.2). To further test whether *egl-9, vhl-1* and *hif-1* act in the same pathway to impinge on RAS/MAPK activity, i.e. cooperatively in the hypoxia response pathway rather than separately, we constructed triple mutants for epistasis analysis. Vulval induction was increased by a deletion in *hif-1* in a manner epi-

static to the *vhl-1(ok161)* or *egl-9(sa307)* deletions (**Fig. 3.15**). In addition, we found that the VI of *let-60(n1046); egl-9(sa307); vhl-1(ok161)* triple mutants was decreased as compared to *let-60(n1046)* single mutants, but not further when compared to either *let-60(n1046); egl-9(sa307)* or *let-60(n1046); vhl-1(ok161)* mutant animals (**Fig. 3.15**). We conclude from this epistasis that EGL-9, VHL-1 and HIF-1 act together not only to control expression of oxygen responsive genes but also to modify RAS/MAPK activity during normoxia.

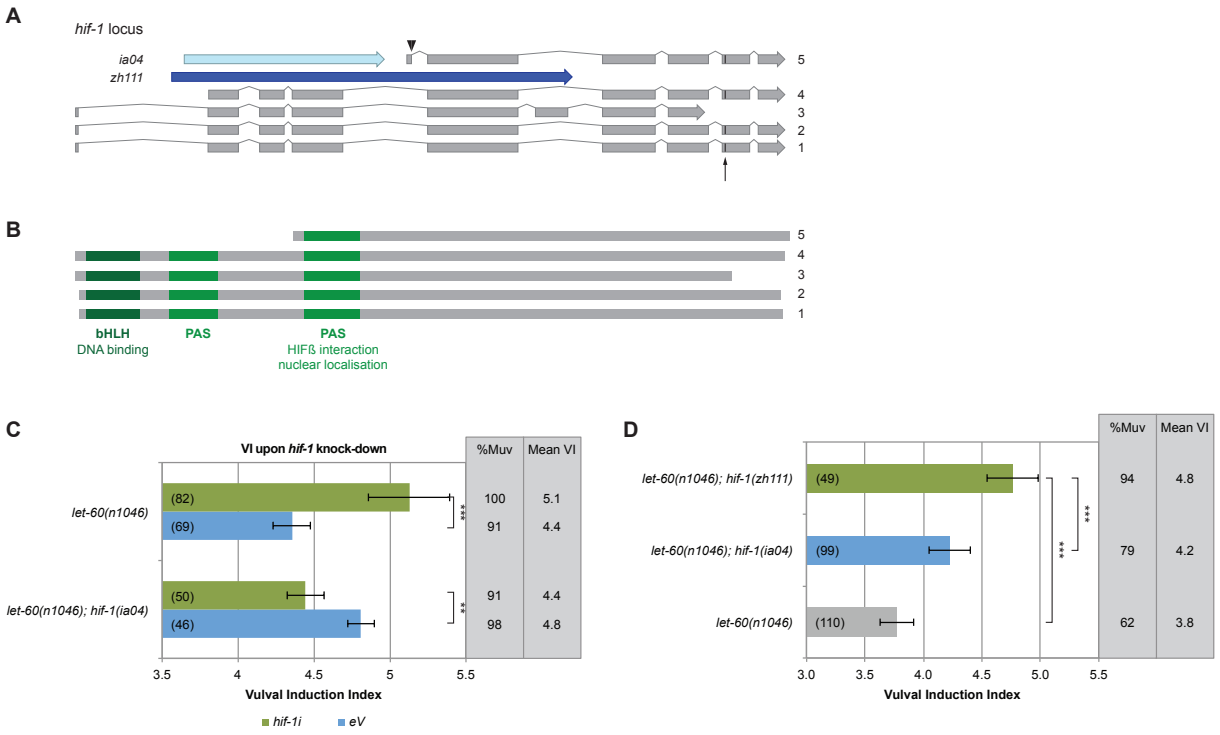

Figure 3.14. (A) Schematic representation of the *hif-1* genomic locus. The locus encodes five isoforms and four are partially deleted in the *ia04* allele. The larger *zh111* deletion obtained by CRISPR/Cas9 removes parts of all isoforms. The arrow indicates the P621 site of EGL-9 hydroxylation that is not present in one isoform. The arrowhead points to the splice donor site that contains a SNP in a number of isolates including CB4856 and impairs splicing. **(B)** the protein domains of the five HIF-1 isoforms are indicated. The shortest isoform, that is impaired in CB4856, does not contain the DNA binding domain but one of the PAS protein interaction domains. **(C)** RNAi of *hif-1* increases the VI of *let-60(n1046)* animal and decreases the VI of *let-60(n1046); hif-1(ia04)* mutants. **(D)** The VI of *let-60(n1046)* mutants is increased when combined with the *hif-1(ia04)* allele and more strongly increased when combined with the *hif-1(zh111)* allele. p values were derived from bootstrapping 1000 samples, where *** $p < 0.001$ and ** $p < 0.01$. Error bars indicate the 95% confidence interval and the number of animals analysed is indicated in brackets.

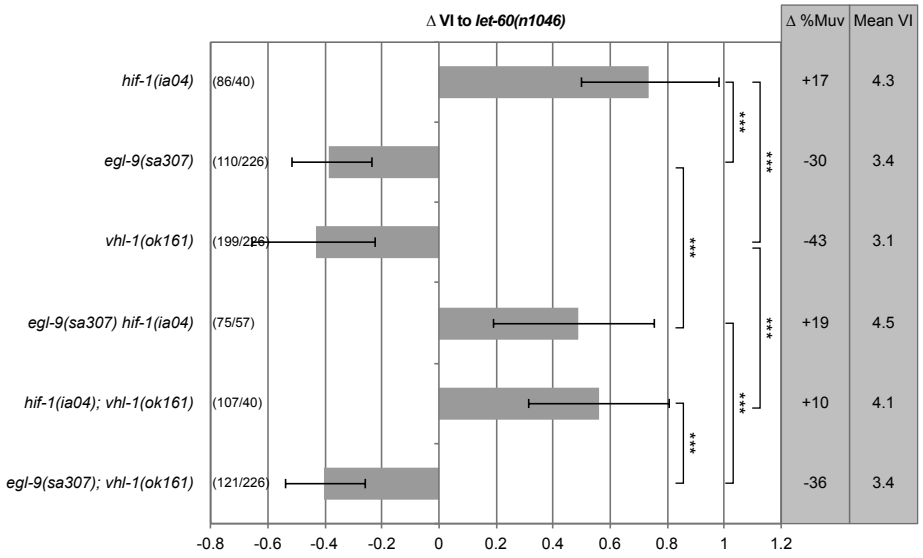

Figure 3.15. Epistasis analysis between LET-60 and the core hypoxia response pathway. Loss of EGL-9 or VHL-1 decreases the VI and the loss of HIF-1 increases the VI in a manner epistatic to both EGL-9 and VHL-1. The differences in VI are indicated in comparison to the respective *let-60(n1046)* single mutant sibling. p values were derived from bootstrapping 1000 samples, where *** $p < 0.001$. Error bars indicate the 95% confidence interval and the number of animals analysed is indicated in brackets (double or triple mutant / *let-60(n1046)* sibling). The mean VI value refers to the double / triple mutant.

3.3.8 Loss of EGL-9 does not affect vulval cell fates

We had found that vulval induction was changed by the loss of EGL-9 or HIF-1 in animals carrying mutations in members of the RAS/MAPK cascade but not in animals mutant for *lin-12* (*gf* or *lf*) (see also chapter 3.2). It could be assumed that alterations in signalling result in a different pattern or intensity of downstream marker genes, such as the 1° cell fate marker *egl-17::gfp* (Burdine et al. 1998) or the 2° cell fate marker *lip-1::gfp* (Berset et al. 2001). We tested this hypothesis by crossing these reporters into the *egl-9(n586lf)* temperature-sensitive mutant background. We raised animals at the non-restrictive (15 °C - 20 °C) and the restrictive temperature (25 °C) when vulval induction is reduced (**Fig. 3.9B**). For both markers analysed, we did not notice any difference in either localisation or fluorescence intensity in the absence of EGL-9 (**Fig. 3.16**). From these findings, we conclude that *egl-9* is involved in fine-tuning rather than instructing RAS/MAPK signalling strength or that it acts in a parallel pathway.

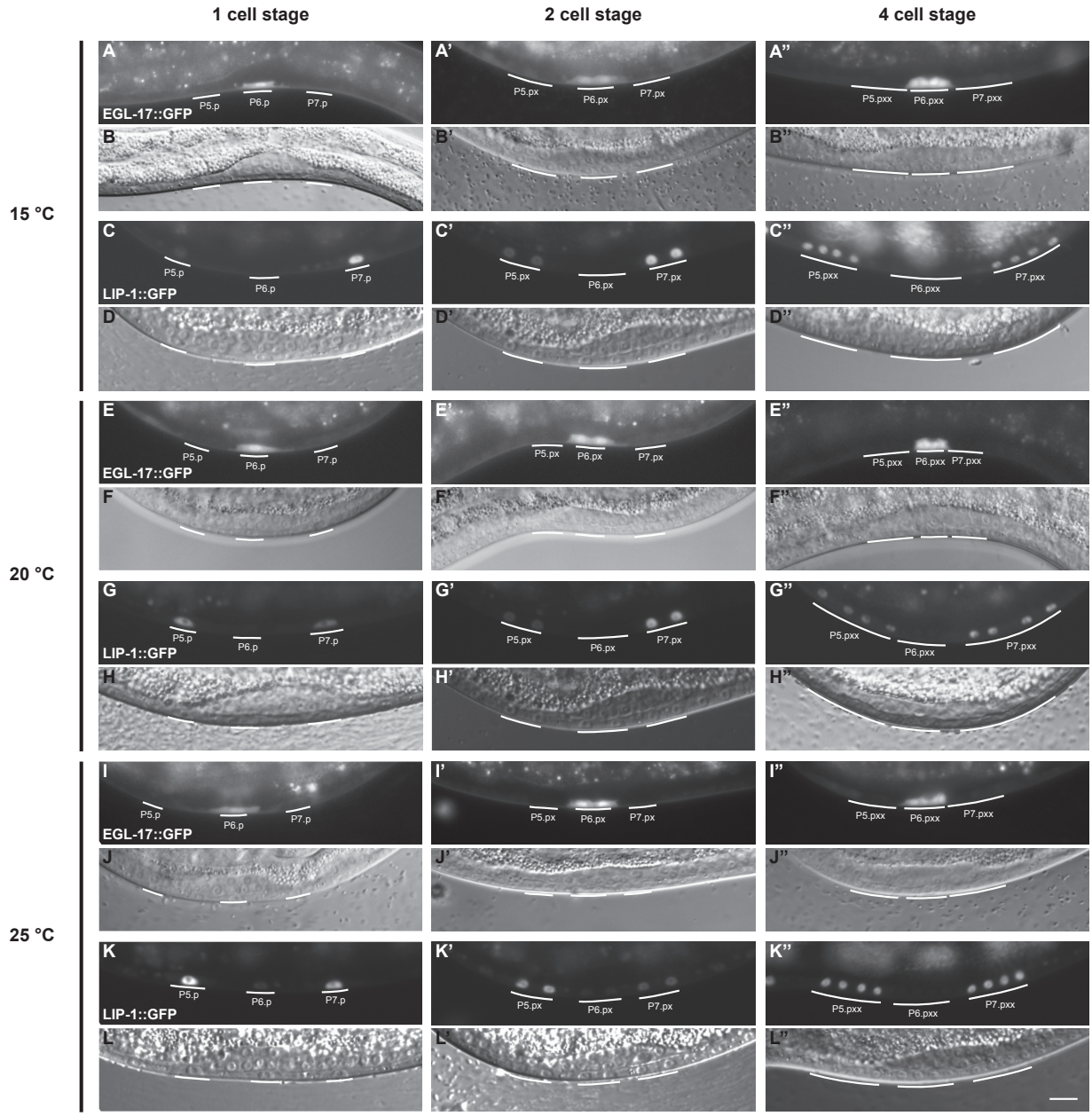

Figure 3.16. Vulval cell fates are not changed in *egl-9(n586ts)* mutant animals. The localisation of EGL-17::GFP is not changed in *egl-9(n586ts)* mutant animals raised at the permissive temperatures 15 °C **(A)** and 20 °C **(E)** or the restrictive temperature 25 °C **(I)** and most prominent in P6.p and descendants. 1, 2 and 4 cell stages are shown. Similarly, the localisation of LIP-1::GFP is unchanged in *egl-9(n586ts)* mutant animals raised at the permissive temperatures 15 °C **(C)** and 20 °C **(G)** or the restrictive temperature 25 °C **(K)** and most prominent in P5.p and P7.p and descendants. 1, 2 and 4 cell stages are shown. The scale bar indicates 10 µm.

3.3.9 Hypoxia affects the RAS/MAPK signalling pathway downstream of LET-23/EGFR and upstream of LIN-1/ETS

We have shown that hypoxia inhibits RAS/MAPK signalling in the vulva i) upstream of or in parallel with the ETS family transcription factor LIN-1 (Beitel et al. 1995) (see chapter 3.2) and ii) in part independently of *hif-1* (see chapter 3.2 and **Fig. 3.17**). We further found that hypoxic inhibition of RAS/MAPK activity depends on *egl-9* and *vhl-1* in the *let-60(n1046)* mutant background, since induction was not further changed upon hypoxia in presence of either deletion allele (**Fig. 3.17**). Moreover, we did not see any effect of hypoxia in animals where LET-23 is severely mislocalised, i.e. in animals mutant for *lin-2, lin-7* or *lin-10* (Haag et al. 2014). In contrast, there was an intermediate reduction in the VI of *let-23(sy1)* mutant animals (see chapter 3.2) in which LET-23 activity is reduced due to decreased basolateral localisation but not abolished (Simske et al. 1996). Finally, hypoxia did not suppress the Muv of animals mutant for *lin-15*, which acts upstream of *let-23* and in parallel to *lin-3* to inhibit vulval induction (Huang et al. 1994; Clark et al. 1994) and there was no effect on the VI of animals mutant for BAR-1/ß-catenin or LIN-12/Notch. Together, these results strongly suggest that hypoxia acts specifically on the RAS/MAPK signalling cascade, genetically upstream of or in parallel to LIN-1 but downstream of LET-23.

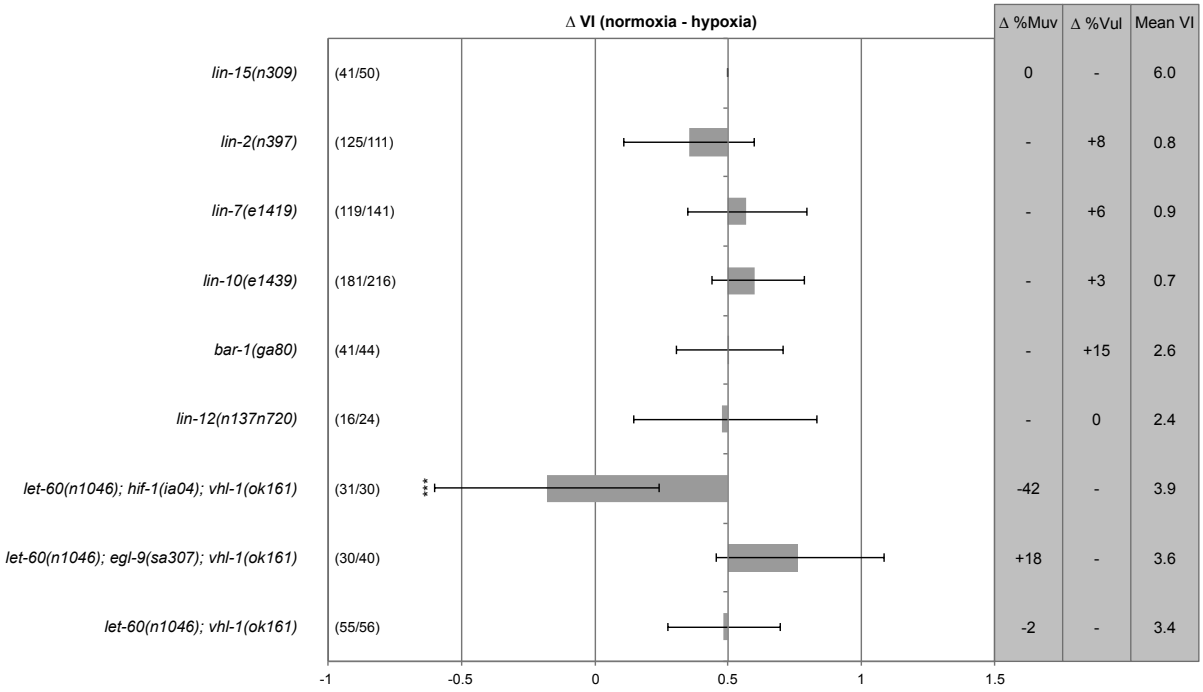

Figure 3.17. Difference in VI of hypoxia treated animals compared with animals raised in normoxia. p values were derived from bootstrapping 1000 samples, where *** $p < 0.001$. The mean VI is indicated for the hypoxic situation. The number of animals analysed is indicated in brackets (hypoxia / normoxia). Error bars indicate the 95% confidence interval.

3.3.10 During normoxia HIF-1 and EGL-9 are dispensable in the germline but HIF-1 is required for the hypoxic reduction of RAS/MAPK activity

Hypoxic exposure suppressed RAS/MAPK activity during vulval development, meiotic germ cell progression and the specification of the excretory duct cell precursor in the embryo (see chapter 3.2 draft). We had further observed that both EGL-9 and HIF-1 are required in the vulva during normoxia and that RAS/MAPK activity is reduced during hypoxia partially independently of HIF-1. Analogously, we tested the requirement for EGL-9 and HIF-1 in the germline, both during normoxia and hypoxia. Neither did the loss of EGL-9 reduce the percentage of stacked oocytes in *let-60(ga89ts)* animals raised at the restrictive temperature nor did the loss of HIF-1 increase the phenotype (**Fig. 3.18**). Since the phenotype of *let-60(ga89)* mutant animals is > 90% penetrant and strong at 25 °C and may prevent the detection of any further enhancement, we tested the *hif-1(zh111)* allele at 23 °C but did not see any effect compared to the single mutant (data not shown). Hypoxic treatment reduced the percentage of stacked oocytes at 25 °C significantly in *let-60(ga89)* as well as in *let-60(ga89); egl-9(sa307)* mutants (see chapter 3.2 and **Fig. 3.18**) but not in *let-60(ga89); hif-1(zh111)* mutant animals (**Fig. 3.18**) suggesting a requirement of functional HIF-1 upon hypoxia. Together, these results propose that firstly, HIF-1 regulates RAS/MAPK signalling in the germline during hypoxia and secondly, that EGL-9 does not regulate HIF-1 stability during normoxia suggesting the presence of an alternative HIF-1 hydroxylase acting in the germline.

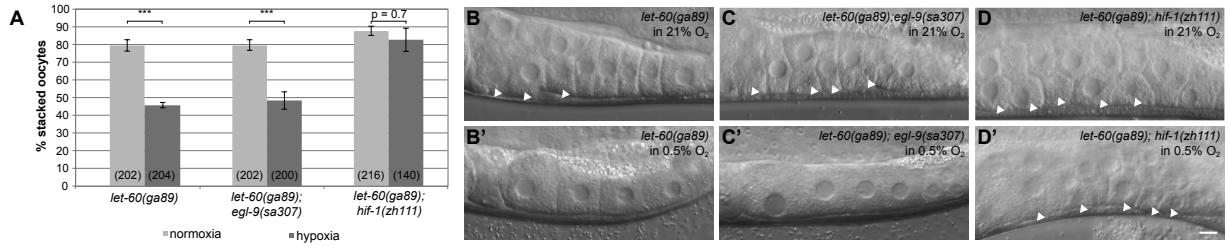

Figure 3.18. (A) Percentage of stacked oocytes of *let-60(ga89gf)* mutant animals carrying either the *hif-1(zh111lf)* or *egl-9(sa307lf)* deletion allele that were raised at the restrictive temperature (25 °C) and in normoxia or hypoxia. Error bars indicate the standard error of the mean and p-values were calculated in a Fisher's exact test where *** $p < 0.001$. The numbers of animals scored are indicated in brackets. **(B)-(D)** Example images of *let-60(ga89gf), let-60(n1046); egl-9(sa307lf)* and *let-60(ga89gf); hif-1(zh111lf)* mutants raised at 25 °C and normoxia **(B, C, D)** or hypoxia **(B', C', D')**. Triangles indicate stacked oocytes. The scale bar indicates 5 µm.

3.3.11 Acknowledgements

We wish to thank all members of the Hajnal laboratory as well as J. Kammenga, B. Beck-Schimmer and K. Basler for critical input and extensive support in this project. We further thank Kim Gauthier for providing the LIN-10::GFP construct and Judith Grolleman for creating the *zh111* deletion. We thank J. Ahringer and J. Reboul for RNAi clones and the *Caenorhabditis elegans* Genetic Center for strains. This work was supported by grants from the Swiss National fond SNF to A.H. and the Kanton Zürich.

3.4 Biarsenical labelling of tetracysteine-tagged proteins is promising in *C. elegans*

3.4.1 Introduction

The imaging of proteins in living cells is a powerful tool to study aspects such as dynamics, trafficking, protein-protein interactions and many more. Fluorescent tags like GFP and variants are widely used to visualise protein expression or localisation (Day and Davidson 2009). However, the considerable size of these fluorescent proteins (approx. 27 kDa) can interfere with protein function or stability (Giepmans et al. 2006) and issues with photostability and cytoplasmic accumulation have been encountered (Shcherbo et al. 2007). Another limitation is the lack of multiplexing, once a protein has been modified with a specific fluorescent tag. Griffin et al. (1998) introduced a new technique whereby proteins are labelled with a small tetra-cysteine tag consisting of the six-amino acid motif CCPGCC. Here, a small fluorescein derivative, such as fluorescein arsenical hairpin binder (FlAsH) or a red-shifted variant resofurin arsenical hairpin binder (ReAsH), is used in a non-fluorescent complex with ethanedithiol (EDT_2). The freed compound can bind to the tetra-cysteine motif upon which fluorescence becomes visible (Hoffmann et al. 2010). FlAsH (MW 664) and ReAsH (MW 545) are comparable in size to MitoTracker® (MW 500-600) and similarly membrane permeable. The tetra-cysteine-based biarsenical labelling system has been applied successfully to study protein localisation and turnover in pulse-chase experiments (Gaietta et al. 2002; Pattnaik and Panda 2009), protein-protein interactions by using the dyes for FRET (Hoffmann et al. 2005), for electron microscopy (Gaietta et al. 2002), affinity purification (Thorn et al. 2008) or SDS-PAGE (Kottegoda et al. 2008). Although biarsenical labelling has proven difficult in the Golgi apparatus or the extracellular space, hence in oxidising environments, successful imaging has been reported with the prior use of reducing agents that keep cysteine thiols accessible for the dyes (Gaietta et al. 2006). The versatility of the system convinced us to test the method in *C. elegans* with a prospect of visualising a presumptive LIN-3/EGF gradient produced by the AC during vulval development that has, as of to date, only been visualised indirectly (Yoo et al. 2004).

3.4.2 Preliminary results

In a first step, we inserted the CCPGCC tetra-cysteine tag (TC-tag) at the C-terminus of functional reporter plasmids. We used the sequence 5'- TGC TGC CCA GGA TGC TGC -3' that we had codon-optimised for *C. elegans* as described (Redemann et al. 2011). We employed reporter plasmids that are widely used as co-injection markers (Frøkjær-Jensen et al. 2008; Arribere et al. 2014; Dickinson et al. 2015), specifically the *Pmyo-2::mCherry::unc-54* 3' UTR and *Pmyo-3::gfp::unc-54* 3' UTR as well as a plasmid containing a 6.3 kb fragment of *lin-3* (Hajnal lab). The visual output (mCherry or GFP expression and a Muv respectively) provides information on the functionality of the TC-tagged transgenes. We micro-injected worms to obtain animals carrying one of the reporters as an extra-chromosomal array and were able to isolate

animals with TC-tagged *lin-3* and *Pmyo-2::mCherry* but not yet *Pmyo-3::gfp*. We adapted protocols used to stain with MitoTracker® (Rimann and Hajnal 2007; Morf et al. 2013), since the size of the dye is comparable to both FlAsH and ReAsH. We applied working concentrations of 5 µM, 7.5 µM and 10 µM for several hours or overnight. We did not detect considerable amounts of background staining with either construct, when we used the BAL washing buffer from the kit (ThermoFisher). However, there was no specific fluorescence where we would have expected the presence of LIN-3 protein (not shown). For the *Pmyo-2::mCherry* construct, the FlAsH staining in the pharynx of array carrying worms was detectable as fluorescence and was specific to animals carrying the array (**Fig. 3.19** and not shown), which proposes that the dye had bound specifically to the mCherry expressed in the pharynx. In further experiments, we will similarly apply ReAsH on worms that carry extra-chromosomal arrays of *Pmyo-3::gfp* that is expressed in body wall muscles (Frøkjær-Jensen et al. 2008).

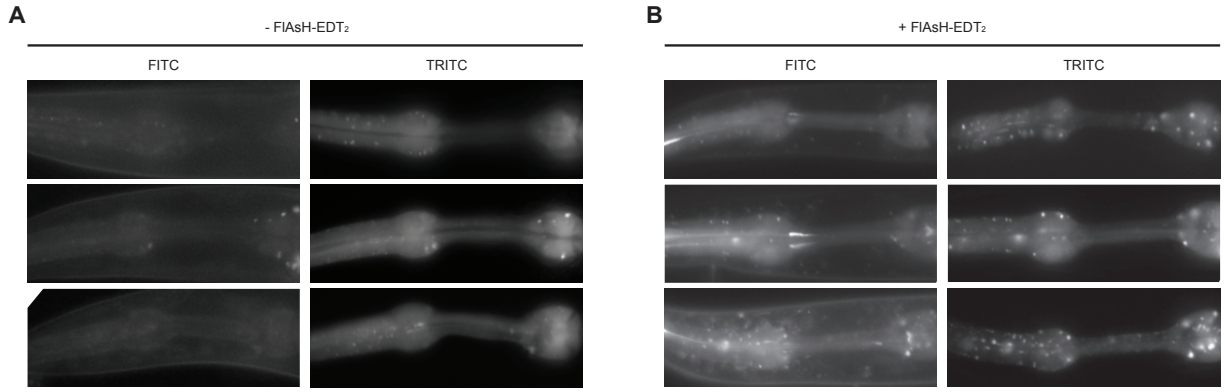

Figure 3.19. FlAsH-EDT_2 staining of *Pmyo-2::mCherry* in the pharynx. **(A)** In control animals treated without the compound, no fluorescence is detectable with the FITC filter set („green", left), although the *Pmyo-2::mCherry* construct is expressed and visible with the TRITC filter set („red", right). **(B)** FlAsH-EDT_2 (left) stains the pharynx of animals carrying the *Pmyo-2::mCherry* array (right).

3.4.3 Further steps in the establishment and usage of biarsenical dyes

To our knowledge, biarsenical staining has not been applied on *C. elegans* and only via injection on *D. melanogaster* eyes in vivo (Venken et al. 2008). Our very preliminary data indicate that biarsenical dyes can permeate the cuticle of the worm to stain proteins expressed from extra-chromosomal arrays and are therefore promising tools as an alternative to GFP-based live imaging. In further experiments, we will test whether we see a similar fluorescence of ReAsH in *Pmyo-3::gfp* transgenic worms as we had seen for FlAsH in *Pmyo-2::mCherry* carrying animals. Moreover, we will tag other fluorescent reporter genes using the tetra-cysteine motif to analyse the spatial concurrence of biarsenical dye and fluorescent protein and improve on the protocol. We did not observe LIN-3 staining and will repeat the experiments with more *lin-3::TC* carrying animals at various stages of development. However, since LIN-3 is

secreted (Hill and Sternberg 1992), prior application of reducing agents may be necessary. In conclusion, biarsenical labelling of TC-tagged proteins appears feasible and promising in *C. elegans*, since i) the dyes seemed able to cross the cuticle and membranes, ii) we did not detect perturbing levels of background staining, iii) TC-tagged proteins can be generated and introduced with minimal effort and iv) viability as well as the development of the worms were not affected.

Discussion

4

4.1 General considerations

4.1.1 Anoxia and hypoxia are ambiguous terms

Studies on oxygen deprivation distinguish between the absence of and a reduction in O_2 (anoxia vs. hypoxia). A precise transition does not exist and the terms appear clearly defined only within a given study. However, anoxia and hypoxia cause profoundly different defects and should thus be evaluated according to well-defined phenotypes rather than the oxygen percentage employed within an experiment in order to prevent confusion and misinterpretation. *C. elegans* is surprisingly resilient against hypoxia and dies only upon prolonged anoxia (> 24h), which is in stark contrast to most other organisms and thought to be accomplished by diffusion (Shen and Powell-Coffman 2003). Here, hypoxia referred to an oxygen concentration below 21% and anoxia to the lack of molecular oxygen (0%). In contrast, another study described genes that confer resistance to hypoxia based on their suppression of lethality in an oxygen concentration of < 0.3% (Mabon et al. 2008). To complicate things further, still others distinguish between “moderate” and “severe” hypoxia. As a matter of fact, the strength of hypoxic insult may determine certain phenotypes rather than hypoxia *per se*. The metabolic rate (as judged from CO_2 production) has been shown to be unchanged at an oxygen concentration as low as 3.6%, slightly reduced down to 2% and severely compromised below (Van Voorhies and Ward 2000). As smooth as the transition between hypoxia and anoxia may be, there are phenotypes clearly defining one or the other situation. In the absence of oxygen (0%), movement, feeding, developmental progression as well as cell divisions cease in worms – a situation known as „suspended animation“ that involves an arrest in the cell cycle (Padilla et al. 2002). Hypoxic treatment (> 0% O_2 and < 21% O_2), on the other hand, does not involve such severe phenotypes and wild-type but not *hif-1* mutants apparently develop normally (Shen and Powell-Coffman 2003). We have analysed the influence of hypoxia on RAS/MAPK signalling in several tissues of the worm and refer to hypoxia as a reduction in oxygen concentration to 0.5%, which we could measure with an oxygen sensor (GOX 100, Greisinger) mounted inside the hypoxic chambers. However, according to the manufacturer, the sensor has an error of 0.1%, which is considerable in this range. To circumvent the falsification of our results by anoxic suspended animation pathways, we only evaluated those experiments, during which worms developed and moved more or less normally (which verified the absence of

suspended animation and thus anoxia) but during which the progeny of *hif-1* mutants was not viable (as is characteristic of hypoxic treatment). For the description of our experiments, we used 0.5% oxygen as an approximation of the concentration applied and considered the phenotypes described as more important. With this approach, we were able to obtain reproducible results and thus emphasise the experimental bias towards oxygen-dependent phenotypes rather than oxygen percentages or generic terms like anoxia and (moderate, severe, strong etc.) hypoxia.

4.1.2 „Isogeneity“ and „wild-type“

When studying a certain cellular or developmental event, the first step most often involves the acquisition of an appropriate mutant. Especially for popular model organisms, researchers have made an effort in collecting newly isolated mutations in commonly accessible databases which substantially simplifies research. Based on common agreement, mutations are engineered in and backcrossed to a reference strain or “wild-type” to create “isogenic” lines. However, particularly in the case of model organisms with a short generation time that are kept within a constant and distinct laboratory environment, evolution at a population level occurs to select individuals with (small) advantages in fitness and establishes an evolutionary distance to the initial wild-type (Caberoy et al. 2003; Folg and Bradley 2005; Gasch et al. 2016). Note that such microevolution of model organisms is unconsciously enforced by favouring their easy-to-handling characteristics. The presence of a mutation can put a selective pressure on specific genes, e.g. to suppress an increased lethality associated with that mutation. Hence, initially isogenic lines become more heterogenic, meaning they differ in the constitution of their genomic background. As much as microevolution is accelerated in simple short-lived model organisms, it can be at least limited by performing regular backcrosses and should be standard practice for organisms that can be stored frozen like *C. elegans* – in theory. In practice, this is rarely done due to the associated additional effort and/or a sheer underestimation of the issue. The fact that a certain mutation of interest is analysed within a non-isogenic environment may account for unexpected, highly variable and even contradictory results and it is the interaction of a trait with its individual genomic and environmental background that produces a measurable phenotype. It is therefore reasonable that the term “wild-type” is not (entirely) valid, since it signifies a reference strain that has undergone laboratory specific genetic adaptation. In the case of *C. elegans*, as of today the “wild-type” reference strain N2 Bristol (Brenner 1974) has already experienced almost 44 years of adaptation which is a considerable amount of time for an organism with a life cycle of only three days. A prominent and disturbing example of adaptation is presented by the *lin-2(n397)* mutant that exhibits a strongly reduced vulval induction index due to a severe mislocalisation of LET-23/EGFR (Horvitz and Ferguson 1985; Hoskins et al. 1996; Kaech et al. 1998). During the course of experiments within the scope of this thesis, the mutant was thawed and backcrossed repeatedly (and frozen immediately thereafter), as the acquisition of random mutations through several generations suppressed the Vul phenotype considerably. An analogous example is given

by the variability in signalling strength that is manifested in a broad range of VIs in sensitised mutants. This is however not solely caused by environmental fluctuations but depends on the set of unrelated or pathway related mutations present in the genome of a strain (Battu et al. 2003; Schmid et al. 2015) and introduced into others upon crossing (**Fig. 3.4, 3.6** and **3.7**). When studying alterations in signalling strength in response to a mutation, it is thus of utmost importance to i) analyse several lines carrying the mutation of interest in order to compensate for differences in the genomic background and ii) to consistently compare the effect of a mutation introduced by mating to the respective control sibling lines rather than to any original strain in order to stay in the same range of unrelated background modifications.

4.1.3 Western blots to measure pERK/ERK and pMEK/MEK ratios are inconclusive

From our genetic data, we had concluded that HIF-1 acts to repress RAS/MAPK signalling whereas VHL-1 and EGL-9 enhance its activity (see chapter 3.2 and **Fig. 3.9, 3.14, 3.15**). Hence, we expected to detect elevated ratios of diphosphorylated (dp) MPK-1/ERK to total MPK-1/ERK as well as elevated phosphorylated (p) MEK-2/MEK to total MEK-2/MEK levels in *hif-1(zh111)* mutant animals and the opposite in *egl-9(sa307)* or *vhl-1(ok161)* mutants. To test this hypothesis, we had performed SDS-PAGE and Western blotting on L4 larvae as described (Nakdimon et al. 2012; Schmid et al. 2015). We chose the *let-60(n1046)* mutant as a reference and the *amx-2(ok1235); let-60(n1046)* mutant animals as a control where we expected increased levels of phosphorylated ERK or MEK (Schmid et al. 2015). To our surprise, however, we were not able to reproduce the results of either publication: Whereas Nakdimon et al. (2012) detected no dpMPK-1 band in N2, the band for the wild-type was obvious on all our blots (data not shown). Second, there was no increase in dpMPK-1/total MPK-1 or pMEK/total MEK in the *let-60(n1046)* mutant sample as compared to the wild-type and third, there was no increase in dpMPK-1 or pMEK in *amx-2(ok1235); let-60(n1046)* mutants as compared to *let-60(n1046)* mutant animals (data not shown). Lastly, there was no difference in dpMPK-1 or pMEK in our *let-60(n1046); egl-9(sa307)* or *let-60(n1046); hif-1(zh111)* mutants in comparison with the *let-60(n1046)* single mutants. Generally speaking, the quantification of the bands representing (di)phosphorylated and total protein was highly variable as had been observed earlier (T. Schmid, personal communication). RAS/MAPK signalling is important not only during vulval development (Kornfeld 1997), but also during duct cell fate specification (Abdus-Saboor et al. 2011) and meiotic cell cycle progression (Church et al. 1995). In relation to the germline, the vulval tissue is rather small and the ERK and MEK levels we had measured in our *egl-9, hif-1* and *vhl-1* mutants may have represented the situation in the germline and masked the levels present in the VPCs. If this was the case, the variability in quantification could have stemmed from natural fluctuations in RAS/MAPK activity, which is supported by our genetic data that had revealed no effect of either HIF-1 or EGL-9 on RAS/MAPK signalling in the germline (see chapter 3.2).

Still, this would not explain why we were not able to reproduce the published data. To circumvent this issue and in addition to analyse MPK-1 dynamics, we intended to introduce a MAPK FRET based biosensor previously reported to be functional in cell culture as well as *C. elegans* ASER neurons (Tomida et al. 2012; Fritz et al. 2013). However, we did not succeed in employing the sensor neither in the VPCs nor in the germline (for a detailed analysis and discussion, the reader is referred to the Master Thesis by S. Boetschi). Since its initial description, there has been a burst in MAPK biosensors and future experiments relating to the projects presented here should include a recently published *C. elegans* sensor that relies on the ratio of cytoplasmic to nuclear intensities (ERK-nKTR). Here, phosphorylation in response to active RAS/MAPK inhibits a nuclear localisation signal and enhances a nuclear export signal (de la Cova et al. 2017).

4.2 Project related considerations

4.2.1 Highly polymorphic genes may modify low polymorphic pathways

The findings of Schmid et al. (2015) and ours suggest the presence of several polymorphic modifiers affecting the WNT and RAS/MAPK pathways during *C. elegans* vulval development. Intriguingly, although the members of these two signalling pathways exhibit some degree of polymorphic divergence, coding SNPs are rare (Thompson et al. 2013 and **Table 7.2**). This fact underscores the essential functions of the WNT and RAS/MAPK pathways during development and a low tolerance for aberrations. A high tolerance for sequence variation in non-essential modifying genes is represented by polymorphic genes containing many coding as well as non-coding SNPs (**Tables 3.7, 3.11, 7.1** and **7.2**). Cumulatively, they can considerably change signalling strength as exemplified in the degree of Vul and Muv phenotypes that strongly depend on the genomic background.

When we consulted the list of polymorphic genes that we had identified in the RNAi screens, we were surprised to find some extent of pathway correlation within the candidates, in particular to oxygen sensing. It seems indeed plausible that several signalling modules (here RAS/MAPK and oxygen pathways) are influenced by the same polymorphic gene in order to facilitate an adaptation to a specific environmental condition encountered by genetically divergent individuals. These candidates were *rskn-1*, which plays a role in anoxia-associated death (Mabon et al. 2008), interacts with *mpk-1* and is an ortholog of human ribosomal protein S6 kinase polypeptide 1 (Simonis et al. 2009), *pqn-26*, a prion like Q/N-rich domain protein which suppresses the egg-laying defective phenotype of *egl-9* mutants when knocked down (Gort et al. 2007) (both within QTL1a in the *let-60(n1046)* mutant background (**Fig. 3.7** and **Table 3.13**) and *best-26*, an orthologue of human bestrophin genes (calcium-activated chloride channels) that also suppressed the *egl-9* mutant phenotype (Gort et al. 2007) (within the QTL1B in the *bar-1(ga80)* mu-

tant background (**Fig. 3.4** and **Table 3.8**). Finally, *F44F1.1* and *pfd-3* were found to modify RAS/MAPK signalling, to suppress the egg-laying defects caused by the lack of EGL-9, and PFD-3 is orthologous to VHL binding protein 1 (Gort et al. 2007; Schmid et al. 2015).
Previously, a difference in oxygen preference of CB4856 and N2 has been ascribed to an oxygen-sensing globin *glb-5,* which is modified by the neuropeptide receptor *npr-1* and both of which are polymorphic (de Bono and Bargmann 1998; Persson et al. 2009). These polymorphisms contribute to the behavioural differences between CB4856 and N2. CB4856 and other wild isolates tend to burrow more extensively into the agar the less food is present, whereas N2 roams on the surface of NGM plates and is thus exposed to higher oxygen concentrations (Hodgkin and Doniach 1997 and our observations). Further, the presence of CB4856 sequence can increase RAS/MAPK and WNT signalling strength. Based on theses relationships, it could thus be hypothesised that RAS/MAPK or WNT signalling strength and oxygen signalling are tuned in concert, i.e. according to oxygen availability, such that burrowing strains need to upregulate fundamental pathways (like RAS/MAPK or WNT) to ensure a correct development despite a reduced metabolic performance. If this hypothesis was true, then the VI of CB4856 animals sensitised with the *let-60(n1046)* mutation should be lower in individuals which had grown inside the agar compared with individuals that had grown on the surface. This notion is supported by our hypoxia experiments, in which the VI of CB4856 animals carrying the *let-60(n1046gf)* mutation was decreased in hypoxia (see chapter 3.2). Alternatively, a lower VI in the standard N2 strain (as compared to CB4856) might be the result of extensive adaptation to the laboratory and exclusive life on the surface with increased oxygen saturation.
Although we have not directly investigated the role of the polymorphic genes mentioned above neither in modifying RAS/MAPK signalling nor in affecting the hypoxia response pathway, we would expect their contribution to both based on the tight interaction between the two pathways as well as with oxygen availability (see chapter 3.2). In this respect, we had decided for a more unconventional approach by studying the relationship between two less polymorphic pathways (RAS/MAPK and the hypoxia response) that had emerged from their shared polymorphic modifiers rather than studying the direct link to these modifiers. Future studies could therefore focus more deeply on this branch.

4.2.2 Pseudogenes – genomic remnants but not necessarily non-functional

Initially, the identification of *F44F1.1* as a polymorphic modifier of RAS/MAPK signalling (Schmid et al. 2015) came as a surprise. As a paralog of *F44F1.3, F44F1.1* may have originated from gene duplication with subsequent mutational events and was formerly defined as a calpain-like sequence (Syntichaki et al. 2002) but then dismissed as pseudogene with unknown (if any) function (WormBase WS225). Pseudogenes need not be non-functional, since RNA can be produced that may regulate related sequences (Tutar 2012). Somewhat supportive of such a function is the fact that *F44F1.1* does not exhibit SNPs between CB4856 and N2 that would presumably

not strongly affect the functionality of a non-coding RNA, but rather a deletion that would indeed impair its ability in post-transcriptional modification. Previous studies have proposed that pseudogenes regulate their own “parental” paralogous sequences either directly by pseudogene-gene pairing or indirectly by acting as microRNA decoys (Poliseno et al. 2010). The latter mechanism has been described for the *PTEN* and *KRAS* loci and excitingly, the *PTEN* pseudogene locus (*PTENP1*) is frequently lost in human cancer (Poliseno et al. 2010) while the *KRASP1* locus was found to be duplicated in neuroblastoma, retinoblastoma and hepatocellular carcinoma (Plantaz et al. 1997; Zimonjic et al. 1999; van der Wal et al. 2003). *F44F1.3* is an orthologue of human atypical calpain 15 (Shaye and Greenwald 2002). Calpains are calcium-dependent cysteine-type endopeptidases involved in cell differentiation, proliferation and cell signalling events (Sorimachi et al. 1997; Sato and Kawashima 2001). A link between *F44F1.3*, its possibly regulatory pseudogene *F44F1.1*, hypoxia and the RAS/MAPK pathway is provided by the following findings. Firstly, *F44F1.1* suppressed the egg-laying defects of *egl-9* mutant worms (Gort et al. 2007). Secondly, calpain expression and activity is enhanced during hypoxic insult (Zhang et al. 1998) and thirdly, calpains degrade HIF-1A in an O_2 independent but Ca^{2+} dependent manner (Zhou 2006). Other studies described an involvement of ERK mediated calpain 2 activation in cell adhesiveness (Glading et al. 2000). Although we were not able to verify the deletion in *F44F1.3* and did not manage to engineer a mutant due to time limitations, we have observed a reduction in the VI of *let-60(n1046)* mutant worms carrying the *F44F1.1(ok1765)* deletion allele indicating an involvement of a calpain pseudogene in RAS/MAPK signalling output. It would be interesting to investigate the function of *F44F1.1* as a pseudogene and regulator of *F44F1.3* further, e.g. by analysing *F44F1.3* mRNA levels in *F44F1.1(ok1765)* mutants vs. wild-type and to study the role of *F44F1.3* in the RAS/MAPK signalling pathway.

4.2.3 EGL-9 function is not restricted to HIF-1 modification

When studying signalling pathways and networks within cells, the relevance of post-translational modification of pathway components is frequently underestimated although it can profoundly alter protein localisation, function or degradation (Krishna and Wold 1993). An impressive example is the hypoxia response pathway that relies to a large part on post-translational modifications (PTM). As a type of PTM, prolyl hydroxylation within LXXLAP motifs promotes the proteasomal degradation of hypoxia inducible factors (HIFA) and is mediated by prolyl hydroxylation domain proteins (PHDs) (Bruick 2001). Prolyl hydroxylation within proline-rich sequences changes the function of a number of proteins, such as the stability of collagen, the formation of elastin fibrils and, perhaps surprising, the stability of Argonaute 2 (Myllyharju 2003; Gorres and Raines 2010). LXXLAP motifs as found in HIFA are present in other proteins where they are similarly modified by PHDs. This is the case for the large subunit of the RNA polymerase II complex (Kuznetsova et al. 2003), activating transcription factor 4 (ATF4) (Koditz et al. 2007), ß2-adrenergic receptor (Xie et al. 2009) or non-muscle actin (Luo et al. 2014). Thus, identifying proteins with a LXXLAP

motif is a promising approach to not only detect and understand the role of prolyl hydroxylation for a given candidate but also to decipher HIFA independent mechanisms during hypoxia. Such a candidate could help discover details of the HIFA independent reduction of RAS/MAPK signalling strength we had observed in worms raised under hypoxia and that seemed to require intact AMX-2 (see chapter 3.2). Using the SIB ExPASy Bioinformatics Resource Portal (Artimo et al. 2012) proteomes can be readily scanned for motifs of interest and we interrogated the *C. elegans* proteome for the presence of LXXLAP motifs. 46 such proteins exist, with a human conservation of the motif only in *H28O16.1* and *ddx-35* (**Table 4.1**). *ddx-35* is an ortholog of human DHX35 with probable ATP-dependent RNA helicase activity (Shaye and Greenwald 2011). Mutations in *ddx-35* that impair its function have not been engineered. *H28O16.1* encodes the alpha subunit of mitochondrial ATP synthase (Shaye and Greenwald 2011), is involved in the induction of the unfolded protein response (UPR) (Runkel et al. 2014) and is induced by serotonin (Gomez-Amaro et al. 2015). Could *H28O16.1* thus be involved in the HIF-1 independent inhibition of RAS/MAPK signalling in the vulva during hypoxia, when serotonin levels rise (Pocock and Hobert 2010) and enhance expression of *amx-2* (Gort et al. 2007) as well as *H28O16.1*? Due to time restrictions, we have no (preliminary) results relating to this hypothesis but we will examine this possibility in future experiments and have started to create translational GFP reporters of *H28O16.1* and similarly planned constructs of *ddx-35* (mutated and wt LXXLAP motifs). Furthermore, if *ddx-35* and *H28O16.1* are indeed targets of hydroxylation by EGL-9, it would be interesting to study their function in normoxia and hypoxia and to verify their prolyl hydroxylation within the LXXLAP motif (via e.g. drug treatment (DIP, $CoCl_2$), mass spectrometry, Co-IPs or in vitro hydroxylation assays).

Table 4.1. *C. elegans* genes containing at least one LXXLAP motif. In the case of human conservation, the motif sequence is indicated.

Gene name	Sequence name	Human conservation	Motif *C. elegans*	Motif *H. sapiens*
unc-89	*C09D1.1*	no	LvvLAP	
vps-39	*T08G5.5*	no	LlqLAP	
-	*T19H5.4*	no	LsqLAP	
-	*B0303.11*	no	LtmLAP	
-	*ZK1290.11*	no	LagLAP	
-	*F44B9.2*	no	LaaLAP	
-	*C06E1.9*	no	LfsLAP	
-	*B0495.5*	no	LraLAP	
-	*C05B5.4*	no	LyeLAP	
-	*K07C5.4*	no	LfrLAP	

-	*T19B4.3*	no	LieLAP	
-	*H28O16.1*	yes	LqfLAP	LqyLAP
-	*F35C8.5*	no	LpiLAP	
chd-3	*T14G8.1*	no	LnfLAP	
cor-1	*R01H10.3*	no	LstLAP	
dapk-1	*K12C11.4*	no	LvcLAP	
ddx-35	*Y67D2.6*	yes	LyeLAP	LteLAP
epi-1	*K08C7.3*	no	LnkLAP	
-	*R09B5.11*	no	LteLAP	
-	*ZK1058.3*	no	LnpLAP	
-	*F41C3.4*	no	LdrLAP	
hif-1	*F38A6.3*	yes	LscLAP	LemLAP, LtlLAP
hpk-1	*F20B6.8*	no	LriLAP	
ceh-38	*F22D3.1*	no	LasLAP	
ceh-21	*T26C11.6*	no	LeeLAP	
hmp-1	*R13H4.4*	no	LekLAP	
mes-1	*F54F7.5*	no	LrtLAP	
mon-2	*F11A10.4*	no	LasLAP	
tyra-2	*F01E11.5*	no	LisLAP	
ostb-1	*T09A5.11*	no	LfiLAP	
ptc-1	*ZK675.1*	no	LlnLAP	
ptr-9	*F54G8.5*	no	LklLAP	
irx-1	*C36F7.1*	no	LalLAP	
lin-45	*Y73B6A.5*	no	LanLAP	
cdc-25.1	*K06A5.7*	no	LwdLAP	
dpy-31	*R151.5*	no	LvsLAP	
pro-1	*R166.4*	no	LfqLAP	
rfc-4	*F31E3.3*	no	LqsLAP	
rhy-1	*W07A12.7*	no	LlrLAP	
rpl-4	*B0041.4*	no	LlkLAP	
uba-2	*W02A11.4*	no	LnmLAP	
sdc-3	*C25D7.3*	no	LheLAP	
slc-17.3	*C02C2.4*	no	LlsLAP	
strd-1	*Y52D3.1*	no	LyyLAP	
unc-103	*C30D11.1*	no	LlrLAP	
ptp-3	*C09D8.1*	no	LllLAP	

4.2.4 Is EGL-9 the sole HIF-1 hydroxylase in *C. elegans*?

To assess tissue-specificity of EGL-9 and HIF-1 function during RAS/MAPK signalling, we have used the *let-60(ga89)* allele and analysed the percentage of stacked oocytes in double mutants at both normoxia and hypoxia (see chapter 3.2 and **Fig. 3.18**). Interestingly and in contrast to the vulval tissue, the absence of EGL-9 did not suppress the phenotype. Since the *ga89* allele exhibits a strong phenotype at 25 °C and may complicate the detection of mutations enhancing the stacking of oocytes, we tested the absence of HIF-1 at both 25°C (**Fig. 3.18**) and 23 °C (not shown), but similarly did not detect a change in the phenotypical outcome. These results indicated that neither EGL-9 nor HIF-1 regulate RAS/MAPK activity in the germline during normoxia. As opposed to this, RAS/MAPK activity was strongly reduced in the germline of hypoxia treated animals in both *let-60(ga89)* and *let-60(ga89); egl-9(sa307)* mutants but not in *let-60(ga89); hif-1(zh111)* mutant animals, which suggested a HIF-1 dependent effect in the absence of oxygen.

These results raised the possibility of a hydroxylase other than EGL-9 that modifies HIF-1 (at least in the germline), though this has not been reported as of yet. Rather, the prevailing understanding is that human HIFA proteins are subject to prolyl hydroxylation by one of three closely related PHDs (also known as EGLN1, 2 and 3) (Bruick 2001) and to asparaginyl hydroxylation by factor inhibiting HIF (FIH-1) (Lando 2002; Hewitson et al. 2002). Apparently, *C. elegans* encodes a single HIF-PHD (EGL-9) (Jiang et al. 2001; Epstein et al. 2001). A FIH gene has not been described in the worm, but the worm genome encodes a low sequence similarity FIH-1 homolog, a JuMonJi (transcription factor) Domain protein *jmjd-5* (The *C. elegans* Sequencing Consortium 1998) that contains an iron and 2-oxoglutarate coordinating JmjC domain with hydroxylase activity (Trewick et al. 2005; Klose et al. 2006). Other prolyl hydroxylases modify collagen but have been shown not to influence HIFA stability (Jaakkola et al. 2001). *C. elegans* produces six collagen prolyl hydroxylase proteins, *dpy-18, phy-2, phy-3, phy-4, C14E2.4* and *Y43F8B.4* (Myllyharju 2003), a procollagen lysyl hydroxylase *let-268* (The *C. elegans* Sequencing Consortium 1998) and *C17G10.1* which is an ortholog of human 2-oxoglutarate and iron dependent oxygenase domain containing 1 (OGFOD1) (Shaye and Greenwald 2011). Consistent with the findings of Jaakkola et al. (2001) the absence of DPY-18 or PHY-2 does not impair HIF-1 degradation (Epstein et al. 2001). Lastly, although OGFOD1 is most closely related to HIF-PHDs it probably does not regulate HIFA stability but rather acts as a ribosomal oxygenase (Singleton et al. 2014; Pugh and Ratcliffe 2017).

In conclusion and to our surprise, relatively little has been done to interrogate the hydroxylation of HIFA by oxygenases other than EGLN. The *C. elegans* germline in particular represents a promising tissue to investigate this option in more detail. Specifically, *jmjd-5* and *C17G10.1* as non-collagen modifying hydroxylases are encouraging candidates.

4.2.5 EGL-9 and NHR-57 may competitively act to control vulval competence

During vulval induction, growth factor signalling via the LET-23 and LIN-12 pathways establishes distinct cell fates to ensure the formation of a functional egg-laying organ (Kornfeld 1997; Yoo et al. 2004). In order to respond to these growth factors, vulval precursor cells need to obtain competence, which is established by Hox gene expression and WNT signalling (Clark et al. 1993; Eisenmann et al. 1998) and seems defined within a temporal window (Wang and Sternberg 1999). Of the twelve ventral epidermal cells, only P3.p-P8.p comprise the vulval equivalence group and divide once irrespective of inductive signalling (Kornfeld 1997). Uninduced cells lose their competence soon after this first division, fuse to the hypodermal syncytium and differentiate as 3° VPCs. In wild-type animals, induction by LIN-3 from the AC takes place prior to this first division and favours a 1° vs 2° cell fate in P6.p. By expressing LIN-3 from a heat-shock promoter at precisely controlled timepoints, Wang and Sternberg (1999) found that VPCs are competent to respond to LIN-3 from the beginning of the first cell division until shortly after division (Wang and Sternberg 1999). If they overexpressed LIN-3 after VPCs had divided, all VPCs adopted the uninduced 3° fate. They further found that the daughters of NOTCH expressing 2° VPCs (P5.p and P7.p) are able to respond to LIN-3 and adopt a 1° fate which contrasts the time-wisely more restricted LIN-3 responsiveness and suggests that 2° cells remain competent for a longer period. In agreement with these observations, others had proposed a function of NOTCH in maintaining competence by delaying cell fate determination (Coffman et al. 1993; Artavanis-Tsakonas et al. 1995). Specifically, NOTCH signalling promotes the G1/S transition thereby inhibiting differentiation (Joshi et al. 2009). The coupling of NOTCH signalling with cell cycle progression is an elegant way to temporally adjust cell fate acquisition and indeed, NICD degradation in the VPCs has been shown to coincide with the G2 phase (Nusser-Stein et al. 2012). Therefore, if VPCs receive both unsufficient LIN-3 and LIN-12 signals, they exit from the cell cycle and differentiate as 3° (Ambros 1999). LIN-12 probably prolongs vulval fate competence to help ensure that a 1° fate is established, since 1° descendants but not 2° cells can sometimes give rise to a partially functional vulva (Sulston and White 1980; Greenwald and Seydoux 1990). This notion is consistent with the finding that once the 1° fate has been established, a VPC cannot be reverted to 2° or 3° (Ambros 1999). Similarly, compromised RAS/MAPK signalling does not necessarily cause all VPCs to adopt the uninduced cell fate but frequently confers a 2° fate to extend the time when a 1° fate can still be acquired (Katz et al. 1995; Katz et al. 1996).

Our results extend the current knowledge on VPC cell fate acquisition and prolongation of competence and suggest that EGL-9 aids in these processes. We discovered that EGL-9 is a NOTCH target promoting induction and that the HIF-1 target NHR-57 mediates the inhibitory effect we observed in *egl-9* mutant animals (see chapter 3.2). Hence, these results add more complexity to vulval fate acquisition and control of cell competence by introducing the environmental component oxygen. In wild-type animals, a translational *nhr-57::gfp* reporter is expressed in the ventral epidermal cells that do not exhibit *egl-9::gfp* expression (see chapter 3.2), i.e. in the Pn.p cells

outside of the vulval equivalence group. Therefore, NHR-57 may act to limit vulval competence in competition with EGL-9 which promotes competence. We assume that early during development and in P6.p, where expression of *egl-9* (as judged from *egl-9::gfp* expression) is weak, NHR-57 may act to moderate competence to prevent a manifestation of stochastic fluctuations in signalling. At the onset of induction, LIN-3 signalling may override this decreased competence to confer a vulval fate and initiate lateral signalling via LIN-12 in order to promote *egl-9* expression and the enhancement as well as the prolongation of vulval competence. While the VI of *let-60(n1046)* mutant animals was increased by a *nhr-57(tm4533)* mutation, presumably due to the loss of NHR-57 function in uninduced cells (see chapter 3.2), the translational *nhr-57::gfp* construct did not suppress the VI (data not shown). Possibly, since the construct is still subject to HIF-1 mediated transcriptional control, an overexpression from an extra-chromosomal array may not suffice for protein accumulation (as suggested by the lack of a GFP signal in vulval cells of wild-type or *let-60(n1046)* mutant animals). As opposed to this, *nhr-57* expressed from a non-HIF-1 regulated promoter is expected to suppress RAS/MAPK activity and we are currently working on a *bar-1* driven reporter to test this hypothesis.

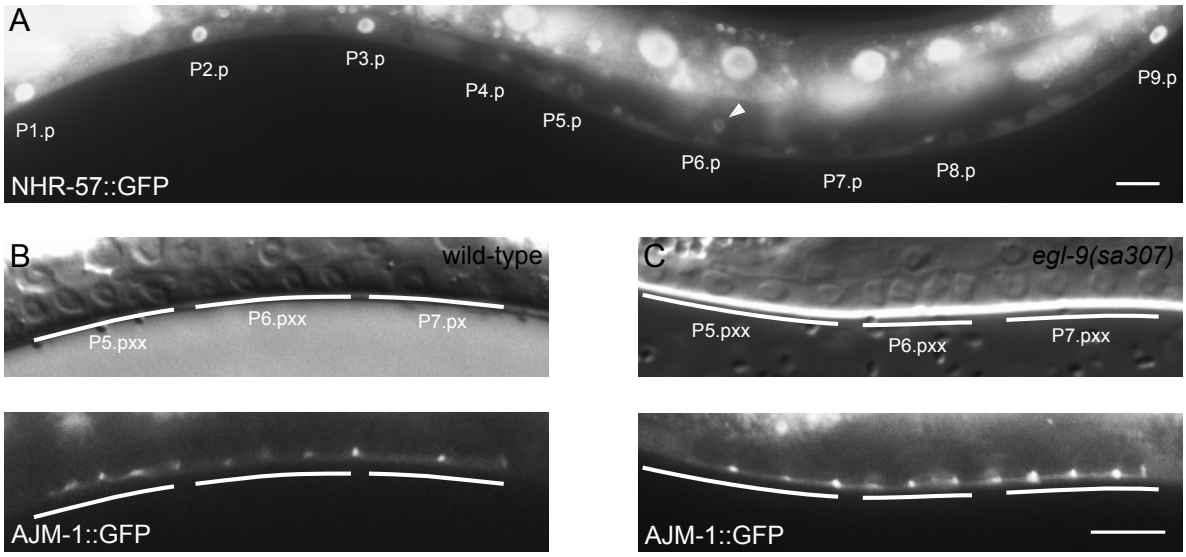

Figure 4.1. NHR-57 and EGL-9 modulate vulval development. **(A)** Expression of an extrachromosomal *nhr-57::gfp* construct in *egl-9(sa307)* mutant animals is prominent in nonvulval cells and visible in the VPCs as well as in the AC (indicated by a triangle). **(B)** In the wild-type, the apical junctions of the vulval competence group are visible, because they do not fuse with *hyp7*. **(C)** AJM-1::GFP expression in *egl-9(sa307)* mutants is unchanged. The scale bars indicate 10 µm.

The epistasis analysis predicts that NHR-57 inhibits vulval induction in parallel with LIN-1/ETS and this is in accordance with our findings that the GFP reporter expression of the RAS/MAPK and NOTCH downstream effectors *egl-17* and *lip-1* is unchanged in *egl-9* mutant animals (**Fig. 3.16**). All of the genes within this new regulatory module – *hif-1, egl-9, nhr-57* and *vhl-1* – exert a regulatory and fine-tuning rather than an essential function during vulval development, since mutations in any of the genes do not cause obvious phenotypes in an otherwise wild-type situation (in terms of vulval development). Likewise, a loss of EGL-9, which causes increased NHR-57 expression in the VPCs (**Fig. 4.1A**), does not lead to the adoption of excessive 3° cell fates and the fusion with the syncytial hypodermis as assessed using an apical junction marker *ajm-1::gfp* (Diogon et al. 2007) (**Fig. 4.1B, C**). Expression of *nhr-57* in the Pn.p cells is presumably not solely regulated by *egl-9* and *hif-1* as reporter fluorescence in *egl-9* mutant animals is strongly enhanced in the non-competent P(1-3).p and P(9-12).p cells in relation to the vulval competence group (P(3-8).p) (**Fig. 4.1A** and see below). We assume that the usage of oxygen in modulating and timing cell competence serves to limit energetically unfavourable signalling pathway activity, especially in less important tissues like the vulva, when oxygen availability is compromised and to preserve essential cellular functions with an absolute necessity of oxygen.

NHR-57 is an ortholog of members of the human nuclear hormone receptors, among which are the glucocorticoid and retinoic acid receptors that act as transcription factors or by regulating the same (Shaye and Greenwald 2011; Varricchio and Migliaccio 2014). Among the possible orthologues, only the glucocorticoid receptor NR3C1 (nuclear receptor subfamily 3 group C member 1) was found to accumulate during hypoxia and participate during erythropoiesis (Bauer et al. 1999; Mense et al. 2006; Elvidge et al. 2006; Varricchio and Migliaccio 2014). While NR3C1 was found expressed during CD8 T cell and cardiomyocyte differentiation, it maintained proliferation in response to stress such as hypoxia (Bauer et al. 1999; Cabral-Teixeira et al. 2015; Yu et al. 2017). In addition to an activation by steroid hormone binding, CDKs and MAPK regulate transcriptional activity of NR3C1 through phosphorylation (Krstic et al. 1997) and others described a physical interaction between NR3C1 with ETS2 proteins to synergistically regulate shared cellular events (Mullick et al. 2001). Intriguingly, *NR3C1* mutations compromising its expression are present in patients suffering from major depression and serotonin positively regulates NR3C1 expression (Mitchell et al. 1990; Mitchell et al. 1992; Laplante et al. 2002; Kumsta et al. 2009; Zhang et al. 2012). This fact is of particular interest, since we propose that RAS/MAPK signalling is reduced during hypoxia in a HIF-1 independent but presumably serotonin dependent manner (see chapter 3.2). Against our initial expectations such a HIF-1 independent regulation could still converge on the same transcription factor, NHR-57, by employing increased serotonin levels present during hypoxia (Pocock and Hobert 2010) and promote *nhr-57* expression to suppress RAS/MAPK activity. Finally, the gene encoding the glucocorticoid receptor contains many coding and noncoding polymorphisms in the human population that have been associated with various diseases (Bray and Cotton 2003; Varricchio and Migliaccio 2014). Similarly, the *nhr-57* locus re-

veals twelve noncoding SNPs between CB4856 and N2 that may affect function (Thompson et al. 2013). In summary, many studies have focused on the presumable *nhr-57* ortholog *NR3C1* and have suggested the involvement of the protein during hypoxia, cell differentiation and proliferation, serotonin signalling and RAS/MAPK signalling outputs – characteristics relating to our present data and hypothesis and that may facilitate in gaining a deeper insight into how exactly NHR-57 acts to control vulval induction.

4.2.6 Crosstalk between HIFA and MAPK

In this thesis, we describe how HIF-1 as a transcription factor and hypoxia as an important environmental component control the output of RAS/MAPK signalling. As a matter of fact, the interaction of HIFA and hypoxia with MAPK has been described earlier. HIF-1 post-translational modification does not only include hydroxylation by PHD proteins (Epstein et al. 2001) but also positively regulating phosphorylation by MAPK, as exemplified in transformed cell lines exhibiting elevated RAS/MAPK levels (Richard et al. 1999). Interestingly, one of the four HIF-1 isoforms of *C. elegans* contains neither a hydroxylation nor a P-X-[S/T]-P MAPK phosphorylation motif (Clark-Lewis et al. 1991) as determined from its amino acid sequence (The *C. elegans* Sequencing Consortium 1998), raising the possibility of a poorly modifiable stable isoform comparable to constitutive HIF1B. On the other hand, hypoxia has been shown to activate RAF by hyper-phosphorylation it on the other hand to activate negative feedback signalling (Seko et al. 1996; de la Cova and Greenwald 2012). Further HIF-1 was shown to interact with LIN-2 in yeast two-hybrid experiments (Li et al. 2004) and described as an ERK target gene (Berra et al. 2000). The activation of HIF-1 by a gain in RAS/MAPK activity could explain our findings that the loss of HIF-1 affected vulval induction of *let-60(n1046)* mutants during normoxia, when HIF-1 protein is normally degraded. To assess the extent, to which elevated RAS/MAPK activity increases HIF-1 protein levels, we had crossed a HIF-1::GFP translational reporter (Sendoel et al. 2010) into the *let-60(n1046)* mutants. However, we did not observe any increase in fluorescence when EGL-9 was functional, suggesting that oxygen regulated degradation of HIF-1 had eliminated potentially elevated protein levels that may have originated from overactive RAS/MAPK signalling. Though, it might be that the fluorescent reporter construct was not visible in the mutants, because expression was in general rather weak also in *egl-9* mutant animals. Unfortunately, we could not perform SDS-PAGE and Western blotting to detect HIF-1 protein in these mutants as the antibody was not available. Nevertheless, future experiments may include the biochemical analysis of HIF-1::GFP levels in *let-60(n1046)* or *lin-12(n137n720)* mutant animals as well as hypoxia to confirm or analyse respectively whether HIF-1 protein accumulates as had been suggested previously.

4.2.7 Further experiments

This last paragraph is dedicated to a summary of some of the experiments that were not conducted because of timely constraints but may be part of follow-up studies.
We have identified several polymorphic candidate polymorphic modifier genes within the QTLs affecting WNT and RAS/MAPK signalling that await verification by mutant analysis and a detailed description. In addition, the hypothesis and involvement of a pseudogene-gene interactive mechanism by *F44F1.1* and *F44F1.3* on RAS/MAPK activity could be evaluated.
In the second project, we have investigated the requirement for HIF-1 and EGL-9 in RAS/MAPK signalling during vulval development and the germline both during normoxia and hypoxia and found considerable differences in pathway regulation. Thus, the role of the two proteins during duct cell fate specification in normoxia and hypoxia should be analysed and compared to the other tissues. Next, we had started analysing the egg-laying defective phenotype of *egl-9* mutants in more detail. RAS/MAPK activity is required for the uterine uv1 fate to establish the vulva-uterine connection and enable egg-laying (Chang et al. 1999). It is therefore plausible to interrogate uv1 fate acquisition in *egl-9* mutants. Moreover and as mentioned above, *H28O16.1* and *nhr-57* may act in concert with AMX-2 to suppress RAS/MAPK activity in the vulva during hypoxia and in a HIF-1 independent manner. The analysis of mutants and fluorescent reporters (of *amx-2, H28O16.1* and *nhr-57*) in normoxia, hypoxia, upon treatment with the *egl-9* inhibiting drugs $CoCl_2$ or DIP (Romney et al. 2011; Padmanabha et al. 2015) and in *egl-9* mutant animals will provide more information and open up possibilities for subsequent analyses. It should be mentioned at this point that drug treatment using $CoCl_2$ or DIP is indeed a feasible method for our investigations as both drugs strongly suppressed the VI of *let-60(n1046)* mutant animals but had no effect in a wild-type background (data not shown, for method see 5.3.7). Our results also strongly suggest the presence of an alternative hydroxylase acting on HIF-1 in the germline and investigating the involvement of the few hydroxylases encoded in the *C. elegans* genome (e.g. *jmjd-5, C17G10.1*) appears straightforward. Finally, we have just started to understand the regulatory role of the hypoxia response pathway and one of its prime targets NHR-57 in vulval cell fate acquisition and competence and future should and will tell, which NHR-57 targets or interacting proteins act downstream and how exactly cell fate acquisition is controlled.

Material and Methods

5

5.1 DNA methods

5.1.1 Plasmids

The plasmid sequences can be found on the accompanying CD ROM.
pSMa01, 02 and 07 were not part of the projects described in this thesis and are described in the previous Master thesis. For a detailed description of experiments performed with pSMa05, pSMa06, pSMa09 and pSMa10 the reader is referred to the Master thesis by S. Boetschi and to the report by J. Grolleman. The usage of pSMa11-14 is described in the Master thesis of A. Henggeler. SLiCE cloning was established in our lab by J. Grolleman and is described in the respective report.

pSMa03	sgRNA1 targeting *hif-1*. Site-directed mutagenesis using OSMA87 and OSMA88 to insert sgRNA into pUC57. Sequence: GATAGAAAAGTGAGTCCTAA.
pSMa04	sgRNA4 targeting *hif-1*. Site-directed mutagenesis using OSMA93 and OSMA94 to insert sgRNA into pUC57. Sequence: TTCGAATATACACGCCCTTT.
pSMa05	*Pbar-1::ERKyce::unc-54* 3' UTR in pCFJ150. Obtained by Gateway cloning using pIN08, ERKyce_pos221_pDONR and pCH17.
pSMa06	*Pdlg-1* in pDONRP4-P1r. *Pdlg-1* was amplified using OSMA102 and OSMA103.
pSMa08	sgRNA5 targeting *hif-1* P621. Site-directed mutagenesis using OSMA96 and OSMA97 to insert sgRNA into pUC57. Sequence: ATATGATGCAAATGGACGAG.
pSMa09	*pie-1* 3' UTR in pDONRP2r-P3. *pie-1* 3' UTR was amplified using OSMA144 and OSMA145.
pSMa10	*Ppie-1::ERKyce::pie-1* 3' UTR in pCFJ150. Construct obtained by Gateway cloning using pCM1.127, ERKyce_pos221_pDONR and pSMa09.
pSMa11	pDONRP2r-P3 containing *let-23(partial)::mCherry*. *mCherry* was inserted by Gibson cloning: *mCherry* was amplified using OSMA179 and OSMA180 with overhangs into pJE05. OSMA181 and OSMA182 were used to amplify pJE05 without GFP and the fragments were fused.
pSMa12	*Plet-23::let-23::mCherry::let-23* 3' UTR in pCFJ150. Obtained by LR reaction (Gateway cloning) with pSMa11, pJE06 and pJE07.

pSMa13	pDONRP2r-P3 containing *let-23(partial)::SECFP*. *SECFP* was inserted by SLiCE cloning: *SECFP* was amplified using OSMA195 and OSMA197 with overhangs into pJE05. OSMA182 and OSMA196 were used to amplify pJE05 without GFP and the fragments were fused.
pSMa14	pDONRP2r-P3 containing *let-23(partial)::YPet*. *YPet* was inserted by SLiCE cloning: *YPet* was amplified using OSMA195 and OSMA198 with overhangs into pJE05. OSMA182 and OSMA196 were used to amplify pJE05 without GFP and the fragments were fused.
pSMa15	N-terminally tagged *lin-3* with tetracysteine sequence (TGTTGCCCAGGTTGCTGT). Inserted by site-directed mutagenesis using OSMA183 and OSMA184.
pSMa16	sgRNA1 targeting *nhr-57*. Sequence cloned into pMW46. Sequence: TGTAGTGTGTGCCATCAGTT.
pSMa17	sgRNA2 targeting *nhr-57*. Sequence cloned into pMW46. Sequence: TTAGGAGATGGTTATCACTT.
pSMa18	sgRNA4 targeting *nhr-57*. Sequence cloned into pMW46. Sequence: GAACTATTTCTTCAAACGA.
pSMa19	sgRNA5 targeting *nhr-57*. Sequence cloned into pMW46. Sequence: GGCTAAAAAGATATAAGCTT.
pSMa20	Tester for sgRNAs3, 4, 5 targeting *nhr-57*. Cloned into pMW79. Sequence: GGCTAAAAAGATATAAGCTTAGGTCACAATTTTCAGCGTTCCGTGGAACTATTTCTTCAAACGATGG.
pSMa21	sgRNA1 targeting LXXLAP motif in *H28O16.1.* Cloned into pMW46. Sequence: TGCCGCTCCACTCCAATTCT.
pSMa22	sgRNA4 targeting LXXLAP motif in H28O16.1. Cloned into pMW46. Sequence: TATGGAGCCAAGAATTGGAG.
pSMa23	sgRNA3 targeting LXXLAP motif in *H28O16.1.* Cloned into pMW46. Sequence: CAGAGTATGGAGCCAAGAAT.
pSMa24	sgRNA5 targeting LXXLAP motif in H28O16.1. Cloned into pMW46. Sequence: AGCCAAGAATTGGAGTGGAG.
pSMa25	sgRNA2 targeting LXXLAP motif in *ddx-35.* Cloned into pMW46. Sequence: GCCAATTCGTAAAGCCATTC.
pSMa26	sgRNA1 targeting LXXLAP motif in *ddx-35.* Cloned into pMW46. Sequence: GTGCCAAATTCGTAATAGTG.
pSMa27	sgRNA3 targeting LXXLAP motif in *ddx-35.* Cloned into pMW46. Sequence: GCCTGAATGGCTTTACGAAT.
pSMa28	Repair template with mutated LXXLAP motif in *H28O16.1,* cloned into pCR™-Blunt II-TOPO®. Amplified with OSMA234 - OSMA235 and mutated with OSMA236/237.
pSMa29	sgRNA5 targeting *nhr-57.* Sequence cloned into pMW46. Sequence: TCACAATTTTCAGCGTTCCG.
pSMa30	*Pmyo-2::mCherry::unc-54* 3' UTR (Q29), C-terminally tagged with codon-optimised tetracysteine tag (TGCTGCCCAGGATGCTGC). Tag was inserted by site-directed mutagenesis using OSMA283 and OSMA284.

pSMa31	*Pmyo-3::gfp::unc-54* 3' UTR, C-terminally tagged with codon-optimised tetracysteine tag (TGCTGCCCAGGATGCTGC). Tag was inserted by site-directed mutagenesis using OSMA292 and OSMA293.
pSMa32	*Pnhr-57::nhr-57::gfp::nhr-57* 3' UTR in vector backbone with AmpR and *CB-unc-119(+)* (Note that the *CB-unc-119(+)* sequence contains a coding SNP).
pSMa33	*Pbar-1::nhr-57::gfp::nhr-57* 3' UTR in vector backbone with AmpR and *CB-unc-119(+)* (Note that the *CB-unc-119(+)* sequence contains a coding SNP).

5.1.2 PCR

Amplification of DNA sequences was performed with Phusion® High-Fidelity DNA Polymerase (NEB) or LongAmp® Taq DNA Polymerase (NEB) according to the manufacturer's protocol using the following PCR mixes and cycle programs.

Phusion® High-Fidelity DNA Polymerase (NEB)

Component	20 µl reaction
5X Phusion HF or GC buffer*	4 µl
2 mM dNTPs	2 µl
2 mM forward primer	2 µl
2 mM reverse primer	2 µl
Template DNA	variable
Phusion DNA Polymerase	0.2 µl
ddH_2O	to 20 µl

Cycles	Temperature	Time
1x	98 °C	30 sec
30x	98 °C	10 sec
	58 °C	30 sec
	72 °C	30 sec / kb
1x	72 °C	5 - 10 min
	12 °C	∞

*Phusion HF buffer was used for the amplification from plasmid DNA and Phusion GC buffer was used for the amplification from genomic DNA.

LongAmp® Taq DNA Polymerase (NEB)

Component	20 µl reaction
5X LongAmp Taq buffer	4 µl
2 mM dNTPs	2 µl
2 mM forward primer	2 µl
2 mM reverse primer	2 µl
Template DNA	variable
LongAmp DNA Polymerase	0.8 µl
ddH_2O	to 20 µl

Cycles	Temperature	Time
1x	94 °C	2 min
30x	94 °C	30 sec
	58 °C	30 sec
	65 °C	50 sec / kb
1x	65 °C	10 min
	12 °C	∞

PCRs were performed in 0.2 ml Multiply® Pro Tubes (Sarstedt) or 96-well plates cut according to the number of reactions. The BioRad MyCycler Thermocycler was used. 2 – 4 µl PCR product was mixed with PCR-loading dye and loaded onto 1% agarose gels supplied with 0.2 – 0.5 µg/ml ethidium bromide. 1 kb or 2-log ladders (Invitrogen) were used as reference. Gels were run at 120 V for approximately 30 min and the DNA bands were visualised with UV trans illumination.

5.1.3 Oligonucleotides

The primers listed below were ordered from Microsynth AG (www.microsynth.ch) and kept at -20 °C in 100 µM stock solution in TE. For PCR reactions, the primers were diluted with ddH_2O to 2 µM. A working concentration of 10 µM was used for sequencing. The primers listed below are indicated from 5' to 3'. Primers OSMA1 – OSMA25 were part of previous studies and not mentioned here.

F44F1.1

OSMA	26	CAGTTGAGTCTTTTACCCCG
OSMA	27	GATCCAGAAAACAGTCAGCC
OSMA	30	GAACACGAATCCGAACAAATC
OSMA	31	GTCAAAGGAATGGGAATGGTG

F44F1.3

OSMA	28	CAAAGACAGGCACTAAAATGAG
OSMA	29	CTGAGAAGAAGAAGTTTGTGC
OSMA	85	GGACTATATTTCTCGGTGAT
OSMA	86	GGAAGATTGCCAGTAAGAAT

pfd-3

OSMA	32	GTGTCGATAATGCTCAAACT
OSMA	33	ACAAATTCCTCTCTGAACCC
OKJ	1	TCTAATCACATCACCTGTCACAC
OKJ	2	CGAAAATCAATATCCCAAAGCCC
OKJ	3	GCAAATCTA AATGTTTGCGGACAGTCTATCAGCACGGTTTTA GAGC-TAGAAATAGCAAGTTA
OKJ	4	CTAGCTCTAAAACCGTGCTGATAGACTGTCCGCAAACATTTA GAT TTG-CAATTCAATTATATAG
OKJ	5	GCAAATCTAAATGTTTGTCATATTCGACCATTACGTGTTTTAGAG CTAGAAATAGCAAGTTA
OKJ	6	CTAGCTCTAAAA CACGTAATGGTCGAATATGACAAACATTTA GATTTG-CAATTCAATTATATAG
OKJ	7	CTTTTTCCCCGGAAGATCTACGCTCAATTTTTAC
OKJ	8	TGAGCGTAGATCTTCCGGGGAAAAAGAAAATTCC

OKJ	9	CCGTTTTTCGCCCGAAAGATCTCTTGAAATCCCC
OKJ	10	ATTTTAAAGGGGATTTCAAGAGATCTTTCGGGCG
OKJ	11	AAATTAAAGGCGCATAAGGG
OKJ	12	CCGATTTCGTTTTTTTCCACC
OKJ	13	AGGTCGTCTAGTGTCTTTTAG
OKJ	14	AAATTGAACCCGAAACCCTC
OKJ	15	CGTCTATCCATATTCTCAGC
OKJ	16	AACCATGCTCTCCAATTTTG
OKJ	17	ACG GAA GTC AAT TTT GAA GC
OTS	326	GCAAATCTAAATGTTTGAAAAAACGCAAAAAATTCGGTTTTAGAG CTAGAAATAGCAAGTTA
OTS	327	CTAGCTCTAAAACCGAATTTTTTGCGTTTTTTCAAACATTTA GATTTG-CAATTCAATTATATAG
OTS	328	GCAAATCTAAATGTTTGCCGCTCTCGCTGTCAATAAGTTTTA GAGC-TAGAAATAGCAAGTTA
OTS	329	CTAGCTCTAAAACTTATTGACAGCGAGAGCGGCAAACAT TTAGATTTG-CAATTCAATTATATAG
OTS	121	AGTTGGGATTTTTTTGTGCTCC
OTS	122	TGGCTGCTGAGATGTTGATTTTC

egl-9

OSMA	34	CCAATTCCACCTACTGTTTC
OSMA	35	CAGTAAATGTGGTCAGATCG
OSMA	36	CAGATCATCGAAACAGAAGG
OSMA	42	GCCACGTCGTTCATTTTATC
OSMA	43	GCGTAGGGAGATGGAAGAGA
OSMA	113	GTTATTGTCTCGCTTTTGCC
OSMA	114	CCAATTCCACCTACTGTTTC
OSMA	171	CATCATCAGTGTCTTCCCCTC
OSMA	172	CTTGCTCTCACGTATTTCTGC
OSMA	229	GATATCAGTAGACTCGCTCAAGTTTTGAGTC (cDNA)
OSMA	230	GATGATCCGGATATTCAGATCATCGAAACAGAAG (cDNA)
OSMA	231	GAGTCGCTCAATTTCTTTCGCGGTAAATTTG (cDNA)
OSMA	232	GTCGGCAGAGATGTCAACTCTATCTTCATCTG (cDNA)
OSMA	233	GTGGAGAGAGATACTCCCGAGTCAGTAGATTC (cDNA)

hif-1

OSMA	48	CACTTACAATGGCTCGAAAC
OSMA	49	GTAACATCTTCTCCGTTTTC
OSMA	87	GCAAATCTAAATGTTTGATAGAAAAGTGAGTCCTAAGTTTTAGAGC-TAGAAATAGCAAGTTA
OSMA	88	CTAGCTCTAAAACTTAGGACTCACTTTTCTATCAAACATTTAGATTTG-CAATTCAATTATATAG

OSMA	89	CGTTTGCAAAAGTAAAATGAGCAGGGACTCTGAATACCTAG-ATAGAAAAGGGAGTCCTAAAGCGCGTGTATATTCGAAAACTTTTTCAAATCA-GATTTATAG
OSMA	90	GTCCTTTTTGTCCTTTCGTC
OSMA	91	GCAAATCTAAATGTTTTAGGACTCACTTTTCTATCTGTTTTAGAGC-TAGAAATAGCAAGTTA
OSMA	92	CTAGCTCTAAAACAGATAGAAAAGTGAGTCCTAAAACATTTAGATTTG-CAATTCAATTATATAG
OSMA	93	GCAAATCTAAATGTTTTTCGAATATACACGCCCTTTGTTTTAGAGC-TAGAAATAGCAAGTTA
OSMA	94	CTAGCTCTAAAACAAAGGGCGTGTATATTCGAAAAACATTTAGATTTG-CAATTCAATTATATAG
OSMA	95	GATCTTCAATGGGAAGAGCCTGATTTATCGTGCTTGGCAGGATTC-GTTGACACTTATGATATGATGCAAATGGACGAGGGCTTACCAC-CAGAGCTTCAAGCTCTTTACGACTTGCCTGACTTTAC
OSMA	96	GCAAATCTAAATGTTTATATGATGCAAATGGACGAGGTTTTAGAGC-TAGAAATAGCAAGTTA
OSMA	97	CTAGCTCTAAAACCTCGTCCATTTGCATCATATAAACATTTAGATTTG-CAATTCAATTATATAG
OSMA	115	CAAAACTGTCTGAAAACACC
OSMA	116	GAAAATGAATGAGACGAGAGC
OSMA	122	CAATCTTGCCCCATTCATAC
OSMA	123	GTATCTGATGGTGAAAGGGC
OSMA	127	GAGCTCCAACAAAAAGAAGGG
OSMA	128	CTGAACAACAAAGAGCGGTC
OSMA	129	GCGAATGCATTACAACTAGG
OSMA	130	CTTCACCTCTCTCAATTTTCAG
OSMA	131	GTTTCCCTCGTTTCATATGAC
OSMA	132	CTAGGCTGTTGTTCATTTTGC
OSMA	224	CAATCACACCAACCTCAGCTTCAC
OSMA	225	CTGTTGCTGTCCTTGCCAATATGTC
OSMA	289	CTCACGGAGGTATGAGGACAACGG
OSMA	290	GAGGAATGCCGCATGTTCCGATCC

vhl-1

OSMA	50	CGTATGGGGAATGGAATTGC
OSMA	51	CTGTCCTGTAATTCAACTTTCC

ahr-1

OSMA	77	CTCTTTTTATCGCCATCCTTC
OSMA	78	GGAATTGATGGGATTGTTGG

mos1 / ttTi5605

OSMA	62	GAATAGGTGGTAATCGGATGG
OSMA	63	CCCATCTACCGACCTTCTGA
OSMA	64	CATTCCCTACTTGTACACCT
OTS	172	CGGAAACCAAAGGACGAGAG
OTS	173	TGTTTTTGATTGCGTGCGTT
OTS	194	ATCTTTTCTGGCTCTGCTTCTTC
OTS	195	CCTCTTAATGCGTTGTTTCTCTC

pha-1

OSMA	117	CGTTGCTCGATGATTTCTCC
OSMA	118	CAAAATTTTCCCGGTTGTCG
OSMA	119	GAAAAGAGAATCGAACTGTGG

rrf-3

OSMA	120	CAATGGAGCGAACATACATC
OSMA	121	CACATTTTCTCGTTCAAGCC

let-23

OSMA	124	CAAAGAAGTTCAGCAGTCAGC
OSMA	125	CCAGCGACCAAATCCATTAG
OSMA	126	GAAATTTTGTGAAGAAGGGCAG

let-858

OSMA	146	GGGGACAGCTTTCTTGTACAAAGTGGCAATTTTCAAATTTTAAATACTGAATA
OSMA	147	GGGGACAACTTTGTATAATAAAGTTGCTTTCTTTGCTTATTTTTTACTAGTT

cdka-1 / p35

OSMA	175	GTCAACAGGAATAGAGCAAGAG
OSMA	176	CGTGCGATATCCAAATAAGTG

lin-10

OSMA	159	GATTTGTTACGAGGATGTGCAG
OSMA	160	CTGGAAATTAGGCGAAGTGATG
OSMA	161	CTCTCTCTTTTTGCTCAGCC

lin-7

OSMA	162	CTTGATCGGTTTTTGGGAGC
OSMA	163	GAGGAGATGAAGGGATACGAG

unc-119

OSMA	165	GCACACCCCTTTTATGAACG
OSMA	166	CGGGTCTCGTTTGGATTATTG
OSMA	167	CAGTTGTTTCTCGAATTTGGC

lin-3

OSMA	189	GTTCTTCCCACCCCTTATG
OSMA	190	CTGGAGACGATGAAAAACG
OSMA	191	GATGAGCATGACAATGAGA
OSMA	192	CGACACAACTCCACATTCAAC
OSMA	206	GCTGATGTTGAAGATTGCTG
OMMO	135	TGGTCCCTTGAATGGTTTGTC
OMMO	136	CTGTTCGGGAGCACTACGTT
OJE	129	GACTAACAACCAATCTACAG
OAH	138	GAAATCGAGGAGTTGAACTGGC

lin-45

OSMA	199	GTTGCCTCATCATTAATCGC
OSMA	200	GATGATGGGATTTCGATGTG

unc-32

OSMA	211	CTGAGCACTTCACCAATTCC
OSMA	212	GGTATGTGGTCCTAGGCAAG
OSMA	213	CACGACAAGCTACAGGATAG

mpk-1

OSMA	226	CACCCCTGAATTGAACTACG
OSMA	227	GTTTCTCTCTTTTCTACCACG
OSMA	229	CCGGAAAATCGAAAACTTAC

H28O16.1

OSMA	234	GCCGAAGAAATGGTTGAGTTC
OSMA	235	CTACACGGGATACAGACAGAC
OSMA	236	GAGTATCGTGGGATGAATTCCACTGGAGCGGCATCGG
OSMA	237	CTCCAGTGGAATTCATCCCACGATACTCTGGATGCG
OSMA	242	CTTGTGCCGCTCCACTCCAATTCT
OSMA	243	AAACAGAATTGGAGTGGAGCGGCA
OSMA	244	CTTGCAGAGTATGGAGCCAAGAAT
OSMA	245	AAACATTCTTGGCTCCATACTCTG
OSMA	246	CTTGTATGGAGCCAAGAATTGGAG
OSMA	247	AAACCTCCAATTCTTGGCTCCATA
OSMA	248	CTTGAGCCAAGAATTGGAGTGGAG
OSMA	249	AAACCTCCACTCCAATTCTTGGCT

OSMA	260	CTTGCTCCGATGCCGCTCCACTCCAATTCTTGGCTCCATACTCTGGATGCG
OSMA	261	CCCTCGCATCCAGAGTATGGAGCCAAGAATTGGAGTGGAGCGGCATCGGAG

ddx-35

OSMA	238	GTATTTTGCGTACTTTTGGGGC
OSMA	239	GCGCGGAATATAGTCATGTTG
OSMA	240	GTAATAGTGTCCACCGAACTCGAGATGCCATTCAGGCTCAATAAC
OSMA	241	GAATGGCATCTCGAGTTCGGTGGACACTATTACGAATTTGGC
OSMA	250	CTTGGTGCCAAATTCGTAATAGTG
OSMA	251	AAACCACTATTACGAATTTGGCAC
OSMA	252	CTTGGCCAATTCGTAAAGCCATTC
OSMA	253	AAACGAATGGCTTTACGAATTGGC
OSMA	254	CTTGGCCTGAATGGCTTTACGAAT
OSMA	255	AAACATTCGTAAAGCCATTCAGGC
OSMA	262	CTTGCCTTCGGTGCCAAATTCGTAATAGTGTGGAGCCAATTCGTAAAGC-CATTCAGGCTCAATA
OSMA	263	CCCTTATTGAGCCTGAATGGCTTTACGAATTGGCTCCACACTATTACGAATTTG-GCACCGAAGG

nhr-57

OSMA	266	GCGTACGTGATTAGTGGAAC
OSMA	267	CTCTGGAACCTCACAAATTTC
OSMA	294	CTCTCCATACCTTTTTCATTTCCC
OSMA	295	CTGGAACTCGGTGACTATGAC
OSMA	296	CACGTTTGGGACATTTGAAG
OSMA	297	GCATTTCTCACGTAGACTTCCTGG
OSMA	298	GTCATAGTCACCGAGTTCCAG
OSMA	299	CACAGCTGCTCAACGCAAATCCAG
OSMA	300	GACGTAACTTATTTGAGCGGG
OSMA	301	GTAGTTTGTGGCTCTTGGTGTC

tyr-2

OSMA	287	GCTTCAGCCTATTCCAGTTC
OSMA	288	GATTAAGGTGGAGTTAGCGTG

let-60

OTS	38	TCATTCTCCGTCGTCTTC
OTS	39	CATTTTTTTCAGTTCCAGCC
OTS	49	CCAAACTTCTGACTCATC
OMMO	127	CCCTTTGCTGTCTCACTGACT
OMMO	128	CATTTTTTTCAGTTCCAGCC

bar-1

OTS	33	AGATAGACACACACACACAA
OTS	36	GAGCATTGTTGCATGTTGGA
OSMA	327	CTAACAACTTGGAAATGAAATCTTAGCAAAGCCGTGTCAAAACCC
OSMA	328	GTTCGCGAGCCACCAACATTAGGTTCGGATCCAGGTCCATCCCAGTTTTC

dpy-10

AF-ZF	827	CACTTGAACTTCAATACGGCAAGATGAGAATGACTGGAAACCGTACCGCAT-GCGGTGCCTATGG
AF-ZF	831	GTCAGATGATCTACCGGTGTGTCAC
AF-ZF	832	GTCTCTCCTGGTGCTCCGTCTTCAC

rde-1

OMW	207	CGACTTGCTTGCCAAACACTGATG
OMMO	247	ATCCACGAATCACTGGTGTC
OMMO	248	GTCGAGATTGACAGAACGAC
OEL	1	GGCATGCGATTCTCGAATGATGAC

cdk-5

OSN	108	AAGAGCATCCACAGTTTCGTAG
OSN	109	CAGTTCGTTGAATATTGAGTAGC
OSN	110	ATCGATTCTTCCTGCTGGATTGC

lin-2

OJE	61	CGCCTATGAAATCTCAGTTT
OJE	62	CGCGCATTTTCATAATTGCG

dpy-19

OMW	223	GCAGTAGAGAATGGAATCAGATCC
OMW	224	CTTGCATTTCTGTACCGCCCATTC

amx-2

OTS	149	AGGCTCAGGGTACATTTTAG
OTS	150	GTCGTTTCGGTTAATGATGG

sos-1

OAH	295	CAAGCAATTCAAGCAACTGG
OAH	296	TGTCTTTCTCGTGGCGAGACC

sem-5

OAS	605	GATCACCTGATGAGTTGTCTTTCAAG
OAS	606	CAGCAATACTTCTGCGTCATTTCTTG

ttr-11

OSN	7	GGTTCTTGAAATTCGACGCTC
OSN	8	TAAGTCCGTCCACAAACTGGC

mCherry

OEH	86	ATGGTCTCAAAGGGTGAAGAAG
OEH	87	CTTATACAATTCATCCATGCCAC

gfp

OSMA	81	CTTTTCACTGGAGTTGTCCC
OSMA	82	CCATGTGGTCTCTCTTTTCG
OJE	6	TTTGTATAGTTCATCCATGCC
OMW	280	GAAGTCAAGTTTGAAGGTGATACCC

Pegl-9::egl-9::tag

OSMA	264	CACCACCTCCTTCCACAAAC
OSN	73	GCATCACCTTCACCCTCTCC

opIs206[Phif-1::hif-1::gfp::hif-1* 3' UTR*]

OSMA	79	GGGACAACTCCAGTGAAAAG
OSMA	80	CCACACAGTGCCAACTACTC

pSMa05 (*Pbar-1::ERKyce::unc-54* 3' UTR)

OSMA	111	TAGCCAATTTCACACCTTTG
OSMA	112	CTATTTTTTCTCTTCATCCGGC

pSMa06 (*Pdlg-1* in pDONRP4-P1r)

OSMA	102	GGGGACAACTTTGTATAGAAAAGTTGAGCTGTACGACAGTTGCACATTCGG
OSMA	103	GGGGACTGCTTTTTTGTACAAACTTGGCTTCCTTCCTTCGGTGAGGCGTTC

pSMa09 (*pie-1* 3' UTR in pDONRP2r-P3) and
pSMa10 (*Ppie-1::ERKyce::pie-1* 3' UTR)

OSMA	142	GGGGACAACTTTGTATAGAAAAGTTGGATCATTATTTCACTGATTTTCTTCAT
OSMA	143	GGGGACTGCTTTTTTGTACAAACTTGGCTGGAAAAGAAAATTTGATTTTTAA
OSMA	144	GGGGACAGCTTTCTTGTACAAAGTGGGATTTTGCCGTATTTTCCATATTTTGT
OSMA	145	GGGGACAACTTTGTATAATAAAGTTGCATATTCGAATACACTTCCAGAGTCG
OSMA	148	CGAAAGCGAAACAGAGACAG
OSMA	149	GAAGGTCGCTTTTTGGTCG
OSMA	150	GGTGTCGATTTACGAGCTTG
OSMA	151	GTAGGCAGCAGAATGTGTG
OSMA	152	GAGAAAACTACAGACACGGG
OSMA	153	CATTCAGCTTTTTTTGAGTCCG
OSMA	154	GCCTTTAAACCAACCGTAACC

OSMA	155	GTTCACCCTTTTTCTCCAATG
OSMA	156	CCCAATCCGCTCTTTCTAAG
OSMA	168	CGCTAAAAACACTAATCACACG
OSMA	169	CTTTTGACGCCATTTTTTCTCG
OSMA	170	GGTAGTGCAAAGAAGCTTAAGG

pSMa11 (*let-23(partial)::mCherry* in pDONRP2r-P3) and pSMa12 (*Plet-23::let-23::mCherry-let-23* 3' UTR)

OSMA	179	CCGGTAGAAAAAATGGTCTCAAAGGGTGAAGA
OSMA	180	CTCTTCTGATGTTTCCTTATACAATTCATCCATG
OSMA	181	GAGACCATTTTTTCTACCGGTACCCTCCAAGG
OSMA	182	GAAACATCAGAAGAGGCTGAAG
OSMA	185	CGGAGCCTTTTGATTGTAAG
OSMA	186	CCCAACAAATTTTCACCCAAC
OSMA	187	GTTTATGCGTTTCAAGGTGC
OSMA	188	CTCGGATGGACCTGTTATGC
OSMA	201	GAAGGCTGCGAACAAATTGATG
OSMA	202	GCCCTTCTTCACAAAATTTC
OSMA	203	GGAAAGGAAATTGGAGTCTG

pSMa13 (*let-23(partial)::SECFP* in pDONRP2r-P3)

OSMA	195	CCGGTAGAAAAAATGGTTTCTAAGGGAGAGG
OSMA	196	AACCATTTTTTCTACCGGTACCCTCCAAG
OSMA	197	CTCTTCTGATGTTTCGAGCTCATCCATTCCAAGGGTG

pSMa14 (*let-23(partial)::YPet* in pDONRP2r-P3)

OSMA	195	CCGGTAGAAAAAATGGTTTCTAAGGGAGAGG
OSMA	196	AACCATTTTTTCTACCGGTACCCTCCAAG
OSMA	198	CTCTTCTGATGTTTCAGCAGCGGTAAGGAACTCAAGAAG

pSMa15 (*lin-3::TC*)

OSMA	183	GTTTCAGAATCGTGTCTCTGTTGCCCAGGTTGCTGTCCTTCGTGGTTTCGTCAAGAACGTA
OSMA	184	AAACCACGAAGGACAGCAACCTGGGCAACAGAGACACGATTCTGAAACTTTTATTGATATTTG
OSMA	193	CTTAAACCGGCGGTTCGGAAGG
OSMA	194	CCGCCGGTTTAAGAGTCGACG

pSMa30 (P*myo-2::mCherry::tetracysteine::unc-54* 3' UTR)

OSMA	283	ATGGATGAATTGTATAAGTGCTGCCCAGGATGCTGCTAGTACCCAGCTTTCTTGTACAAAG
OSMA	284	GAAAGCTGGGTACTAGCAGCATCCTGGGCAGCACTTATACAATTCATCCATGCCACCTGTCGAG

pSMa31 (P*myo-3::gfp::tetracysteine::unc-54* 3' UTR)

OSMA	292	CATGGATGAACTATACAAATGCTGCCCAGGATGCTGCTAGCATTCGTAGAATTC-CAACTGAGCGCCGGTCGC
OSMA	293	GTTGGAATTCTACGAATGCTAGCAGCATCCTGGGCAGCATTTGTATAGTTCATC-CATGCCATGTGTAATCCC

pSMa32 (P*nhr-57::nhr-57::gfp::nhr-57* 3' UTR)

OSMA	302	CTAACAACTTGGAAATGAAATCACCAACACCTTCTACACAGCTGC
OSMA	303	GTTCTTCTCCTTTACTCATTTGTCCATCAATGATTTTATAGATTTTGTCG
OMMO	76	ATGAGTAAAGGAGAAGAAC
OSMA	304	GAGATCTGGTTCAAATAGCTATTTGTATAGTTCATCCATGC
OSMA	305	GCTATTTGAACCAGATCTCTTC
OSMA	306	CAGTACGGCCGACTAGTAGGAATAAATCATCCCAAAGCCGTTTTTG
OMW	443	CTACTAGTCGGCCGTACTGAGGTGTTGTCGCTTTTATTGGG
OMW	405	ATTTCATTTCCAAGTTGTTAGCG

pSMa33 (P*bar-1::nhr-57::gfp::nhr-57* 3' UTR)

OSMA	326	ATGTTGGTGGCTCGCGAACGAAAATATTG
OSMA	327	CTAACAACTTGGAAATGAAATCTTAGCAAAGCCGTGTCAAAACCC
OSMA	328	GTTCGCGAGCCACCAACATTAGGTTCGGATCCAGGTCCATCCCAGTTTTC

5.1.4 Restriction enzyme digest

Restriction enzymes from Roche or NEB were used and digests were carried out according to the manufacturer's protocol. To remove parental plasmids after site-directed mutagenesis, the sample was digested with DpnI for 3 – 4 h prior to transformation. Digested fragments were purified from residual buffer and enzyme either by PCR purification using the GenElute PCR Clean-Up Kit (Sigma-Aldrich) or by gel extraction using the QIAquick® Gel Extraction Kit (Qiagen). Digested and purified fragments were checked on an agarose gel.

Component	Volume per reaction
10X restriction enzyme buffer	2 µl
Template DNA	variable
Restriction enzyme	0.2 µl
ddH_2O	to 20 µl

5.1.5 Ligation of DNA into vector plasmid

DNA fragments obtained by PCR or plasmid digest were sub-cloned into the pCR™-Blunt II-TOPO® vector (Invitrogen) according to manufacturer's protocol and further modified where necessary. For Gateway® cloning (Invitrogen), purified PCR products were inserted into the respective pDONR™ vector through the BP reaction. The MosSCI expression vectors were obtained by performing the Gateway® LR reaction with the destination vector pCFJ150.

5.1.6 Transformation of *E. coli*

Chemically competent cells (DH10B or Top10) stored at -80°C were thawed on ice for 10 min. For a re-transformation of plasmids, 0.5 µl of the construct were added to 100 µl cells. In case of ligation products, 20 µl of the ligation mix were used. The cells were left on ice for 10 min. The cells were heat-shocked at 42 °C for 1.5 min on a Thermocycler (Eppendorf), after which they were left to recover on ice for 2 min. 800 µl 2x TY medium without ampicillin were added and the cells were incubated at 37 °C for 30 – 60 min. Of bacteria transformed with a retransformation product, 50 µl were streaked onto agar plates containing 50 µg/ml antibiotic. Cells transformed with ligation products were pelleted in the micro-centrifuge for 2 min at 3500 rpm and the supernatant was discarded up to 100 µl. The cells were resuspended and distributed on agar plates with antibiotic (50 µg/ml). Either plates were incubated overnight at 37 °C or over the weekend at room temperature to allow the growth of colonies.

5.1.7 Miniprep

In order to test the presence of a specific DNA sequence in previously transformed cells, a quick miniprep was performed. Single clones were picked from agar plates into 2 ml 2X TY containing 50 µg/ml antibiotic and left to shake at 225 rpm and 37 °C overnight. The bacterial cultures were transferred to 1.5 ml Eppendorf Tubes® and pelleted in the micro-centrifuge for 2 min at 4000 rpm. The supernatant was discarded and per sample, 350 µl STET buffer were added. The pellet was dissolved by vigorous vortexing. To lyse the cells, 25 µl lysozyme solution (10 mg/ml in TE buffer) were added and the sample was inverted several times. The lysozyme was inactivated by the incubation at 95 °C for 1 min on a heating block. The cell lysate was centrifuged for 8 min at 4 °C and 14000 rpm and the cell remnants were removed with a toothpick. The DNA was precipitated by adding 30 µl NaAc (3M, pH = 5.2) and 300 µl isopropanol (100%). The samples were inverted several times and again centrifuged for 8 min at 4 °C and at 14000 rpm, after which the supernatant was discarded. To remove remaining isopropanol, the sample was centrifuged briefly and left to dry before the DNA pellet was resuspended in 40 µl TE buffer and allowed to dissolve at 40 – 50 °C using a heating block. For sequencing, 2 µl were used.

5.1.8 Midiprep

Midipreps were performed with the QIAGEN Plasmid Plus Kit (Qiagen), which was adapted slightly. A bacterial clone was incubated overnight while shaking at 225 rpm in 100 ml 2X TY medium containing 50 µg/ml antibiotic. The bacterial culture was centrifuged at 6000 g for 15 min. The bacterial pellet was resuspended in 4 ml Buffer P1. 4 ml Buffer P2 were added and the sample was inverted several times. The mixture was incubated at room temperature for three minutes, during which the QIAFilter Cartridge was prepared. Subsequently, 4 ml Buffer P3 were added and mixed again thoroughly to neutralise the lysis. The lysate was poured into the barrel of the cartridge and incubated at room temperature for 10 min. Using the plunger, the cleared lysate was transferred into a 15 ml falcon tube containing 2 ml binding buffer BB. The sample was mixed and poured onto a filter column (using an extender). The liquid was drawn through the column by suction. The column was washed by applying 700 µl ETR buffer and suction. A second washing step was performed using 700 µl PE buffer and suction. To remove residual EtOH, the column was placed into a 2 ml tube and centrifuged at 14'000 rpm for 2 min. The column was inserted into a fresh 1.5 ml Eppendorf Tube® and 100 µl TE buffer were added onto the centre of the filter. After a brief incubation, the DNA was eluted by centrifuging at 14'000 rpm for 2 min. Since the quality of this sample was not yet satisfying, we additionally precipitated the DNA in the following way. Twice the volume of 100% ice-cold EtOH and 1/10 of the volume of NaAc (3M, pH = 5.2) was added and the sample left at -20 °C for 30 – 60 min. The sample was centrifuged at 14'000 rpm for 20 min, the supernatant was removed carefully and the initial volume (100 µl) of TE was added. The concentration of the DNA was measured using the NanoDrop™ and adjusted to 1 µg/µl.

5.1.9 Site-directed mutagenesis

To insert specific mutations on a plasmid, overlapping primers of minimally 50 bp were designed (according to the Richard lab, https://openwetware.org/ (OpenWetWare 2017)). The mutation(s) of interest were positioned in both primers and at least four bases from the 5'-terminus as well as at least eight bases from the 3'-terminus. Each primer contained eight or more non-overlapping bases at the 3'-terminus. Finally, both primers were placed such that they started and ended with a G or C. Mutagenesis was carried out in the BioRad MyCycler with the conditions below.

Component	25 µl reaction
5X Phusion HF buffer	5 µl
10 mM dNTPs	2 µl
forward primer	100 ng
reverse primer	100 ng
Template DNA	100 ng
Phusion DNA Polymerase	0.2 µl
ddH_2O	to 25 µl

Cycles	Temperature	Time
1x	98 °C	30 sec
30x	98 °C	10 sec
	58 °C	30 sec
	72 °C	30 sec / kb
1x	72 °C	5 - 10 min
	12 °C	∞

After the PCR the sample was digested with DpnI (NEB) to remove the methylated template plasmid and transformed into chemically competent DH10B or Top10 *E. coli.*

5.1.10 DNA sequencing

DNA sequence data was obtained through in-house Sanger sequencing. For this purpose, 500 – 1000 ng plasmid DNA or 10 – 20 ng per 100 bp DNA obtained via PCR and 1 µM sequencing primer were delivered.

5.1.11 DNA micro-injection

The injection mix containing 150 ng of DNA in 20 µl was cleaned using a filter column (Coxtar, SPIN-X Centrifuge Tube Filter, 0.45 µm Cellulose Acetate) and injected into the gonads of young adult hermaphrodites sticking to 2.5% agarose pads and covered in Halocarbon oil (700) as described previously in (Mello et al. 1991). Injected animals were rescued with M9 buffer onto fresh plates seeded with OP50 *E. coli* and screened for transgenic progeny after a few days.

5.1.12 Ballistic transformation

As an alternative to micro-injection or in case of big DNA constructs, worms were transformed by gene bombardment to obtain low-copy integrations.

Equipment
Biolistic PDS-1000/He from BioRad
rupture discs 1100 psi
macrocarriers
macrocarrier holders
stopping screens

Settings
Gap distance: 1/4''
vacuum: 27/28 inches Hg
Target shelf: second shelf from the bottom

To facilitate the screening of transformants, a worm strain defective in crawling (DP38, *unc-119(ed3)*) and a cloning vector containing the genomic *unc-119* sequence was used. Worms were enriched by liquid culture. For this purpose, two confluent 6 cm NGM plates were added to 100 ml S-medium and supplied with 300 µl $MgSO_4$ (1M), 300 µl $CaCl_2$ (1M), 1 ml KCitrate (pH = 6), 1 ml trace metals, 100 µl cholesterol (5 mg/ml), 1 ml Pen/Strep (100X) and 100 µl nystatin (1000X). As a food source, highly concentrated Na22 *E. coli* were used. The bacteria were enriched overnight in a rich medium as listed below and concentrated ~ 40x. The worm culture was kept at 20 °C on a shaker at 150 rpm to ensure oxygenation.

Component	Amount / volume
Bacto tryptone	24 g
Yeast extract	48 g
Glycerol (50%)	16 ml
ddH_2O	to 2l
autoclave, cool to 60 °C, then add	
KH_2PO_4 (pH = 6)	1 ml

When worms had grown to confluency and a lot of L4 to young adult worms were present, the culture was centrifuged at 1000 – 2000 rpm for 1 min, washed twice with M9 buffer and distributed evenly on two 10 cm NGM plates. To prevent the movement of the worms, the plates were dried on ice with the lid open.
Prior to the collection of the worms, the gold beads were prepared (this step can be done up to one week before). For two bombardments, 16 – 17 mg gold beads were weighed into siliconised Eppendorf Tubes® (0.3 – 3 microns, Chempur) and 1 ml of 70% EtOH was added. The beads were mixed thoroughly in a homogenizer, briefly centrifuged and the supernatant was removed. The beads were then washed three times by adding 1 ml of ddH_2O, mixing in the homogenizer and removing the supernatant after a brief spin. The streaks of gold were gently streaked down with the pipette tip. Finally, 170 µl of 50% glycerol were added. Optionally, the beads can be kept 3 – 4 weeks at room temperature at this point. The beads were again mixed well using the homogenizer and distributed into two siliconised Eppendorf Tubes® (85 µl / tube). The beads were coated while being vortexed continuously, with a one min break in between the additions. 32 µl spermidine, 4 µg DNA and 80 µl $CaCl_2$ (2.5M) were added and the final mixture was vortexed for five min. The beads were centrifuged briefly and the supernatant was removed from the centre. The beads were resuspended in 300 µl 70% EtOH and the gold streaks sticking to the tube wall were pushed down. The supernatant was removed again after spinning and 80 µl 100% EtOH

were added. The beads were vortexed for further five min.
The macrocarriers were cleaned using pressurised gas and inserted into the holder. 10 µl of coated DNA beads were spread evenly on each macrocarrier and left to dry. The rupture disc (1350 psi) was prepared by dipping it in 100% isopropanol and drying with pressurised gas. The bombardment disc was assembled, inserted into the apparatus and the plate(s) with the dried worm culture was bombarded.
The bombarded worms were left to recover for 1 – 2 h at room temperature. They were washed down with M9 into 15 ml falcon tubes, centrifuged at 1000 rpm for 1 min and the supernatant was removed leaving 4 ml. With a cut pipette tip, the worms were distributed onto 25 NGM plates (10 cm) next to the food at the edge of the plates. After approximately one week, crawling worms were searched and cloned to check for insertions.

5.1.13 Lysis of worms

Genomic DNA of worms was obtained by lysing 1 – 10 young adult hermaphrodites in 6 – 10 µl lysis mix. The lysis was performed in 0.2 ml Multiply® Pro Tubes (Sarstedt) in a PCR machine (BioRad MyCycler).

Temperature	Time
60 °C	1 hour
95 °C	10 min
12 °C	∞

Component	Volume (for 10 µl)
10X lysis buffer	1 µl
Proteinase K (10 mg / ml)	0.6 µl
ddH_2O	8.4 µl

5.1.14 Genotyping PCR assays

The genotyping of strains was performed by amplifying the genomic locus partially using NEB LongAmp Taq DNA Polymerase. The presence of a deletion was confirmed via gel electrophoresis and SNPs were verified via DNA sequencing after precipitation of the PCR product.

Locus	Primer pair	Size (mut) / (wt)	Sequencing Primer
F44F1.1(ok1765)	OSMA26 / OSMA27	1.8 kb / 2.9	-
egl-9(sa307)	OSMA35 / 36 OSMA171 / 172	1.0 kb / 1.2 kb 1.1 kb / 1.4 kb	-
egl-9(n586)	OSMA113 / OSMA114	0.6 kb	OSMA113
egl-9(ia60)	OSMA113 / OSMA114	0.6 kb	OSMA113
hif-1(ia04)	OSMA48 / OSMA49 OSMA122 / OSMA123	0.5 kb / 1.7 kb 3.1 kb / 4.5 kb	-

hif-1(zh111)	OSMA122 / OSMA123 OSMA224 / OSMA225	1.0 kb / 4.5 kb 2.0 kb / 4.4 kb	-
vhl-1(ok161)	OSMA50 / OSMA51	0.6 kb / 1.9 kb	-
ahr-1(ia3)	OSMA77 / OSMA78	1.9 kb / 3.0 kb	-
Phif-1::gfp::hif-1(3' UTR)	OSMA79 / OSMA80	0.9 kb	-
gfp	OSMA81 / OSMA82	0.8 kb	-
pha-1(e2123)	OSMA117 / OSMA118	1.1 kb	OSMA119
rrf-3(pk1426)	OSMA120 / OSMA121	2.2 kb / 4.5 kb	-
let-23(sy1)	OSMA124 / OSMA125	1.0 kb	OSMA126
cdka-1/p35(gm335)	OSMA175 / OSMA176	4.0 kb / 5.7 kb	-
amx-2(ok1235)	OTS149 / OTS150	0.5 kb / 2.3 kb	-
let-60(n1046)	OTS38 / OTS39	0.8 kb	OTS49
let-60(ga89)	OTS38 / OTS39	0.8 kb	OTS49
let-60(n2021)	OMMO127 / OMMO128	0.5 kb	OMMO127
bar-1(ga80)	OTS33 / OTS36	0.5 kb	OTS33 / OTS36
lin-10(e1439)	OSMA159 / OSMA160	1.3 kb	OSMA161
lin-7(e1413)	OSMA162 / OSMA163	1.1 kb	OSMA164
unc-119(ed3)	OSMA165 / OSMA166	1.6 kb	OSMA167
lin-45(sy96)	OSMA199 / OSMA200	0.8 kb	OSMA199
unc-32(e189)	OSMA211 / OSMA212	0.8 kb	OSMA213
Pegl-9::gfp::egl-9 3' UTR	OSMA264 / OSN73	0.5 kb	-
nhr-75(tm4533)	OSMA300 / OSMA301	0.5 kb / 1.0 kb	-
tyr-2(ok1363)	OSMA287 / OSMA288	1.0 kb / 1.9 kb	-
rde-1(ne219)	OMW207 / OEL1	5.6 kb	OMW247
cdk-5(ok626)	OSN108 / OSN109 / OSN110	2.1 kb / 2.1 kb + 1.8 kb	-
lin-2(n397)	OJE61 / OJE62	2.0 kb / 9 kb	-
lin-3(e1417)	OMMO135 / OMMO136	0.5 kb	OJE129
dpy-19(e1259)	OMW223 / OMW224	0.7 kb	OMW223
mCherry	OEH86 / OEH87	0.9 kb	-
sos-1(s1031)	OAH295 / OAH296	0.3 kb	OAH295
sem-5(n2019)	OAS605 / OAS606	0.4 kb	OAS605
ttr-11(tm3381)	OSN7 / OSN8	0.5 kb / 0.8 kb	-

Position of introgression	Primer sequence	FLP (N2 to CB)
ZH1-01	TTTTGCGCGTCAAATATGTTGT TGCTTTAACCTATATTTTGAATGCG	+3
ZH1-03	GACCCGACTGCCGTTCTAT CTGCGTCTCCCTATGTTCG	-6
ZH1-05	GAAATCGATTCTTCATTCAGTT GCCCCTGAAACCCGTGGT	+21
ZH1-06	TCAAGAAAAACGGTCATTATGCA CATTGTATCGCACATCGAACG	+8
ZH1-08	GGGGAAAGCAAGATAGACTC CGCTTCCGAACAACCACCT	+7
ZH1-09	CATATCGAAAATCAATCCCGTA AGGAAAAATAAGCTGACCGAAT	+4
ZH1-15	GGCATTTTTTTGGTTCAACATTT CGAAGACTTCCTAAAAGAGTGGCA	-4
ZH1-18a	AATATTTGATTGGATCGTCGCA TTAGAAGTAAATTTGCAGTACCA	-5
ZH1-22	CTCGTTGTGAGACTCTATGGAA TCCATATTTTTTGGCTTCTGAGA	+4
ZH1-23	ATCAAATTTCTCTTGCCTTAATGAT TAGGTGATTCATTTTTGCGGGAA	+2
ZH1-27	CACAGAAGTTTCGAAGTTACAG AAATTGAGGTGGTATTTTCTCAT	+1
ZH1-34	GAAAAACAATCGCTACATAAAC GCCTACACAGAAGAATTATGG	+1
ZH3-02	ACATCACATCATAAGTCAAGC AAAGTGAGAAATCTTGTCCAC	+3
ZH3-04	ATCAGCAGAGAATAGTTTCACA CGAAATGAAGTGGGTATTTGAT	+3
ZH3-5a	CACTGAGGAGACGAGCATTT AATGAAGATCAGAAATGAGCAA	+2
ZH3-10a	GAATTACCGCCATTTGCGTA GTGGTGAAACGTGTGAAGACT	-4
ZH3-11	TCAACGTAGATCAAGCCGAA CAACGTAGGTCGCCTTACA	+2
ZH3-12	AAATTGCCTGAAAACACCGAA CAAGTATTTGGTAAATTGCCAA	+6
ZH3-23	GCGGTCAGTGCCAGAGCAT TATGCAATGCAATTAAAAAATGTC	+1
ZH3-35	GAAAACAAGTAATCAATGCTGC AAGAAGTTTCATGATTAAGGAC	+1

5.1.15 Genotyping by FLP mapping

FLP (fragment length polymorphism) mapping was carried out according to ("A universal method for automated gene mapping") to determine whether the CB4856 Hawaiian or N2 Bristol sequence was present at a specific genomic position. For a schematic overview of the introgression lines created please consult section 3.1. The PCR was carried out using NEB LongAmp Taq DNA Polymerase as described above (5.1.2) with the cycle program below.

Cycles	Temperature	Time
1x	95 °C	2 min
10x	95 °C	20 sec
	61 °C	30 sec
	Decrease by 0.5 °C / cycle	
	72 °C	45 sec
28x	95 °C	20 sec
	56 °C	30 sec
	72 °C	45 sec
1x	72 °C	5 min
	12 °C	∞

For each introgression eight genomic positions were analysed as listed below.

CB4856 introgression	Loci
ewIR5 (Chr I)	ZH1-18a, ZH1-03, ZH1-27, ZH1-34, ZH1-01, ZH1-22, ZH1-23, ZH1-15
ewIR9 (Chr I)	ZH1-03, ZH1-27, ZH1-34, ZH1-01, ZH1-23, ZH1-15, ZH1-08, ZH1-06
ewIR10 (Chr I)	ZH1-01, ZH1-22, ZH1-23, ZH1-15, ZH1-05, ZH1-08, ZH1-09, ZH1-06
ewIR10 (Chr III)	ZH3-04, ZH3-02, ZH3-05a, ZH3-35, ZH3-10a, ZH3-23, ZH3-11, ZH3-12
ewIR17 (Chr I)	ZH1-03, ZH1-27, ZH1-34, ZH1-01, ZH1-23, ZH1-15, ZH1-08, ZH1-06

5.1.16 Generation of an extra-chromosomal translational LET-23::mCherry reporter strain

A translational LET-23::mCherry reporter was created from a pre-existing LET-23::GFP reporter construct. mCherry was amplified from pCFJ90 with overhangs to allow insertion into pJE05 via Gibson assembly®. pJE05 was amplified accordingly and the fragments were assembled. The resulting plasmid pSMa11 containing the partial *let-23* sequence fused to mCherry in the Gateway vector pDONRP2r-P3 was used in a Gateway LR reaction with the 5' and 3' parts of *let-23* (pJE06 and pJE07) and the destination vector pCFJ150 to obtain the final reporter construct pSMa12. The construct was bombarded on the strain DP38 and transgenic lines were isolated.

5.1.17 Generation of *hif-1(zh111)* mutant worms

The Co-CRISPR method was applied according to (Arribere et al. 2014). The sgRNA sequence GATAGAAAAGTGAGTCCTAA was inserted into plasmid #46169 (PU6::unc-119_sgRNA) via site-directed mutagenesis to obtain pSMa03. 25 ng/µl *dpy-10* sgRNA (pJA58) was co-injected into N2 Bristol animals with 25 ng/µl of pSMa03, 500 nM of *dpy-10(cn64)* repair template AF-ZF-827, 500 nM of OSMA89 and 50 ng/µl of pDD162. Candidate worms were selected from plates harbouring a large number of RoI progeny and analysed by PCR for deletions and further sequencing. The *zh111* deletion spans 2464 bp and removes exons three to five between the regions ATTTCAAAAAATTTTTGACA (upstream) and CTAAGTTAAAAAAACAACAG (downstream).

5.1.18 CRISPR/Cas9 to obtain *pfd-3* deletion mutants

CRISPR/Cas9 was employed as described in (Friedland et al. 2013). The sgRNA sequences GCGGACAGTCTATCAGCACG (sgRNA1), GTCATATTCGACCATTACGT (sgRNA2), GAAAAAACGCAAAAAATTCG (sgRNA3) or GCCGCTCTCGCTGTCAATAA (sgRNA4) were inserted into plasmid #46169 (PU6::unc-119_sgRNA) via site-directed mutagenesis. The *pfd-3* genomic sequence was amplified with OKJ1 and OKJ2, sub-cloned and BglII restriction sites were inserted using OKJ7/8 and OKJ9/10 to flank the CDS. The CDS was removed via an enzymatic restriction digest and the resulting plasmid was used as repair template. N2 Bristol animals were injected with 2x 25 ng/µl sgRNA plasmid (sgRNA1 and 2 or sgRNA3 and 4 respectively), 50 ng/µl P*eft-3*::Cas9-SV40 NLS::*tbb-2* 3'UTR, 50 ng/µl repair template and 5 ng/µl pCFJ104. The progeny was screened for deletions by PCR using OTS121 and OTS122. To balance lethal deletions, the strain KR2151 was used.

5.1.19 Generation of an extra-chromosomal P*nhr-57::nhr-57*(CDS)::*gfp::nhr-57* 3' UTR reporter strain

A 1206 bp fragment upstream of the *nhr-57* transcriptional start site was amplified together with the coding genomic region (without the stop codon) using the primers OSMA302 and OSMA303. The *gfp* sequence was amplified from pPD95.75 using the primers OMMO76 and OSMA304. 459 bp of the *nhr-57* 3' UTR were amplified using the primers OSMA305 and OSMA306. A vector backbone containing a *CB-unc-119(+)* rescue as well as the *AmpR* gene was amplified using the primers OMW405 and OMW443. The four fragments were combined into a 10.170 kb plasmid (pSMa32) using Gibson Assembly®. N2 animals were injected (due to a mutation in the *CB-unc-119(+)* gene) with 5 ng/µl pSMa32, 2.5 ng/µl pCFJ104 and 100 ng/µl pBS. Transformants were isolated based on the presence of the co-injection marker.

5.1.20 Generation of an extra-chromosomal P*bar-1::nhr-57*(CDS)::*gfp::nhr-57* 3‘ UTR reporter strain

A 3237 bp fragment upstream of the *bar-1* transcriptional start site was amplified using the primers OSMA327 and OSMA328. The *nhr-57*(CDS)::*gfp::nhr-57* 3’ UTR sequence within a vector backbone containing a *CB-unc-119(+)* rescue as well as the *AmpR* gene was amplified from pSMa05 using the primers OMW405 and OSMA326. The two fragments will be combined into a 12.201 kb plasmid (pSMa33) using Gibson Assembly®. N2 animals will be injected (due to a mutation in the *CB-unc-119(+)* gene) with 5 ng/µl pSMa33, 2.5 ng/µl pCFJ104 and 100 ng/µl pBS. Transformants will be isolated based on the presence of the co-injection marker.

5.2 Protein methods

5.2.1 SDS-PAGE

SDS-PAGE with subsequent Western blotting was performed using pre-cast Novex® Tris-Glycine Mini Gels (Invitrogen) with the XCell SureLock™ Mini-Cell Electrophoresis System including the XCell SureLock® Mini-Cell and the XCell II™ Blot Module. SDS gels were run at 100 V in freshly prepared 1X running buffer. MOPS buffer was used for the separation of medium- to large-sized proteins and MES buffer for small- to medium-sized proteins. Per genotype, 45 L4 larvae were picked into 15 µl 1x SDS loading buffer and proteins were denatured at 95 °C for 5 min. Samples were either frozen at -20 °C or centrifuged for 2 min at 14’000 rpm. 15 µl sample were loaded together with 5 µl Precision Plus Protein™ Dual Color Standards (Biorad).

2X SDS loading buffer	100 mM Tris-HCL pH = 6.8, 4% SDS, 0.2% bromophenol blue, 20% glycerol, 200 mM DTT / ß-mercaptoethanol
20X MOPS running buffer	104.6 g MOPS, 60.6 g Tris, 50 ml SDS (20%), 20 ml EDTA (0.5M), dd$H_2$0 to 0.5l
20X MES running buffer	195.2 g MES, 121.2 g Tris, 20 g SDS, 6 g EDTA, ddH_2O to 1l

5.2.2 Western blot

SDS-PAGE gels were blotted onto PVDF membranes (Merck Millipore) of 5.5 x 8.5 cm using the XCell II™ Blot Module. While the gel was running, the blotting buffer and solution was prepared and cooled to 4 °C. The membrane was activated in 100% MeOH for 5 min and stored in blotting buffer at 4 °C until used. Blotting was carried out at 30 V for 1h at 4 °C. The membrane was removed from the gel sandwich and blocked in 4% milk/TBS-T for 2-4h at room temperature to prevent unspecific binding of antibodies. The membrane was probed with the 1° antibody diluted in 4%

milk/TBS-T while shaking at 4 °C overnight. The antibody was removed and the membrane was washed 3x 15 min with TBS-T at RT before the HRP coupled 2° antibody was added for 60 min at RT. The membrane was washed again with TBS-T 3x 15 min. The HRP reaction was activated using the Amersham™ ECL™ Western blotting detection kit (GE Healthcare) and the membrane was illuminated to visualise the protein bands and protein ladder.
If a second protein of similar size was analysed, the horseradish peroxidase was inactivated by applying 15% H_2O_2 in TBS-T for 30 min. The membrane was washed extensively with TBS-T and probed with the second 1° antibody.

Transfer buffer	600 ml H_2O, 150 ml 100% MeOH, 2.4 g Tris, 10.8 g glycine. Stir with magnetic stirrer to dissolve.

5.2.3 Antibodies

Antibody	Company	Cat. No.	Dilution
Monoclonal mouse anti-GFP	Roche	11814460001	1:2000
Polyclonal rabbit anti-MAP Kinase (ERK-1, ERK-2)	Sigma-Aldrich	M5670	1:5000
Monoclonal mouse anti-MAP Kinase, activated (dephosphorylated ERK-1&2)	Sigma-Aldrich	M8159	1:1000
Polyclonal rabbit anti-alpha tubulin	Abcam	ab18251	1:2000
Monoclonal mouse anti-alpha tubulin	Sigma-Aldrich	T6074	1:2000
Polyclonal HRP goat anti-rabbit	Jackson Immuno Research	111-035-144	1:3000
Polyclonal HRP goat anti-mouse	Jackson Immuno Research	115-035-003	1:3000

5.2.4 Biarsenical labelling

Biarsenical labelling of tetracysteine tagged proteins was performed by adapting published protocols for staining with MitoTracker™, since the molecular weight of the molecules is comparable (MitoTracker™: 531.5 g/mol, TC-FlAsH™ (ThermoFisher Scientific): 664.5 g/mol, TC-ReAsH™ (ThermoFisher Scientific): 545.4 g/mol). At least one small NGM plate crowded with worms was washed into a 1.5 ml Eppendorf tube. After centrifugation at 1000 rpm for 1 min, the liquid was removed to 500 µl and 2.5 µl of the dye (2 mM) was added to obtain a working concentration of 10 µM. The tube was wrapped in aluminium foil. The sample was incubated for at least 8h at RT while shaking. The liquid was removed after briefly centrifuging and the sample was washed twice with BAL wash buffer (ThermoFisher Scientific) that had been diluted according to the manufacturer's protocol. The worms were resuspended in H_2O and transferred back to small

NGM plates seeded with OP50 *E. coli*. After 1h of recovery in the dark, the worms were imaged using standard fluorescence microscopy.

5.3 Animal Methods

5.3.1 Strains and general handling of *C. elegans*

C. elegans strains derived from either N2 Bristol (Brenner 1974) or CB4856 Hawaii (Wicks et al. 2001) were maintained at 15 °C, 20 °C or 25 °C on NGM (Nematode Growth Medium) plates according to standard methods (Brenner 1974). Unless otherwise noted, the mutations used have been described previously and are listed below.

5.3.1.1 Mutations

Linkage group	Allele	Reference	Present in strain
LG I:	*lin-10(e1439)*	(Whitfield et al. 1999)	CB1439
	F44F1.1(ok1765)	(Consortium 2012)	RB1497
	F44F1.3(ok1878)	(Consortium 2012)	VC1418
	H28O16.1(ok2203)	(Consortium 2012)	VC2824
	dpy-5(e907)	(Thacker et al. 2006)	BC13915, BC15199
	hT2 [bli-4(e937) let-?(q782) qIs48]	(McKim et al. 1993)	several
	gon-2(ok465)	(Church and Lambie 2003)	VC1463
	ceh-6(ok3388)	(Consortium 2012)	VC2666
	hIn1 [unc-54(h1040)]	(Zetka and Rose 1992)	KR2151
LG II:	*let-23(sy1)*	(Aroian and Sternberg 1991)	AH13
	lin-7(e1413)	(Simske et al. 1996)	CB1413
	rrf-3(pk1426)	(Sijen et al. 2001)	NL2099
	ttTi5605	(Frøkjær-Jensen et al. 2008)	EG6699

	unc-32(e189) lin-12(n137n720)	(Greenwald et al. 1983)	MT2343
	dpy-19(e1259) lin-12(n137)	(Greenwald and Seydoux 1990)	MT2343
	pha-1(e2123)	(Mani and Fay 2009)	GS6387
LG III:	*cdka-1/p35(gm335)*	(Juo et al. 2007)	AH4538
	unc-119(ed3)	(Maduro and Pilgrim 1995)	several
	tyr-2(ok1363)	(Consortium 2012)	RB1272
	cdk-5(ok626)	(Consortium 2012)	RB814
	hT2 [bli-4(e937) let-?(q782) qIs48]	(McKim et al. 1993)	several
	let-60(n1046)	(Beitel et al. 1990)	
	let-60(zh121)	Maxeiner et al., unpublished data	MT2124 AH3345
	let-60(zh122)	Maxeiner et al., unpublished data	AH3340 SD551
LG IV:	*let-60(ga89)*	(Eisenmann and Kim 1997)	MT4866
	let-60(n2021)	(Beitel et al. 1990)	MT8022
	lin-1(n304)	(Beitel et al. 1995)	CB1417
	lin-3(e1417)	(Hwang 2004)	PS427
	lin-45(sy96)	(Sternberg et al. 1993)	
	sos-1(s1031)	(Chang et al. 2000)	BC1925
	egl-9(sa307)	(Darby et al. 1999)	JT307
	egl-9(n586)	(Darby et al. 1999)	MT1216
	egl-9(ia60)	(Shao et al. 2009)	ZG448
LG V:	*hif-1(ia04)*	(Jiang et al. 2001)	CB6088
	hif-1(zh111)	Maxeiner et al., unpublished data	AH4533
	nhr-57(tm4533)	National BioResource Project	FX04533
	ttr-11(tm3381)	(Consortium 2012)	FX03381
	vhl-1(ok161)	(Epstein et al. 2001)	CB6116
	rde-1(ne219)	(Qadota et al. 2007)	several
LG X:	*sem-5(n2019)*	(Clark et al. 1992)	MT4755
	bar-1(ga80)	(Natarajan et al. 2004)	EW15
	lin-2(n397)	(Horvitz and Ferguson 1985)	MT397

5.3.1.2 Transgenes

Linkage group	Transgene	Reference	Present in strain
LG I:	*ayIs4[Pegl-17p::NLSgfp; dpy-20(+)]*	(Burdine et al. 1998)	NH2466
LG II:	*saIS14[lin-48p::gfp]*	(Johnson et al. 2001)	AH472
LG III:	*zhIs4[lip-1::GFP, unc-119(+)]*	(Berset et al. 2001)	AH142
LG IV:	*zhIs038[let-23::gfp, unc-119(+)]* *ayIs7[hlh-8::gfp fusion + dpy-20(+)]* *swIs79[ajm-1::GFP, seamcell::GFP, unc-119(+)]*	(Haag et al. 2014) (Harfe et al. 1998) (Mohler et al. 1998)	AH1779 PD4666 SU140
LG unknown:	*iaIs38[egl-9p::egl-9::tag + unc-119(+)]* *sIs13915[rCes H28O16.1::GFP + pCeh361]* *opIs206[Phif-1::hif- 1::gfp::hif-1(3'UTR)]* *gaIs47[lin-31::mpk-1(gf); lin-31::D-mek(gf)]*	(Shao et al. 2009) (MCKAY et al. 2003) (Sendoel et al. 2010) (Lackner et al. 1994)	ZG494 BC15199 WS4274 SD573
extra-chromosomal:			
	iaEx101[egl-9p::egl-9(H487A)::tag + unc-119(+)]	(Shao et al. 2009)	ZG686
	zhEx550[let-23::mCherry, unc-119(+)]	Maxeiner et al., unpublished data	AH4568, AH4569, AH4570
	zhEx418[lin-31::rde-1; myo-2::mCherry]	(Haag et al. 2014)	AH2927
	sEx13915 [rCes H28O16.1::GFP + pCeh361]	(MCKAY et al. 2003)	BC13915
	Ex?[elt-2p::rde-1; pRF4[rol-6(su1006)]]	(Pilipiuk et al. 2009)	OLB11
	arEx1528[lin-31p::YFP::lin-45(+)]	(de la Cova and Greenwald 2012)	GS6387
	vhEx37[pttx-3::gfp + plin-31::gfp::lin-10]	Gauthier et al., unpublished data	QR600
	zhEx555[tetracysteine::lin-3 + Pmyo-2::mCherry]	Maxeiner et al., unpublished data	AH4640
	zhEx579[Pmyo-2::mCherry::tetracysteine]	Maxeiner et al., unpublished data	AH4825
	zhEx605[Pnhr-57::gfp::nhr-57 3' UTR + Pmyo-2::mCherry]	Maxeiner et al., unpublished data	AH5707

5.3.1.3 N2/CB4856 introgression lines

CB4856 introgressions as published in (Doroszuk et al. 2009) were used to obtain miRILs with either the *let-60(n1046)* or *bar-1(ga80)* allele. Specifically, we made use of the strains ewIR5, ewIR9, ewIR10 and ewIR17 (LG I). The raw mapping data of the obtained strains are listed and described in 3.1.

5.3.2 Crosses

To obtain homozygous mutant males plates with 20 L4 hermaphrodites were tightly sealed with parafilm and incubated at 30 °C for 5h to favour non-disjunction during meiosis and increase the incident of male sex to occur (adapted from Hodgkin 1993). After a few days, single males were enriched by crossing them to hermaphrodites of the same genotype. 15 hermaphrodites and five males were kept on an NGM plate with a small drop of *E. coli* OP50 for two days. Hermaphrodites were singled out and screened for male F1 progeny. Animals of the F1 generation were either used for further crossing or singled out for subsequent genotyping of the F2 generation.

5.3.3 Worm liquid cultures

To obtain large quantities of worms, e.g. for ballistic transformation, three to six small well-crowded NGM plates were washed down into 100 ml of liquid medium as follows:

Amount	Component
100 ml	S-Basal
300 µl	1M $MgSO_4$
300 µl	1M $CaCl_2$
1 ml	KCitrate pH = 6
1 ml	100X trace metals
1 ml	100X Pen/ Strep
100 µl	1000X Nystatin
100 µl	Cholesterol (5 mg/ml)
4 ml	Na22 worm food (see below)

Worm liquid cultures were incubated at 20 °C on a shaker at 150 rpm for approximately one week or until a sufficient number of worms was obtained. The superbroth media to prepare worm food consists of:

Amount	Component
24 g	Bacto tryptone
48 g	Yeast extract
16 ml	50% Glycerol
2 l	ddH_2O

The mixture was autoclaved and 100 ml KPO_4 was added. The media were inoculated with Na22 *E. coli* and grown overnight at 37 °C. The next day, the culture was centrifuged for 15 min at 4000 rpm and the supernatant was discarded. The pelleted bacteria were dissolved in approximately 60 ml 2xTY and aliquoted into 15 ml falcon tubes that were stored at -20 °C.

5.3.4 Freezing of *C. elegans*

Freshly starved L1 larvae were washed down from three NGM plates with M9 and mixed with an equal amount of freezing solution (30% glycerine in S-basal, autoclaved). The worms were slowly cooled down to -80 °C using boxes filled with isopropanol. A few days later, a test vial was thawed to check for successful freezing.

5.3.5 Cleaning of *C. elegans*

To clean contaminated *C. elegans* strains, ten gravid hermaphrodites were picked into a drop of 1:1 (v/v) 10-15% sodium hypochlorite and 2M NaOH on a clean NGM plate. The following day, clean L1 larvae were picked onto fresh plates.
To obtain more worms or to synchronise strains, animals were washed into 15 ml falcon tubes and centrifuged for 1 min at 1000 rpm. The supernatant was removed leaving 1 ml. 70 µl sodium hypochlorite (10-15%) and 200 µl 2M NaOH were added and the tube was gently rocked for 8-10 min, until adult worms were dissolved. The cleaned eggs were washed three times by filling the tube with M9 buffer or ddH_2O, centrifuging at 2000 rpm for 1 min and removing most of the supernatant. After the final washing step, 6 ml M9 buffer were added and the eggs were allowed to hatch overnight while rocking slightly.

5.3.6 RNAi

Gene knockdown via RNAi feeding was performed according to Kamath et al. (2003). HT115 (DE3) *E. coli* RNAi clones were grown on agar plates containing ampicillin and tetracycline. The RNAi feeding plates containing 3 mM IPTG to induce expression of the dsRNA were prepared 2-3 days prior to seeding of the bacterial clones (for recipe see table below). The bacterial clones were grown in 2xTY containing ampicillin overnight and 350 µl per IPTG NGM plate were applied. 1-2 days later, approximately 10 synchronised L1 larvae were pipetted onto the RNAi feeding

plates and the F2 progeny was analysed (unless stated otherwise).

Protocol for 40 – 50 NGM RNAi feeding plates

Amount	Component
1.5 g	NaCl
1.25 g	Peptone (Tryptone Peptone)
9.5 g	Bacto Agar
0.5 l	ddH_2O
autoclave, when T = 55 °C add while stirring:	
0.5 ml	Cholesterol (5 mg/ml)
12.5 ml	KPO_4 buffer 1M, pH = 6
0.5 ml	1M $MgSO_4$
0.5 ml	1M $CaCl_2$
1.5 ml	1M IPTG
0.5 ml	Ampicillin

The mixture was stirred using a magnetic stirrer for a few minutes and 10 ml medium per plate were poured into 6 cm petri dishes.

5.3.7 Drug treatment on NGM plates

The experiments to treat *C. elegans* with drugs were adapted from (Wang et al. 2007; Locke et al. 2008; Romney et al. 2011; Ackerman and Gems 2012; Padmanabha et al. 2015). The drugs were dissolved to a stock concentration of 100 mM and distributed evenly to 6 cm NGM plates containing 10 ml medium.

Amount for 100 mM stock	Component
46.8 mg	DIP (Sigma)
3000 µl	EtOH
store at -20 °C, use within one month	
47.4 mg	$CoCl_2$ • 6 H_2O (Sigma)
1978 µl	H_2O
filter-sterilise, store at 2-8 °C	

The working concentrations were 10 µM (500 µl of 0.2 mM dilution) and 1 µM (500 µl of 0.02 mM dilution). The plates were left to dry for some hours during which time the worm food was heat-inactivated. We heat-inactivated previously concentrated Na22 *E. coli* prior to feeding, since i) bacterial growth is affected by the drugs and ii) we we wanted to prevent the emergence of bacterial drug metabolites.
One bacterial clone was incubated in 250 ml 2xTY overnight at 37 °C. The following day, the bacterial culture was centrifuged for 15 min at 4000 rpm and resuspended in a total of 25 ml (10x

concentrated). Aliquots of 750 µl (sufficient for two NGM plates) were stored frozen at -20 °C and heat-inactivated for 1h in a 70 °C water bath prior to use. A small aliquot was streaked out onto an agar plate to check the efficiency of heat-killing. 350 µl heat-inactivated Na22 *E. coli* were pipetted onto each NGM plate with or without drug and left to dry for one or two days, after which 10 synchronised L1 larvae were added. The vulval induction index was scored in the F2 generation.

5.4 Instruments

DNA experiments	
PCR machine	BioRad Tetrad® 2 Thermal Cycler
Nanodrop	NanoDrop® ND-1000 Spectrophotometer
Protein experiments	
Western blot	XCell SureLock™ Mini-Cell
	XCell II™ Blot Module
Microscopes	
Fluorescent and Nomarski	Leica DMRA, equipped with a cooled CCD camera (Hamamatsu ORCA-ER)
Dissecting scope	Leica MS5
Fluorescence dissecting scope	Leica MZDLIII
Injection scope	Leica DM-IRB
Further instruments	
Centrifuges	Eppendorf Centrifuge 5804
	Eppendorf Centrifuge 5417 R
Homogenizer	Fastprep®-24, MP Biomedicals

5.5 Media and buffers

S-Basal	5.85 g NaCl, 50 ml KPO_4, 1 l H_2O
2xTY (pH = 7)	16 g Bacto Tryptone, 10 g Yeast extract, 5 g NaCl, ddH_2O to 1 l, autoclave
KCitrate (1M, pH = 6)	21.01 g Citric acid monohydrate, adjust to pH = 6 with solid KOH (approx. 17 g) fill to 100 ml with ddH_2O, autoclave
KH_2PO_4 (1M, pH = 6)	136.1 g KH_2PO_4, adjust to pH = 6 with solid KOH (approx. 15 g), fill to 1 l with ddH_2O, autoclave
KPO_4 buffer (1M, pH = 6)	87.8 ml 2M KH_2PO_4, 12.3 ml 2M K_2HPO_4, 100 ml ddH_2O

Worm lysis buffer (10X)	500 mM KCl, 100 mM Tris (pH = 8.2), 25 mM $MgCl_2$, 4.5% NP-40, 4.5% Tween 20, 0.1% Gelatine
M9	3 g KH_2PO_4, 6 g Na_2HPO_4, 5 g NaCl, ddH_2O to 1l, autoclave and cool to 55 °C, then add 1 ml $MgSO_4$
STET	8% Sucrose, 5% Triton-X 100, 50 mM EDTA, 50 mM Tris (pH = 8)
50x TAE	242 g Tris base, 57.1 ml Glacial acetic acid, 100 ml 0.5M EDTA (pH = 8), ddH_2O to 1 l
TE	2 ml Tris (1M, pH = 7.5), 0.4 ml EDTA (0.5M), 197.6 ml ddH_2O
Trace metals	0.346 g $FeSO_4 \cdot 7\ H_2O$, 0.930 g Na_2EDTA, 0.098 g $MnCl_2 \cdot 4\ H_2O$, 0.144 g $ZnSO_4 \cdot 7\ H_2O$, 0.012 g $CuSO_4 \cdot 5\ H_2O$, ddH_2O to 500 ml, autoclave, keep in dark at 4 °C
TBS-T	50 ml 1M Tris, 150 ml 5M NaCl, 2.5 ml Tween 20, 5 l ddH_2O

5.6 Software used for data analysis

Leica operating software	Openlab 5.0.1, VisiView®
Image processing	ImageJ 1.48f Adobe Illustrator CS6, Version 16.0.4
DNA analysis	CLC Main Workbench 7 GeneMapper (AppliedBiosystems)
Statistical software	R 3.3.3 Spyder 3.0.0 (The Scientific PYthon Development EnviRonment)

5.7 Python, R and ImageJ macro scripts

The following Python, R and ImageJ scripts can be found on the accompanying CD-ROM and are described briefly in the following table.

Name	Purpose
bootstrapping_VI.R	Input data is bootstrapped 1000 times and mean and p values as well as the 95% confidence intervals are given.
evaluation_sgRNA.py	A DNA sequence is given as input and sgRNA sequences and their evaluation scores analysed according to Doench et al., 2014 are saved in an Excel sheet.
fishers_exact_test.py	Performs the Fisher's exact test of independence to test whether proportions of two variables are different from each other.
bootdif.R	The difference of the mean of two samples is bootstrapped 1000 times. The output is the mean difference, the sample means and the 95% confidence intervals.
background_correction.ijm	The programme uses a folder containing sample and background images as an input. Using the "Calculator Plus" option in ImageJ, the sample images are background subtracted and saved in a new folder.
sorting_stages.ijm	The programme uses a folder with sample images of various cell stages and sorts the images into cell stage specific folders according to the user's decision.
zproject_1cs_allVPCs.ijm zproject_2cs_allVPCs.ijm zproject_4cs_allVPCs.ijm	Image stacks to quantify are opened and background subtracted. A z project is performed ("sum slices") and the intensity values are measured within a selection given by the user. Programmes adapted for 1-, 2- and 4-cell stages.
stk_to_tiff.ijm	Macro opens images with file extension ".stk" and saves as ".tiff" files. This can be applied prior to other ImageJ applications that fail to work with ".stk".

References

6

Abdus-Saboor I, Mancuso VP, Murray JI, et al (2011) Notch and Ras promote sequential steps of excretory tube development in *C. elegans*. Development 138:3545–3555. doi: 10.1242/dev.068148

Aberle H, Bauer A, Stappert J, et al (1997) β-catenin is a target for the ubiquitin–proteasome pathway. EMBO J 16:3797–3804. doi: 10.1093/emboj/16.13.3797

Ackerman D, Gems D (2012) Insulin/IGF-1 and Hypoxia Signaling Act in Concert to Regulate Iron Homeostasis in *Caenorhabditis elegans*. PLoS Genet 8:e1002498. doi: 10.1371/journal.pgen.1002498

Ahearn IM, Haigis K, Bar-Sagi D, Philips MR (2011) Regulating the regulator: post-translational modification of RAS. Nat Rev Mol Cell Biol 13:39–51. doi: 10.1182/blood-2006-05-024752

Almasy L, Blangero J (2008) Human QTL linkage mapping. Genetica 136:333–340. doi: 10.1007/s10709-008-9305-3

Altun ZF, Hall DH (2009) Hermaphrodite Introduction. WormAtlas.

Ambros V (1999) Cell-cycle regulation of NOTCH signaling during *C. elegans* vulval development. Development 126:1947–1956.

Amit S (2002) Axin-mediated CKI phosphorylation of beta-catenin at Ser 45: a molecular switch for the Wnt pathway. Genes & Development 16:1066–1076. doi: 10.1101/gad.230302

Andersen EC, Shimko TC, Crissman JR, et al (2015) A Powerful New Quantitative Genetics Platform, Combining *Caenorhabditis elegans* High-Throughput Fitness Assays with a Large Collection of Recombinant Strains. G3: Genes, Genomes, Genetics 5:911–920. doi: 10.1534/g3.115.017178

Aroian RV, Sternberg PW (1991) Multiple functions of *let-23*, a *Caenorhabditis elegans* receptor tyrosine kinase gene required for vulval induction. Genetics 128:251–267.

Arribere JA, Bell RT, Fu BXH, et al (2014) Efficient marker-free recovery of custom genetic modifications with CRISPR/Cas9 in *Caenorhabditis elegans*. Genetics 198:837–846. doi: 10.1534/genetics.114.169730

Artavanis-Tsakonas S (1999) Notch Signaling: Cell Fate Control and Signal Integration in Development. Science 284:770–776. doi:10.1126/science.284.5415.770

Artavanis-Tsakonas S, Matsuno K, Fortini M (1995) Notch signaling. Science 268:225–232. doi: 10.1126/science.7716513

Artimo P, Jonnalagedda M, Arnold K, et al (2012) ExPASy: SIB bioinformatics resource portal. Nucleic Acids Res 40:W597–W603. doi: 10.1093/nar/gks400

Axelrod JD (2009) Progress and challenges in understanding planar cell polarity signaling. Semin Cell Dev Biol 20:964–971. doi: 10.1016/j.semcdb.2009.08.001

Ayyadevara S, Ayyadevara R, Vertino A, et al (2003) Genetic Loci Modulating Fitness and Life Span in *Caenorhabditis elegans*: Categorical Trait Interval Mapping in CL2a × Bergerac-BO Recombinant-Inbred Worms. Genetics 163:557–570.

Banasiak KJ, Xia Y, Haddad GG (2000) Mechanisms underlying hypoxia-induced neuronal apoptosis. Prog Neurobiol 62:215–249.

Barach AL, Bickerman HA (1954) The effect of anoxia on tumor growth with special reference to sarcoma 180 implanted in C57 mice. Cancer Res 14:672–676.

Barontini M, Dahia PLM (2010) VHL disease. Best Pract Res Clin Endocrinol Metab 24:401–413. doi: 10.1016/j.beem.2010.01.002

Battu G, Hoier EF, Hajnal A (2003) The *C. elegans* G-protein-coupled receptor SRA-13 inhibits RAS/MAPK signalling during olfaction and vulval development. Development 130:2567–2577. doi: 10.1242/dev.00497

Bauer A, Tronche F, Wessely O, et al (1999) The glucocorticoid receptor is required for stress erythropoiesis. Genes & Development 13:2996–3002.

Bänziger C, Soldini D, Schütt C, et al (2006) Wntless, a conserved membrane protein dedicated to the secretion of Wnt proteins from signaling cells. Cell 125:509–522. doi: 10.1016/j.cell.2006.02.049

Beck I, Ramirez S, Weinmann R, Caro J (1991) Enhancer element at the 3[prime]-flanking region controls transcriptional response to hypoxia in the human erythropoietin gene. J Biol Chem 266:15563–15566.

Beitel GJ, Clark SG, Horvitz HR (1990) *Caenorhabditis elegans ras* gene *let-60* acts as a switch in the pathway of vulval induction. Nature 348:503–509. doi: 10.1038/348503a0

Beitel GJ, Tuck S, Greenwald I, Horvitz HR (1995) The *Caenorhabditis elegans* gene *lin-1* encodes an ETS-domain protein and defines a branch of the vulval induction pathway. Genes & Development 9:3149–3162. doi: 10.1101/gad.9.24.3149

Berra E, Beniziri E, Ginouvès A, et al (2003) HIF prolyl-hydroxylase 2 is the key oxygen sensor setting low steady-state levels of HIF-1 in normoxia. EMBO J 22:4082–4090. doi: 10.1093/emboj/cdg392

Berra E, Milanini J, Richard DE, et al (2000) Signaling angiogenesis via p42/p44 MAP kinase and hypoxia. Biochem Pharmacol 60:1171–1178.

Berset T, Hoier EF, Battu G, et al (2001) Notch inhibition of RAS signaling through MAP kinase phosphatase LIP-1 during *C. elegans* vulval development. Science 291:1055–1058. doi: 10.1126/science.1055642

Beukers W, Zwarthoff EC, Hercegovac A (2014) HRAS mutations in bladder cancer at an early age and the possible association with the Costello Syndrome. European Journal of Human Genetics 22:837. doi: 10.1038/ejhg.2013.251

Birner P (2000) Overexpression of hypoxia-inducible factor 1[alpha] is a marker for an unfavorable prognosis in early-stage invasive cervical cancer. Cancer Res 60:4693–4696.

Birner P, Schindl M, Obermair A, et al (2001) Expression of hypoxia-inducible factor 1[alpha] in epithelial ovarian tumors: its impact on prognosis and on response to chemotherapy. Clin Cancer Res 7:1661–1668.

Bishop T, Lau KW, Epstein ACR, et al (2004) Genetic Analysis of Pathways Regulated by the von Hippel-Lindau Tumor Suppressor in *Caenorhabditis elegans*. PLoS Biol 2:e289. doi: 10.1371/journal.pbio.0020289

Bivona TG, Quatela SE, Bodemann BO, et al (2006) PKC regulates a farnesyl-electrostatic switch on K-Ras

that promotes its association with Bcl-XL on mitochondria and induces apoptosis. Mol Cell 21:481–493. doi: 10.1016/j.molcel.2006.01.012

Blais JD, Addison CL, Edge R, et al (2006) Perk-Dependent Translational Regulation Promotes Tumor Cell Adaptation and Angiogenesis in Response to Hypoxic Stress. Molecular and Cellular Biology 26:9517–9532. doi: 10.1128/MCB.01145-06

Blumenson LE, Bross ID (1976) A possible mechanism for enhancement of increased production of tumor angiogenic factor. Growth 40:205–209.

Bos R, Zhong H, Hanrahan CF, et al (2001) Levels of Hypoxia-Inducible Factor-1 During Breast Carcinogenesis. JNCI Journal of the National Cancer Institute 93:309–314. doi: 10.1093/jnci/93.4.309

Bovill EG, van der Vliet A (2011) Venous Valvular Stasis–Associated Hypoxia and Thrombosis: What Is the Link? Annu. Rev. Physiol. 73:527-45. doi: 10.1146/annurev-physiol-012110-142305

Bowerman B, Meneghini MD, Ishitani T, et al (1999) MAP kinase and Wnt pathways converge to downregulate an HMG-domain repressor in *Caenorhabditis elegans*. Nature 399:793–797. doi: 10.1038/21666

Boyden LM, Mao J, Belsky J, et al (2002) High Bone Density Due to a Mutation in LDL-Receptor–Related Protein 5. N Engl J Med 346:1513–1521. doi: 10.1056/NEJMoa013444

Bray PJ, Cotton RGH (2003) Variations of the human glucocorticoid receptor gene (NR3C1): Pathological and in vitro mutations and polymorphisms. Human Mutation 21:557–568. doi: 10.1136/bmj.319.7221.1337

Bray SJ (2006) Notch signalling: a simple pathway becomes complex. Nat Rev Mol Cell Biol 7:678–689. doi: 10.1016/S1534-5807(04)00097-8

Breitlin R, Li Y, Tesson BM, et al (2008) Genetical Genomics: Spotlight on QTL Hotspots. PLoS Genet. doi: 10.1371/journal.pgen.1000232

Brenner S (1974) THE GENETICS OF *CAENORHABDITIS ELEGANS*. Genetics 77:71–94.

Brizel DM (1996) Tumor oxygenation predicts for the likelihood of distant metastases in human soft tissue sarcoma. Cancer Res 56:941–943.

Brou C, Logeat F, Gupta N, et al (2000) A novel proteolytic cleavage involved in Notch signaling: the role of the disintegrin-metalloprotease TACE. Mol Cell 5:207–216.

Bruick RK (2001) A Conserved Family of Prolyl-4-Hydroxylases That Modify HIF. Science 294:1337–1340. doi: 10.1126/science.1066373

Bruinsma JJ, Jirakulaporn T, Muslin AJ, Kornfeld K (2002) Zinc ions and cation diffusion facilitator proteins regulate Ras-mediated signaling. Developmental Cell 2:567–578.

Brummer T, Naegele H, Reth M, Misawa Y (2003) Identification of novel ERK-mediated feedback phosphorylation sites at the C-terminus of B-Raf. Oncogene 22:8823–8834. doi: 10.1038/sj.onc.1207185

Budde MW, Roth MB (2010) Hydrogen Sulfide Increases Hypoxia-inducible Factor-1 Activity Independently of von Hippel-Lindau Tumor Suppressor-1 in *C. elegans*. Molecular Biology of the Cell 21:212–217. doi: 10.1091/mbc.E09-03-0199

Burdine RD, Branda CS, Stern MJ (1998) EGL-17(FGF) expression coordinates the attraction of the migrating sex myoblasts with vulval induction in *C. elegans*. Development 125:1083–1093.

Bülow HE, Boulin T, hobert O (2004) Differential functions of the C. elegans FGF receptor in axon outgrowth and maintenance of axon position. Neuron 42:367–374.

Caberoy NB, Welch RD, Jakobsen JS, et al (2003) Global Mutational Analysis of NtrC-Like Activators in *Myxococcus xanthus*: Identifying Activator Mutants Defective for Motility and Fruiting Body Development. Journal of Bacteriology 185:6083–6094. doi: 10.1128/JB.185.20.6083-6094.2003

Cabral-Teixeira J, Martinez-Fernandez A, Cai W, et al (2015) Cholesterol-derived glucocorticoids control early fate specification in embryonic stem cells. Stem Cell Research 15:88–95. doi: 10.1016/j.scr.2015.04.010

Cadigan KM, Fish MP, Rulifson EJ, Nusse R (1998) Wingless repression of *Drosophila* frizzled 2 expression shapes the Wingless morphogen gradient in the wing. Cell 93:767–777.

Cairns RA, Hill RP (2004) Acute Hypoxia Enhances Spontaneous Lymph Node Metastasis in an Orthotopic Murine Model of Human Cervical Carcinoma. Cancer Research 64:2054–2061. doi: 10.1158/0008-5472.CAN-03-3196

Campos-Ortega JA (1994) Cellular interactions in the developing nervous system of *Drosophila*. Cell 77:969–975.

Cha DS, Datla US, Hollis SE, et al (2012) The Ras-ERK MAPK regulatory network controls dedifferentiation in *Caenorhabditis elegans* germline. Biochim Biophys Acta 1823:1847–1855. doi: 10.1016/j.bbamcr.2012.07.006

Chan N, Koritzinsky M, Zhao H, et al (2008) Chronic Hypoxia Decreases Synthesis of Homologous Recombination Proteins to Offset Chemoresistance and Radioresistance. Cancer Research 68:605–614. doi: 10.1158/0008-5472.CAN-07-5472

Chan N, Milosevic M, Bristow RG (2007) Tumor hypoxia, DNA repair and prostate cancer progression: new targets and new therapies. Future Oncology 3:329–341. doi: 10.1158/0008-5472.CAN-05-0729

Chandra A, Grecco HE, Pisupati V, et al (2011) The GDI-like solubilizing factor PDEδ sustains the spatial organization and signalling of Ras family proteins. Nat Cell Biol 14:148–158. doi: 10.1364/OE.17.006493

Chang C, Hopper NA, Sternberg PW (2000) *Caenorhabditis elegans* SOS-1 is necessary for multiple RAS-mediated developmental signals. EMBO J 19:3283–3294. doi: 10.1093/emboj/19.13.3283

Chang C, Newman AP, Sternberg PW (1999) Reciprocal EGF signaling back to the uterus from the induced *C. elegans* vulva coordinates morphogenesis of epithelia. Curr Biol 9:237–246.

Chao MY, Larkins-Ford J, Tucey TM, Hart AC (2005) *lin-12* Notch functions in the adult nervous system of *C. elegans*. BMC Neuroscience 2005 6:1 6:45. doi: 10.1186/1471-2202-6-45

Chaplin DJ, Durand RE, Olive PL (1986) Acute hypoxia in tumors: implications for modifiers of radiation effects. Int J Radiat Oncol Biol Phys 12:1279–1282.

Chaudary N, Hill RP (2007) Hypoxia and Metastasis. Clinical Cancer Research 13:1947–1949. doi: 10.1158/1078-0432.CCR-06-2971

Chen C, Pore N, Behrooz A, et al (2001) Regulation of *glut1* mRNA by Hypoxia-inducible Factor-1. J Biol Chem 276:9519–9525. doi: 10.1074/jbc.270.43.25915

Chen N, Greenwald I (2004) The lateral signal for LIN-12/Notch in *C. elegans* vulval development comprises redundant secreted and transmembrane DSL proteins. Developmental Cell 6:183–192.

Chen RH, Sarnecki C, Blenis J (1992) Nuclear localization and regulation of *erk*- and *rsk*-encoded protein kinases. Molecular and Cellular Biology 12:915–927. doi: 10.1128/MCB.12.3.915

Cherfils J, Zeghouf M (2013) Regulation of Small GTPases by GEFs, GAPs, and GDIs. Physiological Reviews 93:269–309. doi: 10.1152/physrev.00003.2012

Choi SH, Wales TE, Nam Y, et al (2012) Conformational locking upon cooperative assembly of *notch* transcription complexes. Structure 20:340–349. doi: 10.1016/j.str.2011.12.011

Christodoulides C, Scarda A, Granzotto M, et al (2006) *WNT10B* mutations in human obesity. Diabetologia 49:678–684. doi: 10.1007/s00125-006-0144-4

Chujo T, Suzuki T (2012) Trmt61B is a methyltransferase responsible for 1-methyladenosine at position 58 of human mitochondrial tRNAs. RNA 18:2269–2276. doi: 10.1261/rna.035600.112

Chung C-M, Lin T-H, Chen J-W, et al (2014) Common quantitative trait locus downstream of *RETN* gene identified by genome-wide association study is associated with risk of type 2 diabetes mellitus in Han Chinese: a Mendelian randomization effect. Diabetes Metab Res Rev 30:232–240. doi: 10.1371/journal.pone.0009718

Church DL, Guan KL, Lambie EJ (1995) Three genes of the MAP kinase cascade, *mek-2, mpk-1/sur-1* and *let-60 ras*, are required for meiotic cell cycle progression in *Caenorhabditis elegans*. Development 121:2525–2535.

Church DL, Lambie EJ (2003) The Promotion of Gonadal Cell Divisions by the *Caenorhabditis elegans* TRPM Cation Channel GON-2 Is Antagonized by GEM-4 Copine. Genetics 165:563–574.

Clandinin TR, Katz WS, Sternberg PW (1997) *Caenorhabditis elegans HOM-C* genes regulate the response of vulval precursor cells to inductive signal. Developmental Biology 182:150–161. doi: 10.1006/dbio.1996.8471

Clark SG, Chisholm AD, Horvitz HR (1993) Control of cell fates in the central body region of *C. elegans* by the homeobox gene *lin-39.* Cell 74:43–55. doi: 10.1016/0092-8674(93)90293-Y

Clark SG, Lu X, Horvitz HR (1994) The *Caenorhabditis elegans* locus *lin-15*, a negative regulator of a tyrosine kinase signaling pathway, encodes two different proteins. Genetics 137:987–997.

Clark SG, Stern MJ, Horvritz HR (1992) *C. elegans* cell-signalling gene *sem-5* encodes a protein with SH2 and SH3 domains. Nature 356:340–344. doi: 10.1038/356340a0

Clark-Lewis I, Sanghera JS, Pelech SL (1991) Definition of a consensus sequence for peptide substrate recognition by p44 *mpk*, the meiosis-activated myelin basic protein kinase. J Biol Chem 266:15180–15184.

Clevers H, Nusse R (2012) Wnt/β-catenin signaling and disease. Cell 149:1192–1205. doi: 10.1016/j.cell.2012.05.012

Cliffe A, Hamada F, Bienz M (2003) A role of Dishevelled in relocating Axin to the plasma membrane during wingless signaling. Curr Biol 13:960–966.

Clifford SC, Walsh S, Hewson K, et al (1999) Genomic organization and chromosomal localization of the human *CUL2* gene and the role of von Hippel-Lindau tumor suppressor-binding protein (CUL2 and VBP1) mutation and loss in renal-cell carcinoma development. Genes, Chromosomes and Cancer 26:20–28. doi: 10.1016/S0344-0338(86)80001-2

Coffman CR, Skoglund P, Harris WA, Kintner CR (1993) Expression of an extracellular deletion of Xotch diverts cell fate in Xenopus embryos. Cell 73:659–671.

Collard BCY, Jahufer MZZ, Brouwer JB, Pang ECK (2005) An introduction to markers, quantitative trait loci (QTL) mapping and marker-assisted selection for crop improvement: The basic concepts. Euphytica 142:169–196.

Comerford KM (2002) Hypoxia-inducible factor-1-dependent regulation of the multidrug resistance (*MDR1*) gene. Cancer Res 62:3387–3394.

Corsi AK, Brodigan TM, Jorgensen EM, Krause M (2002) Characterization of a dominant negative *C. elegans* Twist mutant protein with implications for human Saethre-Chotzen syndrome. Development 129:2761–2772.

Coudreuse DYM, Roël G, Betist, M C, Destrée O, Korswagen, H C (2006) Wnt Gradient Formation Requires Retromer Function in Wnt-Producing Cells. Science 312:921–924. doi: 10.1126/science.1124856

Cox AD, Der CJ (2014) Ras history. Small GTPases 1:2–27. doi: 10.1016/j.tcb.2004.09.014

Crews C, Alessandrini A, Erikson R (1992) The primary structure of MEK, a protein kinase that phosphorylates the ERK gene product. Science 258:478–480. doi: 10.1126/science.1411546

Crittenden SL, Eckmann CR, Wang L, et al (2003) Regulation of the mitosis/meiosis decision in the *Caenorhabditis elegans* germline. Philos Trans R Soc Lond, B, Biol Sci 358:1359–1362. doi: 10.1098/rstb.2003.1333

Crosnier C, Stamataki D, Lewis J (2006) Organizing cell renewal in the intestine: stem cells, signals and combinatorial control. Nat Rev Genet 7:349–59. doi: 10.1038/nrg1840

D'Souza B, Miyamoto A, Weinmaster G (2008) The many facets of Notch ligands. Oncogene 27:5148–5167. doi: doi:10.1038/onc.2008.229

Dang LH, Bettegowda C, Huso DL, et al (2001) Combination bacteriolytic therapy for the treatment of experimental tumors. Proceedings of the National Academy of Sciences 98:15155–15160. doi: 10.1053/sonc.2001.20744

Daniels SE, Bhattacharrya S, James A, et al (1996) A genome-wide search for quantitative trait loci underlying asthma. Nature 383:247–250. doi: 10.1038/383247a0

Darby C, Cosma CL, Thomas JH, Manoil C (1999) Lethal paralysis of *Caenorhabditis elegans* by *Pseudomonas aeruginosa*. Proc Natl Acad Sci USA 96:15202–15207. doi: 10.1139/y94-106

DasGupta R, Fuchs E (1999) Multiple roles for activated LEF/TCF transcription complexes during hair follicle development and differentiation. Development 126:4557–4568. doi: 10.1002/bdra.20705

Davidson IC, Sanger C, Thomlinson RH (1955) HIGH-PRESSURE OXYGEN AND RADIOTHERAPY. The Lancet 265:1091–1095. doi: 10.1016/S0140-6736(55)90589-4

de Bono M, Bargmann CI (1998) Natural variation in a neuropeptide Y receptor homolog modifies social behavior and food response in *C. elegans*. Cell 94:679–689.

de la Cova C, Greenwald I (2012) SEL-10/Fbw7-dependent negative feedback regulation of LIN-45/Braf signaling in *C. elegans* via a conserved phosphodegron. Genes & Development 26:2524. doi: 10.1101/gad.203703.112

de la Cova CA, Townley R, Regot S, Greenwald I (2017) A Real-Time Biosensor for ERK Activity Reveals Signaling Dynamics during *C. elegans* Cell Fate Specification. Developmental Cell 42:542–553.e4. doi: 10.1016/j.devcel.2017.07.014

Deng X, Ruvolo P, Carr B, May WS (2000) Survival function of ERK1/2 as IL-3-activated, staurosporine-resistant Bcl2 kinases. Proc Natl Acad Sci USA 97:1578–1583.

Denko NC (2008) Hypoxia, HIF1 and glucose metabolism in the solid tumour. Nat Rev Cancer 8:705–713. doi: 10.4161/cc.5.8.2681

Deschner EE, Gray LH (1959) Influence of Oxygen Tension on X-Ray-Induced Chromosomal Damage in Ehrlich Ascites Tumor Cells Irradiated *in Vitro* and *in Vivo*. Radiation Research 11:115. doi: 10.2307/3570739

DeVore DL, Horvitz HR, Stern MJ (1995) An FGF receptor signaling pathway is required for the normal cell migrations of the sex myoblasts in *C. elegans* hermaphrodites. Cell 83:611–620.

Dewhirst MW, Cao Y, Moeller B (2008) Cycling hypoxia and free radicals regulate angiogenesis and radiotherapy response. Nat Rev Cancer 8:425–437. doi: 10.1016/j.ijrobp.2007.01.071

Dickinson DJ, Pani AM, Heppert JK, et al (2015) Streamlined Genome Engineering with a Self-Excising Drug Selection Cassette. Genetics 200:1035–1049. doi: 10.1534/genetics.115.178335

Diogon M, Wissler F, Quintin S, et al (2007) The RhoGAP RGA-2 and LET-502/ROCK achieve a balance of actomyosin-dependent forces in *C. elegans* epidermis to control morphogenesis. Development 134:2469–2479. doi: 10.1242/dev.005074

Doench JG, Hartenian E, Graham DB, et al (2014) Rational design of highly active sgRNAs for CRISPR-Cas9 mediated gene inactivation. Nat Biotechnol 32:1262–1267. doi: 10.1073/pnas.0506580102

Doherty D, Feger G, Younger-Shepherd S, et al (1996) Delta is a ventral to dorsal signal complementary to Serrate, another Notch ligand, in *Drosophila* wing formation. Genes & Development 10:421–434.

Donnelly P (2008) Progress and challenges in genome-wide association studies in humans. Nature 456:728–731. doi: 10.1038/nature07631

Doroszuk A, Snoek LB, Fradin E, et al (2009) A genome-wide library of CB4856/N2 introgression lines of *Caenorhabditis elegans*. Nucleic Acids Res 37:e110–e110. doi: 10.1093/nar/gkp528

Downward J (2003) Targeting RAS signalling pathways in cancer therapy. Nat Rev Cancer 3:11–22. doi: 10.1038/nrc969

Edwards AC, Mackay TFC (2009) Quantitative trait loci for aggressive behavior in *Drosophila melanogaster*. Genetics 182:889–897. doi:10.1534/genetics.109.101691

Eichler EE, Flint J, Gibson G, et al (2010) Missing heritability and strategies for finding the underlying causes of complex disease. Nat Rev Genet 11:446–450. doi: 10.1038/nrg2809

Eisenmann DM, Kim SK (1997) Mechanism of Activation of the *Caenorhabditis Elegans Ras* Homologue *let-60* by a Novel, Temperature-Sensitive, Gain-of-Function Mutation. Genetics 146:553–565.

Eisenmann DM, Kim SK (2000) Protruding vulva mutants identify novel loci and Wnt signaling factors that function during *Caenorhabditis elegans* vulva development. Genetics 156:1097.

Eisenmann DM, Maloof JN, Simske JS, et al (1998) The beta-catenin homolog BAR-1 and LET-60 Ras coordinately regulate the Hox gene *lin-39* during *Caenorhabditis elegans* vulval development. Development 125:3667–3680.

Ellisen LW, Bird J, West DC, et al (1991) TAN-1, the human homolog of the *Drosophila notch* gene, is broken by chromosomal translocations in T lymphoblastic neoplasms. Cell 66:649–661.

Eltzschig HK, Carmeliet P (2011) Hypoxia and Inflammation. N Engl J Med 364:656–665. doi: 10.1056/NEJMra0910283

Elvidge GP, Glenny L, Appelhoff RJ, et al (2006) Concordant Regulation of Gene Expression by Hypoxia and 2-Oxoglutarate-dependent Dioxygenase Inhibition. J Biol Chem 281:15215–15226. doi: 10.1128/MCB.22.21.7405-7416.2002

Epstein ACR, Gleadle JM, McNeill LA, et al (2001) *C. elegans* EGL-9 and Mammalian Homologs Define a Family of Dioxygenases that Regulate HIF by Prolyl Hydroxylation. Cell 107:43–54. doi: 10.1016/S0092-8674(01)00507-4

Espinosa L, Inglés-Esteve J, Aguilera C, Bigas A (2003) Phosphorylation by Glycogen Synthase Kinase-3β Down-regulates Notch Activity, a Link for Notch and Wnt Pathways. J Biol Chem 278:32227–32235. doi: 10.1074/jbc.275.13.9099

Farmer SR (2005) Regulation of PPARγ activity during adipogenesis. Int J Obes Relat Metab Disord 29:S13–S16. doi: 10.1038/sj.ijo.0802907

Fehon RG, Kooh PJ, Rebay I, et al (1990) Molecular interactions between the protein products of the neurogenic loci *Notch* and *Delta*, two *EGF*-homologous genes in *Drosophila*. Cell 61:523–534.

Ferdinand P, Roffe C (2016) Hypoxia after stroke: a review of experimental and clinical evidence. Exp & Trans Stroke Med 8:1213. doi: 10.1186/1745-6215-15-99

Ferguson EL, Horvitz HR (1989) The multivulva phenotype of certain *Caenorhabditis elegans* mutants results from defects in two functionally redundant pathways. Genetics 123:109–121.

Ferguson EL, Sternberg PW, Horvitz HR (1987) A genetic pathway for the specification of the vulval cell lineages of *Caenorhabditis elegans*. Nature 326:259–267. doi: 10.1038/326259a0

Fernandez-Medarde A, Santos E (2011) Ras in Cancer and Developmental Diseases. Genes & Cancer 2:344–358. doi: 10.1177/1947601911411084

Félix M-A, Barkoulas M (2012) Robustness and flexibility in nematode vulva development. Trends Genet 28:185–195. doi: 10.1016/j.tig.2012.01.002

Fisher RA (1918) XV.—The Correlation between Relatives on the Supposition of Mendelian Inheritance. Trans R Soc Edinb 52:399–433. doi: 10.1017/S0080456800012163

Fitzgerald K, Greenwald I (1995) Interchangeability of *Caenorhabditis elegans* DSL proteins and intrinsic signalling activity of their extracellular domains *in vivo*. Development 121:4275–4282.

Fitzgerald K, Wilkinson HA, Greenwald I (1993) *glp-1* can substitute for *lin-12* in specifying cell fate decisions in *Caenorhabditis elegans*. Development 119:1019–1027.

Folg DG, Bradley TJ (2005) Adaptive Evolution in the Lab: Unique Phenotypes in Fruit Flies Comprise a Fertile Field of Study. Integrative and Comparative Biology 45:492–499. doi: 10.1093/icb/45.3.492

Forbes SA, Bindal N, Bamford S, et al (2010) COSMIC: mining complete cancer genomes in the Catalogue of Somatic Mutations in Cancer. Nucleic Acids Res 39:D945–D950. doi: 10.1093/nar/gkq929

Friedland AE, Tzur YB, Esvelt KM, et al (2013) Heritable genome editing in *C. elegans* via a CRISPR-Cas9 system. Nat Methods 10:741–743. doi: 10.1007/978-1-59745-202-1_10

Frise E, Knoblich JA, Younger-Shepherd S, et al (1996) The *Drosophila* Numb protein inhibits signaling of the Notch receptor during cell-cell interaction in sensory organ lineage. Proc Natl Acad Sci USA 93:11925–11932.

Fritz RD, Letzelter M, Reimann A, et al (2013) A Versatile Toolkit to Produce Sensitive FRET Biosensors to Visualize Signaling in Time and Space. Sci Signal 6:rs12–rs12. doi: 10.1016/j.jneumeth.2006.05.017

Frödin M, Gammeltoft S (1999) Role and regulation of 90 kDa ribosomal S6 kinase (RSK) in signal transduction. Mol Cell Endocrinol 151:65–77.

Frøkjær-Jensen C, Wayne Davis M, Hopkins CE, et al (2008) Single-copy insertion of transgenes in *Caenorhabditis elegans*. Nat Genet 40:1375–1383. doi: 10.1128/MCB.5.12.3484

Gaietta G, Deerinck TJ, Adams SR, et al (2002) Multicolor and Electron Microscopic Imaging of Connexin Trafficking. Science 296:503–507. doi: 10.1126/science.1068793

Gaietta GM, Giepmans BNG, Deerinck TJ, et al (2006) Golgi twins in late mitosis revealed by genetically encoded tags for live cell imaging and correlated electron microscopy. Proc Natl Acad Sci USA 103:17777–17782. doi: 10.1126/science.1057330

Gallahan D, Callahan R (1987) Mammary tumorigenesis in feral mice: identification of a new int locus in mouse mammary tumor virus (Czech II)-induced mammary tumors. Journal of Virology 61:66–74.

Galli S, Jahn O, Hitt R, et al (2009) A new paradigm for MAPK: structural interactions of hERK1 with mitochondria in HeLa cells. PLoS ONE 4:e7541. doi: 10.1371/journal.pone.0007541

Gao S, Christensen S, Kimble J, Henderson ST (1997) Functional domains of LAG-2, a putative signaling ligand for LIN-12 and GLP-1 receptors in *Caenorhabditis elegans*. Molecular Biology of the Cell 8:1751.

Gasch AP, Payseur BA, Pool JE (2016) The Power of Natural Variation for Model Organism Biology. Trends in Genetics 32:147–154. doi: 10.1016/j.tig.2015.12.003

Ghosh R, Andersen EC, Shapiro JA, et al (2012) Natural Variation in a Chloride Channel Subunit Confers Avermectin Resistance in *C. elegans*. Science 335:574–578. doi: 10.1534/genetics.107.080101

Giaccia A, Siim BG, Johnson RS (2003) HIF-1 as a target for drug development. Nat Rev Drug Discov 2:803–811. doi: 10.1038/nrd1199

Giepmans BNG, Adams SR, Ellisman MH, Tsien RY (2006) The Fluorescent Toolbox for Assessing Protein Location and Function. Science 312:217–224. doi: 10.1126/science.1124618

Giles RH, van Es JH, Clevers H (2003) Caught up in a Wnt storm: Wnt signaling in cancer. Biochim Biophys Acta 1653:1–24.

Glading A, Chang P, Lauffenburger DA, Wells A (2000) Epidermal Growth Factor Receptor Activation of Calpain Is Required for Fibroblast Motility and Occurs via an ERK/MAP Kinase Signaling Pathway. J Biol Chem 275:2390–2398. doi: 10.1074/jbc.275.4.2390

Gleadle J, Ratcliffe P (2001) Hypoxia. John Wiley & Sons, Ltd, Chichester

Gleason JE, korswagen HC, Eisenmann DM (2002) Activation of Wnt signaling bypasses the requirement for RTK/Ras signaling during *C. elegans* vulval induction. Genes & Development 16:1281–1290. doi: 10.1101/gad.981602

Gleason JE, Szyleyko EA, Eisenmann DM (2006) Multiple redundant Wnt signaling components function in two processes during *C. elegans* vulval development. Developmental Biology 298:442–457. doi: 10.1016/j.ydbio.2006.06.050

Goldberg M, Dunning S, Bunn H (1988) Regulation of the erythropoietin gene: evidence that the oxygen sensor is a heme protein. Science 242:1412–1415. doi: 10.1126/science.2849206

Golden J, Riddle D (1982) A pheromone influences larval development in the nematode *Caenorhabditis elegans*. Science 218:578–580. doi: 10.1126/science.6896933

Gomez-Amaro RL, Valentine ER, Carretero M, et al (2015) Measuring Food Intake and Nutrient Absorption in *Caenorhabditis elegans*. Genetics 200:443–454. doi: 10.1534/genetics.115.175851

Gong Y, Slee RB, Fukai N, et al (2001) LDL receptor-related protein 5 (LRP5) affects bone accrual and eye development. Cell 107:513–523.

Gorres KL, Raines RT (2010) Prolyl 4-hydroxylase. Critical Reviews in Biochemistry and Molecular Biology 45:106–124. doi: 10.1111/j.1365-313X.2004.02279.x

Gort EH, van Haaften G, Verlaan I, et al (2007) The TWIST1 oncogene is a direct target of hypoxia-inducible factor-2α. Oncogene 27:1501–1510. doi: 10.1038/sj.onc.1210795

Gómez-Orte E, Sáenz-Narciso B, Moreno S, Cabello J (2013) Multiple functions of the noncanonical Wnt pathway. Trends Genet 29:545–553. doi: 10.1016/j.tig.2013.06.003

Graeber TG (1994) Hypoxia induces accumulation of p53 protein, but activation of a G1-phase checkpoint by low-oxygen conditions is independent of p53 status. Mol Cell Biol 14:6264–6277.

Graeber TG, Osmanian C, Jacks T, et al (1996) Hypoxia-mediated selection of cells with diminished apoptotic potential in solid tumours. Nature 379:88–91. doi: 10.1038/379088a0

Grant K, Hanna-Rose W, Han M (2000) *sem-4* Promotes Vulval Cell-Fate Determination in *Caenorhabditis elegans* through Regulation of *lin-39* Hox. Developmental Biology 224:496–506. doi: 10.1006/dbio.2000.9774

Gray LH, Conger AD, Ebert M, et al (1953) The concentration of oxygen dissolved in tissues at the time of irradiation as a factor in radiotherapy. Br J Radiol 26:638–648.

Green JL, Inoue T, Sternberg PW (2008) Opposing Wnt Pathways Orient Cell Polarity during Organogenesis. Cell 134:646–656. doi: 10.1016/j.cell.2008.06.026

Green JWM, Snoek LB, Kammenga JE, Harvey SC (2013) Genetic mapping of variation in dauer larvae development in growing populations of *Caenorhabditis elegans*. Heredity 111:306–313. doi: 10.1534/g3.112.002212

Greenwald I (1994) Structure/function studies of lin-12/Notch proteins. Curr Opin Genet Dev 4:556–562.

Greenwald I, Seydoux G (1990) Analysis of gain-of-function mutations of the *lin-12* gene of *Caenorhabditis elegans*. Nature 346:197–199. doi: 10.1038/346197a0

Greenwald IS, Sternberg PW, Robert Horvitz H (1983) The *lin-12* locus specifies cell fates in *Caenorhabditis elegans*. Cell 34:435–444. doi: 10.1016/0092-8674(83)90377-X

Griffin BA, Adams SR, Tsien RY (1998) Specific Covalent Labeling of Recombinant Protein Molecules Inside Live Cells. Science 281:269–272. doi: 10.1126/science.281.5374.269

Gu Y, Hukriede NA, Fleming RJ (1995) Serrate expression can functionally replace Delta activity during neuroblast segregation in the *Drosophila* embryo. Development 121:855–865. doi: 10.1002/bdra.20705

Gumbiner BM (2000) Regulation of Cadherin Adhesive Activity. J Cell Biol 148:399–404. doi: 10.1083/jcb.144.2.351

Gutschner T, Baas M, Diederichs S (2011) Noncoding RNA gene silencing through genomic integration of RNA destabilizing elements using zinc finger nucleases. Genome Research 21:1944. doi: 10.1101/gr.122358.111

Haag A, Gutierrez P, Bühler A, et al (2014) An *In Vivo* EGF Receptor Localization Screen in *C. elegans* Identifies the Ezrin Homolog ERM-1 as a Temporal Regulator of Signaling. PLoS Genet 10:e1004341. doi: 10.1371/journal.pgen.1004341

Hajnal A, Whitfield CW, Kim SK (1997) Inhibition of *Caenorhabditis elegans* vulval induction by *gap-1* and by *let-23* receptor tyrosine kinase. Genes & Development 11:2715–2728.

Han M, Golden A, Han Y, Sternberg PW (1993) *C. elegans lin-45 raf* gene participates in *let-60 ras*-stimulated vulval differentiation. Nature 363:133–140. doi: 10.1038/363133a0

Han M, Sternberg PW (1990) *let-60*, a gene that specifies cell fates during *C. elegans* vulval induction, encodes a *ras* protein. Cell 63:921–931.

Hare GMT (2004) Anaemia and the brain. Curr Opin Anaesthesiol 17:363–369.

Harfe BD, Gomes AV, Kenyon C, et al (1998) Analysis of a *Caenorhabditis elegans* Twist homolog identifies conserved and divergent aspects of mesodermal patterning. Genes & Development 12:2623–2635. doi: 10.1101/gad.12.16.2623

Harris AL (2002) Hypoxia - a key regulatory factor in tumour growth. Nat Rev Cancer 2:38–47. doi: 10.1038/nrc704

Hart MJ, de los Santos R, Albert IN, et al (1998) Downregulation of beta-catenin by human Axin and its association with the APC tumor suppressor, beta-catenin and GSK3 beta. Curr Biol 8:573–581.

Harvey JJ (1964) An Unidentified Virus which causes the Rapid Production of Tumours in Mice. Nature 204:1104-1105.

He T (1998) Identification of c-MYC as a Target of the APC Pathway. Science 281:1509–1512. doi: 10.1126/science.281.5382.1509

Hedgecock EM, Culotti JG, Hall DH (1990) The *unc-5, unc-6,* and *unc-40* genes guide circumferential migrations of pioneer axons and mesodermal cells on the epidermis in *C. elegans.* Neuron 4:61–85.

Henderson ST, Gao D, Lambie EJ, Kimble J (1994) *lag-2* may encode a signaling ligand for the GLP-1 and LIN-12 receptors of *C. elegans*. Development 120:2913–2924. doi: 10.1002/bdra.20705

Herman MA, Vassilieva LL, Horvitz HR, et al (1995) The *C. elegans* gene *lin-44*, which controls the polarity of certain asymmetric cell divisions, encodes a Wnt protein and acts cell nonautonomously. Cell 83:101–110.

Herman R (2005) Introduction to sex determination. WormBook.

Hewitson KS, McNeill LA, Riordan MV, et al (2002) Hypoxia-inducible Factor (HIF) Asparagine Hydroxylase Is Identical to Factor Inhibiting HIF (FIH) and Is Related to the Cupin Structural Family. J Biol Chem 277:26351–26355. doi: 10.1021/bi016014e

Hill RJ, Sternberg PW (1992) The gene *lin-3* encodes an inductive signal for vulval development in *C. elegans.* Nature 358:470–476. doi: 10.1038/358470a0

Hill WG, Mulder HA (2011) Genetic analysis of environmental variation. Genet Res 92:381–395. doi: 10.1017/S0016672310000546

Hodgkin J (1993) Molecular cloning and duplication of the nematode sex-determining gene *tra-1*. Genetics 133:543–560.

Hodgkin J, Doniach T (1997) Natural Variation and Copulatory Plug Formation in *Caenorhabditis Elegans.* Genetics 146:149.

Hoffmann C, Gaietta G, Bünemann M, et al (2005) A FlAsH-based FRET approach to determine G protein–coupled receptor activation in living cells. Nat Methods 2:171–176. doi: 10.1074/jbc.C400302200

Hoffmann C, Gaietta G, Zürn A, et al (2010) Fluorescent labeling of tetracysteine-tagged proteins in intact cells. Nat Protoc 5:1666–1677. doi: 10.1038/nprot.2010.129

Holmquist-Mengelbier L, Fredlund E, Löfstedt T, et al (2006) Recruitment of HIF-1α and HIF-2α to common target genes is differentially regulated in neuroblastoma: HIF-2α promotes an aggressive phenotype. Cancer Cell 10:413–423. doi: 10.1016/j.ccr.2006.08.026

Hori K, Sen A, Artavanis-Tsakonas S (2013) Notch signaling at a glance. J Cell Sci 126:2135–2140. doi: 10.1242/jcs.127308

Horvitz H, Chalfie M, Trent C, et al (1982) Serotonin and octopamine in the nematode *Caenorhabditis elegans.* Science 216:1012–1014. doi: 10.1126/science.6805073

Horvitz HR, Ferguson EL (1985) Identification and Characterization of 22 Genes That Affect the Vulval Cell Lineages of the Nematode *Caenorhabditis elegans*. Genetics 110:17.

Hoskins R, Hajnal AF, Harp SA, Kim SK (1996) The *C. elegans* vulval induction gene *lin-2* encodes a member of the MAGUK family of cell junction proteins. Development 122:97–111.

Howard RM (2002) *C. elegans* EOR-1/PLZF and EOR-2 positively regulate Ras and Wnt signaling and function redundantly with LIN-25 and the SUR-2 Mediator component. Genes & Development 16:1815–1827. doi: 10.1101/gad.998402

Huang LE, Gu J, Schau M, Bunn HF (1998) Regulation of hypoxia-inducible factor 1 is mediated by an O_2-dependent degradation domain via the ubiquitin-proteasome pathway. Proceedings of the National Academy of Sciences 95:7987–7992. doi: 10.1074/jbc.271.44.27280

Huang LS, Tzou P, Sternberg PW (1994) The *lin-15* locus encodes two negative regulators of *Caenorhabditis elegans* vulval development. Molecular Biology of the Cell 5:395–411.

Huang P, Senga T, Hamaguchi M (2007) A novel role of phospho-β-catenin in microtubule regrowth at centrosome. Oncogene 26:4357–4371. doi: 10.1038/sj.onc.1210217

Huang Y, Wang KK (2001) The calpain family and human disease. Trends in Molecular Medicine 7:355–362.

Hubbard EJ, Wu G, Kitajewski J, Greenwald I (1997) *sel-10*, a negative regulator of *lin-12* activity in *Caenorhabditis elegans*, encodes a member of the CDC4 family of proteins. Genes & Development 11:3182–3193.

Huelsz-Prince G, van Zon JS (2017) Canalization of *C. elegans* Vulva Induction against Anatomical Variability. Cell Syst 4:219–230.e6. doi: 10.1016/j.cels.2017.01.009

Hultén LM, Levin M (2009) The role of hypoxia in atherosclerosis. Current Opinion in Lipidology 20:409–414. doi: 10.1097/MOL.0b013e3283307be8

Hwang BJ (2004) A cell-specific enhancer that specifies *lin-3* expression in the *C. elegans* anchor cell for vulval development. Development 131:143–151. doi: 10.1242/dev.00924

Iino Y, Hirotsu T, Saeki S, Yamamoto M (2000) The Ras-MAPK pathway is important for olfaction in *Caenorhabditis elegans*. Nature 404:289–293. doi: 10.1038/35005101

Illig T, Gieger C, Zhai G, et al (2009) A genome-wide perspective of genetic variation in human metabolism. Nat Genet 42:137–141. doi: 10.1038/ng.507

Inoue T, Oz HS, Wiland D, et al (2004) *C. elegans* LIN-18 Is a Ryk Ortholog and Functions in Parallel to LIN-17/Frizzled in Wnt Signaling. Cell 118:795–806. doi: 10.1016/j.cell.2004.09.001

Ivan M, Kondo K, Yang H, et al (2001) HIFalpha Targeted for VHL-Mediated Destruction by Proline Hydroxylation: Implications for O_2 Sensing. Science 292:464–468. doi: 10.1126/science.1059817

Ivanov I, Lo KC, Hawthorn L, et al (2006) Identifying candidate colon cancer tumor suppressor genes using inhibition of nonsense-mediated mRNA decay in colon cancer cells. Oncogene 26:2873–2884. doi: 10.1038/sj.onc.1210098

Jaakkola P, Mole DR, Tian YM, et al (2001) Targeting of HIF-alpha to the von Hippel-Lindau Ubiquitylation Complex by O_2-Regulated Prolyl Hydroxylation. Science 292:468–472. doi: 10.1126/science.1059796

Jaegal Shim PWSJL (2000) Distinct and Redundant Functions of μ1 Medium Chains of the AP-1 Clathrin-Associated Protein Complex in the Nematode *Caenorhabditis elegans*. Molecular Biology of the Cell 11:2743.

Jain S, Maltepe E, Lu MM, et al (1998) Expression of ARNT, ARNT2, HIF1α, HIF2α and Ah receptor mRNAs in the developing mouse. Mechanisms of Development 73:117–123. doi: 10.1016/S0925-4773(98)00038-0

Jansen RC, Nap JP (2001) Genetical genomics: the added value from segregation. Trends Genet 17:388–391.

Jiang B-H, Rue E, Wang GL, et al (1996) Dimerization, DNA Binding, and Transactivation Properties of Hypoxia-inducible Factor 1. J Biol Chem 271:17771–17778. doi: 10.1126/science.1470918

Jiang H, Guo R, Powell-Coffman JA (2001) The *Caenorhabditis elegans hif-1* gene encodes a bHLH-PAS protein that is required for adaptation to hypoxia. Proc Natl Acad Sci USA 98:7916–7921. doi: 10.1126/science.1059796

Jiang LI, Sternberg PW (1998) Interactions of EGF, Wnt and HOM-C genes specify the P12 neuroectoblast fate in *C. elegans*. Development 125:2337–2347.

Jinek M, Chylinski K, Fonfara I, et al (2012) A Programmable Dual-RNA–Guided DNA Endonuclease in Adaptive Bacterial Immunity. Science 337:816–821. doi: 10.1126/science.1225829

Johnson AD, Fitzsimmons D, Hagman J, Chamberlin HM (2001) EGL-38 Pax regulates the ovo-related gene *lin-48* during *Caenorhabditis elegans* organ development. Development 128:2857–2865.

Joshi I, Minter LM, Telfer J, et al (2009) Notch signaling mediates G1/S cell-cycle progression in T cells via cyclin D3 and its dependent kinases. Blood 113:1689–1698. doi: 10.1182/blood-2008-03-147967

Juo P, Harbaugh T, Garriga G, Kaplan JM (2007) CDK-5 Regulates the Abundance of GLR-1 Glutamate Receptors in the Ventral Cord of *Caenorhabditis elegans*. Molecular Biology of the Cell 18:3883–3893. doi: 10.1091/mbc.E06-09-0818

Jurgensen JS (2004) Persistent induction of HIF-1[alpha] and -2[alpha] in cardiomyocytes and stromal cells of ischemic myocardium. FASEB J 18:1415–1417.

Kadowaki T, Wilder E, Klingensmith J, et al (1996) The segment polarity gene *porcupine* encodes a putative multitransmembrane protein involved in Wingless processing. Genes & Development 10:3116–3128. doi: 10.1101/gad.10.24.3116

Kaech SM, Whitfield CW, Kim SK (1998) The LIN-2/LIN-7/LIN-10 complex mediates basolateral membrane localization of the *C. elegans* EGF receptor LET-23 in vulval epithelial cells. Cell 94:761–771.

Kamath RS, Fraser AG, Dong Y, et al (2003) Systematic functional analysis of the *Caenorhabditis elegans* genome using RNAi. Nature 421:231–237. doi: 10.1038/nature01278

Kanazawa A, Tsukada S, Sekine A, et al (2004) Association of the gene encoding wingless-type mammary tumor virus integration-site family member 5B (WNT5B) with type 2 diabetes. Am J Hum Genet 75:832–

843. doi: 10.1086/425340

Kato S, Endoh H, Masuhiro Y, et al (1995) Activation of the Estrogen Receptor Through Phosphorylation by Mitogen-Activated Protein Kinase. Science 270:1491–1494. doi: 10.1126/science.270.5241.1491

Katou T, Namise M, Kitagaki H, et al (2009) QTL mapping of sake brewing characteristics of yeast. J Biosci Bioeng 107:383–393. doi: 10.1016/j.jbiosc.2008.12.014

Katz WS, Hill RJ, Clandinin TR, Sternberg PW (1995) Different Levels of the *C. elegans* growth factor LIN-3 promote distinct vulval precursor fates. Cell 82:297–307. doi: 10.1016/0092-8674(95)90317-8

Katz WS, Lesa GM, Yannoukakos D, et al (1996) A point mutation in the extracellular domain activates LET-23, the *Caenorhabditis elegans* epidermal growth factor receptor homolog. Molecular and Cellular Biology 16:529–537.

Kemp PJ, Peers C (2007) Oxygen sensing by ion channels. Essays Biochem 43:77–90. doi: 10.1042/bse0430077

Kimble J, Simpson P (1997) THE LIN-12/Notch SIGNALING PATHWAY AND ITS REGULATION. Annu Rev Cell Dev Biol 13:333–361. doi: 10.1146/annurev.cellbio.13.1.333

Kimble JE, White JG (1981) On the control of germ cell development in *Caenorhabditis elegans*. Developmental Biology 81:208–219.

Kinzler K, Nilbert M, Su L, et al (1991) Identification of FAP locus genes from chromosome 5q21. Science 253:661–665. doi: 10.1126/science.1651562

Kinzler KW, Vogelstein B (1996) Lessons from hereditary colorectal cancer. Cell 87:159–170.

Kirsten WH, Mayer LA (1967) Morphologic responses to a murine erythroblastosis virus. J Natl Cancer Inst. 39:311-35.

Klein EA, Casey G, Silverman R (2006) Genetic susceptibility and oxidative stress in prostate cancer: Integrated model with implications for prevention. Urology 68:1145–1151. doi: 10.1016/j.urology.2006.08.1074

Klemke RL, Cai S, Giannini AL, et al (1997) Regulation of cell motility by mitogen-activated protein kinase. J Cell Biol 137:481–492.

Klose RJ, Kallin EM, Zhang Y (2006) JmjC-domain-containing proteins and histone demethylation. Nat Rev Genet 7:715–727. doi: 10.1128/MCB.19.11.7630

Koditz J, Nesper J, Wottawa M, et al (2007) Oxygen-dependent ATF-4 stability is mediated by the PHD3 oxygen sensor. Blood 110:3610–3617. doi: 10.1182/blood-2007-06-094441

Kolch W (2005) Coordinating ERK/MAPK signalling through scaffolds and inhibitors. Nat Rev Mol Cell Biol 6:827–837. doi: 10.1128/MMBR.68.2.320-344.2004

Kopan R, Ilagan MXG (2013) The Canonical Notch Signaling Pathway: Unfolding the Activation Mechanism. J Cell Sci 126:216–233. doi: 10.1242/jcs.127308

Koritzinsky M, Magagnin MG, van den Beucken T, et al (2006) Gene expression during acute and prolonged hypoxia is regulated by distinct mechanisms of translational control. EMBO J 25:1114–1125. doi: 10.1128/MCB.18.6.3112

Koritzinsky M, Seigneuric R, Magagnin MG, et al (2005) The hypoxic proteome is influenced by gene-specific changes in mRNA translation. Radiotherapy and Oncology 76:177–186. doi: 10.1016/j.radonc.2005.06.036

Kornfeld K (1997) Vulval development in *Caenorhabditis elegans*. Trends Genet 13:55–61.

Korswagen HC (2002) The Axin-like protein PRY-1 is a negative regulator of a canonical Wnt pathway in *C. elegans*. Genes & Development 16:1291–1302. doi: 10.1101/gad.981802

Korswagen HC, Herman MA, Clevers HC (2000) Distinct ß-catenins mediate adhesion and signalling functions in *C. elegans*. Nature 406:527–532. doi: 10.1038/35020099

Kottegoda S, Aoto PC, Sims CE, Allbritton NL (2008) Biarsenical−Tetracysteine Motif as a Fluorescent Tag for Detection in Capillary Electrophoresis. Anal Chem 80:5358–5366. doi: 10.1021/ac8003242

Koukourakis MI, Giatromanolaki A, Sivridis E, et al (2002) Hypoxia-inducible factor (HIF1A and HIF2A), angiogenesis, and chemoradiotherapy outcome of squamous cell head-and-neck cancer. International Journal of Radiation Oncology - Biology - Physics 53:1192–1202. doi: 10.1016/S0360-3016(02)02848-1

Koumenis C, Bi M, Ye J, et al (2007) Hypoxia and the unfolded protein response. Meth Enzymol 435:275–293. doi: 10.1016/S0076-6879(07)35014-3

Koumenis C, Naczki C, Koritzinsky M, et al (2002) Regulation of Protein Synthesis by Hypoxia via Activation of the Endoplasmic Reticulum Kinase PERK and Phosphorylation of the Translation Initiation Factor eIF2. Molecular and Cellular Biology 22:7405–7416. doi: 10.1128/MCB.22.21.7405-7416.2002

Kourembanas S, Marsden PA, McQuillan LP, Faller DV (1991) Hypoxia induces endothelin gene expression and secretion in cultured human endothelium. J Clin Invest 88:1054–1057. doi: 10.1172/JCI115367

Krishna RG, Wold F (1993) Post-Translational Modifications of Proteins. Methods In Protein Sequence Analysis 167–172. doi: 10.1007/978-1-4899-1603-7_21

Krstic MD, Rogatsky I, Yamamoto KR, Garabedian MJ (1997) Mitogen-activated and cyclin-dependent protein kinases selectively and differentially modulate transcriptional enhancement by the glucocorticoid receptor. Molecular and Cellular Biology 17:3947–3954.

Kumsta R, Moser D, Streit F, et al (2009) Characterization of a glucocorticoid receptor gene (GR, NR3C1) promoter polymorphism reveals functionality and extends a haplotype with putative clinical relevance. Am J Med Genet 150B:476–482. doi: 10.1002/ajmg.b.20709

Kurban G, Hudon V, Duplan E, et al (2006) Characterization of a von Hippel Lindau Pathway Involved in Extracellular Matrix Remodeling, Cell Invasion, and Angiogenesis. Cancer Research 66:1313–1319. doi: 10.1158/0008-5472.CAN-05-2560

Kuznetsova AV, Meller J, Schnell PO, et al (2003) von Hippel-Lindau protein binds hyperphosphorylated large subunit of RNA polymerase II through a proline hydroxylation motif and targets it for ubiquitination. Proc Natl Acad Sci USA 100:2706–2711. doi: 10.1038/sj.onc.1203985

Lackner MR, Kornfeld K, Miller LM, et al (1994) A MAP kinase homolog, *mpk-1,* is involved in *ras*-mediated induction of vulval cell fates in *Caenorhabditis elegans.* Genes & Development 8:160–173.

Lambie EJ, Kimble J (1991) Two homologous regulatory genes, *lin-12* and *glp-1,* have overlapping functions. Development 112:231–240.

Lando D (2002) FIH-1 is an asparaginyl hydroxylase enzyme that regulates the transcriptional activity of hypoxia-inducible factor. Genes & Development 16:1466–1471. doi: 10.1101/gad.991402

Laplante P, Diorio J, Meaney MJ (2002) Serotonin regulates hippocampal glucocorticoid receptor expression

via a 5-HT7 receptor. Brain Res Dev Brain Res 139:199–203.

Lee J, Jongeward GD, Sternberg PW (1994) *unc-101*, a gene required for many aspects of *Caenorhabditis elegans* development and behavior, encodes a clathrin-associated protein. Genes & Development 8:60–73.

Leips J, Mackay TF (2000) Quantitative trait loci for life span in *Drosophila melanogaster*: interactions with genetic background and larval density. Genetics 155:1773–1788.

Li S, Armstrong CM, Bertin N, et al (2004) A map of the interactome network of the metazoan *C. elegans.* Science 303:540–543. doi: 10.1126/science.1091403

Li Y, Álvarez OA, Gutteling EW, et al (2006) Mapping Determinants of Gene Expression Plasticity by Genetical Genomics in *C. elegans.* PLoS Genet 2:e222. doi: 10.1371/journal.pgen.0020222

Liao D, Corle C, Seagroves TN, Johnson RS (2007) Hypoxia-Inducible Factor-1 Is a Key Regulator of Metastasis in a Transgenic Model of Cancer Initiation and Progression. Cancer Research 67:563–572. doi: 10.1158/0008-5472.CAN-06-2701

Lieber T, Kidd S, Alcamo E, et al (1993) Antineurogenic phenotypes induced by truncated Notch proteins indicate a role in signal transduction and may point to a novel function for Notch in nuclei. Genes & Development 7:1949–1965.

Lieber T, Wesley CS, Alcamo E, et al (1992) Single amino acid substitutions in EGF-like elements of Notch and Delta modify *Drosophila* development and affect cell adhesion *in vitro*. Neuron 9:847–859.

Liti G, Louis EJ (2012) Advances in Quantitative Trait Analysis in Yeast. PLoS Genet 8:e1002912. doi: 10.1371/journal.pgen.1002912

Livingston DM, Kung AL, Wang S, et al (2000) Suppression of tumor growth through disruption of hypoxia-inducible transcription. Nat Med 6:1335–1340. doi: 10.1038/82146

Lo M-C, Gay F, Odom R, et al (2004) Phosphorylation by the beta-catenin/MAPK complex promotes 14-3-3-mediated nuclear export of TCF/POP-1 in signal-responsive cells in *C. elegans*. Cell 117:95–106.

Locke C, Berry K, Kautu B, et al (2008) Paradigms for Pharmacological Characterization of *C. elegans* Synaptic Transmission Mutants. JoVE. doi: 10.3791/837

Logan CY, Nusse R (2004) The Wnt signaling pathway in development and disease.

Loor G, Schumacker PT (2008) Role of hypoxia-inducible factor in cell survival during myocardial ischemia–reperfusion. Cell Death Differ 15:686–690. doi: 10.1161/01.CIR.103.12.1695

Lopez AL, Chen J, Joo H-J, Drake M, Shidate M, Kseib C, Arur S (2013) DAF-2 and ERK Couple Nutrient Availability to Meiotic Progression during *Caenorhabditis elegans* Oogenesis. Developmental Cell 27:227-240.

Lu J, Ma Z, Hsieh J-C, et al (2009) Structure–activity relationship studies of small-molecule inhibitors of Wnt response. Bioorganic & Medicinal Chemistry Letters 19:3825–3827. doi: 10.1016/j.bmcl.2009.04.040

Luo W, Lin B, Wang Y, et al (2014) PHD3-mediated prolyl hydroxylation of nonmuscle actin impairs polymerization and cell motility. Molecular Biology of the Cell 25:2788–2796. doi: 10.1091/mbc.E14-02-0775

Luttrell LM, Roudabush FL, Choy EW, et al (2001) Activation and targeting of extracellular signal-regulated kinases by beta-arrestin scaffolds. Proc Natl Acad Sci USA 98:2449–2454. doi: 10.1073/pnas.041604898

Mabon ME, Mao X, Jiao Y, et al (2008) Systematic Identification of Gene Activities Promoting Hypoxic Death.

Genetics 181:483–496. doi: 10.1534/genetics.108.097188

Madan A, Curtin PT (1993) A 24-base-pair sequence 3' to the human erythropoietin gene contains a hypoxia-responsive transcriptional enhancer. Proceedings of the National Academy of Sciences 90:3928–3932. doi: 10.1073/pnas.90.9.3928

Maduro M, Pilgrim D (1995) Identification and cloning of *unc-119*, a gene expressed in the *Caenorhabditis elegans* nervous system. Genetics 141:977–988.

Mahon PC (2001) FIH-1: a novel protein that interacts with HIF-1alpha and VHL to mediate repression of HIF-1 transcriptional activity. Genes & Development 15:2675–2686. doi: 10.1101/gad.924501

Main Page (2017). OpenWetWare. https://openwetware.org/mediawiki/index.php?title=Main_Page&oldid=999162.

Makino Y, Cao R, Svensson K, et al (2001) Inhibitory PAS domain protein is a negative regulator of hypoxia-inducible gene expression. Nature 414:550–554. doi: 10.1038/35107085

Maloof JN, Whangbo J, Harris JM, et al (1999) A Wnt signaling pathway controls *hox* gene expression and neuroblast migration in *C. elegans*. Development 126:37–49.

Mandriota SJ, Turner KJ, Davies DR, et al (2002) HIF activation identifies early lesions in VHL kidneys. Cancer Cell 1:459–468. doi: 10.1016/S1535-6108(02)00071-5

Mani K, Fay DS (2009) A Mechanistic Basis for the Coordinated Regulation of Pharyngeal Morphogenesis in *Caenorhabditis elegans* by LIN-35/Rb and UBC-18–ARI-1. PLoS Genet 5:e1000510. doi: 10.1371/journal.pgen.1000510

Marais R, Wynne J, Treisman R (1993) The SRF accessory protein Elk-1 contains a growth factor-regulated transcriptional activation domain. Cell 73:381–393.

Martini E (1923) Die Zellkonstanz und ihre Beziehungen zu anderen zoologischen Vorwürfen. Z Anat Entwickl Gesch 70:179–259. doi: 10.1007/BF02117179

Masson N, Willam C, Maxwell PH, et al (2001) Independent function of two destruction domains in hypoxia-inducible factor-α chains activated by prolyl hydroxylation. EMBO J 20:5197–5206. doi: 10.1093/emboj/20.18.5197

Maxwell PH, Wiesener MS, Chang G-W, et al (1999) The tumour suppressor protein VHL targets hypoxia-inducible factors for oxygen-dependent proteolysis. Nature 399:271–275. doi: 10.1038/ng0594-85

Maydan JS, Lorch A, Edgley ML, et al (2010) Copy number variation in the genomes of twelve natural isolates of *Caenorhabditis elegans*. BMC Genomics 11:62. doi: 10.1186/1471-2164-11-62

McGrath PT, Rockman MV, Zimmer M, et al (2009) Quantitative Mapping of a Digenic Behavioral Trait Implicates Globin Variation in *C. elegans* Sensory Behaviors. Neuron 61:692–699. doi: 10.1016/j.neuron.2009.02.012

MCKAY SJ, JOHNSEN R, KHATTRA J, et al (2003) Gene Expression Profiling of Cells, Tissues, and Developmental Stages of the Nematode *C. elegans*. Cold Spring Harbor Symposia on Quantitative Biology 68:159–170. doi: 10.1016/S0167-7799(97)01169-4

McKim KS, Peters K, Rose AM (1993) Two types of sites required for meiotic chromosome pairing in *Caenorhabditis elegans*. Genetics 134:749–768.

Mello CC, Draper BW, Prless JR (1994) The maternal genes *apx-1* and *glp-1* and establishment of dorsal-ventral polarity in the early *C. elegans* embryo. Cell 77:95–106. doi: 10.1016/0092-8674(94)90238-0

Mello CC, Kramer JM, Stinchcomb D, Ambros V (1991) Efficient gene transfer in *C.elegans*: extrachromo-

somal maintenance and integration of transforming sequences. EMBO J 10:3959–3970.

Mense SM, Sengupta A, Zhou M, et al (2006) Gene expression profiling reveals the profound upregulation of hypoxia-responsive genes in primary human astrocytes. Physiological Genomics 25:435–449. doi: 10.1152/physiolgenomics.00315.2005

Mickey KM, Mello CC, Montgomery MK, et al (1996) An inductive interaction in 4-cell stage *C. elegans* embryos involves APX-1 expression in the signalling cell. Development 122:1791–1798.

Mignone F, Gissi C, Liuni S, Pesole G (2002) Untranslated regions of mRNAs. Genome Biol 3:reviews0004.1.

Miller JR, Moon RT (1997) Analysis of the Signaling Activities of Localization Mutants of β-Catenin during Axis Specification in Xenopus. J Cell Biol 139:229–243. doi: 10.1101/gad.10.12.1443

Milloz J, Duveau F, Nuez I, Félix M-A (2008) Intraspecific evolution of the intercellular signaling network underlying a robust developmental system. Genes & Development 22:3064–3075. doi: 10.1101/gad.495308

Miskowski J, Li Y, Kimble J (2001) The *sys-1* gene and sexual dimorphism during gonadogenesis in *Caenorhabditis elegans*. Developmental Biology 230:61–73. doi: 10.1006/dbio.2000.9998

Mitchell JB, Betito K, Rowe W, et al (1992) Serotonergic regulation of type II corticosteroid receptor binding in hippocampal cell cultures: evidence for the importance of serotonin-induced changes in cAMP levels. Neuroscience 48:631–639.

Mitchell JB, Iny LJ, Meaney MJ (1990) The role of serotonin in the development and environmental regulation of type II corticosteroid receptor binding in rat hippocampus. Brain Res Dev Brain Res 55:231–235.

Moghal N, Garcia LR, Khan LA, et al (2003) Modulation of EGF receptor-mediated vulva development by the heterotrimeric G-protein Gαq and excitable cells in *C. elegans*. Development 130:4553–4566. doi: 10.1242/dev.00670

Moghal N, Sternberg PW (2003) The epidermal growth factor system in *Caenorhabditis elegans*. Exp Cell Res 284:150–159.

Mohler WA, Simske JS, Williams-Masson EM, et al (1998) Dynamics and ultrastructure of developmental cell fusions in the *Caenorhabditis elegans* hypodermis. Current Biology 8:1087–1091. doi: 10.1016/S0960-9822(98)70447-6

Morf MK, Rimann I, Alexander M, et al (2013) The *Caenorhabditis elegans* homolog of the Opitz syndrome gene, *madd-2/Mid1*, regulates anchor cell invasion during vulval development. Developmental Biology 374:108–114. doi: 10.1016/j.ydbio.2012.11.019

Mousnier A, Kubat N, Massias-Simon A, et al (2007) von Hippel Lindau binding protein 1-mediated degradation of integrase affects HIV-1 gene expression at a postintegration step. Proc Natl Acad Sci USA 104:13615–13620. doi: 10.1101/gad.11.12.1561

Mueller JC, Fuchs J, Hofer A, et al (2005) Multiple regions of α-synuclein are associated with Parkinson's disease. Annals of Neurology 57:535–541. doi: 10.1212/WNL.51.6.1757

Mullick J, Anandatheerthavarada HK, Amuthan G, et al (2001) Physical Interaction and Functional Synergy between Glucocorticoid Receptor and Ets2 Proteins for Transcription Activation of the Rat Cytochrome P-450c27 Promoter. J Biol Chem 276:18007–18017. doi: 10.1073/pnas.94.1.127

Mulualem T, Bekeko Z (2016) Advances in Quantitative Trait Loci, Mapping and Importance of Markers Assisted Selection in Plant Breeding Research. International J of Plant Breeding and Genetics 10:58–68.

doi: 10.3923/ijpbg.2016.58.68

Muralidharan P, Szappanos HC, Ingley E, Hool L (2016) Evidence for redox sensing by a human cardiac calcium channel. Scientific Reports 6:srep19067. doi: doi:10.1038/srep19067

Murphy LO, Smith S, Chen R-H, et al (2002) Molecular interpretation of ERK signal duration by immediate early gene products. Nat Cell Biol. doi: 10.1038/ncb822

Myllyharju J (2003) Prolyl 4-hydroxylases, the key enzymes of collagen biosynthesis. Matrix Biol 22:15–24.

Nakdimon I (2011) Regulation of the *C. elegans* RAS/MAPK pathway by the tumor suppressor PTEN DAF-18 and nutritional cues.

Nakdimon I, Walser M, Fröhli E, Hajnal A (2012) PTEN Negatively Regulates MAPK Signaling during *Caenorhabditis elegans* Vulval Development. PLoS Genet 8:e1002881. doi: 10.1371/journal.pgen.1002881

Natarajan L, Jackson BM, Szyleyko E, Eisenmann DM (2004) Identification of evolutionarily conserved promoter elements and amino acids required for function of the *C. elegans* beta-catenin homolog BAR-1. Developmental Biology 272:536–557. doi: 10.1016/j.ydbio.2004.05.027

Natarajan L, Witwer NE, Eisenmann DM (2001) The divergent *Caenorhabditis elegans* beta-catenin proteins BAR-1, WRM-1 and HMP-2 make distinct protein interactions but retain functional redundancy *in vivo.* Genetics 159:159–172.

Nelson FK, Riddle DL (1984) Functional study of the *Caenorhabditis elegans* secretory-excretory system using laser microsurgery. J Exp Zool 231:45–56. doi: 10.1002/jez.1402310107

Nelson WJ, Nusse R (2004) Convergence of Wnt, ß-Catenin, and Cadherin Pathways. Science 303:1483–1487. doi: 10.1126/science.1094291

Neuhausen SL, Swensen J, Miki Y, et al (1994) A P1-based physical map of the region from D17S776 to D17S78 containing the breast cancer susceptibility gene *BRCA1*. Hum Mol Genet 3:1919–1926. doi: 10.1093/hmg/3.11.1919

Newman AP, White JG, Sternberg PW (1995) The *Caenorhabditis elegans lin-12* gene mediates induction of ventral uterine specialization by the anchor cell. Development 121:263–271. doi: 10.1002/bdra.20705

Nicolas M, Wolfer A, Raj K, et al (2003) Notch1 functions as a tumor suppressor in mouse skin. Nat Genet 33:416–421. doi: 10.1038/ng1099

Nishisho I, Nakamura Y, Miyoshi Y, et al (1991) Mutations of chromosome 5q21 genes in FAP and colorectal cancer patients. Science 253:665–669. doi: 10.1126/science.1651563

Nordstrom-O'Brien M, van der Luijt RB, van Rooijen E, et al (2010) Genetic analysis of von Hippel-Lindau disease. Human Mutation 31:521-537. doi: 10.1002/humu.21219

Nusser-Stein S, Beyer A, Rimann I, et al (2012) Cell-cycle regulation of NOTCH signaling during *C. elegans* vulval development. Mol Syst Biol 8:618. doi: 10.1038/msb.2012.51

Overgaard J (2007) Hypoxic Radiosensitization: Adored and Ignored. JCO 25:4066–4074. doi: 10.1200/JCO.2007.12.7878

Öberg C, Li J, Pauley A, et al (2001) The Notch Intracellular Domain Is Ubiquitinated and Negatively Regulated by the Mammalian Sel-10 Homolog. J Biol Chem 276:35847–35853. doi: 10.1038/19096

Padilla PA, Nystul TG, Zager RA, et al (2002) Dephosphorylation of Cell Cycle–regulated Proteins Correlates with Anoxia-induced Suspended Animation in *Caenorhabditis elegans*. Mol Biol Cell 5:1473-1483. doi: 10.1091/mbc.01-12-0594

Padmanabha D, Padilla PA, You Y-J, Baker KD (2015) A HIF-Independent Mediator of Transcriptional Responses to Oxygen Deprivation in *Caenorhabditis elegans*. Genetics 199:739–748. doi: 10.1534/genetics.114.173989

Palopoli MF, Rockman MV, TinMaung A, et al (2008) Molecular basis of the copulatory plug polymorphism in *Caenorhabditis elegans*. Nature 454:1019–1022. doi: 10.1111/j.0014-3820.2000.tb00544.x

Papadopoulos N, Nicolaides N, Wei Y, et al (1994) Mutation of a mutL homolog in hereditary colon cancer. Science 263:1625–1629. doi: 10.1126/science.8128251

Park EC, Ghose P, Shao Z, et al (2012) Hypoxia regulates glutamate receptor trafficking through an HIF-independent mechanism. EMBO J 31:1379–1393. doi: 10.1038/emboj.2011.499

Park FD, Tenlen JR, Priess JR (2004) *C. elegans* MOM-5/frizzled functions in MOM-2/Wnt-independent cell polarity and is localized asymmetrically prior to cell division. Curr Biol 14:2252–2258. doi: 10.1016/j.cub.2004.12.019

Park SK, Choi VN, Hwang BJ (2013) LIN-12/notch regulates *lag-1* and *lin-12* expression during anchor cell/ventral uterine precursor cell fate specification. Mol Cells 35:249–254. doi: 10.1038/nature02089

Pasyukova EG, Vieira C, Mackay TF (2000) Deficiency mapping of quantitative trait loci affecting longevity in *Drosophila melanogaster*. Genetics 156:1129–1146.

Paterson AH, Lan C, Hewitt JD, et al (1988) Resolution of quantitative traits into Mendelian factors by using a complete linkage map of restriction fragment length polymorphisms. Nature 335:721–726. doi: 10.1038/335721a0

Patterson AJ, Zhang L (2010) Hypoxia and Fetal Heart Development. Current molecular medicine 10:653.

Pattnaik AK, Panda D (2009) Biarsenical Labeling of Tetracysteine-Tagged Proteins for Tracking Existing and Newly Synthesized Pools of Proteins.

Pepper AS-R, Killian DJ, Hubbard EJA (2003) Genetic Analysis of *Caenorhabditis elegans glp-1* Mutants Suggests Receptor Interaction or Competition. Genetics 163:115–132.

Percy MJ, Beer PA, Campbell G, et al (2008a) Novel exon 12 mutations in the HIF2A gene associated with erythrocytosis. Blood 111:5400–5402. doi: 10.1182/blood-2008-02-137703

Percy MJ, Furlow PW, Lucas GS, et al (2008b) A Gain-of-Function Mutation in the HIF2A Gene in Familial Erythrocytosis. N Engl J Med 358:162–168. doi: 10.1056/NEJMoa073123

Persico A, Cervigni RI, Barretta ML, et al (2010) Golgi Partitioning Controls Mitotic Entry through Aurora-A Kinase. Molecular Biology of the Cell 21:3708–3721. doi: 10.1091/mbc.E10-03-0243

Persson A, Gross E, Laurent P, et al (2009) Natural variation in a neural globin tunes oxygen sensing in wild *Caenorhabditis elegans*. Nature 458:1030–1033. doi: 10.1038/nature07820

Peruzzi B, Athauda G, Bottaro DP (2006) The von Hippel-Lindau tumor suppressor gene product represses oncogenic beta-catenin signaling in renal carcinoma cells. Proceedings of the National Academy of Sciences 103:14531–14536. doi: 10.1074/jbc.M010202200

Peters JM, McKay RM, McKay JP, Graff JM (1999) Casein kinase I transduces Wnt signals. Nature 401:345–350. doi: 10.1073/pnas.88.21.9578

Peters RL, Rabstein LS, VanVleck R, Kelloff GJ, Huebner RJ (1974) Naturally occurring sarcoma virus of the BALB/cCr mouse. J Natl Cancer Inst. 53:1725-9.

Pilipiuk J, Lefebvre C, Wiesenfahrt T, et al (2009) Increased IP3/Ca^{2+} signaling compensates depletion of LET-413/DLG-1 in *C. elegans* epithelial junction assembly. Developmental Biology 327:34–47. doi: 10.1016/j.ydbio.2008.11.025

Plantaz D, Mohaptra G, Matthay KK, et al (1997) Gain of chromosome 17 is the most frequent abnormality detected in neuroblastoma by comparative genomic hybridization. The American Journal of Pathology 150:81.

Pocock R, Hobert O (2010) Hypoxia activates a latent circuit for processing gustatory information in *C. elegans*. Nat Neurosci 13:610–614. doi: 10.1038/nn.2537

Poliseno L, Salmena L, Zhang J, et al (2010) A coding-independent function of gene and pseudogene mRNAs regulates tumour biology. Nature 465:1033–1038. doi: 10.1038/nature09144

Price MA, Cruzalegui FH, Treisman R (1996) The p38 and ERK MAP kinase pathways cooperate to activate Ternary Complex Factors and *c-fos* transcription in response to UV light. EMBO J 15:6552–6563.

Priess JR (2005) Notch signaling in the *C. elegans* embryo. WormBook. doi: 10.1895/wormbook.1.4.1

Prior IA, Hancock JF (2012) Ras trafficking, localization and compartmentalized signalling. Semin Cell Dev Biol 23:145–153. doi: 10.1016/j.semcdb.2011.09.002

Prior IA, Lewis PD, Mattos C (2012) A Comprehensive Survey of Ras Mutations in Cancer. Cancer Research 72:2457–2467. doi: 10.1158/0008-5472.CAN-11-2612

Pugh CW, Ratcliffe PJ (2017) New horizons in hypoxia signaling pathways. Exp Cell Res 356:116–121. doi: 10.1016/j.yexcr.2017.03.008

Pugh CW, Tan CC, Jones RW, Ratcliffe PJ (1991) Functional analysis of an oxygen-regulated transcriptional enhancer lying 3' to the mouse erythropoietin gene. Proceedings of the National Academy of Sciences 88:10553–10557. doi: 10.1073/pnas.88.23.10553

Purcell SM, Wray NR, Stone JL, et al (2009) Common polygenic variation contributes to risk of schizophrenia and bipolar disorder. Nature 460:748–752. doi: 10.1038/nature08185

Qadota H, Inoue M, Hikita T, et al (2007) Establishment of a tissue-specific RNAi system in *C. elegans*. Gene 400:166–173. doi: 10.1016/j.gene.2007.06.020

Radtke F, Raj K (2003) The role of Notch in tumorigenesis: oncogene or tumour suppressor? Nat Rev Cancer 3:756–767. doi: 10.1038/nrc1186

Rasheed S, Gardner MB, Huebner RJ (1978) *In vitro* isolation of stable rat sarcoma viruses. Proceedings of the National Academy of Sciences 75:2972-2976.

Raval RR, Lau KW, Tran MGB, et al (2005) Contrasting Properties of Hypoxia-Inducible Factor 1 (HIF-1) and HIF-2 in von Hippel-Lindau-Associated Renal Cell Carcinoma. Molecular and Cellular Biology 25:5675–5686. doi: 10.1128/MCB.25.13.5675-5686.2005

Ravichandran KS (2001) Signaling via Shc family adapter proteins. Oncogene 20:6322–6330. doi: 10.1038/sj.onc.1204776

Ravichandran KS, Lorenz U, Shoelson SE, Burakoff SJ (1995) Interaction of Shc with Grb2 regulates association of Grb2 with mSOS. Molecular and Cellular Biology 15:593–600.

Rebay I, Fleming RJ, Fehon RG, et al (1991) Specific EGF repeats of Notch mediate interactions with Delta and Serrate: implications for Notch as a multifunctional receptor. Cell 67:687–699.

Reboul J, Vaglio P, Tzellas N, et al (2001) Open-reading-frame sequence tags (OSTs) support the existence of at least 17,300 genes in *C. elegans*. Nat Genet 27:332–336. doi: 10.1038/85913

Redemann S, Schloissnig S, Ernst S, et al (2011) Codon adaptation–based control of protein expression in *C. elegans*. Nat Methods 8:250–252. doi: 10.1038/nature01278

Repasky GA, Chenette EJ, Der CJ (2004) Renewing the conspiracy theory debate: does Raf function alone to mediate Ras oncogenesis? Trends Cell Biol 14:639–647. doi: 10.1016/j.tcb.2004.09.014

Reszka AA, Seger R, Diltz CD, et al (1995) Association of mitogen-activated protein kinase with the microtubule cytoskeleton. Proc Natl Acad Sci USA 92:8881–8885.

Reya T, Clevers H (2005) Wnt signalling in stem cells and cancer. Nature 434:843–850. doi: doi:10.1038/nature03319

Richard DE, Berra E, Gothie E, et al (1999) p42/p44 Mitogen-activated Protein Kinases Phosphorylate Hypoxia-inducible Factor 1 (HIF-1) and Enhance the Transcriptional Activity of HIF-1. J Biol Chem 274:32631–32637. doi: 10.1074/jbc.274.46.32631

Richard N Day MWD (2009) The fluorescent protein palette: tools for cellular imaging. Chemical Society reviews 38:2887. doi: 10.1039/b901966a

Rimann I, Hajnal A (2007) Regulation of anchor cell invasion and uterine cell fates by the *egl-43 Evi-1* proto-oncogene in *Caenorhabditis elegans*. Developmental Biology 308:187–195. doi: 10.1016/j.ydbio.2007.05.023

Rischin D, Peters L, Fisher R, et al (2005) Tirapazamine, Cisplatin, and Radiation Versus Fluorouracil, Cisplatin, and Radiation in Patients With Locally Advanced Head and Neck Cancer: A Randomized Phase II Trial of the Trans-Tasman Radiation Oncology Group (TROG 98.02). JCO 23:79–87. doi: 10.1200/JCO.2005.01.072

Robbins J, Blondel BJ, Gallahan D, Callahan R (1992) Mouse mammary tumor gene *int-3*: a member of the notch gene family transforms mammary epithelial cells. Journal of Virology 66:2594–2599.

Roberts PJ, Der CJ (2007) Targeting the Raf-MEK-ERK mitogen-activated protein kinase cascade for the treatment of cancer. Oncogene 26:3291–3310. doi: 10.1038/72799

Rocheleau CE, Downs WD, Lin R, et al (1997) Wnt signaling and an APC-related gene specify endoderm in early *C. elegans* embryos. Cell 90:707–716.

Rocks O, Gerauer M, Vartak N, et al (2010) The palmitoylation machinery is a spatially organizing system for peripheral membrane proteins. Cell 141:458–471. doi: 10.1016/j.cell.2010.04.007

Rodriguez-Viciana P, Sabatier C, McCormick F (2004) Signaling Specificity by Ras Family GTPases Is Determined by the Full Spectrum of Effectors They Regulate. Molecular and Cellular Biology 24:4943–4954. doi: 10.1128/MCB.24.11.4943-4954.2004

Roe J-S, Kim H, Lee S-M, et al (2006) p53 Stabilization and Transactivation by a von Hippel-Lindau Protein. Mol Cell 22:395–405. doi: 10.1016/j.molcel.2006.04.006

Roehl H, Kimble J (1993) Control of cell fate in *C. elegans* by a GLP-1 peptide consisting primarily of ankyrin repeats. Nature 364:632–635. doi: 10.1038/364632a0

Romney SJ, Ben S Newman, Thacker C, Leibold EA (2011) HIF-1 Regulates Iron Homeostasis in *Caenorhabditis elegans* by Activation and Inhibition of Genes Involved in Iron Uptake and Storage. PLoS Genet

7:e1002394. doi: 10.1371/journal.pgen.1002394

Rual JF, Ceron J, Koreth J, et al (2004) Toward Improving *Caenorhabditis elegans* Phenome Mapping With an ORFeome-Based RNAi Library. Genome Research 14:2162–2168. doi: 10.1101/gr.2505604

Rubinfeld B, Robbins P, El-Gamil M, et al (1997) Stabilization of beta-catenin by Genetic Defects in Melanoma Cell Lines. Science 275:1790–1792. doi: 10.1126/science.275.5307.1790

Runkel ED, Baumeister R, Schulze E (2014) Mitochondrial stress: Balancing friend and foe. Experimental Gerontology 56:194–201. doi: 10.1016/j.exger.2014.02.013

Ruvkun G, Hobert O (1998) The Taxonomy of Developmental Control in *Caenorhabditis elegans.* Science 282:2033–2041. doi: 10.1126/science.282.5396.2033

Saha M, Carriere A, Cheerathodi M, et al (2012) RSK phosphorylates SOS1 creating 14-3-3-docking sites and negatively regulating MAPK activation. Biochem J 447:159–166. doi: 10.1093/nar/gkg584

Salceda S, Caro J (1997) Hypoxia-inducible Factor 1α (HIF-1α) Protein Is Rapidly Degraded by the Ubiquitin-Proteasome System under Normoxic Conditions. J Biol Chem 272:22642–22647. doi: 10.1126/science.275.5298.400

Salser SJ, Loer CM, Kenyon C (1993) Multiple HOM-C gene interactions specify cell fates in the nematode central nervous system. Genes & Development 7:1714–1724.

Sato A, Kojima T, Ui-Tei K, et al (1999) Dfrizzled-3, a new *Drosophila* Wnt receptor, acting as an attenuator of Wingless signaling in wingless hypomorphic mutants. Development 126:4421–4430. doi: 10.1002/bdra.20705

Sato K, Kawashima S (2001) Calpain function in the modulation of signal transduction molecules. Biol Chem 382:743–751. doi: 10.1515/BC.2001.090

Satoh S, Daigo Y, Furukawa Y, et al (2000) *AXIN1* mutations in hepatocellular carcinomas, and growth suppression in cancer cells by virus-mediated transfer of *AXIN1*. Nat Genet 24:245–250. doi: 10.1128/MCB.16.3.745

Satoh T, Nakafuku M, Kaziro Y (1992) Function of Ras as a molecular switch in signal transduction. J Biol Chem 267:24149–24152.

Sawa H, Lobel L, Horvitz HR (1996) The *Caenorhabditis elegans* gene *lin-17*, which is required for certain asymmetric cell divisions, encodes a putative seven-transmembrane protein similar to the *Drosophila* frizzled protein. Genes & Development 10:2189–2197.

Scaltriti M, Baselga J (2006) The Epidermal Growth Factor Receptor Pathway: A Model for Targeted Therapy. Clinical Cancer Research 12:5268–5272. doi: 10.1158/1078-0432.CCR-05-1554

Schaeffer HJ (1998) MP1: A MEK Binding Partner That Enhances Enzymatic Activation of the MAP Kinase Cascade. Science 281:1668–1671. doi: 10.1126/science.281.5383.1668

Schindl M (2002) Overexpression of hypoxia-inducible factor 1[alpha] is associated with an unfavorable prognosis in lymph node-positive breast cancer. Clin Cancer Res 8:1831–1837.

Schlesinger A, Shelton CA, Maloof JN, et al (1999) Wnt pathway components orient a mitotic spindle in the early *Caenorhabditis elegans* embryo without requiring gene transcription in the responding cell. Genes & Development 13:2028–2038.

Schlessinger J (1993) How receptor tyrosine kinases activate Ras. Trends in Biochemical Sciences 18:273–275.

Schmid TJ (2014) Quantitative genetic analysis of *C. elegans* vulval development.

Schmid T, Snoek LB, Fröhli E, et al (2015) Systemic Regulation of RAS/MAPK Signaling by the Serotonin Metabolite 5-HIAA. PLoS Genet 11:e1005236. doi: 10.1371/journal.pgen.1005236

Sears R (2000) Multiple Ras-dependent phosphorylation pathways regulate Myc protein stability. Genes & Development 14:2501–2514. doi: 10.1101/gad.836800

Seko Y, Tobe K, Ueki K, et al (1996) Hypoxia and Hypoxia/Reoxygenation Activate Raf-1, Mitogen-Activated Protein Kinase Kinase, Mitogen-Activated Protein Kinases, and S6 Kinase in Cultured Rat Cardiac Myocytes. Circulation Research 78:82–90. doi: 10.1161/01.RES.78.1.82

Semenza GL (2003) Targeting HIF-1 for cancer therapy. Nat Rev Cancer 3:721–732. doi: 10.1038/nrc1187

Semenza GL (2007) Evaluation of HIF-1 inhibitors as anticancer agents. Drug Discovery Today 12:853–859. doi: 10.1016/j.drudis.2007.08.006

Semenza GL, Nejfelt MK, Chi SM, Antonarakis SE (1991) Hypoxia-inducible nuclear factors bind to an enhancer element located 3' to the human erythropoietin gene. Proceedings of the National Academy of Sciences 88:5680–5684. doi: 10.1073/pnas.88.13.5680

Semenza GL, Wang GL (1992) A nuclear factor induced by hypoxia via de novo protein synthesis binds to the human erythropoietin gene enhancer at a site required for transcriptional activation. Mol Cell Biol 12:5447–5454.

Sendoel A, Kohler I, Fellmann C, et al (2010) HIF-1 antagonizes p53-mediated apoptosis through a secreted neuronal tyrosinase. Nature 465:577–583. doi: 10.1038/nature09141

Seydoux G, Greenwald I (1989) Cell autonomy of *lin-12* function in a cell fate decision in *C. elegans*. Cell 57:1237–1245.

Shackleford GM, Shivakumar S, Shiue L, et al (1993) Two Wnt genes in *Caenorhabditis elegans.* Oncogene 8:1857–64.

Shannon AM, Bouchier-Hayes DJ, Condron CM, Toomey D (2003) Tumour hypoxia, chemotherapeutic resistance and hypoxia-related therapies. Cancer Treatment Reviews 29:297–307. doi: 10.1016/S0305-7372(03)00003-3

Shao Z, Zhang Y, Powell-Coffman JA (2009) Two Distinct Roles for EGL-9 in the Regulation of HIF-1-Mediated Gene Expression in *Caenorhabditis elegans.* Genetics 183:821–829. doi: 10.1534/genetics.109.107284

Sharma-Kishore R, White JG, Southgate E, Podbilewicz B (1999) Formation of the vulva in *Caenorhabditis elegans*: a paradigm for organogenesis. Development 126:691–699.

Shaul YD, Seger R (2006) ERK1c regulates Golgi fragmentation during mitosis. J Cell Biol 172:885–897. doi: 10.1038/sj.cr.7290105

Shaye DD, Greenwald I (2002) Endocytosis-mediated downregulation of LIN-12/Notch upon Ras activation in *Caenorhabditis elegans.* Nature 420:686–690. doi: 10.1038/nature01234

Shaye DD, Greenwald I (2011) OrthoList: A Compendium of *C. elegans* Genes with Human Orthologs. PLoS ONE 6:e20085. doi: 10.1371/journal.pone.0020085

Shcherbo D, Merzlyak EM, Chepurnykh TV, et al (2007) Bright far-red fluorescent protein for whole-body imaging. Nat Methods 4:741–746. doi: 10.1038/nmeth1083

Shen C, Powell-Coffman JA (2003) Genetic Analysis of Hypoxia Signaling and Response in *C. elegans.* Ann N Y Acad Sci 995:191–199. doi: 10.1111/j.1749-6632.2003.tb03222.x

Sherwood DR, Sternberg PW (2003) Anchor Cell Invasion into the Vulval Epithelium in *C. elegans.* Developmental Cell 5:21–31. doi: 10.1016/S1534-5807(03)00168-0

Shweiki D, Itin A, Soffer D, Keshet E (1992) Vascular endothelial growth factor induced by hypoxia may mediate hypoxia-initiated angiogenesis. Nature 359:843–845. doi: 10.1038/359843a0

Sijen T, Fleenor J, Simmer F, et al (2001) On the Role of RNA Amplification in dsRNA-Triggered Gene Silencing. Cell 107:465–476. doi: 10.1016/S0092-8674(01)00576-1

Simon MC, Keith B (2008) The role of oxygen availability in embryonic development and stem cell function. Nat Rev Mol Cell Biol 9:285–296. doi: 10.1172/JCI17669

Simonis N, Rual JF, Carvunis AR, et al (2009) Empirically-controlled mapping of the *Caenorhabditis elegans* protein-protein interactome network. Nat Methods 6:47.

Simske JS, Kaech SM, Harp SA, Kim SK (1996) LET-23 Receptor Localization by the Cell Junction Protein LIN-7 during *C. elegans* Vulval Induction. Cell 85:195–204. doi: 10.1016/S0092-8674(00)81096-X

Singh N, Han M (1995) *sur-2*, a novel gene, functions late in the *let-60 ras*-mediated signaling pathway during *Caenorhabditis elegans* vulval induction. Genes & Development 9:2251–2265. doi: 10.1101/gad.9.18.2251

Singleton RS, Liu-Yi P, Formenti F, et al (2014) OGFOD1 catalyzes prolyl hydroxylation of RPS23 and is involved in translation control and stress granule formation. Proceedings of the National Academy of Sciences 111:4031–4036. doi: 10.1073/pnas.1314482111

Sorimachi H, Ishiura S, Suzuki K (1997) Structure and physiological function of calpains. Biochem J 328 (Pt 3):721–732.

Soto-Ortolaza AI, Heckman MG, Labbé C, et al (2013) GWAS risk factors in Parkinson's disease: LRRK2 coding variation and genetic interaction with PARK16. American Journal of Neurodegenerative Disease 2:287–299.

Spiegel J, Cromm PM, Zimmermann G, et al (2014) Small-molecule modulation of Ras signaling. Nature Chemical Biology 10:613–622. doi: doi:10.1038/nchembio.1560

Spradling A, Ganetsky B, Hieter P, et al (2006) New Roles for Model Genetic Organisms in Understanding and Treating Human Disease: Report From The 2006 Genetics Society of America Meeting. Genetics 172:2025.

Sternberg PW (1988) Lateral inhibition during vulval induction in *Caenorhabditis elegans*. Nature 335:551–554. doi: 10.1038/335551a0

Sternberg PW (2005) Vulval development. WormBook. doi: 10.1895/wormbook.1.6.1

Sternberg PW, Golden A, Han M (1993) Role of a raf Proto-Oncogene during *Caenorhabditis elegans* Vulval Development. Philosophical Transactions of the Royal Society B: Biological Sciences 340:259–265. doi: 10.1098/rstb.1993.0066

Sternberg PW, Horvitz HR (1986) Pattern formation during vulval development in *C. elegans.* Cell 44:761-772.

Stessman HA, Bernier R, Eichler EE (2014) A genotype-first approach to defining the subtypes of a complex disease. Cell 156:872–877. doi: 10.1016/j.cell.2014.02.002

Storz JF, Scott GR, Cheviron ZA (2010) Phenotypic plasticity and genetic adaptation to high-altitude hypoxia in vertebrates. Journal of Experimental Biology 213:4125–4136. doi: 10.1242/jeb.048181

Struhl G, Fitzgerald K, Greenwald I (1993) Intrinsic activity of the Lin-12 and Notch intracellular domains *in vivo.* Cell 74:331–345.

Sugimura R, Li L (2010) Noncanonical Wnt signaling in vertebrate development, stem cells, and diseases. Birth Defects Res C Embryo Today 90:243–256. doi: 10.1002/bdrc.20195

Sulston JE, Horvitz HR (1977) Post-embryonic cell lineages of the nematode, *Caenorhabditis elegans*. Developmental Biology 56:110–156. doi: 10.1016/0012-1606(77)90158-0

Sulston JE, Schierenberg E, White JG, Thomson JN (1983) The embryonic cell lineage of the nematode *Caenorhabditis elegans*. Developmental Biology 100:64–119. doi: 10.1016/0012-1606(83)90201-4

Sulston JE, White JG (1980) Regulation and cell autonomy during postembryonic development of *Caenorhabditis elegans.* Developmental Biology 78:577–597.

Sundaram M, Han M, Yochem J (1997) Ras is required for a limited number of cell fates and not for general proliferation in *Caenorhabditis elegans*. Molecular and Cellular Biology 17:2716.

Sundaram M, Yochem J, Han M (1996) A Ras-mediated signal transduction pathway is involved in the control of sex myoblast migration in *Caenorhabditis elegans.* Development 122:2823–2833.

Swarup S, Verheyen EM (2012) Wnt/Wingless Signaling in *Drosophila*. Cold Spring Harbor Perspectives in Biology 4:a007930–a007930. doi: 10.1101/cshperspect.a007930

Swiatek PJ, Lindsell CE, del Amo FF, et al (1994) Notch1 is essential for postimplantation development in mice. Genes & Development 8:707–719.

Syntichaki P, Xu K, Driscoll M, Tavernarakis N (2002) Specific aspartyl and calpain proteases are required for neurodegeneration in *C. elegans.* Nature 939–944.

Szewczyk NJ, Peterson BK, Jacobson LA (2002). Activation of Ras and the mitogen-activated protein kinase pathway promotes protein degradation in muscle cells of *Caenorhabditis elegans*. Mol Cell Biol 22:4181-8.

Takebe N, Nguyen D, Yang SX (2013) Targeting Notch signaling pathway in cancer: Clinical development advances challenges. Pharmacol Ther. doi: 10.1016/j.pharmthera.2013.09.005

Takeda H, Lyle S, Lazar AJF, et al (2006) Human sebaceous tumors harbor inactivating mutations in LEF1. Nat Med 12:395–397. doi: 10.1038/nrc1096

Takeshita H (2005) Asymmetric cortical and nuclear localizations of WRM-1/ß-catenin during asymmetric cell division in *C. elegans.* Genes & Development 19:1743–1748. doi: 10.1101/gad.1322805

Takuno S, Terauchi R, Innan H (2012) The power of QTL mapping with RILs. PLoS ONE 7:e46545. doi: 10.1371/journal.pone.0046545

Tan PB, Lackner MR, Kim SK (1998) MAP Kinase Signaling Specificity Mediated by the LIN-1 Ets/LIN-31 WH Transcription Factor Complex during *C. elegans* Vulval Induction. Cell 93:569–580. doi: 10.1016/S0092-8674(00)81186-1

Tan PBO, Kim SK (1999) Signaling specificity: the RTK/RAS/MAP kinase pathway in metazoans. Trends in Genetics 15:145–149. doi: 10.1016/S0168-9525(99)01694-7

Teicher BA (1994) Hypoxia and drug resistance. Cancer Metastasis Rev 13:139–168. doi: 10.1016/0360-3016(84)90522-4

Teicher BA, Lazo JS, Sartorelli AC (1981) Classification of antineoplastic agents by their selective toxicities toward oxygenated and hypoxic tumor cells. Cancer Res 41:73–81.

Tetsu O, McCormick F (1999) β-Catenin regulates expression of cyclin D1 in colon carcinoma cells. Nature 398:422–426. doi: 10.1074/jbc.272.16.10859

Thacker C, Sheps JA, Rose AM (2006) *Caenorhabditis elegans dpy-5* is a cuticle procollagen processed by a proprotein convertase. Cell Mol Life Sci 63:1193–1204. doi: 10.1007/s00018-006-6012-z

The *C. elegans* Sequencing Consortium (1998) Genome Sequence of the Nematode *C. elegans:* A Platform for Investigating Biology. Science 282:2012–2018. doi: 10.1126/science.282.5396.2012

The *C. elegans* Deletion Mutant Consortium (2012) Large-Scale Screening for Targeted Knockouts in the *Caenorhabditis elegans* Genome. G3: Genes, Genomes, Genetics 2:1415–1425. doi: 10.1534/g3.112.003830

Thomlinson RH (1977) Hypoxia and tumours. J Clin Pathol Suppl (R Coll Pathol) 11:105–113.

Thomlinson RH (1965) Tumour anoxia and the response to radiation. Sci Basis Med Annu Rev 74–90.

Thomlinson RH, Gray LH (1955) The histological structure of some human lung cancers and the possible implications for radiotherapy. Br J Cancer 9:539–549.

Thompson O, Edgley M, Strasbourger P, et al (2013) The million mutation project: A new approach to genetics in *Caenorhabditis elegans*. Genome Research 23:1749–1762. doi: 10.1101/gr.157651.113

Thompson OA, Snoek LB, Nijveen H, et al (2015) Remarkably Divergent Regions Punctuate the Genome Assembly of the *Caenorhabditis elegans* Hawaiian Strain CB4856. Genetics 200:975–989. doi: 10.1534/genetics.115.175950

Thorn KS, Naber N, Matuska M, et al (2008) A novel method of affinity-purifying proteins using a bis-arsenical fluorescein. Protein Science 9:213–217. doi: 10.1110/ps.9.2.213

Thorpe CJ, Schlesinger A, Carter JC, Bowerman B (1997) Wnt signaling polarizes an early *C. elegans* blastomere to distinguish endoderm from mesoderm. Cell 90:695–705.

Tian H, McKnight SL, Russell DW (1997) Endothelial PAS domain protein 1 (EPAS1), a transcription factor selectively expressed in endothelial cells. Genes & Development 11:72–82. doi: 10.1101/gad.11.1.72

Timmons L, Fire A (1998) Specific interference by ingested dsRNA. Nature 395:854–854. doi: 10.1038/27579

Tomida T, Oda S, Takekawa M, et al (2012) The Temporal Pattern of Stimulation Determines the Extent and Duration of MAPK Activation in a *Caenorhabditis elegans* Sensory Neuron. Sci Signal 5:ra76–ra76. doi: 10.1038/35005101

Trent C, Tsung N, Horvitz HR (1983) Egg-Laying Defective Mutants of the Nematode CAENORHABDITIS ELEGANS. Genetics 104:619.

Trewick SC, McLaughlin PJ, Allshire RC (2005) Methylation: lost in hydroxylation? EMBO Rep 6:315–320. doi: 10.1101/GAD.927301

Tsuchiya H, Iseda T, Hino O (1996) Identification of a Novel Protein (VBP-1) Binding to the von Hippel-Lindau (VHL) Tumor Suppressor Gene Product. Cancer Research 56:2881–2885.

Tuck S, Greenwald I (1995) *lin-25*, a gene required for vulval induction in *Caenorhabditis elegans.* Genes &

Development 9:341–357.

Tutar Y (2012) Pseudogenes. Comparative and Functional Genomics 2012:1–4. doi: 10.1186/1471-2164-10-277

Ureña J, Fernández-Chacón R, Benot AR, et al (1994) Hypoxia induces voltage-dependent Ca^{2+} entry and quantal dopamine secretion in carotid body glomus cells. Proc Natl Acad Sci USA 91:10208–10211.

Valenta T, Hausmann G, Basler K (2012) The many faces and functions of β-catenin. EMBO J 31:2714–2736. doi: 10.1093/emboj/cdg204

van Amerongen R (2012) Alternative Wnt Pathways and Receptors. Cold Spring Harbor Perspectives in Biology 4:a007914–a007914. doi: 10.1101/cshperspect.a007914

van de Wetering M, Cavallo R, Dooijes D, et al (1997) Armadillo coactivates transcription driven by the product of the *Drosophila* segment polarity gene *dTCF.* Cell 88:789–799.

van den Brenk HA, Moore V, Sharpington C, Orton C (1972) Production of metastases by a primary tumour irradiated under aerobic and anaerobic conditions *in vivo*. Br J Cancer 26:402–412.

van den Heuvel M, Nusse R, Johnston M, Lawrence PA (1989) Distribution of the *wingless* gene product in *Drosophila* embryos: a protein involved in cell-cell communication. Cell 59:739–749.

van der Wal JE, Hermsen MAJA, Gille HJP, et al (2003) Comparative genomic hybridisation divides retinoblastomas into a high and a low level chromosomal instability group. J Clin Pathol 56:26–30.

Van Voorhies WA, Ward S (2000) Broad oxygen tolerance in the nematode *Caenorhabditis elegans*. J Exp Biol 203:2467–2478.

van Zon JS, Kienle S, Huelsz-Prince G, et al (2015) Cells change their sensitivity to an EGF morphogen gradient to control EGF-induced gene expression. Nature Communications 2015 6:7053. doi:10.1038/ncomms8053

Vannucci SJ (2004) Hypoxia-ischemia in the immature brain. Journal of Experimental Biology 207:3149–3154. doi: 10.1242/jeb.01064

Varricchio A, Migliaccio AR (2014) The role of glucocorticoid receptor (GR) polymorphisms in human erythropoiesis. American Journal of Blood Research 4:53.

Vaupel P, Mayer A (2007) Hypoxia in cancer: significance and impact on clinical outcome. Cancer Metastasis Rev 26:225–239. doi: 10.1016/j.ijrobp.2006.07.1376

Vazquez AI, de los Campos G, Klimentidis YC, et al (2012) A Comprehensive Genetic Approach for Improving Prediction of Skin Cancer Risk in Humans. Genetics 192:1493–1502. doi: 10.1534/genetics.112.141705

Veeman MT, Axelrod JD, Moon RT (2003) A second canon. Functions and mechanisms of beta-catenin-independent Wnt signaling. Developmental Cell 5:367–377.

Venken KJT, Kasprowicz J, Kuenen S, et al (2008) Recombineering-mediated tagging of *Drosophila* genomic constructs for *in vivo* localization and acute protein inactivation. Nucleic Acids Res 36:e114–e114. doi: 10.1093/nar/gkn486

Vigil D, Cherfils J, Rossman KL, Der CJ (2010) Ras superfamily GEFs and GAPs: validated and tractable targets for cancer therapy? Nat Rev Cancer 10:842–857. doi: 10.1038/nrc2960

Villalonga P, Lopez-Alcala C, Bosch M, et al (2001) Calmodulin Binds to K-Ras, but Not to H- or N-Ras, and Modulates Its Downstream Signaling. Molecular and Cellular Biology 21:7345–7354. doi: 10.1128/

MCB.21.21.7345-7354.2001

Vora S, Phillips BT (2015) Centrosome-Associated Degradation Limits β-Catenin Inheritance by Daughter Cells after Asymmetric Division. Current Biology 25:1005–1016. doi: 10.1016/j.cub.2015.02.020

Waggoner LE, Zhou GT, Schafer RW, Schafer WR (1998) Control of Alternative Behavioral States by Serotonin in *Caenorhabditis elegans.* Neuron 21:203–214. doi: 10.1016/S0896-6273(00)80527-9

Wang GL, Jiang BH, Rue EA, Semenza GL (1995) Hypoxia-inducible factor 1 is a basic-helix-loop-helix-PAS heterodimer regulated by cellular O_2 tension. Proceedings of the National Academy of Sciences 92:5510–5514. doi: 10.1073/pnas.92.12.5510

Wang GL, Semenza GL (1993) Characterization of hypoxia-inducible factor 1 and regulation of DNA binding activity by hypoxia. J Biol Chem 268:21513–21518.

Wang M, Sternberg PW (2000) Patterning of the *C. elegans* 1 degrees vulval lineage by RAS and Wnt pathways. Development 127:5047–5058.

Wang M, Sternberg PW (1999) Competence and Commitment of *Caenorhabditis elegans* Vulval Precursor Cells. Developmental Biology 212:12–24. doi: 10.1006/dbio.1999.9357

Wang Y, Xie W, Wang D (2007) Transferable properties of multi‐biological toxicity caused by cobalt exposure in *Caenorhabditis elegans*. Environmental Toxicology and Chemistry 26:2405–2412. doi: 10.1897/06-646R1.1

Warburg O (1956) On the Origin of Cancer Cells. Science 123:309–314. doi: 10.1126/science.123.3191.309

Warner TT, Schapira AHV (2003) Genetic and environmental factors in the cause of Parkinson's disease. Annals of Neurology 53:S16–S25. doi: 10.1002/ana.10487

Waskiewicz AJ (1997) Mitogen-activated protein kinases activate the serine/threonine kinases Mnk1 and Mnk2. EMBO J 16:1909–1920. doi: 10.1093/emboj/16.8.1909

Weinmaster G, Roberts VJ, Lemke G (1992) Notch2: a second mammalian Notch gene. Development 116:931–941.

Weis WI, Stamos JL (2013) The β-Catenin Destruction Complex. Cold Spring Harbor Perspectives in Biology. doi: 10.1101/cshperspect.a007898

Wen C, Metzstein MM, Greenwald I (1997) SUP-17, a *Caenorhabditis elegans* ADAM protein related to *Drosophila* KUZBANIAN, and its role in LIN-12/NOTCH signalling. Development 124:4759–4767.

Whangbo J, Kenyon C (1999) A Wnt signaling system that specifies two patterns of cell migration in *C. elegans*. Mol Cell 4:851–858.

White JG, Southgate E, Thomson JN, Brenner S (1976) The Structure of the Ventral Nerve Cord of *Caenorhabditis elegans*. Philosophical Transactions of the Royal Society B: Biological Sciences 275:327–348. doi: 10.1098/rstb.1976.0086

Whitfield CW, Benard C, Barnes T, et al (1999) Basolateral Localization of the *Caenorhabditis elegans* Epidermal Growth Factor Receptor in Epithelial Cells by the PDZ Protein LIN-10. Molecular Biology of the Cell 10:2087–2100. doi: 10.1091/mbc.10.6.2087

WHO Cancer Control Programme. (2017) World Health Organization, www.who.int/cancer/en/.

Wicks SR, Yeh RT, Gish WR, et al (2001) Rapid gene mapping in *Caenorhabditis elegans* using a high density polymorphism map. Nat Genet 28:160–164. doi: 10.1038/88878

Wiesener MS (2003) Widespread hypoxia-inducible expression of HIF-2[alpha] in distinct cell populations of different organs. FASEB J 17:271–273.

Wilkinson HA, Fitzgerald K, Greenwald I (1994) Reciprocal changes in expression of the receptor *lin-12* and its ligand *lag-2* prior to commitment in a *C. elegans* cell fate decision. Cell 79:1187–1198.

Williams WR, Anderson DE, Rao DC (2005) Genetic epidemiology of breast cancer: Segregation analysis of 200 Danish pedigrees. Genet Epidemiol 1:7–20. doi: 10.1080/19485565.1966.9987639

Wood LD, Parsons DW, Jones S, et al (2007) The Genomic Landscapes of Human Breast and Colorectal Cancers. Science 318:1108–1113. doi: 10.1002/jcc.20084

Wortzel I, Seger R (2011) The ERK Cascade: Distinct Functions within Various Subcellular Organelles. Genes & Cancer 2:195–209. doi: 10.1177/1947601911407328

Wouters BG, Koritzinsky M (2008) Hypoxia signalling through mTOR and the unfolded protein response in cancer. Nat Rev Cancer 8:851–864. doi: 10.1074/jbc.M204733200

Wouters BG, van den Beucken T, Magagnin MG, et al (2005) Control of the hypoxic response through regulation of mRNA translation. Semin Cell Dev Biol 16:487–501. doi: 10.1016/j.semcdb.2005.03.009

Wright S (1921) Systems of mating. Parts I-V. Genetics 6:111-178.

Xiao G, Zhu J, Gao S (2014) Regulation of Wnt/β-catenin signaling by posttranslational modifications. Cell & Bioscience 4:13. doi: 10.1186/2045-3701-4-13

Xie L, Xiao K, Whalen EJ, et al (2009) Oxygen-Regulated 2-Adrenergic Receptor Hydroxylation by EGLN3 and Ubiquitylation by pVHL. Sci Signal 2:ra33. doi: 10.1126/scisignal.2000444

Yang S-L, Wu C, Xiong Z-F, Fang X (2015) Progress on hypoxia-inducible factor-3: Its structure, gene regulation and biological function. Molecular Medicine Reports 12:2411–2416. doi: 10.3892/mmr.2015.3689

Yeon SY, Jo YS, Choi EJ, et al (2017) Frameshift Mutations in Repeat Sequences of *ANK3, HACD4, TCP10L, TP53BP1, MFN1, LCMT2, RNMT, TRMT6, METTL8* and *METTL16* Genes in Colon Cancers. Pathol Oncol Res 1–6. doi: 10.1007/s12253-017-0287-2

Yoder JH, Chong H, Guan K-L, Han M (2003) Modulation of KSR activity in *Caenorhabditis elegans* by Zn ions, PAR-1 kinase and PP2A phosphatase. EMBO J 23:111–119. doi: 10.1038/sj.emboj.7600025

Yoo AS, Bais C, Greenwald I (2004) Crosstalk between the EGFR and LIN-12/Notch pathways in *C. elegans* vulval development. Science 303:663–666. doi: 10.1126/science.1091639

Yoon CH, Lee J, Jongeward GD, Sternberg PW (1995) Similarity of *sli-1*, a regulator of vulval development in *C. elegans*, to the mammalian proto-oncogene *c-cbl*. Science 269:1102–1105.

Yost C, Torres M, Miller JR, et al (1996) The axis-inducing activity, stability, and subcellular distribution of beta-catenin is regulated in *Xenopus* embryos by glycogen synthase kinase 3. Genes & Development 10:1443–1454. doi: 10.1101/gad.10.12.1443

Young ND (1996) QTL mapping and quantitative disease resistance in plants. Annu Rev Phytopathol 34:479–501. doi: 10.1146/annurev.phyto.34.1.479

Young SD, Hill RP (1990) Effects of reoxygenation on cells from hypoxic regions of solid tumors: analysis of transplanted murine tumors for evidence of DNA overreplication. Cancer Res 50:5031–5038.

Young SD, Marshall RS, Hill RP (1988) Hypoxia induces DNA overreplication and enhances metastatic potential of murine tumor cells. Proceedings of the National Academy of Sciences 85:9533–9537. doi: 10.1073/pnas.85.24.9533

Yu B, Zhang K, Milner JJ, et al (2017) Epigenetic landscapes reveal transcription factors that regulate CD8+ T cell differentiation. Nat Immunol 18:573–582. doi: 10.1093/bioinformatics/btr064

Yu F, White SB, Zhao Q, Lee FS (2001) HIF-1 binding to VHL is regulated by stimulus-sensitive proline hydroxylation. Proceedings of the National Academy of Sciences 98:9630–9635. doi: 10.1096/fj.00-0732fje

Zetka MC, Rose AM (1992) The meiotic behavior of an inversion in *Caenorhabditis elegans.* Genetics 131:321–332.

Zhang J, Patel JM, Block ER (1998) Hypoxia-specific upregulation of calpain activity and gene expression in pulmonary artery endothelial cells. American Journal of Physiology - Lung Cellular and Molecular Physiology 275:L461–L468.

Zhang L, Hill RP (2004) Hypoxia Enhances Metastatic Efficiency by Up-Regulating *Mdm2* in KHT Cells and Increasing Resistance to Apoptosis. Cancer Research 64:4180–4189. doi: 10.1158/0008-5472.CAN-03-3038

Zhang TY, Labonté B, Wen XL, et al (2012) Epigenetic Mechanisms for the Early Environmental Regulation of Hippocampal Glucocorticoid Receptor Gene Expression in Rodents and Humans. Neuropsychopharmacology 38:111–123. doi: 10.1016/j.jad.2006.01.016

Zhou J (2006) Calpain Mediates a von Hippel-Lindau Protein-independent Destruction of Hypoxia-inducible Factor-1. Molecular Biology of the Cell 17:1549–1558. doi: 10.1091/mbc.E05-08-0770

Zimonjic DB, Keck CL, Thorgeirsson SS, Popescu NC (1999) Novel recurrent genetic imbalances in human hepatocellular carcinoma cell lines identified by comparative genomic hybridization. Hepatology 29:1208–1214. doi: 10.1128/MCB.13.4.2432

Zinovyeva AY, Yamamoto Y, Sawa H, Forrester WC (2008) Complex Network of Wnt Signaling Regulates Neuronal Migrations During *Caenorhabditis elegans* Development. Genetics 179:1357–1371. doi: 10.1534/genetics.108.090290

Zipperlen P, Nairz K, Rimann I, et al (2005) A universal method for automated gene mapping. Genome Biol 6:R19. doi: 10.1186/gb-2005-6-2-r19

Appendix 7

7.1 Supplementary data

Table 7.1. List of polymorphic genes within the QTL1A region in the *bar-1(ga80)* mutant background. Brackets indicate that several isoforms are affected by the SNP.

Gene	Sequence name	Amino acid change
rpn-10	*B0205.3*	[Asn75Thr, Asn75Thr]
-	*B0205.9*	Val273Leu
-	*B0379.2*	Ser85Cys
mut-16	*B0379.3*	[Ser449Phe, Ser445Phe, Ser445Phe]
-	*B0379.7*	[Ala347Glu, Ala347Glu]
-	*B0511.12*	Ala347Glu, Ser795Gly, Gly1307Glu, Ser186Gly
-	*B0511.14*	His549Tyr
npp-14	*C03D6.4*	Glu4Asp, Ser773Ile, Thr930Ser, Ser1144Pro, Ser1157Pro, Leu266Phe
asfl-1	*C03D6.5*	His218Leu, Met230Val
lab-1	*C03D6.6*	Gly159Asp
-	*C04F12.1*	Asn423Lys
fce-1	*C04F12.10*	[Ile124Val, Ile124Val]
-	*C04F12.6*	Val170Ala
-	*C04F12.8*	Asn70Ser
rnh-1.3	*C04F12.9*	Asn77Tyr
dao-5	*C25A1.10*	[Asp620Tyr, Asp345Tyr]
tag-272	*C34B2.1*	Ala56Thr
-	*C35E7.5*	[Thr867Ala, Thr867Ala]
rig-5	*C36F7.4*	[Leu66His, Leu66His, Leu66His]
-	*F16C3.3*	Asn203Ile
-	*F26E4.2*	Glu113Ala
-	*F26E4.4*	[Asp147Asn, Asp147Asn, Asp147Asn]
ncx-4	*F35C12.2*	Gly251Arg

-	*F35C12.3*	[Ser152Phe, Ser152Phe, Ser328Phe, Ser328Phe, Ser328Phe, Ser-302Phe]
oct-1	*F52F12.1*	[Glu320Lys, Glu320Lys, Glu337Lys]
col-64	*F52F12.2*	Tyr50Phe
mom-4	*F52F12.3*	[Arg423Pro, Arg423Pro]
gpx-8	*F55A3.5*	Arg23Cys
-	*F59C6.14*	[Gln139Arg, Gln102Arg]
-	*K07A1.1*	Phe167Ser

Table 7.2. Polymorphisms in selected genes. If several isoforms are affected by the SNP, they are indicated in brackets. Note that a SNP occurrence frequency of 80% was set as a threshold.

	Gene	Sequence name	Polymorphism
QTL1b region and associated	*pfd-3*[1]	*T06G6.9*	Ala5Val
	-	*F44F1.1*[2]	deletion
	-	*F44F1.3*[1]	Gly131Ser, His217Leu, Pro408Gln, Ala418Thr, Asp-468Gly
	amx-2[1]	*B0019.1*	Leu617Pro, Asn535Ser, Thr532Ser, Arg521Gly, As-n461Ser, Val410Ile
hypoxia response pathway	*egl-9*[1]	*F22E12.4*	[Pro16Ser, Pro16Ser, Pro16Ser, Pro16Ser, Pro16Ser]
	vhl-1[3]	*F38A6.3*	none
	hif-1[1]	*F38A6.3*	[Lys258Arg, Lys258Arg, Lys258Arg, Lys258Arg, Ly-s42Arg], splice site donor
	aha-1[1]	*C25A1.11*	none
EGFR/RAS/MAPK pathway	*lin-3*[1]	*F36H1.4*	none
	let-23[1]	*ZK1067.1*	none
	sem-5[1]	*C14F5.5*	none
	sos-1[1]	*T28F12.3*	none
	lin-7[1]	*Y54G11A.10*	none
	lin-10[1]	*C09H6.2*	none
	lin-2[1]	*F17E5.1*	[Glu536Asp, Glu195Asp]
	let-60[1]	*ZK792.6*	none
	gap-1[3]	*T24C12.2*	none
	lin-45[1]	*T24C12.2*	none
	mek-2[1]	*Y54E10BL.6*	none
	mpk-1[3]	*F43C1.2*	none
	lin-31[1]	*K10G6.1*	none
	lin-1[1]	*C37F5.1*	Ille63Thr
	lin-15[1]	*unknown (WS261)*	[Asp844Gly, Asp844Gly], Asn656Lys
NOTCH pathway	*lin-12*[1]	*R107.8*	none
	lip-1[3]	*C05B10.1*	none
	lag-2[1]	*Y73C8B.4*	Ala227Val
	lag-1[1]	*K08B4.1*	[Asp342Asn, Asp340Asn]

further genes	-	*H28O16.1*[1)]	none
	nhr-57[1)]	*T05B4.2*	none
	cdk-5[1)]	*T27E9.3*	none
	cdka-1/ p35[3)]	*T27E9.3*	none
	ddx-35[1)]	*Y67D2.6*	Ille218Met
	bar-1[3)]	*C54D1.6*	none
	lin-39[1)]	*C07H6.7*	[Pro13Ser, Pro13Ser]

[1)] Sequence contains synonymous SNPs.

[2)] non-coding sequence (pseudogene).

[3)] Sequence does not contain any synonymous SNPs.

7.2 Abbreviations

5-HIAA	5-Hydroxyindoleacetic acid
°C	Degree Celsius
1°	Primary
2°	Secondary
3°	Tertiary
AC	Anchor cell
Amp / Tet	Ampicillin / Tetracycline
AmpR	Ampicillin resistance gene
ANK	Ankyrin
bHLH	Basic helix-loop-helix
bp	Base pair
$CaCl_2$	Calcium chloride
Cas	CRISPR-associated system
CB4856	*C. elegans* Hawaii strain
cDNA	Complementary DNA
CDS	Coding sequence
C. elegans	*Caenorhabditis elegans*
CGC	*Caenorhabditis Genetics* Center
Co^{2+}	Cobalt ion
$CoCl_2$	Cobalt chloride
CRISPR	Clustered regularly interspaced short palindromic repeats
CSL	CBF1, Suppressor of Hairless, Lag-1, transcription factor
DIC	Differential interference contrast
DIP	2,2'-Dipyridyl

DLL	Delta-like ligand
DMOG	Dimethyloxalylglycine
DNA	Deoxyribonucleic acid
dNTP	Deoxyribonucleotide
dpy	Dumpy phenotype
DSB	Double strand break
5-HIAA	5-Hydroxyindoleacetic acid
°C	Degree Celsius
1°	Primary
2°	Secondary
3°	Tertiary
AC	Anchor cell
Amp / Tet	Ampicillin / Tetracycline
AmpR	Ampicillin resistance gene
ANK	Ankyrin
bHLH	Basic helix-loop-helix
bp	Base pair
$CaCl_2$	Calcium chloride
Cas	CRISPR-associated system
CB4856	*C. elegans* Hawaii strain
cDNA	Complementary DNA
CDS	Coding sequence
C. elegans	*Caenorhabditis elegans*
CGC	*Caenorhabditis Genetics* Center
Co^{2+}	Cobalt ion
$CoCl_2$	Cobalt chloride
CRISPR	Clustered regularly interspaced short palindromic repeats
CSL	CBF1, Suppressor of Hairless, Lag-1, transcription factor
DIC	Differential interference contrast
DIP	2,2'-Dipyridyl
DLL	Delta-like ligand
DMOG	Dimethyloxalylglycine
DNA	Deoxyribonucleic acid
dNTP	Deoxyribonucleotide
dpy	Dumpy phenotype
DSB	Double strand break
dsRNA	Double stranded DNA
DTC	Distal tip cell
E. coli	*Escherichia coli*

EGF	Epidermal growth factor
EGFR	Epidermal growth factor receptor
egl	Egg-laying defective phenotype
EIF	Eukaryotic initiation factor
EPO	Erythropoietin
ER	Endoplasmatic reticulum
ERK	Extracellular-signal regulated kinase
EtBr	Ethidium bromide (DNA stain)
EtOH	Ethanol
eQTL	Expression quantitative trait locus
Fe^{2+}	Ferrous
Fe^{3+}	Ferric
F1	First filial generation
F2	Second filial generation
FAP	Familial adenomatous polyposis
FGF	Fibroblast growth factor
FGFR	Fibroblast growth factor receptor
$FlAsH\text{-}EDT_2$	Fluorescin arsenical hairpin binder-ethanedithiol
FLP	Fragment length polymorphism
g	Gram
GAP	GTPase activating protein
GEF	Guanine nucleotide exchange factor
gf	Gain-of-function
GFP	Green fluorescent protein
GWAS	Genome-wide association study
h	Hour
H_2O_2	Hydrogen peroxide
HIF	Hypoxia inducible factor
HRE	Hypoxia response element
HRP	Horseradish peroxidase
InDel	Insertion/deletion
IPTG	Isopropyl ß-D-1-thiogalactopyranoside
Kan	Kanamycin
kb	Kilobases
kD	Kilo dalton
l	Liter
L1 - L4	Larval stage 1 to 4
LB	Lysogeny broth
let	LEThal

lf	Loss-of-function
lin	Abnormal cell LINeage
LIP	Lateral-singal-induced phosphatase
LNG	LIN-12, NOTCH, GLP-1
LNR	LIN-12/NOTCH Repeat
LOD	Likelihood of disequilibrium
LongAmp	Long amplification polymerase
M	Molar
MAPK	Mitogen activated protein kinase
Mb	Mega bases
mCherry	Red monomeric (m) fluorescent protein
mg	Milligram
min	Minute
miIL	Mutation included introgression line
miRIL	Mutation included recombinant inbred line
ml	Milliliter
µl	Microliter
µm	Micrometer
mm	Millimeter
mM	Millimolar
µg/ml	Microgram per milliliter
MosSCI	Mos1-mediated Single Copy Insertion
mRNA	Messenger RNA
ms	Millisecond
Muv	Multivulva phenotype
MW	Molecular weight
N2	N2 Bristol, wild-type *C. elegans* strain
NGM	Nematode Growth Medium
NLS	Nuclear localisation signal
nm	Nanometer
NICD	Notch intracellular domain
nt	Nucleotide
O_2	Oxygen
ODDD	Oxygen dependent degradation domain
oligo	Oligonucleotide
ORF	Open reading frame
ORFeome	Complete set of open reading frames in a genome
P0	Parental generation
PAGE	Polyacrylamide gel electrophoresis

PAS	Per, ARNT, Sim
PCR	Polymerase chain reaction
Pen / Strep	Penicillin / Streptomycin
PEST	Sequence rich in Pro (P), Glu (E), Ser (S) and Thr (T)
PHD	Prolyl hydroxylase domain
PI3K	Phosphoinositide 3-kinase
PLC	Phospholipase C
Pn.a cells	Neuroblast cell lineage
Pn.p cells	Ventral ectodermal blast cells
Pvl	Protruding vulva phenotype
QTL	Quantitative trait locus
RAM	RBPJ-associated
RAS	Rat sarcoma
RCC	Renal cell carcinoma
ReAsH-EDT_2	Resofurin arsenical hairpin binder-ethanedithiol
rf	Reduction of function
RIL	Recombinant inbred line
RNA	Ribonucleic acid
RNAi	RNA interference
Rol	Roller phenotype
ROS	Reactive oxygen species
rpm	Rounds per minute
RSK	Ribosomal protein S6 kinase
RT	Room temperature
RTK	Receptor tyrosine kinase
s	Second
SDS	Sodium dodecyl sulfate
sgRNA	Single guide RNA
SLiCE	Seamless Ligation Cloning Extract
SNP	Single nucleotide polymorphisms
STET	Saline / Tris / EDTA / Triton
synMuv	Synthetic Multivulva
TAD	Transactivation domain
TAE	Tris / glacial acetic acid / EDTA
TC	Tetra-cysteine
TE	Tris-EDTA
TM	Transmembrane
TY	Trypton yeast extract
unc	Uncoordinated movement phenotype

UPR	Unfolded protein response
UTR	Untranslated region
UV	Ultraviolet
VEGF	Vascular endothelial growth factor
VEGFR	Vascular endothelial growth factor receptor
VHL	Von Hippel-Lindau
VI	Vulval induction index
VPC	Vulval precursor cell
VU	Ventral uterus
Vul	Vulvaless phenotype
v/v	Volume per volume
wt	Wild-type
Zn	Zinc

7.3 Curriculum vitae

SABRINA MAXEINER

Margrit-Rainer-Strasse 11A
8050 Zurich
sabrina.maxeiner@gmail.com
Mobile +41 76 595 36 33
Date of birth: 28.02.1990
Swiss / German

Strengths in the preparation and implementation of project ideas.
Solid communication skills adapted to the level of the counterpart.
Reliable, highly organised and independent.

PROFESSIONAL EXPERIENCE

01/2013 - present **University of Zurich, Institute of Molecular Life Sciences**
Doctoral Researcher
- training and mentoring of a master student and several semester students
- coordination of a small team of experts to plan and craft customized experimental gas chambers
- presentation of project outcomes at international conferences

06/2016 – present **Life Science Learning Center (LSLC), Zurich**
Teacher
- Running of practical biology courses for high school students and teachers
- Introducing high school students to research at university

04/2012 – 12/2012 **SUBWAY® Zurich**
Sandwich Artist® and Assistant to the Store Manager
- Regular inspections of equipment and fixtures
- Solicitation of customer feedback and ensuring customer satisfaction
- Spontaneous deputizing during rush hours in nearby subsidiary

06/2012 – 08/2012 **University of Zurich, Institute of Molecular Life Sciences**
Scientific assistant
- Internship in developmental biology, completion with highest grade

07/2011 – 09/2011 **University of Zurich, Institute of Molecular Life Sciences**
Scientific assistant
- Internship in cellular and molecular biology, completion with highest grade
- Autonomous work in strict compliance with the guidelines as defined by the Good Laboratory Practice

EDUCATION

01/2013 – present **University of Zurich, Institute of Molecular Life Sciences**
- Master & Doctoral study within the Fast Track program for outstanding students

09/2009 – 08/2012 **University of Zurich**
- Bachelor studies in natural sciences in biology, grade: 5.7

03/2009 – 06/2009 **English Language College Langports, Brisbane, Australia**
- Certificate of Advanced English (CAE), C1
- Certificate in Proficiency of English (CPE), C2

AWARDS

2009 **Schweizer Jugend forscht**
- High school thesis judged among the 50 best in the Canton of Zurich

2009 **SRF Einstein**
- Audience award, 3rd position for presentation of high school thesis

LANGUAGES

German (native language)

English (C1)

French (B2)

COMPUTER SKILLS

MS Office Suite

Statistical software: R, Python, MATLAB

Image processing software: Adobe Illustrator, Fiji

References available upon request.

7.4 Acknowledgements

This thesis would not have been possible without a number of people and I would like to leave a few words to express my cordial thanks to all these who have accompanied me through the past years and supported me in achieving my goals.

Firstly, my thanks go to Prof. Dr. Alex Hajnal who guided me through the turmoil of a doctoral thesis and helped me follow a satisfying path. I am grateful for the valuable time he sacrificed to discuss scientific issues, his open ear and understanding in non-work related trouble, his never-ending optimism and his knack for motivating people over and over again. He is not only our boss and slightly absent-minded professor, but also the “lab dad” who takes care of his students and the working atmosphere.

Further, my thanks go to all present and former members of our lab who contributed to a lively atmosphere. Erika Fröhli, the good spirit and organised “lab mum” apparently knew a solution to any problem be it work-related or private, and the world seemed lighter after talking to her. She turned tears and anger into relief and laughter. The lab lost a great person when she left for her well-earned retirement. Irene Hofmann, although working in the adjacent building and therefore physically a little more distant, is the woman who truly keeps things running. She eliminated and reminded of administrative issues before they could arise and in that saved me a large amount of labour and trouble. Special thanks go to Dr. Michael Walser who fortunately decided to re-join our lab as a Postdoc after a temporary position at the hospital and with whom I had the luck to share an office. His enthusiasm, motivation and humour brought me back to a work-mode smoothly and softly every Monday morning that tends to arrive incredibly quickly. Thank you for your trust, the discussions that were sometimes deep, sometimes silly and relaxing and sometimes heavy. I would argue that his expertise in Adobe as well as lab techniques has saved many nerves and experiments – not only mine but of the entire lab. More special thanks are dedicated to Michael Daube, who fortunately joined our lab as a technician after his time in the Hengartner lab. He is the slightly odd bird and there is always an anecdote in stock. Whenever there was something missing, he immediately took care of it, he invested intense time and effort to provide us with protocols, lists, material, in short with whatever is necessary. I speak for the institute when I say you enrich any good week and save any bad week with the regular TGIFs, not only because you organise them but because how you organise them – with so much care and attention that everyone feels at ease.

Moreover, my thanks address Dr. Juan Miguel Escobar, he was always up for a discussion – with or without *cafecito*. I am grateful to Jonas Hartmann for his direct way and valuable discussions about science, private life and how future might look like, to Sabrina Steiert for the close friendship we could establish during our time together in the lab, to Dr. Qiutan Yang for her contagious light-heartedness, to Dr. Daniel Roiz for sharing his extensive scientific knowledge and for speaking his mind, to Dr. Matthias Morf for scientific support, Charlotte Lambert, Philipp Leu, Dr. Itay

Nakdimon and Dr. Stephanie Nusser-Stein for their contribution to such a nice atmosphere. I thank Adrian Henggeler, the “coffee-bell” in the morning, for his friendliness, easiness and humour that so often compensated for failed experiments or a bad mood and I thank Andrea Haag for her cheeriness and fun company with a glass of wine or two. Another thank you goes to Louisa Mereu who conveyed the ease with which she managed work and family to the lab and everyone working therein, to Silvan Spiri for an awesome teamwork in teaching high school classes, scientific and private discussions and the musical instrument equipment via the family business and to Aleksandra Fergin for her impressive mix of funny, serious, honest and dedicated attitude. I am grateful to our Ticino-Italy fraction presented by Tea Kohlbrenner and Svenia Dilaria Heinze – with you ladies, no problem seems to exist and I would not miss the times we spent at the TGIF in having a good time and forget bad days. Still further thanks go to Dr. Evelyn Lattmann for her persistent good mood and helpfulness, to Dr. Tinri Aegerter-Wilmsen for interesting non-science related discussions about everything and anything, to Christoph alias Stefan alias Christian alias *Whatevercomestomind* Umbricht for his wittiness and sarcasm, to Ting Deng, to Steve Grein, to Elisa Pircher and to Kirsti Arumae. I would like to mention here and thank Giuseppe Ianiri and Hatip Zenuni for their provision of worm and bacteria plates as well as media. Without their support, the lab would not be running as smoothly as it was and is.

There are several students who have closely worked with me and supported my work. I had the honour to guide Seraina Boetschi through her Master thesis and although experiments did not work out as intended, she pursued her goals and managed to find her way out of disappointments. She is not only a great colleague to work with, but became a dear friend and I am happy that she does not work far away and comes over for visiting us frequently. Katharina Jovic spent several months with us to work on the RNAi screen to find modifiers of WNT and RAS/MAPK signalling and did so with great success. I value the discussions and fun moments I shared with her. Judith Grolleman is a person who always bounces back and has indulged us with her exuberant attitude and baking qualities. It was an indescribable experience to witness and attend her personal and scientific development, through which she became a dear friend. Finally, I want to thank Kateřina Apolínová, the summer entertainer of our lab. She spent nine weeks with us and worked with me on the RNAi screen while developing her scientific confidence and bringing life into the lab.

I would like to express my gratefulness to Reto Maier and Daniel Schnarwiler. They have helped in designing the hypoxic chambers, provided all the material necessary and most importantly, manufactured them and supported me with in troubleshooting. Without you, the project would have taken another direction and I am relieved it did not. Along the line, I want to thank Dr. Tanja Restin who carried out the initial hypoxia experiments with me by providing her own material. She did not only kick-start the story on hypoxia, but also took me for a coffee and shared scientific knowledge with me.

I was accompanied and support by the members of the thesis committee meeting and I have to say I chose them well. I highly appreciated the yearly meetings to discuss the progress of my

work but also to spend intense and interesting hours to define further steps. A cordial thank you to Prof. Dr. Konrad Basler for his always realistic input and sincere support, to Prof. Dr. Beatrice-Beck Schimmer for her reassuring smile and warmth and to Prof. Dr. Jan Kammenga who came from the Netherlands to share his ideas and constructive comments.

Although the Hengartner lab was gradually closed, I had the pleasure to work with several people still. Thanks go to Luca Ducoli for his cheeriness combined with scientific seriousness, to Dr. Sergio Pinto for sharing his extensive scientific knowledge, to Dr. Deni Subasic for the fun moments we had as lab bench mates, to Polina Kamkina for the fun times in the lab and during social events and to all former lab members.

Prof. Dr. Daniel Kiper, Dr. Alex Butschi, Helen Stauffer and Claudia Bischoff gave me the opportunity to enrich my doctoral thesis with the regular supervision and tuition of high school classes and offered me the freedom to shape the lessons or create courses. I am grateful not only for this experience but also for the numerous times when I was able to receive the most valuable present: Gratefulness and interest of students and their teachers.

Last but certainly not least, there are my family and friends. They have guided me, caught me in tough times, cheered me up, brought me back to reality – they have lived the years with me. My dear partner and friend Tobias Schmid probably had to endure most of my moodiness but is still there with me. Thank you Tobi for being there whatever the situation, for giving me advice, reassurement and togetherness. I want to thank my brother Sascha and my dad Harald for their realistic view of the world and their ability to calm me in emotional crises, my mom Cornelia and Sascha's partner Lina for their warmth and emotional support. On the Schmid family side, I want to thank Vreni and Guido, Fabian and Ines as well as the little naughty boys Mats and Levi for fun times with games, cats, beer and wine. I want to thank all of you for being a family to me and enriching life.

It has been and is a pleasure to work with all of you and have you by my side respectively. Although there were periods where times seemed to stand still, the past five years have flown by and became filled with invaluable memories that I will gladly keep with myself. I want to close by stressing that although in the end, I had to undertake the doctoral adventure by my own, I would not have succeeded in passing the "finish line" of that curvy marathon without all of you.

Danke, Thank you, Merci, Grazie, Kiitos.

Zurich, February 2018